

Alma Mater Studiorum - Università di Bologna  
in cotutela con UNIVERSIDAD NACIONAL DEL LITORAL - SANTA FE

**DOTTORATO DI RICERCA IN  
SCIENZE VETERINARIE**

Ciclo 34

**Settore Concorsuale:** 07/H1 - ANATOMIA E FISIOLOGIA VETERINARIA

**Settore Scientifico Disciplinare:** VET/01 - ANATOMIA DEGLI ANIMALI  
DOMESTICI

**GROSS AND MICROSCOPIC MORPHOLOGICAL ANATOMICAL STUDY  
OF THE GUINEA PIG (*Cavia porcellus*) AND THE CAPYBARA  
(*Hydrochoerus hydrochaeris*), AIMED AT THE PREPARATION OF A  
COMPARATIVE ANATOMICAL ATLAS OF THE DIFFERENT SYSTEMS**

**Presentata da:** Margherita De Silva

**Coordinatore Dottorato**  
Carolina Castagnetti

**Supervisore**  
Annamaria Grandis

**Supervisore**  
Ana María Canal

**Co-supervisore**  
Roberto Chiocchetti

**Esame finale anno 2022**

## ABSTRACT

In recent years, there has been an exponential increase in the so-called “new pets”, including the domestic guinea pig (*Cavia porcellus*) and the capybara (*Hydrochoerus hydrochaeris*), two closely related Caviid rodents native to South America. Both historically bred for food purposes, they have more recently become increasingly popular as pets in the European and American continents, respectively. This led to an increasing veterinary interest in deepening the knowledge regarding their normal anatomy, as a basic contribution to other fields of veterinary medicine, including diagnostic imaging, surgery, and pathological anatomy.

Being part of a bilateral framework co-tutelage agreement leading to a joint Doctoral Degree between the *Alma Mater Studiorum* of Bologna, Italy and the *Universidad Nacional del Litoral* of Santa Fe, Argentina, this research project was partly carried out in Italy (study of guinea pigs) and partly in Argentina (study of capybaras). It consisted in the macroscopic study, through anatomical dissections of carcasses of both species as well as the use of anatomical casts, and in the histological study of the various systems in the two species, and was aimed at creating a gross and microscopic comparative anatomical atlas.

In summary, from the morphological anatomical study of the respiratory system emerged that the left lung of the guinea pig presented a typical accessory lobe, which was absent in the capybara, and that the bronchial tree of the guinea pig was more articulated, providing numerous segmental branches originating from the lobar bronchi. From the study of the abdominal aorta, it emerged that it originated separate celiac and cranial mesenteric arteries in the capybara, whereas the guinea pig had a single celiacomesenteric trunk; furthermore, the renal arteries of the guinea pig were found to be single, double or even triple in the guinea pigs studied, whereas they were found to be single on both sides in all the capybaras studied. From the study of the cardiovascular system, it emerged that the myocardium of the capybara heart was vascularized solely by a left coronary artery, whereas a right coronary artery was present in all guinea pig hearts. As for the urogenital system, the capybara only presented two sexual accessory glands, the seminal vesicles and the prostate gland, whereas, in the guinea pig, coagulating and bulbourethral glands were also identified. Moreover, the uterus of the capybara, unlike that of the guinea pig, was characterized by a double cervix. Finally, the capybara cerebrum, which presented a highly developed hypophysis, had a higher degree of

gyrification of the cerebral cortex and more conspicuous neocortical fissures, as opposed to the guinea pig's cerebrum.

From the histological study of the different systems, the most noteworthy differences emerged regarding the gastrointestinal apparatus. The oesophagus was lined by a highly keratinized stratified squamous epithelium in the capybara, as opposed to the nonkeratinized epithelium of the guinea pig's oesophagus, whereas the stomach, lined by a glandular epithelium in both species, with the exception of the nonglandular cardiac region, was lined with a keratinized epithelium in the capybara only. Further studies are necessary in order to confirm the present findings.

The creation of a comparative anatomical atlas of gross and microscopic anatomy of the capybara and the guinea pig might prove useful for clinical, zootechnical and research purposes.

# INDEX

<b>Introduction.....</b>	<b>pag. 1</b>
--------------------------	---------------

## FIRST PART

<b>Features of the species.....</b>	<b>pag. 3</b>
<i>Cavia porcellus</i>	
Taxonomy.....	pag. 3
Origins.....	pag. 4
History of domestication.....	pag. 5
Legislation.....	pag. 6
<i>Hydrochoerus hydrochaeris</i>	
Taxonomy.....	pag. 7
Origins.....	pag. 9
History of domestication.....	pag. 9
Legislation.....	pag. 11
<b>Gross and microscopic anatomy.....</b>	<b>pag. 12</b>
<b>Respiratory system.....</b>	<b>pag. 12</b>
Nasal cavities.....	pag. 12
Larynx.....	pag. 13
Trachoea.....	pag. 14
Lungs.....	pag. 16
<b>Digestive system.....</b>	<b>pag. 18</b>
Buccal cavity.....	pag. 18
Teeth.....	pag. 19
Tongue.....	pag. 21
Oesophagus.....	pag. 24
Stomach.....	pag. 25
Small intestine.....	pag. 27
Large intestine .....	pag. 30
Liver.....	pag. 32
Pancreas.....	pag. 34
<b>Cardiovascular system.....</b>	<b>pag. 36</b>
Heart.....	pag. 36
Large arterial and venous vessels.....	pag. 40
<b>Urogenital system.....</b>	<b>pag. 45</b>
Urinary system.....	pag. 45
Male genital system.....	pag. 47
Female genital system.....	pag. 51

<b>Lymphatic system</b> .....	pag. 54
Spleen.....	pag. 54
Thymus.....	pag. 56
Lymph nodes.....	pag. 57
<b>Endocrine system</b> .....	pag. 58
Adrenal glands.....	pag. 58
Pineal gland.....	pag. 60
Thyroid gland.....	pag. 61
Parathyroid gland.....	pag. 61
Pituitary gland.....	pag. 61
<b>Central nervous system</b> .....	pag. 62

## SECOND PART

<b>Materials &amp; methods</b> .....	pag. 66
<b>Gross anatomy</b> .....	pag. 67
Dissection procedure.....	pag. 67
Preparation techniques of anatomical casts.....	pag. 68
<b>Microscopic anatomy</b> .....	pag. 70
Classical histology techniques.....	pag. 70
<b>Statistics</b> .....	pag. 72
<b>Results</b> .....	pag. 73
<b>Atlas of macroscopic anatomy</b> .....	pag. 73
<b>Atlas of microscopic anatomy</b> .....	pag. 137
<b>Discussion</b> .....	pag. 162
<b>Conclusions</b> .....	pag. 189
<b>Bibliography</b> .....	pag. 193

# INTRODUCTION

The domestic guinea pig (*Cavia porcellus*) and the capybara (*Hydrochoerus hydrochaeris*) are two rodents native to South America belonging to the Caviidae family. The two species share many characteristics but differ in size, morphology, and habits.

The importance of these rodents lies in the fact that they are not only raised for food purposes and the capybara is also part of aquatic ecosystems, but they have become the so-called "new pets", the guinea pig in Europe, as well as the capybara in America. In South America, capybaras provide value for the ecosystem as part of the food chain, they are hunted for their meat and leather, and they have proved easy to domesticate, becoming increasingly popular exotic pets. Historically bred for food in South America, guinea pigs, on the other hand, have been extensively used as laboratory animals for human research; however, to this day, they are largely widespread as exotic pets all over the world.

The descriptive study of the macroscopic and microscopic anatomy of the guinea pig and the capybara is aimed at integrating the available information and interpreting the conformation of their systems. It is hoped that the results of the present study will deepen the knowledge regarding their normal anatomy, highlighting similarities and differences between the two species, as basic contribution to several fields of veterinary medicine, such as clinical practice, diagnostic imaging, surgery and pathological anatomy, thus improving their clinical and zootechnical management.

The research project is part of a bilateral framework co-tutelage agreement leading to a joint Doctoral Degree award between the *Alma Mater Studiorum* of Bologna, Italy and the *Universidad Nacional del Litoral* of Santa Fe, Argentina. The project was therefore partly carried out in Italy (anatomical study of guinea pigs) and partly in Argentina (anatomical study of capybaras), consisted in the anatomical study of the various systems in the two species, and led to the creation of a gross and microscopic comparative anatomical atlas, which might prove useful for zootechnical and research purposes, as well as for clinicians for an easier at-a-glance interpretation of anatomical abnormalities and pathological conditions, with important therapeutic implications.

## **FIRST PART**

## FEATURES OF THE SPECIES

### *Cavia porcellus*

#### **Taxonomy**

Guinea pigs (*Cavia porcellus*) are hystricomorph rodents indigenous to South America that have long been used as animal models of human disease, but have also become increasingly popular as exotic pets in Europe and North America (Pritt, 2012; Pignon and Mayer, 2020).

The scientific name *Cavia porcellus* was attributed to the domestic guinea pig by the naturalist Erxleben at the end of the 18th century (Pritt, 2012).

The taxonomic classification of the domestic guinea pig, according to Linnaeus (1758) is as follows:

Kingdom: Animalia;  
Subkingdom: Bilateria;  
Infrakingdom: Deuterostomia;  
Phylum: Chordata;  
Subphylum: Vertebrata;  
Infraphylum: Gnathostomata;  
Superclass: Tetrapoda;  
Class: Mammalia;  
Subclass: Theria;  
Infraclass: Eutheria;  
Order: Rodentia;  
Suborder: Hystricomorpha;  
Infraorder: Hystricognathi;  
Family: Caviidae;  
Subfamily: Caviinae;  
Genus: *Cavia*;  
Species: *C. porcellus*.

The suborder Hystricomorpha includes the guinea pig, the porcupine, the chinchilla, the capybara, and other rodents characterized by anatomical features such as large infraorbital foramina, deep pterygopalatine fossae, and prominent zygomatic arches (Wagner, 1976). Compared to rodents belonging to the suborders Sciuromorpha (squirrel-like) and Myomorpha (rat-like), hystricomorph rodents exhibit relative differences in the masticatory apparatus (Myers et al., 2006). Characteristics peculiar to the family Caviidae include the number of digits (4 at the level of each forelimb and 3 at the level of each hind limb with the hairless palmar and plantar surfaces), the presence of a single pair of inguinal mammae, and a vestigial tail (Harkness et al., 2002; Donnelly and Brown, 2004).





*Cavia porcellus*

## Origins

*Cavia porcellus* is no longer found naturally in the wild; its most likely wild ancestors are closely-related cavy species, such as *Cavia aperea*, *Cavia fulgida* and *Cavia tschudii*, still found today in several regions of South America, where they live in small groups in grassland areas (Weir, 1974; Harkness and Wagner, 1995).

Guinea pigs, despite the misleading nickname, are native to the Andean regions of South America (corresponding to the present-day Ecuador, Peru, Bolivia and Colombia), where they were domesticated by the Incas starting as early as 5000 BC for food and religious purposes (Morales, 1995; Diamond, 2002). During the period ranging between 1200 and the Spanish conquest of 1532, the indigenous peoples of the Andes selected several varieties of domestic guinea pigs through selective breeding; these breeds formed the basis of many modern domestic guinea-pig breeds (Nowak, 1999). *Cavia porcellus* continues to constitute an important food source in the Andean highlands to date; many households in the region raise the animal for food, which subsists on the families' vegetable leftovers (Morales, 1995).

Guinea pigs were then imported to Europe about 500 years ago by Dutch, English and Spanish traders by sea during the European colonization of South America in the 16th century, only to appear in North America from the 17th century, where they became popular exotic pets among the upper classes and royalty, including Queen Elizabeth I (Wagner, 1976; Morales, 1995).



Geographical distribution of *Cavia porcellus* in South America (from: Morales, 1995)

## History of domestication

*Cavia porcellus* has a long history of domestication, both in Europe and South America (Portorno et al., 2007; Lord et al., 2020).

Domestication over the centuries has led to the birth of a new species, *Cavia porcellus*, the domestic guinea pig, closely related to some species of wild guinea pig, especially *Cavia aperea*, but also *Cavia cutleri*, *C. fulgida* and *C. tschudii* (Wagner, 1976; Caras, 2002), and currently reared for food purposes by the Andean populations of South America (Morales, 1995). The wild guinea pig is still present in nature today in Peru, Venezuela, Argentina, Brazil, Uruguay and Paraguay, where it occupies a great variety of habitats, such as rocks, grasslands, forest borders and swamps, living in small herds of 5 to 10 animals inside burrows, and feeding on native vegetation, such as polyphite meadows, mainly at dusk, to denote their nocturnal attitudes (Cooper and Schiller, 1975a; Wagner, 1976; Morales, 1995). Peru is now home to the largest number of domestic and wild guinea pigs, followed by Ecuador, Bolivia and Colombia (Pritt, 2012). In Europe and North America, the domestic guinea pig is currently kept as a pet and is intended for scientific research. The use of the guinea pig as a laboratory animal, which began in 1780 with Lavoisier in the context of studies on heat production, reached its peak in 1960 in North America (Pritt, 1998). Among the discoveries made thanks to the use of the guinea pig in research, are the development of diphtheria antitoxin in 1901, the discovery of the antibiotic streptomycin in 1952, the discovery of the mechanisms involved in cochlear stimulation in 1961, and the identification of the structure of antibodies in 1971 (Pritt, 1998; Pritt, 2012). Historically, the research fields in which the guinea pig has been used are allergology, genetics, immunology, pharmacology, infectious diseases, nutrition, audiology and otology, optic neuropathies, scurvy, leukemia, allergic encephalomyelitis, ulcerative colitis, ketoacidosis, cardiovascular medicine, and reproductive biology (Harkness et al., 2010; Pritt,

2012). Other characteristics that make it of interest for scientific research are the high sensitivity to antibiotics (penicillins, tetracyclines and erythromycin) and the inability to synthesize vitamin C endogenously (Cozzi et al., 2006; Harkness et al., 2010).

In North America, the term *guinea pig* (common name of *Cavia porcellus* in the English language) has taken on the meaning of laboratory animal in the current lexicon, to testify how the use in scientific research has become a distinctive element of the species itself (Pritt, 1998; Pritt, 2012). Researchers Dunkin and Hartley in 1926 selected with out-breeding techniques the short-haired albino strain (or Dunkin Hartley, from the name of the scientists), widely (but not exclusively) used in biomedical research for more of a century (Wagner, 1976).

## **Legislation**

The EEC Directive 86/609 of 26 November 1986 and the Legislative Decree n. 116 of 26 January 1992 are currently the reference standards for the use and protection of all animal species used for scientific and experimental purposes in Europe and in Italy. The current legislation examines all the elements and factors that make up and experiment (definition of experiment and experimental animal, establishment, competent authority in the figure of the Ministry of Health, training of professional figures); it also defines requirements, obligations and fulfilments for the use of animals for scientific purposes, including the requirement for authorization of an experimental protocol and housing parameters, as well as defining the administrative or penal sanctions for those who violate the relevant provisions (Cozzi et al., 2006).

The possession and use of guinea pigs for breeding and private purposes is disciplined by the Animal Protection Ordinance 455.1 of 23 April 2008, which disciplines the treatment, possession, use and interventions on vertebrate animals, cephalopods (Cephalopoda) and decapods (Reptantia). According to the aforementioned Ordinance, no training is required for the private detention of guinea pigs; the sale of >100 animals per year requires a cantonal authorization and special training for the keeping and breeding of these animals (art. 101 lett. C no. 3, 102 para. 4 OPAn). Being social animals, guinea pigs must be kept in groups of at least two animals (art.13, annex 2 table 1 special requirement 47 OPAn). Animals must be given adequate and regular access to water and food, particularly, coarse-grained food such as hay (art.4 OPAn). The care of guinea pigs, intended to prevent illness and injury, includes the regular brushing of long-haired guinea pigs, the regular and neat trimming of the claws of guinea pigs, and the treatment or, where appropriate, humane killing of sick or injured animals (art. 5, 177, 179 OPAn). Animals cannot be exposed to excessive noise for a long time (art.12 OPAn). Breeding of guinea pigs must aim at obtaining healthy guinea pigs (art.25 OPAn), and the keeper of animals must take appropriate measures to prevent guinea pigs from reproducing excessively (art. 25 para. 4 OPAn). Parks for livestock farming must be illuminated with natural light or a suitable artificial light, that must not be perceived by animals as flickering (annex 2 preliminary observation J OPAn). The minimum requirements for parks are the following (art.7, 10, annex 2 table 1 number 40 OPAn): they must not allow animals to escape and must not compromise their health; their dimensions must be adequate for the animals to perform the

typical ethogram of the species; they must be equipped with hiding places and present adequate bedding and object to gnaw, such as soft wood or freshly cut branches. The parks must comply with the minimum requirements according to Annex 2 of the ordinance on the protection of animals. A park for two guinea pigs must have a minimum area of 0.5 m<sup>2</sup>. For each additional animal, 0.2 m<sup>2</sup> must be added. For guinea pigs not intended for breeding, the ventilated rooms must have a minimum surface area of 3800 cm<sup>2</sup> for each detention unit, with a minimum height of 30 cm, and an area per animal of 350, 700 or 900 cm<sup>2</sup>, for animals weighing, respectively, less than 300 g, between 300 and 700 g, and more than 700 grams. Further specific detention requirements are the presence of an unperforated bottom with adequate bedding, such as dusted shavings, roughage such as hay or straw, gnawing items such as compressed fodder cubes or pieces of soft wood, and a hiding place with at least two entrances or with a longitudinal wall that allows all animals to withdraw at the same time. Guinea pigs that are kept outdoors must have access to a place that guarantees them protection from extreme weather conditions such as rain, humidity, wind, cold and direct sunlight (art.6 OPAn). It is forbidden to create and manage parks with guinea pigs accessible to the public during events (art. 24 letter f OPAn).

## ***Hydrochoerus hydrochaeris***

### **Taxonomy**

The taxonomic classification of the capybara is as follows (Linnaeus, 1766):

Kingdom: Animalia;

Subkingdom: Bilateria;

Infrakingdom: Deuterostomia;

Phylum: Chordata;

Subphylum: Vertebrata;

Infraphylum: Gnathostomata;

Superclass: Tetrapoda;

Class: Mammalia;

Subclass: Theria;

Infraclass: Eutheria;

Order: Rodentia;

Suborder: Hystricomorpha;

Infraorder: Hystricognathi;

Family: Caviidae;

Subfamily: Hydrochoerinae;

Genus: *Hydrochoerus*;

Species: *H. hydrochaeris*.

The history of the scientific nomenclature for the capybara is long and turbulent (Moreira et al., 2013). Recently, there has been great inconsistency in the genus name adopted and in its spelling. Much of the debate is due to uncertainty over which name takes historical precedence, but some variants seem to be the result of simple spelling errors (Moreira et al., 2013). However, it is to be emphasized that, as a general rule, the species should be referred to by the generic name *Hydrochoerus* (Brisson, 1762), and the species name *Hydrochoerus hydrochaeris* Linnaeus, 1766 (for the capybara, living east of the Andes) and *H. isthmius* Goldman, 1912 (for the lesser capybara, found west of the Andes). The lesser capybara (*Hydrochoerus isthmius*) of eastern Panama, northwestern Venezuela, and northern and western Colombia is recognized as a distinct species from *H. hydrochaeris* based on anatomical differences, particularly its smaller size, and on the basis of genetic studies (Peceño 1983; Mones; 1984; Mones and Ojasti, 1986). Unlike *H. hydrochaeris*, *H. isthmius*, is characterized by wider frontal bones in proportion to the total skull length, a proportionally larger lower diastema, and shorter and thicker pterygoids (Mones and Ojasti, 1986). *H. hydrochaeris* has a larger body mass, weighing 35 to 65.5 kg (Mones and Ojasti, 1986). According to some authors, the name that should be adopted for the capybara family is Hydrochoeridae (Vucetich et al., 2012). However, it is worth noting that most authors consider that the capybara is a member of the subfamily Hydrochoerinae within the family Caviidae (Rowe and Honeycutt 2002; Honeycutt 2013).

The common name of *Hydrochoerus hydrochaeris*, “capybara”, originates from a word in the indigenous Tupi language, which in the 16th century was the most widely spread language in South America: *kapii'gwara* meaning “grass eater” (Houaiss et al., 2001; Moreira et al., 2013).



*Hydrochoerus hydrochaeris*

## Origins

The capybara or greater capybara (*H. hydrochaeris*) is a cavy rodent native to South America and is considered to be the largest and heaviest living rodent (Moreira et al., 2013).

The genus *Hydrochoerus* has two species with distinct distributions. The lesser capybara – *H. isthmius* – is distributed to the west of the Andes, in Panama, Colombia and Venezuela. The larger species – *H. hydrochaeris* – is found east of the Andes, specifically Eastern Colombia, Venezuela, and the Guianas, the Amazonian Ecuador, Peru, Bolivia, Brazil, Paraguay, Uruguay and northeastern Argentina south to Queuén Chico River in the Buenos Aires Province. Chile is the only country in South America that has no capybaras, and Panama is the only Central American country where they are found (Mones and Ojasti, 1986). Both species inhabit a wide variety of lowland habitats near ponds, lakes, rivers, streams, reservoirs, and swamps, in regions with tropical or temperate climates and live in herds (Mones and Ojasti, 1986). These habitats include gallery forests, seasonally flooded savannas, and wetlands (Moreira and Macdonald, 1996). The maximum elevation recorded for the capybara is 1,500 m in the Chapada dos Veadeiros National Park, Goiás State, Brazil (Moreira, 1995).

*Hydrochoerus hydrochaeris* evolved in South America during the last 10 million years (Ojasti, 1973). It is a mammalian and herbivorous rodent, practically unknown in its ecology, behavior and biology until the 1960s, when several biological studies started to be carried out. The capybara is the largest native mammal that shares the ecological niche of the herbivore. Therefore, its function within the ecosystem is to transform plant biomass -grassland- into meat, that is, into animal biomass. Its effects on vegetation, nutrient circulation and energy supply to secondary biophages including man, can be considered as its fundamental role in savanna ecosystems (Ojasti, 1973; Sarango et al., 2011).

The New World hystricognath rodents (caviomorphs) to this day represent one of the most diverse and widespread suborders among the over 800 mammalian species of South America (Woods, 1982). Having been isolated from other rodents from the Oligocene to Miocene (some 50 million years), neotropical rodents evolved separately from those in other continents, and occupied a diversity of niches, especially those vacated following the extinction of notoungulates (Webb and Marshall, 1982). As a result, many contemporary species of hystricognaths are comparable in ecological and morphological terms to other terrestrial herbivores such as ungulates, macropods and lagomorphs (Dubost, 1968; Mares and Ojeda, 1982). Specifically, New World hystricognaths are generally more cursorial and larger in size than most rodents, and not burrowing (Moreira and Macdonalds, 1996). Consequently, the New World hystricognaths contain the majority of large extant rodent species (Dubost, 1988) and constitute an important component of the neotropical mammal fauna (Moreira and Macdonalds, 1996).

## History of domestication

Capybaras, which, to date, range throughout south american tropical wetlands, have been, over the years largely extirpated from their former habitats due to agricultural practices and poaching, and have adapted well to human management and conservation efforts and are frequently raised on ranches as valued sources of both meat and leather (Moreira et al., 2013).

The first descriptions of the species date back to the Iberian colonization of South America in the late fifteenth century: the early explorers encountered this diverse species characterized by an unusual anatomy and behavior, which led them to name the new-found endemic animals after the most analogous European species (Ojasti, 1973; Moreira et al., 2013). In 1576, for example, Pero de Gândavo (2004) described the capybara as “a type of pig.” However, capybaras were sufficiently unlike any known European species for most explorers to simply adopt a phonetic representation of the local name. Therefore, in 1557, the capybara was called *catiware* by the german Hans Staden (1557), *capiyûára* in 1560 by the spaniard José de Anchieta (1997), and *capijuara* in 1625 by the portuguese Fernão Cardim (1980). The name *capybara* actually originates from a word in the indigenous Tupi, which in the sixteenth century was the most widely spread language in South America: *kapii’gwara* meaning grass eater (*ka’pii* = “grass” + *gwara* = “eater”; Houaiss et al., 2001). The anglo-irish Oliver Goldsmith (1870), in 1774, listed the species as being among the “quadrupeds of the hog kind”. The first detailed description of the capybara by a naturalist came in the midseventeenth century from observations made in Pernambuco State, Brazil. The german naturalist Georg Marcgrave, which made up part of the scientific commission of the Dutch colony in northeastern Brazil, described the capybara, from a morphological, behavioral and ecological point of view, in the *Historia Naturalis Brasiliae* (1648), which is the reference used by all subsequent naturalists up to Linnaeus (Moreira et al., 2013).

Today, despite being protected in most countries, capybaras are hunted in South America for pest control or for meat, due to their favorable ecological features for agricultural domestication, such as fast growth rate, high reproductive rate, sociality and a cheap diet (Moreira and Macdonald, 1996). Local extinctions have occurred throughout their range over the years due to the high environmental pressures subsequent to the conversion of neotropical forest into grasslands; however, they are not considered an endangered species. Venezuela is the only south american country where capybaras are commercially harvested on a large-scale. Subsistence hunting of capybara is allowed in some forest districts of Peru, in some argentinean provinces, and in seasonally flooded savannahs along the brasilian Amazon Valley. In Colombia and Brazil, there exist ranches for the captive breeding of capybaras, although apparently not economically feasible (Moreira and Macdonald, 1996).



*Geographical distribution of the two principal subspecies of capybara: Hydrochoerus hydrochaeris and Hydrochoerus isthmus (from Ibáñez Orihuela et al., 2019)*

## Legislation

In Italy, since 1996, the possession of capybaras by private individuals is prohibited by law, as it is a species that is included in the Ministerial Decree Ministerial Decree 04/19/96 “List of animal species which may constitute a danger to public health and safety and whose detention is prohibited”, in annex A, for the protection of wild animals. All genera and species of the Hydrochoeridae family fall within the sphere of influence of the ban.

According to the Animal Protection Ordinance 455.1 of 23 April 2008, chapter 4 (“wild animals”), for the private detention of capybaras, a permit is required in accordance with chapter 4, section 2, Article 89 of the aforementioned Ordinance. Specifically, the parks must comply with the minimum requirements according to Annex 2 of the ordinance on the protection of animals. For groups of up to 5 animals a minimum area of 150 square meters is required in an outdoor park, of 20 square meters in an internal park. For each additional animal, it is necessary to add 10 square meters in the outdoor park, 2.5 square meters in the indoor park. Furthermore, the following requirements are necessary: the presence of screens to ensure the possibility of avoiding and withdrawing, the regular availability of fresh branches for the care of the teeth and for behavioral needs, and the possibility of bathing, through the use of basins of water of at least 6 square meters with a minimum depth of 0.5 meters for every 5 animals.



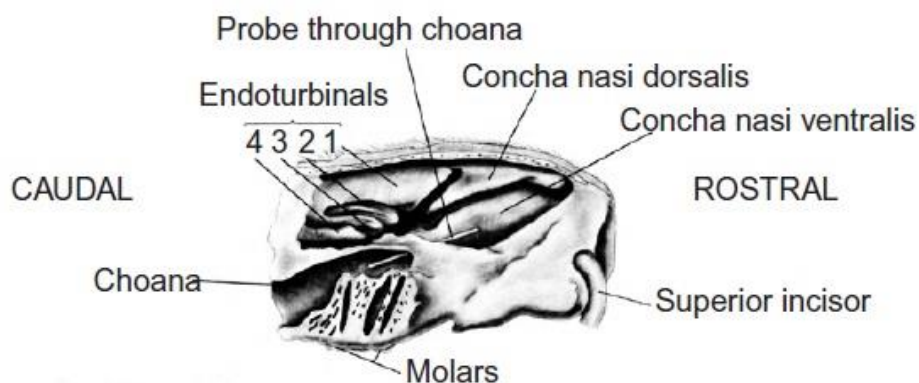
# GROSS AND MICROSCOPIC ANATOMY

## Respiratory system

### Nasal cavities

#### *Cavia porcellus*

The guinea pig is an obligate nasal breather (Nixon, 1974), with the nasal cavity extending from the nostrils to the choanae and bounded dorsally by the nasal bones, and latero-ventrally by the incisive and maxillary bones (Cooper and Schiller, 1975a). On cross section, the nasal cavity is T-shaped: it is broadened dorsally and gradually narrows down ventrally (Cooper and Schiller, 1975a). The cutaneous stratified squamous epithelium covers the external nasal orifices and the nasal vestibules (Breazile and Brown, 1976; O'Malley, 2005). The epithelium changes abruptly to a ciliated pseudostratified columnar epithelium with goblet cells within the nasal cavity (Breazile and Brown, 1976). The guinea pig lacks maxillary, frontal and sphenoid sinuses (Hargaden and Singer, 2012), although some sources refer to the maxillary recess as the maxillary sinus (Cooper and Schiller, 1975a). Guinea pigs have large and well-developed nasolacrimal ducts, located at the level of the lateral wall of the nasal cavity (Cooper and Schiller, 1975a). The nasal septum is characterized by a defect which allows the communication between the two nasal fossae; rostral to the ostium, is located the vomeronasal organ, involved in pheromone detection (Cooper and Schiller, 1975a; Hargaden and Singer, 2012). The caudodorsal wall of the nasal cavities of the guinea pig is lined by an olfactory epithelium that gives this species a developed sense of smell (Breazile and Brown, 1976; O'Malley, 2005). Each nasal fossa terminates caudally with the choanae which communicate with the nasopharynx (Cooper and Schiller, 1975a). The nasopharynx is relatively short and its floor is formed by the soft palate which is continuous with the base of the tongue (Cooper and Schiller, 1975a; Breazile and Brown, 1976). On the dorsolateral walls of the nasopharynx and dorsal to the soft palate are located the openings of the Eustachian tube (Hargaden and Singer, 2012).



*Guinea pig nasal cavity. Left lateral view after removal of the nasal septum. (from: Cooper and Schiller, 1975a)*

### ***Hydrochoerus hydrochaeris***

The nasal plane of the capybara lies dorsally in the head, due to its adaptation to a semi-aquatic life, and is divided by a semi-pointed philtrum, with the nostrils arranged laterally (Moreto et al., 2017). Externally, the capybara nasal cavity is supported by paired cartilages; internally, the rostral end of the nasal septum divides the nasal cavity into the right and left vestibules. The free margin of the nasal septum gives attachment to the cartilages that support the dorsal and lateral walls of the nostrils. Internally, each nasal vestibule extends from the nostril caudally to the nasal cavity, which is further divided into a right and left cavity by the nasal septum which joins the dorsal surface of the hard palate (Moreto et al., 2017). The largest portion of the nasal cavity is occupied by the spiral-shaped turbinates, with their respective meatuses (Moreto et al., 2017). A peculiarity of the endocranial morphology of caviomorphs, including capybaras, is the presence of a system of paranasal sinuses, which is rare among rodents, but that has been documented in hystricomorphs (Ferreira et al., 2022). The cavities of the paranasal sinus system are referred to as sinuses and recesses, and they are pneumatic cavities between two layers of cortical bones resulting from bone remodeling during ontogeny. Cranial pneumatization in capybaras is present in the frontal and lacrimal bones, originating the frontal sinus, the frontal recess and the lacrimal recess (Ferreira et al., 2022).



*Longitudinal section of a capybara head, showing the nasal septum (from: Moreto et al., 2017)*

## **Larynx**

### ***Cavia porcellus***

The larynx of the guinea pig is square-shaped and has the typical structure of that of other mammals: it is composed of five cartilages (epiglottis, thyroid, cricoid, and paired arytenoids) but the laryngeal ventricle is absent (Cooper and Schiller, 1975a; O'Malley, 2005). Despite their advanced vocalization ability, guinea pigs have poorly developed vocal cords (Breazile and Brown, 1976; Brewer and Cruise, 1997). The laryngeal cavity is composed of the vestibule, the glottis, and the infraglottis (Cooper and Schiller, 1975a). The laryngeal opening, caudal to the pharynx, is bound laterally by the right and left aryepiglottic folds, by the epiglottis ventrally and by the arytenoid cartilages dorsally (Hargaden and Singer, 2012). The palatal ostium lying

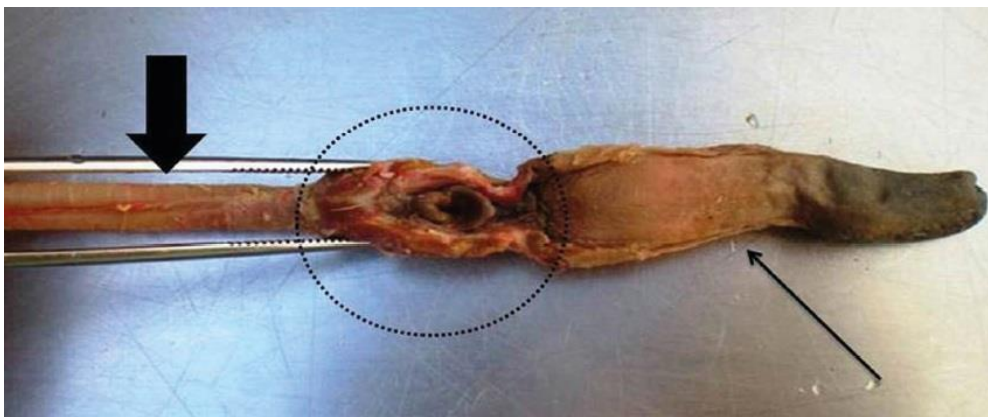
centrally is an aperture that forms the only connection between the oropharynx and the pharynx; around this ostium, folds of the soft palate, called the velopharyngeal recesses are present, which can be damaged during an inaccurate endotracheal intubation in this species (Timm et al., 1987; O'Malley, 2005)

### ***Hydrochoerus hydrochaeris***

The larynx of the capybara is bounded by cartilage, it is short and conical in shape, and is located ventrally in the neck, in communication with the trachea ventrocaudally (Moreto et al., 2017).

The larynx is formed by four cartilages: the cricoid, the thyroid, the arytenoid (with a cuneiform and a corniculate processes) and the epiglottis. Structurally, the laryngeal cartilages are hyaline and elastic (Moreto et al., 2017). The epiglottic cartilage of capybaras is leaf-shaped, has a sharp free edge, and its base is fixed onto the thyroid cartilage. Histologically, the epiglottis is composed of elastic fibers (Moreto et al., 2017). The thyroid cartilage is constituted, ventrally, by a body, and, laterally, by two rectangular laminae. The thyroid is composed of hyaline fibers (Moreto et al., 2017). The arytenoid cartilage is inserted onto the cranial extremity of the cricoid cartilage. It consists of two processes: the corniculate (cranial) and the cuneiform (caudal) processes. Histologically, the arytenoid cartilage is predominantly hyaline (Moreto et al., 2017). The cricoid cartilage has the appearance of a complete ring located at the caudal end of the larynx, with an expanded dorsal lamina and a narrower ventral arch; histologically, it has a hyaline structure (Moreto et al., 2017).

Histologically, the larynx is mostly lined by a respiratory epithelium (Junqueira & Carneiro 2004; Moreto et al., 2017). A non-keratinized stratified squamous epithelium lines the surface of the vocal cords and epiglottis (Moreto et al., 2017). The submucosa of the larynx is composed of loose connective tissue, harboring defense cells, diffuse lymphatic tissue, sparse lymph nodes and mixed glands in some regions (Samuelson, 2007).



***Trachea*** (bold arrow), ***larynx*** (dotted circle) and ***tongue of a capybara***. Dorsal view (from: Moreto et al., 2017)

## **Trachea**

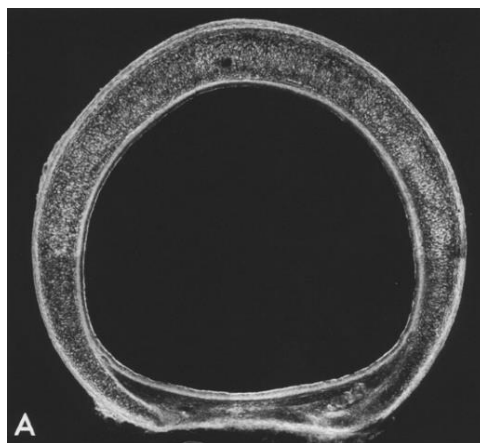
### ***Cavia porcellus***

The trachea of guinea pigs is composed of 35 to 40 cartilaginous tracheal rings joined dorsally by annular ligaments (Cooper and Schiller, 1975a). A ciliated pseudostratified columnar epithelium lines the trachea (Breazile and Brown, 1976), with the proportion of ciliated cells gradually decreasing distally until the terminal bronchi, which present only 15%

of ciliated cells (Rhodi, 1959). The trachea stems into the primary bronchi at the level of the third rib (Breazile and Brown, 1976). The right primary bronchus is shorter and wider than the left (Cooper and Schiller, 1975a). Similarly to other rodents, all intrapulmonary airways are bronchioles branching directly from the primary bronchi (Brewer and Cruise, 1997); the bronchioles, in turn, give rise to the respiratory bronchioles with alveoli (Hargaden and Singer, 2012). A peculiarity of the guinea pig is that the distal bronchi have a very prominent smooth muscle, which is arranged in a spiral manner (Brewer and Cruise, 1997). The trachea is well innervated; however, the smaller airways are characterized by little to no innervation (O'Donnell et al., 1978). Guinea pig airways are highly sensitive to histamine, showing early and late allergic reactions, and their bronchi are more sensitive to constriction by acetylcholine compared to other species (Brewer and Cruise, 1997; Hargaden and Singer, 2012).

A comparative anatomic-topographic and morphometric study of the main, lobar and segmental bronchi of the rabbit, guinea pig and ferret (Tagliavia, 2014) has shown, in the guinea pig, the bronchial, arterial and venous pulmonary architecture described below. The main left and right bronchi arising from the tracheal bifurcation extend caudally into the hilum of the left and right lungs, respectively. The right main bronchus immediately emits the right cranial lobar bronchus, then detaching the middle lobar bronchus, and finally continues as the right caudal lobar bronchus, which gives rise to the accessory bronchus.

The left main bronchus, shortly after the tracheal bifurcation, emits the left cranial lobar bronchus and then continues as the left caudal lobar bronchus. The pulmonary arteries throughout their course remain in close connection with their respective bronchial branches, in a lateral position with respect to the corresponding bronchus. The pulmonary veins are localized on the medial side of the respective bronchi, but do not maintain a close relationship with them. The diameters of the bronchi and satellite vessels at the level of the right lung are comparable, while at the level of the left lung the bronchi are smaller than the respective vessels. The pulmonary arteries of the right lung are larger in diameter than the veins, whereas, in the left lung, the opposite is true. The aforementioned study also highlighted, contrary to what has been reported in the literature (Schlesinger and McFadden, 1981), a dichotomous organization of the bronchial ramifications of the guinea pig, instead of a monopodial organization (Tagliavia, 2014).



*Guinea pig trachea* (frozen section). Transversal section of distended cervical trachea (from: Amiri and Gabella, 1988)

### ***Hydrochoerus hydrochaeris***

The trachea of the capybara is a flexible, cartilaginous, and membranous tube, formed by incomplete C-shaped tracheal rings connected by ligaments, which extends from the cricoid cartilage of the larynx and terminates distally by bifurcating into the tracheal carina (Moreto et

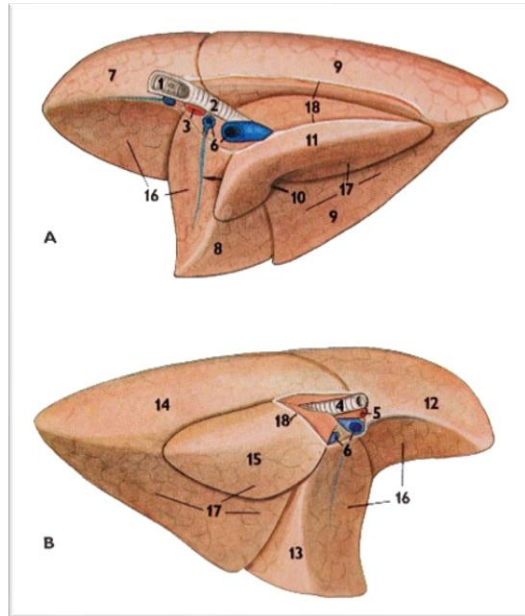
al., 2017). It has been reported that the number of tracheal rings ranges from 35 to 46 (Moreto et al., 2017). The tracheal rings are incomplete and joined to each other by smooth muscle tissue. Internally, the trachea is lined by a respiratory epithelium. Structurally, the tracheal wall is composed of hyaline cartilage, a muscular layer on its dorsal surface and, finally, an adventitious layer of connective tissue (Moreto et al., 2017).

## Lungs

### *Cavia porcellus*

Since the heart of the guinea pig occupies a relatively large portion of the thorax, it leaves a narrow space for the lungs on each side (O'Malley, 2005). The guinea pig lungs are polylobed and proportionally voluminous (Cozzi et al., 2006). The right lung is the most developed and extends to the eighth rib (Cozzi et al., 2006). It consists of four lobes (cranial, middle, accessory and caudal), each separated by deep fissures, with the cranial lobe being the smallest in size and the caudal lobe being the largest and extending to the eighth rib. The right middle lobe has a concave cardiac impression on its medial surface, whereas the right caudal lobe has a concave diaphragmatic surface; the accessory lobe is irregularly-shaped with a ventral notch for the caudal vena cava and a concave diaphragmatic surface (O'Malley, 2005; Cozzi et al., 2006; Hargaden and Singer, 2012). The left lung, on the other hand, not as developed as the right, is composed of three lobes: cranial, middle and caudal (Brezile and Brown, 1976; O'Malley, 2005). The left cranial lobe is divided into a smaller cranial segment and a larger caudal segment by an intralobar fissure, and its medial surface is concave to accommodate the heart (Cooper and Schiller, 1975a; Orti et al., 2004). The left middle lobe is small and has a medial notch for the oesophagus and a concave diaphragmatic surface. The left caudal lobe is large and its concave medial border is in contact with the middle lobe (Cooper and Schiller, 1975a; Hargaden and Singer, 2012). Because of the lack of intralobular septa in the lungs, an extensive collateral ventilation is possible in this species, due to a communication between the two pleural hemicavities (Cozzi et al., 2006). The respiratory bronchioles give rise to the terminal sacs with alveolar outpockets, where alveolar development is nearly complete at birth in this species (Brewer and Cruise, 1997; Hargaden and Singer, 2012). Because of their peculiar respiratory physiology, guinea pigs have been used as experimental animal models for lung function impairment and airway hyperresponsiveness (Hargaden and Singer, 2012). Some peculiarities of the guinea pigs, in contrast to other species, such as rats, mice and rabbits (Doidge and Satchel, 1982), is the sympathetic innervation of the trachealis muscle causing it to relax; moreover, highly sensitive mechanoreceptors present in the upper airways cause laryngeal spasm in response to mechanical stimuli such as endotracheal intubation (Hargaden and Singer, 2012). Furthermore, in contrast to mice and rats, guinea pig airways are sensitive to histamine, showing early and late allergic reactions (Hargaden and Singer, 2012).

Regarding the cellular population of the respiratory system, it is characterized by numerous fibroblasts secreting anti-inflammatory cytokines, endothelial cells at the level of the pulmonary capillary bed, numerous goblet cells in the upper tract, non-ciliated Clara cells (only at the bronchiolar level), and brush cells (Brewer and Cruise, 1997). At the alveolar level, type I cells (respiratory alveocytes) and type II cells (large pulmonary surfactant-secreting alveocytes, protecting from oxidative stress), endothelial cells, interstitial cells, macrophages and many neutrophils that play a role in the phagocytosis of intravascular foreign bodies (Brewer and Cruise, 1997). There are also mast cells associated with abundant pleural smooth muscle (Brewer and Cruise, 1997) and many eosinophils in the loose connective tissue at the subepithelial lamina propria level of the respiratory tract (Hudson, 1968).



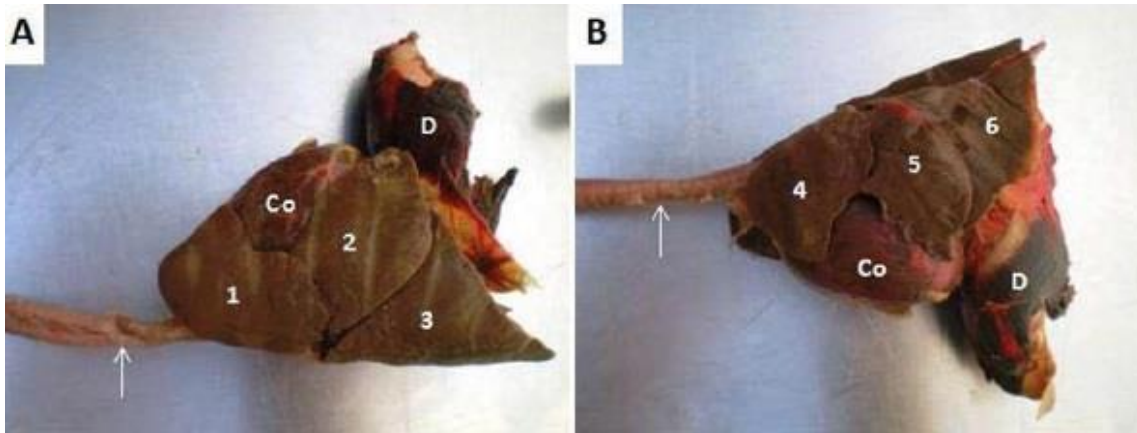
**Guinea pig right (A) and left (B) lungs, medial view.** 4: trachea; 5: pulmonary artery; 6: pulmonary veins; 7: right cranial lung lobe; 8: right middle lung lobe; 9: right caudal lung lobe; 10: 11: right accessory lung lobe; 12-13: cranial and caudal portions of left cranial lung lobe; 14: left caudal lung lobe; 15: left accessory lung lobe; 16: cardiac impression (from: Popesko et al., 1992).

### ***Hydrochoerus hydrochaeris***

Each lung is covered by a serous membrane, the pleura, and divided by deep fissures into well demarcated lobes (Moreto et al., 2017). The right lung of the capybara has four lobes (cranial, middle, caudal and accessory, the latter divided into a medial and a lateral portions by the accessory intralobar fissure). An interlobar notch is present between the cranial and middle lobes, and an interlobar fissure divides the right middle lobe from the caudal. The left lung is bilobated, presenting a cranial and a caudal lobes, separated by an interlobar fissure. The left cranial lung lobe is further divided, by the cranial intralobar notch, into a cranial and a caudal portions (Moreto et al., 2017).

The bronchial tree consists of the tracheal carina bifurcating into the left and right extrapulmonary primary bronchi. These then give rise to the intrapulmonary bronchi, bronchioles, terminal bronchioles and respiratory bronchioles eventually subdividing into alveolar ducts and sacs made up of several alveoli (Moreto et al., 2017).

The mucosa of the bronchi is the same as the one that lines the trachea (respiratory epithelium), gradually turning into a simple ciliate cylindrical epithelium at the level of the bronchioles and smaller branches and becoming a simple cubic epithelium in the final portions. Structurally, the bronchial wall is cartilaginous and surrounded by connective tissue rich in elastic fibers. The bronchioles, on the other hand, do not present a cartilaginous component (Moreto et al., 2017).



*Capybara* right (A) and left (B) lungs, lateral view. 1. cranial right lung lobe; 2. middle right lung lobe; 3. caudal right lung lobe; 4: cranial portion of the left cranial lung lobe; 5: caudal portion of the left cranial lung lobe; 6: caudal left lung lobe (from: Moreto et al., 2017).

## Digestive system

### Buccal cavity

#### *Cavia porcellus*

The entire alimentary tract of guinea pigs, from pharynx to anus, is 2.3 meters long (Jilge, 1980; Hargaden and Singer, 2012).

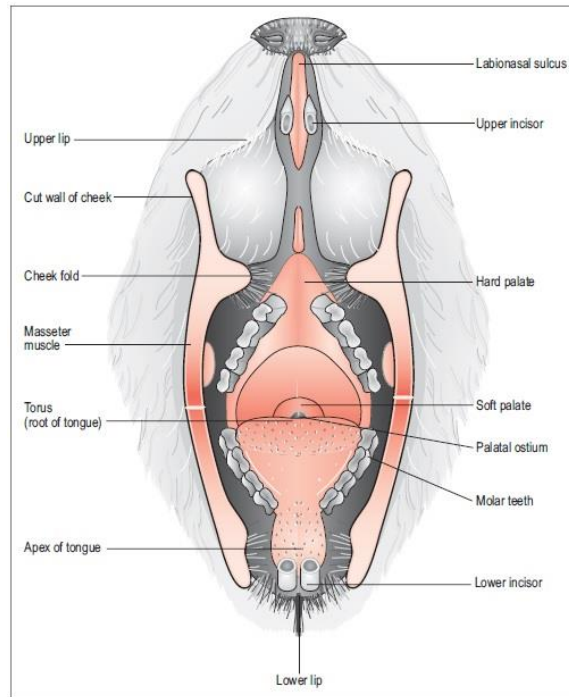
The oral cavity of the guinea pig is small and is occupied by a large and elongated tongue (O'Malley, 2005). The lateral walls of the oral cavity are composed of buccal pads and bristle areas (Hargaden and Singer, 2012). The buccal pads are the upper and lower cheek folds which project inwards during gnawing and divide the buccal cavity into two different regions, separating the incisors from the molar teeth (O'Malley, 2005). The bristle areas are small circular flaps covered by hair which are located in the middle of the diastema (Cooper and Schiller, 1975b). Cheek pouches are absent in guinea pigs (Hargaden and Singer, 2012). Salivary glands are present and the oral cavity communicates caudally with the pharynx (O'Malley, 2005). The mastication muscles are well developed, demonstrating the gnawing and grinding masticatory behavior of the species (Breazile and Brown, 1976).

The guinea pig has five pairs of salivary glands: the parotid, the mandibular, the zygomatic, and the major and minor sublingual glands, with the paired mandibular glands coming into contact with each other ventrally on the midline (Quesenberry et al., 2004). The salivary ducts open into the oral cavity at the level of the molar teeth (O'Malley, 2005).

The nasopharynx and oropharynx are separated by the soft palate, with the palatal ostium being the only communication with the oral cavity (Timm et al., 1987).

Tonsils are absent in guinea pigs however, lymphoid nodules are incorporated inside folds located in the pharynx wall (O'Malley, 2005).

Due to the unique structure of the pharynx, oral gavage and endotracheal intubation can be challenging in guinea pigs (Hargaden and Singer, 2012).



**Guinea pig oral cavity.** Section of the buccal structures (from: O'Malley, 2005)

### ***Hydrochoerus hydrochaeris***

The mouth of the capybara presents highly labile lips and is located in the lower front part of the box-shaped cranium, so as to have the mouth and teeth directly in contact with the ground when grazing, which proves useful especially when the grass is short and the food is scarce (Ojasti, 1973; Herrera, 2013)

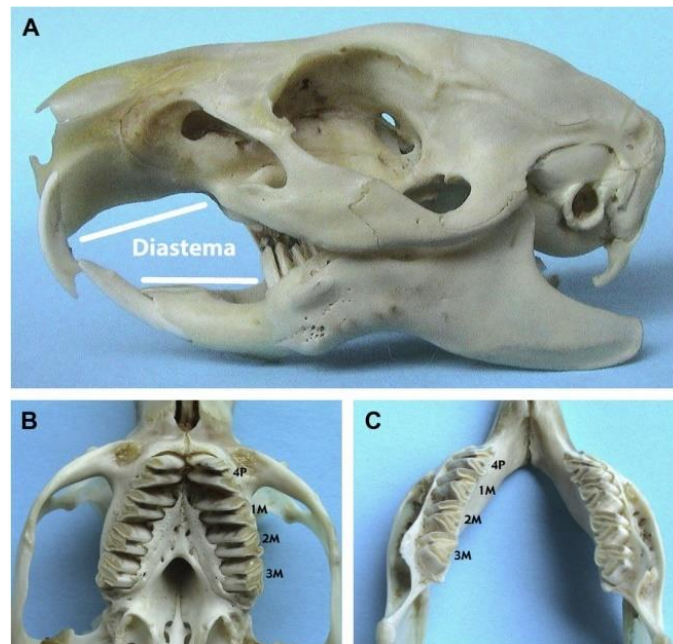
The oral cavity of the capybara communicates, posteriorly, with the pharynx through a well developed and extended soft palate (*velum palati*) which becomes constricted and forms a funnel-shaped palatal ostium that is attached to the whole circumference of the fauces and the root of the tongue, and is surrounded by a sphincter muscle and by posterior muscular pillars (Ojasti, 1973; Mones and Ojasti, 1986). As in guinea pigs, the oral opening is proportionally narrower than in other domestic species such as carnivores (Legendre, 2016).

## **Teeth**

### ***Cavia porcellus***

The total dental formula of guinea pigs is 20: I 1/1, C 0/0, P 1/1, M 3/3, with a diastema between incisors and cheek teeth (O'Malley, 2005). All teeth are aradicular and characterized by a continuous growth, causing frequent malocclusion in both molar and incisor teeth (O'Malley, 2005). Incisors are white and chisel-shaped (O'Malley, 2005). The maxillary molariforms are laterally oriented, whereas the mandibular cheek teeth arch medially toward the tongue, causing tongue entrapment in case of molar malocclusion (Breazile and Brown, 1976; O'Malley, 2005). Unlike the capybara, the rostral portion of the mandible is more dorsally angled, the row of teeth is convex, the ramus of the mandible is thin and the mandibular condyle is cranially protruding (Cherem and Ferigolo, 2012).





**Dentition of the guinea pig.** A: lateral view of the skull; B: Ventrodorsal view of the maxilla; C: dorsoventral view of the mandible displaying the cheek teeth. 4P: premolar; 1M: first molar; 2M: second molar; 3M: third molar (from Legendre, 2016).

### ***Hydrochoerus hydrochaeris***

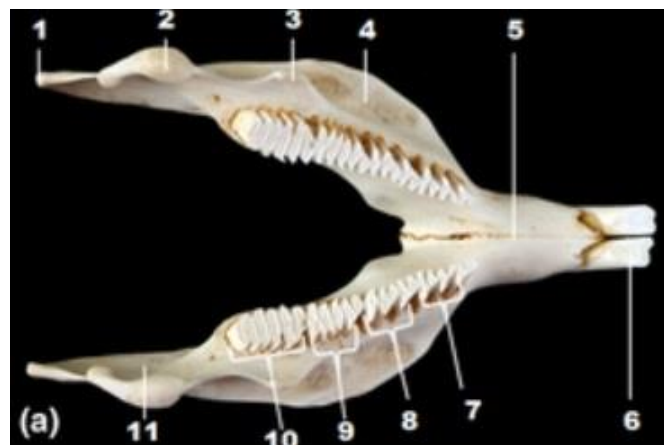
The adult dental formula of the capybara, as in other caviomorpha, is 20 teeth: I 1/1, C0/0, P 1/1, M3/3 (Pereira et al., 2020). As in guinea pigs and hystricomorph rodents, being herbivorous rodents, the teeth of the capybara are all elodont, with large chewing surfaces adapted to a more voluminous abrasive diet (Pereira et al., 2020). The large and sharp incisors are separated from the molariforms by a large diastema (Herrera, 2013). Mandibular and maxillary incisors produce a scissor-like effect for efficient cropping of grasses (Herrera, 2013). All teeth grow continually to compensate for the wear occurring due to prolonged gnawing (Legendre, 2003). Due to the convoluted pattern of the teeth enamel, associated with the strong mandibular musculature and the antero-posterior movements of the jaws, capybaras can grind grasses down to very small particles (Herrera, 2013).

The upper third molar presents an occlusal surface that corresponds to the sum of the length of the upper premolar and of the first and second molars (Pereira et al., 2020). Incisors are antero-medially grooved; cheek teeth are composed of cordiform or lamellar prisms separated by cement layers. Incisors are broader in adult males than in adult females (Ojasti, 1973; Mones and Ojasti, 1986).

Unlike guinea pigs, capybaras have a trapezoidal mandible, with a bulging angular process, and the upper third molars are much more developed than the other molariform teeth, which is associated with their herbivorous diet (Bode et al., 2013; Pereira et al., 2020).



**Ventral view of the capybara skull.** 13. upper incisor; 14. incisive bone; 15. interincisive foramen; 16. palatine fissure; 17. vomer; 18. maxilla; 19. palatine crest; 20. palatine bone; 21. presphenoid; 22. pterygoid; 23. basisphenoid; 24. occipital condyle; 25. foramen magnum; 26. upper premolar; 27. upper first molar; 28. upper second molar; 29. upper third molar; 30. mandibular fossa; 31. caudal alar foramen; 32. foramen lacerum; 33. tympanic bulla; 34. paracondylar process of occipital (from Pereira et al., 2020)

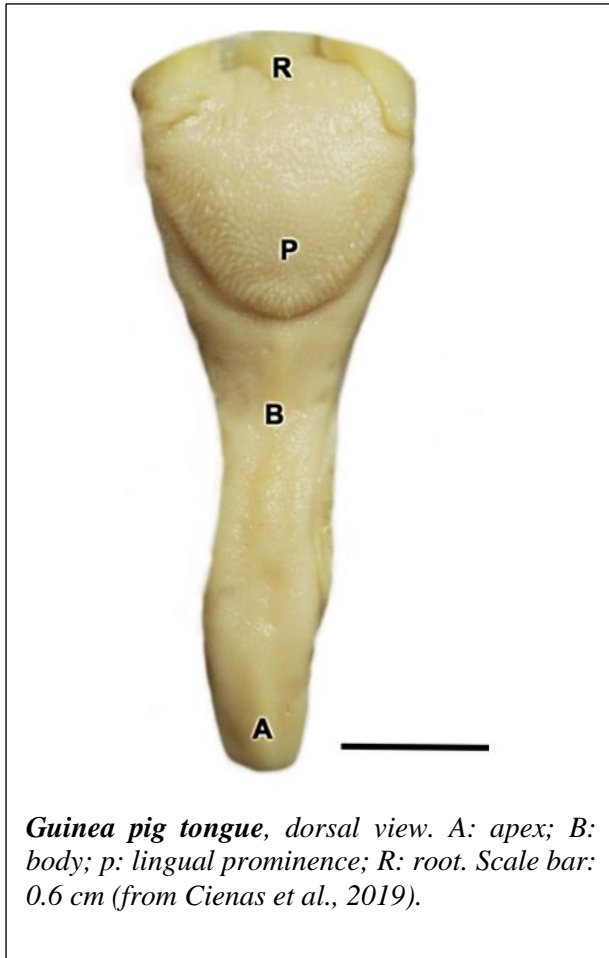


**Dorsal view of the capybara mandible.** 1. Angular process; 2. condyloid process; 3. coronoid process; 4. masseteric fossa; 5. mandibular symphysis; 6. lower incisor; 7. lower premolar; 8. lower first molar; 9. lower second molar; 10. lower third molar; 11. pterygoid fossa (from Pereira et al., 2020)

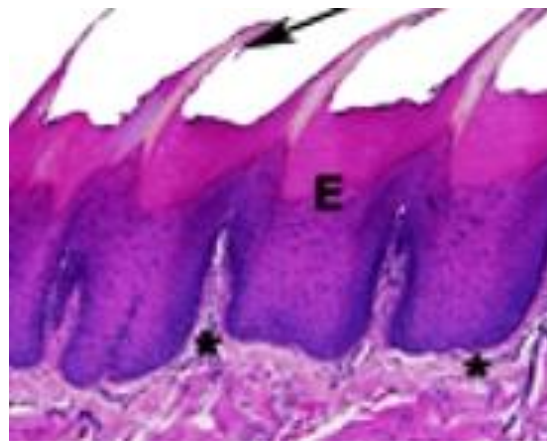
## Tongue

### *Cavia porcellus*

The tongue of guinea pigs is voluminous and elongated, and occupies most of the floor of the oral cavity and oropharynx, and is bounded laterally by the mandible (O'Malley, 2005). The average rostrocaudal length of the tongue is 3.5 cm and is composed of three parts: an apex, a body and a root (Cienas et al., 2019). The apex is rounded and lacks a median sulcus; the body is wider and features a lingual prominence in proximity to the molar teeth; the root, caudally, is the most voluminous section (Cienas et al., 2019). A distinguishable lingual frenulum is not always present (Brezile and Brown, 1976). Four types of papillae, namely filiform, fungiform, foliate and vallate on the dorsal surface of the tongue have been identified (Cienas et al., 2019).



Filiform papillae are distributed throughout the total extension of the tongue surface; fungiform papillae are less numerous and with a more heterogeneous distribution; foliate papillae are well-developed, located on the caudal region bilaterally and organized in in five pairs of parallel folds; two parallel vallate papillae are found close to the tongue root. These are well developed and consisting in a specialized structure consisting in a double epithelial projection with a columnar aspect, that is not found in other similar species (Cienas et al., 2019). The caudal third of the tongue is characterized by a mound composed of extensive papillae (Cooper and Schiller, 1975b). The base of the tongue, caudally, is continuous with the soft palate, covering most of the back of the throat, except for a small central opening, the palatal ostium, which forms the only connection between the oropharynx and the pharynx (Timm et al., 1987; O'Malley, 2005). The palatal ostium has also been referred to as the intrapharyngeal ostium, which is also observed in other hystrycomorph rodents such as chinchillas and capybaras (Hargaden and Singer, 2012).

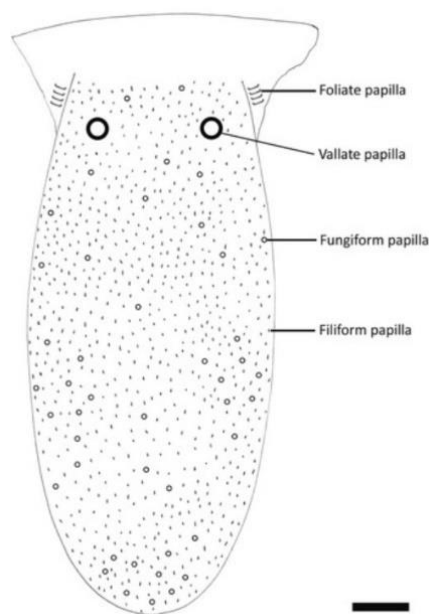


**Histological aspect of the guinea pig tongue. Long filiform papillae (arrow) with a thick epithelium (E) and thin lamina propria (\*) (from Cienas et al., 2019)**

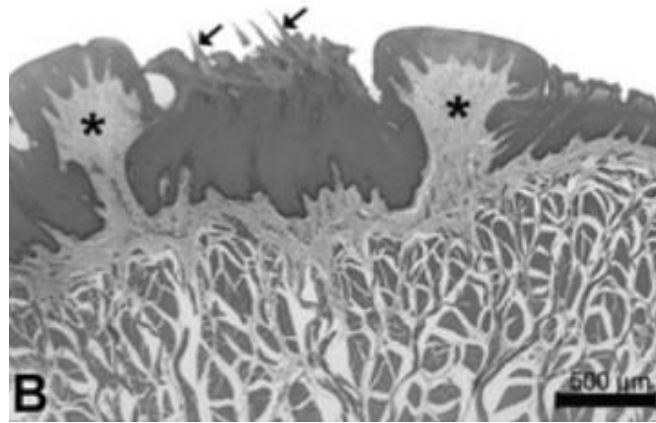
### ***Hydrochoerus hydrochaeris***

The capybara tongue is elongated along its antero-posterior axis and rounded at the anterior extremity. The anterior part is narrow, whereas the posterior part is broader, and covered by a pair of circumvallate papillae (Mone and Ojasti, 1986). Histologically, the epithelium of the tongue of the capybara is a keratinized stratified squamous epithelium, including basal cells

and corneal cell types and a thick keratin layer (Watanabe et al., 2013). The dorsal mucosa of the capybara tongue, with the exception of the root of the tongue, is composed of filiform, fungiform, vallate and foliate papillae. Filiform papillae are densely distributed over the whole surface of the tongue body, but mostly on the apex and lateral edges of the central third of the tongue. Foliate and vallate papillae are present mostly on the posterior third of the dorsal mucosa of the tongue, with the foliate being located on the lateral surface, and the vallate on the dorso-posterior surface. The epithelial layer consists of a lining of keratinized stratified squamous epithelial cells. The lamina propria is characterized by dense connective tissue presenting primary and secondary papillar projections. Pyriform taste buds occupying the epithelial layer of fungiform, vallate and foliate papillae are characterized by granular endoplasmic reticulum throughout the perinuclear area, the Golgi apparatus and mitochondria (Watanabe et al., 2013)



*Schematic overview of the dorsal surface of the capybara tongue, showing the distribution of the different types of papillae found on the tongue surface. Scale bar: 10 mm (from: Watanabe et al., 2013)*



*Photomicrograph showing features of fungiform papillae (\*) and adjacent filiform papillae (arrows). Azo-Carmine staining. 300x (from Watanabe et al., 2013)*

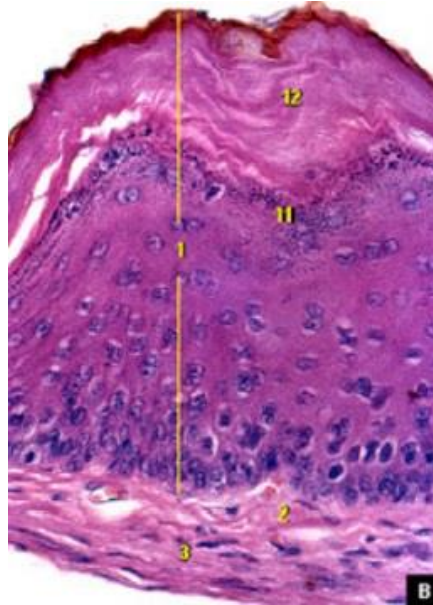
## **Oesophagus**

### ***Cavia porcellus***

The oesophagus runs on the median plane dorsal to the trachea, whereas it is displaced towards the left at the entrance of the thoracic inlet (O'Malley, 2005). The oesophagus of guinea pigs is lined by a stratified squamous epithelium. It is composed of striated muscles at its proximal extremity, by smooth muscle more distally. It enters the stomach through the cardia near the lesser curvature at an oblique angle, forming the so-called angular notch with the stomach (Cooper and Schiller, 1975b; O'Malley, 2005).

### ***Hydrochoerus hydrochaeris***

Anatomically, the oesophagus of the capybara can be divided into three regions: a cranial, a middle and a caudal portions (Carrascal Velasquez et al., 2016). Macroscopically, the union of the terminal portion of the oesophagus with the gastric fundus gives rise to a cardiac incisure (de Barros Moraes et al., 2002). The lumen of the oesophagus is covered with a keratinized longitudinal folded membrane, adapted to allow the passage of abrasive fibers (Herrera, 2013; Mones and Ojasti, 1986). Histologically, all three oesophageal regions are lined with a keratinized stratified epithelium, which tends to be thicker at the apex of the oesophageal folds as well as in its terminal part, proximal to the stomach. The caudal region presents a well-developed stratum granulosum. The submucosa, composed of loose connective tissue, does not present any glands. The muscular layer is covered, externally, by a serous and/or adventitious layer, and its fibers present a circular and a longitudinal orientations in all three regions. The muscular layer, moreover, consists of striated skeletal muscle fibers with a well-developed nervous plexus (Carrascal Velasquez et al., 2016).

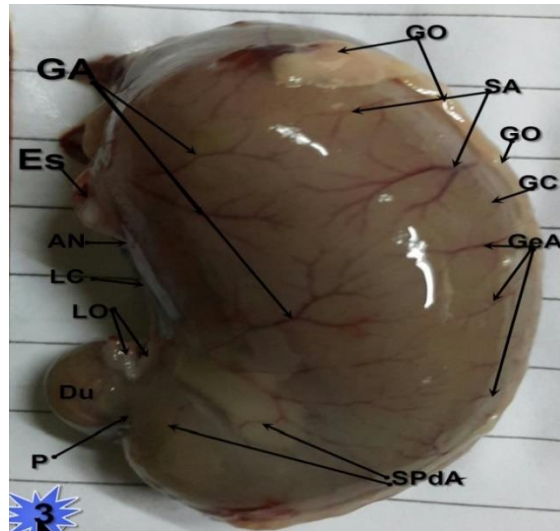


**Photomicrograph of the oesophagus of the capybara.** Longitudinal section of the caudal region of the oesophagus. 1: epithelium; 2: lamina propria; 3: lamina muscularis; 4: submucosa; 11: granular stratum; 12: keratin. H-E stain. 400x (from Carrascal Velasquez et al., 2016).

## Stomach

### *Cavia porcellus*

Guinea pigs are monogastric and have a completely glandular stomach, unlike other rodents (Harkness et al., 2002; O'Malley, 2005). The stomach is topographically located in the left cranial abdomen and comes in contact with the left lobe of the liver and the small intestine (Breazile and Brown, 1976). The stomach has a smooth mucosa and it comprises four regions which are the cardia, the fundus, the body and the pylorus (Breazile and Brown, 1976; Hargaden and Singer, 2012). Its lesser curvature, poorly developed, forms a so-called angular notch with the oesophagus (O'Malley, 2005). The fundus of the stomach consists of a large pouch located to the left and cranial to the cardia; the body of the stomach lies to the right of the fundus and ends in the thick-walled pylorus, which consists, internally, of longitudinal folds (Cooper and Schiller, 1975b; Breazile and Brown, 1976). Similarly to other species, the greater and lesser omentum extend from the stomach (Cooper and Schiller, 1975b). The major muscular component of the guinea pig stomach is a continuous layer of circular musculature extending from the greater curvature to the lesser curvature, with the external longitudinal layer being completely absent at the level of the lesser curvature (de Barros Moraes et al., 2005). The gastric emptying time in guinea pigs is 2 hours with the gastrointestinal transit time being approximately 20 hours total (Jilge, 1980).



**Guinea pig stomach:** parietal surface. AN: angular notch; Du: duodenum; Es: oesophagus; GA: gastric artery; GeA: Gastroepiploic artery; GO: greater omentum; GC: greater curvature; LC: lesser curvature; LO: lesser omentum; P: pylorus; SA: splenic artery; SPdA: superior pancreaticoduodenal artery (from Abd AL-Rhman, 2016)

### ***Hydrochoerus hydrochaeris***

Macroscopically, the stomach of the capybara consists of five portions: the cardiac portion, the fundus, the gastric diverticulum, the body and the pylorus (de Barros Moraes et al., 2002).

It can be classified as a simple stomach (monogastric), entirely glandular, in the form of an “inverted J-shaped” curved sack (de Barros Moraes et al., 2002). It presents a greater and a lesser curvature measuring on average, 38.8 cm and 5.4 cm in length, respectively (de Barros Moraes et al., 2002). The transversal and longitudinal diameters of the stomach of the capybara measure 11.02 and 18.23 cm in length, respectively (de Barros Moraes et al., 2002). Externally, it is characterized by the presence of gastric bands (teniae) that vary in number from 2 to 3: two large gastric teniae, located on the parietal face and on the visceral face in proximity of the greater curvature, and, in some animals, a third smaller gastric tenia exists on the parietal face of the organ in proximity of the lesser curvature, which delimits small outpouchings called haustras (de Barros Moraes et al., 2002). Where the terminal portion of the oesophagus meets the gastric fundus, a cardiac incisure forms; in addition, at the level of the lesser curvature, an angular incisure occurs besides the well-demarcated pyloric antrum (de Barros Moraes et al., 2002).

A cranial expansion of the gastric fundus is located to the left of the median plane, known as the gastric diverticulum (de Barros Moraes et al., 2002).

The average gastric volumetric capacity of the capybara is 1498.6 ml (850-2010 ml) (de Barros Moraes et al., 2002).

The gastric mucosa is demarcated by numerous and tortuous longitudinal gastric folds all along its extension, from the cardiac to the pyloric portions (de Barros Moraes et al., 2002).

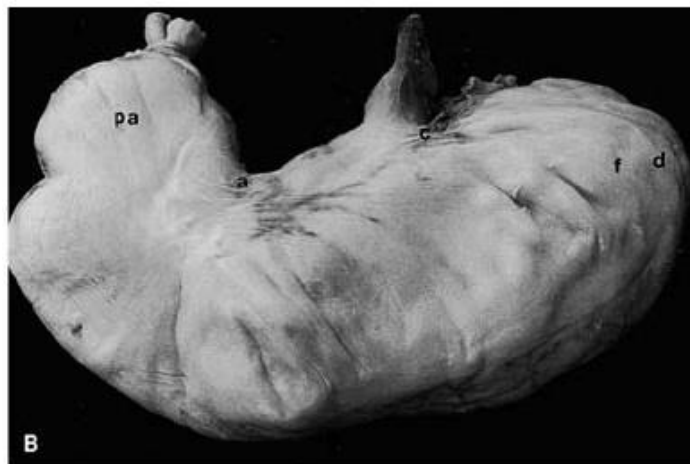
The mucous tunic is also characterized by several recesses located between successive gastric folds, described as gastric areas, where numerous openings occur, the so-called gastric pits, representing the openings of the gastric glands (de Barros Moraes et al., 2002).

Histologically, the mucous tunic is composed of a simple prismatic epithelium, a lamina propria that in some areas bulges out from the interior of the epithelium, and a well-developed muscular tunic of the mucosa. The tunica submucosa is well developed and distinguishable and

containing numerous arterioles and venules. The muscular tunic consists of a longitudinal stratum, an external oblique stratum, a circular stratum and an internal oblique stratum. The serous tunic is composed of loose connective tissue and a simple squamous epithelium (de Barros Moraes et al., 2002).

As far as the muscular organization of the stomach is concerned, the internal oblique fibres, together with the external longitudinal fibers, extend from the cardiac portion of the stomach to the lesser curvature and participate in the formation of the so-called Ansa cardiaca (de Barros Moraes et al., 2005), differing therefore from the arrangement seen in most domestic animals, where the internal oblique fibers alone contribute to the formation of the Ansa cardiaca (Nickel et al., 1979; Getty, 1982). Unlike the muscular organization of the stomach of guinea pigs, the circular muscular layer of the stomach of capybara does not extend to the greater curvature; conversely, unlike guinea pigs, the external longitudinal layer is present in both the greater and lesser curvatures (de Barros Moraes et al., 2005).

From a cytological point of view, a simple prismatic glandular epithelium lines all the gastric regions. Specifically, the cardiac portion of the stomach is lined with a glandular epithelium with cardiac glands containing parietal acidophilus cells and mucous cells located at the neck of the cardiac glands (de Barros Moraes et al., 2002). The fundus, body and gastric diverticulum are lined with gastric glands containing main (pepsinogenic), parietal and mucous neck cells inside the glandular epithelium. The lamina propria of the gastric diverticulum emits septa towards the glandular epithelium, whereas the muscular tunic of the mucosa of the gastric diverticulum has an enlarged appearance (de Barros Moraes et al., 2002). The gastric diverticulum, moreover, is characterized by enteric neurons with eccentric nuclei located in the submucosa, comprising the submucous plexus. Finally, the gastric pylorus is characterized by pyloric glands containing mucous neck cells and parietal cells (de Barros Moraes et al., 2002).



*Capybara stomach, parietal face. a: angular incisure; c: cardiac incisure; f: gastric fundus; d: gastric diverticulum; pa: pyloric antrum (from: de Barros Moraes et al., 2002)*

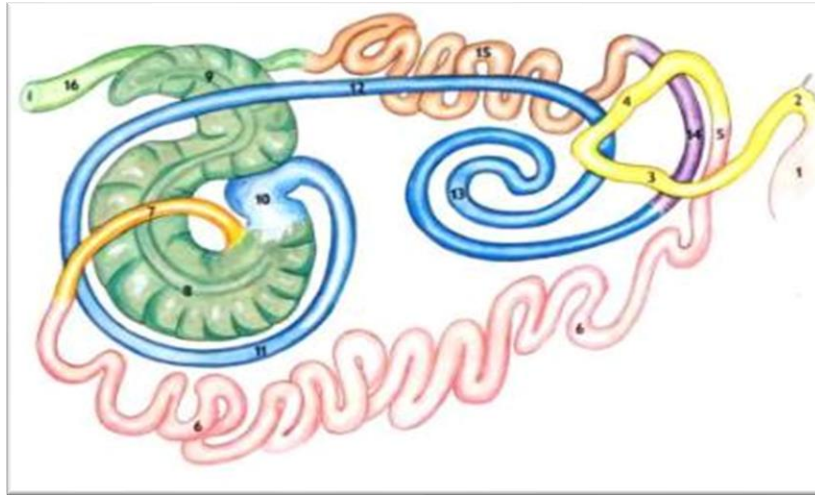
## **Small intestine**

### ***Cavia porcellus***

The small intestine of the guinea pig is the longest portion of the alimentary tract, measuring about 125 cm in length, and lies on the right side of the abdominal cavity (Breazile and Brown, 1975b; O'Malley, 2005). The duodenum, the jejunum and the ileum are not distinguishable macroscopically (Breazile and Brown, 1976; Hargaden and Singer, 2012). The



duodenum is the shortest (10.12 cm long), while the jejunum is the longest (95 cm long), whereas the ileum measures about 10 cm (Cooper and Schiller, 1975b). The ileum enters the cecum at the ileocecal papilla (Hargaden and Singer, 2012). Peyer lymphoid patches are present in the lamina propria of the small intestine and gradually increase in number moving distally (O'Malley, 2005; Hargaden and Singer, 2012).



**Guinea pig digestive system.** Right view. 1. stomach; 2-4. cranial, descending, ascending duodenum; 4: duodeno-jejunal flexure; 6: jejunum; 7: ileum; 8-9: body and apex of the cecum; 10-13: ascending colon; 14: transverse colon; 15: descending colon; 16: rectum. (From: Popesko et al., 1992).

### ***Hydrochoerus hydrochaeris***

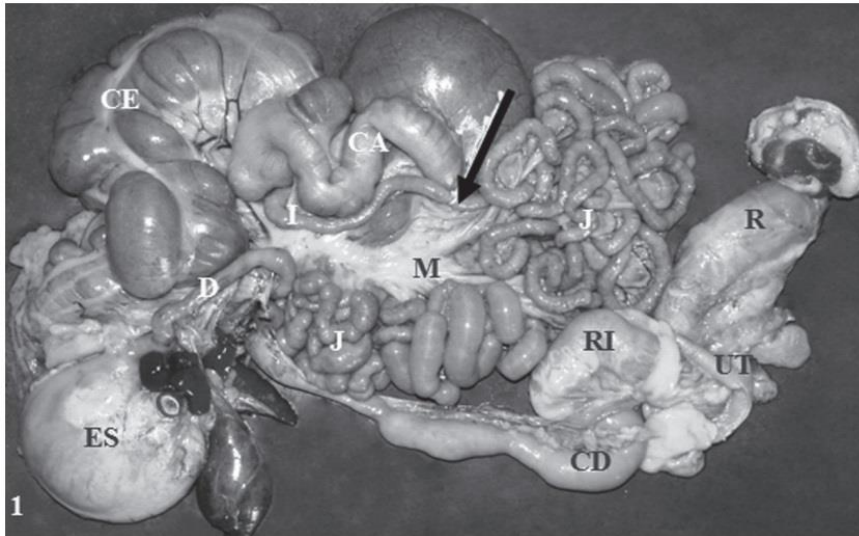
The gross anatomy of the capybara small intestine does not differ significantly from that of other domestic mammals, such as dogs and swines (Nickel et al., 1979).

The small intestine has a homogeneous diameter which is markedly smaller in comparison to that of the large intestine (de Freitas et al., 2008). The first part of the duodenum is directed towards the right abdominal wall and continues with the cranial duodenal flexure, which is dorsally fixed to the roof of the abdominal cavity through the mesoduodenum. It continues in the caudal direction as descending duodenum flexing from right to left (caudal duodenal flexure), and caudally to the root of the mesentery, forming the ascending duodenum. The ascending duodenum, fixed to the descending colon through the duodenocolic fold, is directed cranially and in proximity to the stomach. A marked duodeno-jejunal flexure marks the transition between the duodenum and the jejunum. The descending and ascending parts are arranged in a U-shape around the root of the mesentery (de Freitas et al., 2008).

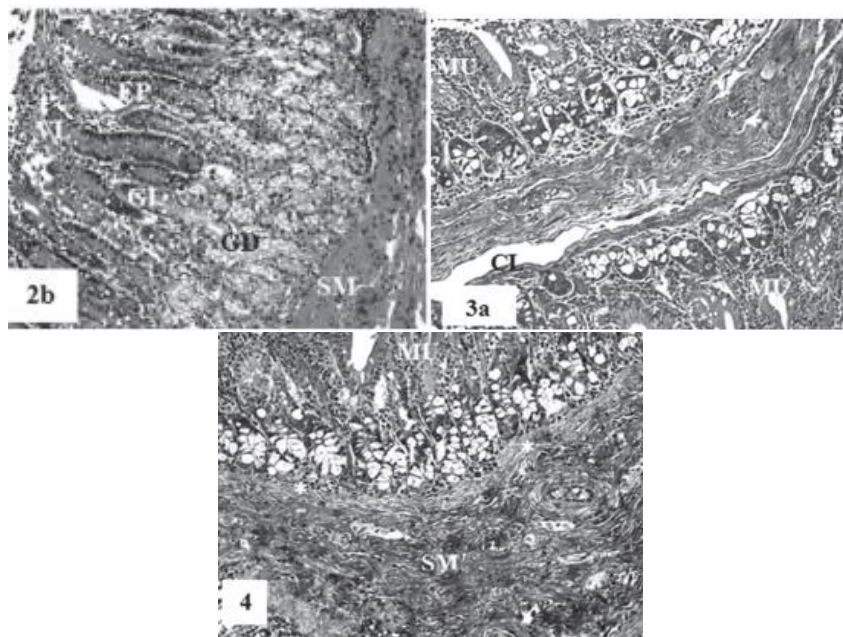
The jejunum was the most easily identifiable segment due to its length and typical convolutions. Macroscopically, the transition between the jejunum and the ileum is hardly identifiable in terms of change in diameter; however, slight differences can be identified in terms of wall consistency on palpation. The mesentery, a wide and abundantly vascularized peritoneal fold with little adipose tissue, supports the jejunal loops. The ileum appears as a straight tubular segment located just after the jejunum, supported by the mesoileum, and opening into the visceral surface of the cecum. The ileocecal fold connects the visceral surface of the cecum to the antimesenteric margin of the ileum (de Freitas et al., 2008).

The minimum and maximum length of the small intestine is 441 to 1734 cm in females and 355 to 1123 in male capybaras (de Freitas et al., 2008), which represent intermediate values between canine and swine small intestinal lengths (Nickel et al., 1979). The ratio between small

intestine length and body length is 12:1, and is not influenced by sex (de Freitas et al., 2008). Correlation between the length of each small intestine length and body length is positive, but statistically significant only for the duodenum. The small intestine wall, histologically, consists of a mucosa, a submucosa, a muscular tunic and a serosa. The mucosa is composed of intestinal and duodenal glands, serosal and mucosal in type, respectively. The muscular layer of the mucosa is made up of two distinct layers in the jejunum and ileum, whereas it is made up of a thin single layer in the duodenum. The submucosa, consisting in dense connective tissue, does not show any glands. The internal layer of the muscular tunic presents helicoidal fiber bundles (de Freitas et al., 2008).



***Isolated female capybara gastrointestinal tract (liver removed): CA: ascending colon; CD: descending colon; CE: cecum; D: duodenum; ES: stomach; I: ileum; J: jejunum; M: mesentery; R: rectum; RI: Kidney; UT: uterine horn; the arrow indicated the union between the jejunum and the ileum (from: de Freitas et al., 2008)***



*Photomicrographs of the duodenum (2b), jejunum (3a), and ileum (4) of the capybara. Duodenum: EP: simple columnar epithelium, covered by intestinal villi (VL); GI: intestinal glands; GD: duodenal glands. Jejunum: Submucosa (SM) with arterioles (\*) and venules (\*) and lymph capillaries (CL). Ileum: tunica mucosa (MU); GI: intestinal glands; lamina muscularis (\*), and submucosa (SM). H-E. 20x (from: de Freitas et al., 2008)*

## **Large intestine**

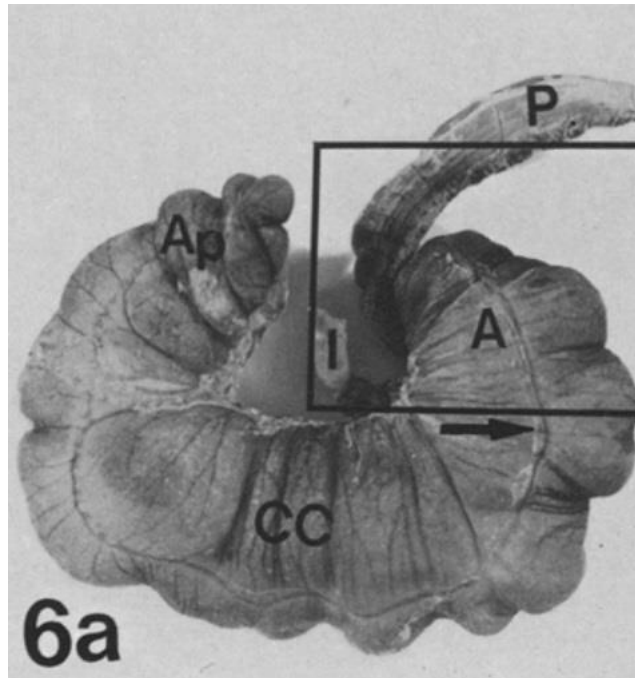
### ***Cavia porcellus***

The large intestine of the guinea pig extends from the ileocecal valve and ends with the anus and is approximately 70-75 cm in length, lacking a sigmoid colon or a cecal appendix (Brazile and Brown, 1976; Cooper and Schiller, 1975b).

The cecum is large and well developed, it has a thin wall and fills most of the left ventral abdominal cavity (O'Malley, 2005). It is the largest dilatation of the gastroenteric canal, measuring 15-20 cm in length and containing 65% of the gastrointestinal contents, making up 15% of the animal's body weight (Manning et al., 1984; O'Malley, 2005; Hargaden and Singer, 2012). The cecum is responsible for the production of vitamins (Hargaden and Singer, 2012). On its outer surface, it presents three white longitudinal smooth muscular bands, the so-called teniae ceci: the dorsal, the ventral and the medial, which create lateral saccular outpouchings called haustra (Cooper and Schiller, 1975b).

The colon measures 70 cm in length and is dark green in color. It is anatomically divided into an ascending, a transverse, and a descending portions, on the basis of their topography in the abdominal cavity, as in other mammals, but it is functionally divided into a shorter proximal and a longer distal portions (Cooper and Schiller, 1975a; O'Malley, 2005). The descending colon terminates with the 10 cm-long rectum, macroscopically similar to the colon (Cooper and Schiller, 1975b).

The mesenteric side of the mucosa of the proximal colon presents a longitudinal furrow which separate the digesta into the high protein cecotrophs and the poor-quality protein destined to become fecal pellets (O'Malley, 2005). The longitudinal furrow at the level of the proximal colon is deep and lined by mucous cells which trap bacteria and high protein particles, which are then transported back to the cecum by antiperistalsis for fermentation (Cheeke, 1987). Cecotrophy or coprophagy (eating the soft cecotrophes directly from the anus) occurs several times per day, and it is thought to contribute as a source of vitamin B and protein utilization in guinea pigs (Hargaden and Singer, 2012).



**Guinea pig cecum.** Ventral view. A. ampulla ceci; AP: apex ceci; CC: corpus ceci; I: ileum; P: proximal colon (from: Snipes, 1982)

### ***Hydrochoerus hydrochaeris***

The large intestine of the capybara consists of the cecum, the colon, the rectum and the anal canal. The colon is distinctly differentiated into three portions: the ascending, the transverse and the descending colon. The intestinal portion interposed between the ascending and the transverse colon is referred to as right colic flexure, whereas the portion interposed between the transverse colon and the descending colon is referred to as left colic flexure (Vazquez et al., 2012).

The cecum is the largest part of the intestine and composed of a base, a body and an apex, analogously to other rodents, such as the guinea pig (Snipes et al., 1982). The outer surface of the cecum presents four teniae (dorsal, ventral, lateral and medial), forming haustra or sacculations. The proximal loop of the ascending colon is joined by the cecocolic fold, which is attached to the medial tenia of the cecum, to the cecum. The four teniae of the cecum join variably with each other at the level of the cecal apex (Vazquez et al., 2012).

The ascending colon presents small haustras along its entirety, and is divided into a proximal ansa, and a distal or spiral ansa. The proximal ansa is characterized by teniae on its surface and is directed cranially, from left to right, towards the base and body of the cecum, to which is attached through the cecocolic fold. The distal ansa has a spiral arrangement and is located in the right cranial abdomen, in contact ventrally with the apex of the cecum; it does not present any teniae. The spiral ansa has a centripetal gyrus to the left, a central flexure, and a centrifugal gyrus directed towards the right side, which is continuous with the transverse colon in the right colic flexure. The internal surface of the ascending colon is characterized by longitudinal and transversal muscular folds, extending from the cecum to the beginning of the spiral ansa (Vazquez et al., 2012).

The deep layer of the greater omentum inserts on the transverse colon, extending from the right to the left colic flexure (Vazquez et al., 2012).

The descending colon is supported by a loose and mobile mesocolon, allowing large mobility of this tract (Vazquez et al., 2012).

Histologically, all large intestinal tracts are characterized by a mucosa, a submucosa, a muscular tunic and a serosa. The mucosa is lined with a simple cylindrical epithelium containing PAS-positive goblet cell, more represented at the rectum level. The submucosal layer consists of loose connective tissue, consisting of variably-sized blood vessels and lymphoid nodules and nerve plexuses. The muscular tunic consists of smooth muscle fibers organized in a circular internal layer and in a longitudinal external layer, with well- developed nerve plexuses between the two. The muscular layer increases in thickness towards the rectum. The serous tunic consists of a thin layer of loose connected tissues, covered by the mesothelium (Carrascal Velasquez, 2017).



*Ventral view of the abdominal organs of the capybara. 1: cecum; 2: proximal ansa of the ascending colon; 3: distal or spiral ansa of ascending colon; 4: teniae of the cecum; 5: small intestine; 6: stomach (from Vazquez et al., 2012).*

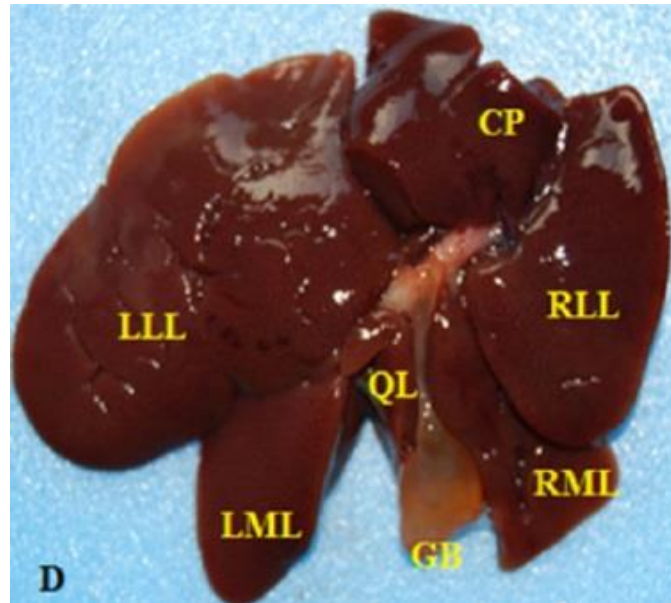
## **Liver**

### ***Cavia porcellus***

The liver constitutes the largest gland and has a smooth dark red-brown appearance (O'Malley, 2005; Hargaden and Singer, 2012). It consists of six lobes: right, medial left lateral, left medial, caudate, and quadrate, that are not well demarcated and tend to blend with each other (O'Malley, 2005; Hargaden and Singer, 2012). A peculiarity of guinea pigs, similarly to humans, some bats, and non-human primates, is the inability to produce the hepatic enzyme L-gulonolactone oxidase, fundamental for the catalization of endogenous vitamin C biosynthesis (Nishikimi et al., 1992).

Guinea pigs have a well-developed, thin-walled oval gallbladder that lies in a fossa of the quadrate liver lobe on its medial aspect, and is drained by the cystic duct (Breazile and Brown, 1976; Cooper and Schiller, 1975b). The hepatic ducts and the cystic duct join to form the common bile ducts which drains into the duodenum through an ampullary swelling (Higgings,

1927; Hargaden and Singer, 2012). A sphincter located proximal to the ampullary swelling allows the bile to flow into the duodenum and prevents regurgitation of the bile backwards into the ducts (Higgins, 1927; Hargaden and Singer, 2012). Histologically, the guinea pig liver presents a lobular architecture with poorly-defined border and portal tracts consisting of vascular structures and biliary canaliculi (Bhattacharjya et al., 2003). Parenchymal cords are composed of hepatocytes that are cuboidal to polygonal in appearance, and radially distributed from the central lobular vein. Liver lobules are hexagonal or oval in shape, incomplete and separated by connective tissue (Bhattacharjya et al., 2003); the PAS-stained hepatocytes contain glycogen and hemosiderin neutral mucins showing a variable staining pattern, either granular or, most frequently, clustered and diffuse (Rosas et al., 2010).



**Guinea pig liver**, visceral surface. CP: caudate process; GP: gallbladder; QL: quadrate lobe; LML: left medial lobe; LLL: left lateral lobe; PP: papillary process; RLL: right lateral lobe; RML: right medial lobe (from Stan, 2018).

### ***Hydrochoerus hydrochaeris***

Macroscopically, the liver of the capybara is thicker in its central portion, with thinner margins, with the lobes well demarcated and separated by deep fissures nearly reaching the portal fissure, with the exception of the incisure that separates the left medial lobe from the quadrate lobe (Cao et al., 2017). It consists of five lobes, overlapping each other for a considerable extension (Cao et al., 2017). The lobulation of the liver of the capybara, as well as its histological structure, resemble those of domestic carnivorous species (Getty, 1982; König and Liebich, 2011; Cao et al., 2017). The left lateral lobe is the most voluminous and oval-shaped, followed, in terms of size, by the right medial lobe and the left medial lobe, the quadrate lobe (tongue-shaped), with the right lateral lobe being the smallest. On the visceral surface of the liver is located the caudate lobe, made up of a caudate process on the right side and a papillary process towards the left, both further subdivided by secondary fissures (Cao et al., 2017). A small gallbladder is present, located in the fossa between the right medial lobe and the quadrate lobe (Cao et al., 2017). The diaphragmatic surface of the liver is convex and attached to the diaphragm via the falciform ligament, formed by the union of the well-developed right and left coronary ligaments. The liver presents a deep oesophageal impression (Cao et al., 2017). On its outer surface, each hepatic lobe is covered by a thin layer of connective tissue (Cao et al., 2017).

Histologically, the liver structure is characterized by a lobular architecture and portal tracts consisting of vessels and bile canaliculi. Liver lobules do not appear polygonal in shape as in most species such as the dog and cat (König and Liebich, 2011), but present poorly-defined margins (Cao et al., 2017). The capybara liver lobules also differ from the hexagonal/oval lobules of the guinea pig (Bhattacharjya et al., 2003), partially separated by connective tissue. Portal spaces were filled with vascular structures, with their endothelia surrounded by smooth muscle fibers, whereas the central vein appeared optically empty and surrounded by endothelial tissue. Hepatocytes are irregularly polyhedral, variable-sized, with an eosinophilic cytoplasm and a rounded central basophilic nucleus with a nucleolus and a dispersed chromatin (Cao et al., 2017). Similarly to guinea pigs (Rosas et al., 2010), the content of hepatocytes, analyzed through the PAS method, consists of glycogen and neutral mucins, showing a granular or diffuse staining pattern (Cao et al., 2017). The histological organization of the liver of the capybara resembles that reported for other domestic mammals and experimental rodents (Cao et al., 2017).

The liver is irrigated by the hepatic artery, which carries oxygen-rich blood, and by the portal vein, which is rich in nutrients. The hepatic artery originates from the trifurcation of the celiac artery, an unpaired vessel that originates from the descending aorta, analogously to most mammals (Sejín et al., 2003). The hepatic artery enters the liver through the portal fissure, located on the visceral face of the liver, accompanied by the portal vein, originating from the mesenteric vein that carries venous blood coming from the pancreas, intestine, spleen and stomach (Sejín et al., 2003).



*Capybara liver, diaphragmatic surface. 1: coronary ligaments; 2: falciform ligament; 3: oesophageal impression (from Cao et al., 2017)*

## **Pancreas**

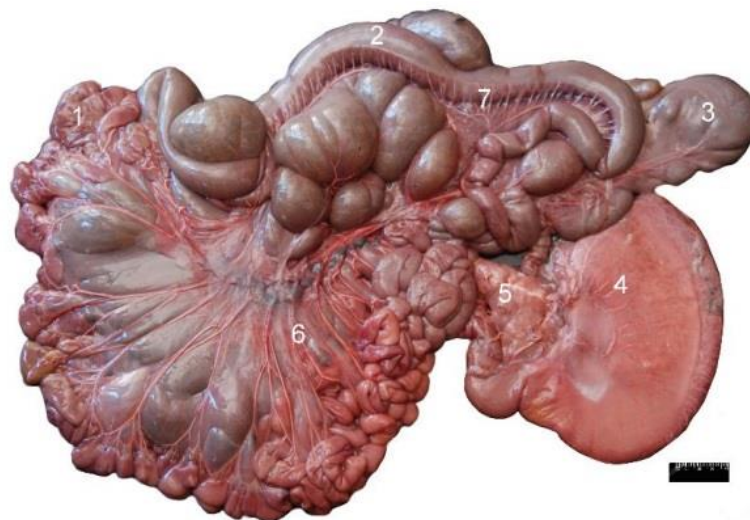
### ***Cavia porcellus***

The well-developed pancreas of the guinea pig, as in other species, extends to the spleen and lies in contact with the descending duodenum incorporated in the mesoduodenum; it has a triangular shape, consists of three lobes and is pink-red in color (Brezile and Brown, 1976;

O'Malley, 2005). According to Cozzi et al. (2006), the pancreas consists of two lobes, a cranial lobe and a caudal lobe. Similarly to other species, the pancreas is composed of the islets of Langerhans located throughout the parenchyma (Breazile and Brown, 1976). The pancreatic lobes are divided into lobules; the lobular ducts drain into the single pancreatic duct which joins the common bile duct before opening into the duodenum (Breazile and Brown, 1976), although, according to some authors, the pancreatic duct drains separately into the duodenum approximately 7 cm distal to the common bile duct (Cooper and Schiller, 1975b; Mann et al., 1920; Cozzi et al., 2006). An accessory pancreatic duct is absent in guinea pigs (Cooper and Schiller, 1975b).

### ***Hydrochoerus hydrochaeris***

The pancreas of the capybara is intraperitoneal and lies transversally in relation to the posterior abdominal wall, with its larger portion being located left to the median plane. It measures 8 to 12 cm in length and weighs 29 to 50 g. It presents an irregularly elongated prismatic shape, is red in color and is divided into a head, a body and a tail (Percegonia et al., 2004). The caudal edge (tail) is lobulated. The cranial border is in contact with the ascending duodenum, the tail with the descending duodenum, the right border with the duodenal curvature. Ventrally, it comes in contact with the greater gastric curvature. Caudally, the tail of the pancreas relates with the transverse colon and is in contact with the small intestine. The left border communicates with the spleen, the upper pole of the left kidney and the left adrenal gland. Dorsally, it is in contact with the aorta, the caudal vena cava and the renal vein (Percegonia et al., 2004). The ventral face of the pancreas is vascularized by thin branches originating from the hepatic artery, the cranial border and right portion of the pancreas are vascularized by the gastroduodenal and gastroepiploic artery, whereas the splenic artery vascularized the pancreas body and tail; finally, the pancreaticoduodenal artery, originating from the cranial mesenteric artery, vascularizes the tail of the pancreas (Privado-Filho, 2000). The pancreatic duct extends transversally and empties into the first portion of the duodenum through a distinctive papilla of the common bile duct, approximately 4-5 cm below its opening. Histologically, the exocrine pancreas is an acinar gland, it is lobulated and the lobes are poorly demarcated by connective tissue. The pancreatic duct, histologically, is lined by a cuboidal epithelium. The pancreatic acini consist of a single layer of pyramidal epithelial cells that rest on a delicate basal layer. The pancreatic islets are small in size and with poorly-limited borders (Percegonia et al., 2004)



***Capybara isolated gastrointestinal tract. Dorsal view. 1: jejunum; 2: ileum; 3: cecum; 4: stomach; 5: pancreas; 6: jejunal arteries; 7: ileal arteries (from: Ibanez Orihuela et al., 2019)***



# Cardiovascular system

## Heart

### *Cavia porcellus*

The guinea-pig heart has a globular appearance with a shape of a truncated cone flattened laterally, and occupies a large part of the small thoracic cavity (O'Malley, 2005; Hargaden and Singer, 2012). It lies in the midline between the 2nd and the 4th intercostal spaces, approximately 1 cm cranial to the xyphoid process, and has a ventro-caudal inclination (Cooper and Schiller, 1975a; O'Malley, 2005; Heatley, 2009; Hargaden and Singer, 2012). It is four-chambered and surrounded by a pericardium consisting of two layers: an outer fibrous layer and an inner thin serous layer (O'Malley, 2005; Hargaden and Singer, 2012). The guinea pig heart measures approximately 2 cm in length (long axis from apex to base), and its maximum diameter at the heart base level is of 5 to 6 cm. Its weight corresponds on average to 0.43% of the body weight (1.4 grams in a specimen of 500 grams of weight) (Hoffmann, 1956). Externally, the atria are separated from the ventricles by a deep coronary sulcus to accommodate the coronary veins and arteries (Breazile and Brown, 1976). The guinea pig heart, in comparison with the rat, presents a reduced coronary flow (Cozzi et al., 2006). Two shallow interventricular sulci separate dorsally and ventrally the two ventricles (Cooper and Schiller, 1975a). The atria are separated internally by the atrial septum and externally by the aorta and pulmonary trunk, whereas the ventricles are separated internally by a thick intraventricular septum. The left and right auricles are well-developed (Cooper and Schiller, 1975a). The right ventricular lumen contains a septomarginal septum, also known as moderator band, that is not always present in the left ventricular lumen (Breazile and Brown, 1976; Hargaden and Singer, 2012). The apex of the heart, as in other animals, is formed by the thicker and larger left ventricle (Barone, 2006a; Hargaden and Singer, 2012). The means of fixation of the heart include the thin pericardium, the large vessels, the pulmonary trunk, and the sternum-pericardial ligament that anchors it to the sternum, albeit to a lower extent in comparison with other laboratory rodents (Hoffmann, 1956).

A comparative macroscopic anatomical study of the rabbit and guinea pig hearts has set in light the morphological characteristics of the atrioventricular and semilunar cardiac valves

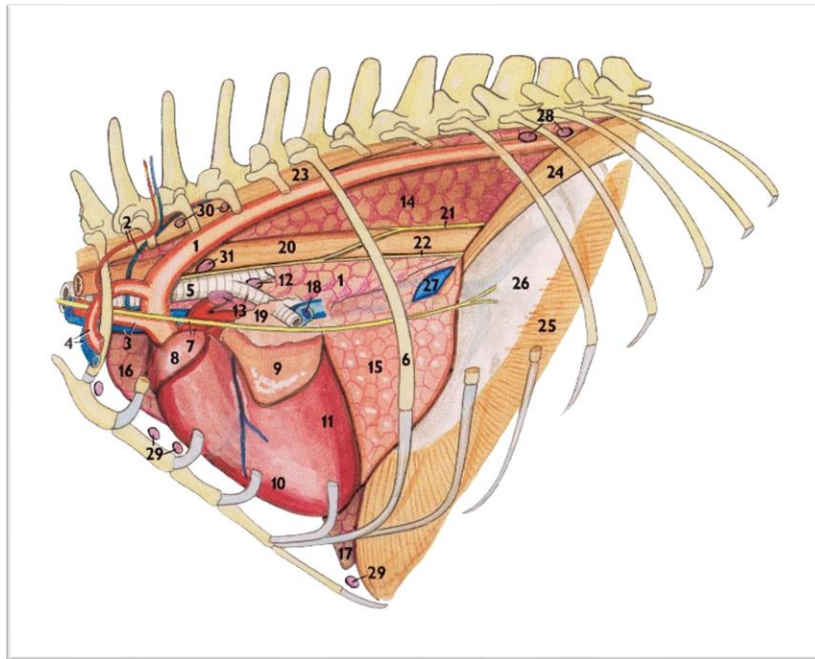
(Ates and Cakir, 2010). The tricuspid valve was found to be composed of 3 cusps in the majority of the animals examined, of 2 cusps in a minority of subjects, whereas the mitral valve was found to be composed of 2 cusps in all analyzed hearts. A poorly-demarcated separation was highlighted between the cusps of both atrioventricular valves. The aortic and pulmonary semilunar valves were found to consist of 3 cusps each. A single anterior papillary muscle and a single septal papillary muscle were detected at the level of the right ventricle. The number of posterior papillary muscles of the right ventricle was found to present individual variability. Two papillary muscles were observed at the level of the free wall of the left ventricle. Tendinous cords connecting the papillary muscles and the cusps of the atrioventricular valves were detected in both ventricles (Ates and Cakir, 2010).

It has been reported that, at the level of the atrial and ventricular surfaces of the mitral and tricuspid valves of the guinea pig "micro appendages" are physiologically present, referable to a wavy and irregular layer of endothelial cells at the microscopic level (Hill and Folan-Curran, 1993). These microvilli are more represented at the level of the tricuspid valve, confirming the hypothesis that the pleomorphism at the level of the valvular surfaces is the result of intracardiac haemodynamic factors: a higher blood pressure leads to a reduced development of the aforementioned micro appendages, and viceversa. The function of these structures has not yet been clarified, but two hypotheses have been advanced regarding their role: that of expanding the surface of the endothelial cells, and to intervene in their metabolism

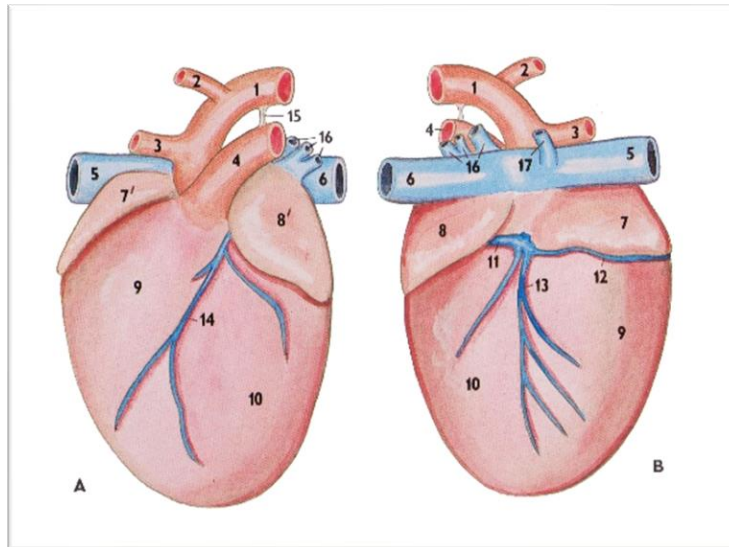
(Hill and Folan-Curran, 1993).

The guinea pig electrocardiogram wave forms are similar to humans, with a well distinguishable T wave and a QRS complex (Cozzi et al., 2006). The total blood volume of a guinea pig is 70-75 ml/kg of blood (O'Malley, 2005). The systolic pressure is 80-94 mmHg, the diastolic 55-58 mmHg, with a heart rate of 229-319 beats per minute (Cozzi et al., 2006). In comparison with other rodents, such as the rat and mouse, the guinea pig presents a reduced number of erythrocytes and a reduced hemoglobin hematic concentration (Cozzi et al., 2006).

The guinea pig myocardiocytes are not as rigid as the rat's, making the rat's cardiac myocardium characterized by a stronger contractile force at comparable myoplasmic calcium concentrations (Kapelko and Navikova, 1993).



***Topographical anatomy of the organs of the thoracic cavity of the guinea pig. Left view, after removal of part of the left lung. 1: aorta; 2: costocervical artery and vein; 3: brachiocephalic trunk, cranial vena cava; 4: left subclavian artery and vein; 5: trachea; 6: sixth rib; 7: pulmonary trunk, left phrenic nerve; 8: right auricle; 9: left auricle; 10: right ventricle; 11: left ventricle; 12: right main bronchus and medial tracheobronchial lymph node; 13: left main bronchus and left tracheobronchial lymph node; 14: right caudal lung lobe; 15: right accessory lobe; 16: right cranial lobe; 17: middle lobe; 18: pulmonary vein; 19: left lung dissected; 20: oesophagus; 21: dorsal vagal trunk; 22: ventral vagal trunk; 24-26: diaphragm; 27: caudal vena cava; 28: Inn. aortic thoracic; 29: sternal lymph nodes; 30: intercostal lymph nodes; 31: mediastinal lymph nodes. (from: Popesko et al., 1992)***



**Guinea pig heart.** Auricular (A) and atrial (B) surfaces. 1: aorta; 2: left subclavian a.; 3: brachiocephalic trunk; 4: pulmonary trunk; 5: cranial vena cava; 6: caudal vena cava; 7 and 7': right atrium and right auricle; 8 and 8': left atrium and left auricle; 9: right ventricle; 10: left ventricle; 11: coronary sinus; 12: right cardiac vein; 13: median cardiac vein; 14: interventricular paraconal vein; 15: arterial ligament; 16: pulmonary veins; 17: right azigos vein. (from: Popesko et al., 1992)

### ***Hydrochoerus hydrochaeris***

The capybara heart lies in the middle mediastinum and extends cranio-caudally from the second intercostal space to the sixth rib (Magariños et al., 2018). It is surrounded by the pericardium, composed of a fibrous and a serous layers, very closely interconnected. The visceral layer or epicardium is completely attached to the myocardium. The fibrous pericardium is covered by the pericardial pleura. The fibrous pericardium is attached to the sternum and diaphragm through the phrenicopericardial ligament. The cardiac grooves and major cardiac vessels are covered by very little subepicardial fat. The intervenous tubercle inside the right atrium (Tuberculum intervenosum) is poorly developed. The right atrial cavity presents a low number of pectinate muscles. The terminal crest separates the sinus vena cavae from the right atrium, and it forms the cranial and right margin of the orifice of the cranial vena cava, located on the roof of the atrium. The floor of the atrium is almost entirely occupied by the atrioventricular ostium and its valve. The right papillary muscles, serving as anchor point for the chordae tendinae of the cusps of the right atrioventricular valve, can be subdivided into: the large papillary muscle (*M. papillaris magnus*), which is preponderant and located on the marginal wall; the subarterial papillary muscle (*M. papillaris subarteriosus*), inserted on the septal wall under the conus arteriosus; and the small papillary muscles (*Mm. papillares parvi*), inserted on the septal wall (Magariños et al., 2018).

The right papillary muscles are interspersed with septomarginal trabeculae. The well-developed right septomarginal trabecula lays between the subarterious papillary muscle and the magnus papillary muscle. Carnous trabeculae are located mostly in the blood intake chamber, especially towards the apex and interventricular sulci, and are absent in the conus arteriosus. The marginal wall of the right ventricle, as well as the septal wall are characterized by well developed carnos trabeculae. The magnus papillary muscle gives off chordae tendineae to the septal and angular cusps of the right atrioventricular valve. The subarterial papillary muscle, of intermediate size, sends chordae tendineae mainly to the septal and parietal cusp of the right atrioventricular valve. The small papillary muscles send chordae tendineae exclusively to the parietal cusp of the right atrioventricular valve (Magariños et al., 2018). The left atrium is

characterized by fewer pectinate muscles than the right. The floor of the left atrium is almost entirely occupied by the left atrioventricular ostium and its valve. The left ventricular cavity is partially divided into two compartments by the septal cusp of the mitral valve, creating a so-called subatrial chamber for blood intake, located under the atrioventricular orifice and continuing to the apex of the heart, and a blood expulsion chamber, or arterial chamber, reaching the aortic ostium. The septal wall presents two left papillary muscles, the caudal subatrial papillary muscle (*M. papillaris subatrialis*), and the more cranial subatrial papillary muscle (*M. papillaris subauricularis*) located opposite to each other. Both papillary muscles are simple and emit chordae tendineae towards both cusps of the mitral valve. The septal wall also gives insertion to the left septomarginal trabeculae. The carnosus trabeculae of the left ventricle are less numerous, however more developed and located over almost the entire length of the left ventricle. Small left septomarginal trabeculae are interspersed between the trabeculae carnosae. A large carnosus trabecula located between both papillary muscles occupies a large part of the dorsoventral extension of the septal wall of the left ventricle. The largest left septomarginal trabecula extends from this carnosus trabecula, with a ventrocaudal direction, towards the middle of the subatrial papillary muscle. The cardiac skeleton of the capybara lacks any osseous or cartilaginous components (Magariños et al., 2018).

Regarding the atrioventricular conduction system of capybara hearts, according to Trindade de Veglia (2016), it is, overall, similar to the organization seen in other species and humans, with the atrioventricular node, the bundle of His, which divides into a right and left branches distributed through the subendocardium of the papillary muscles of both ventricles. However, it differs in that it lacks a true left trunk that divides into anterior and posterior branches, as seen in cattle; instead, a fan-arranged bundle of fibers originating from the bundle of His widely distribute through the multiple papillary muscles of the left ventricle, more similarly to what happens in humans (Trindade de Veglia, 2016).

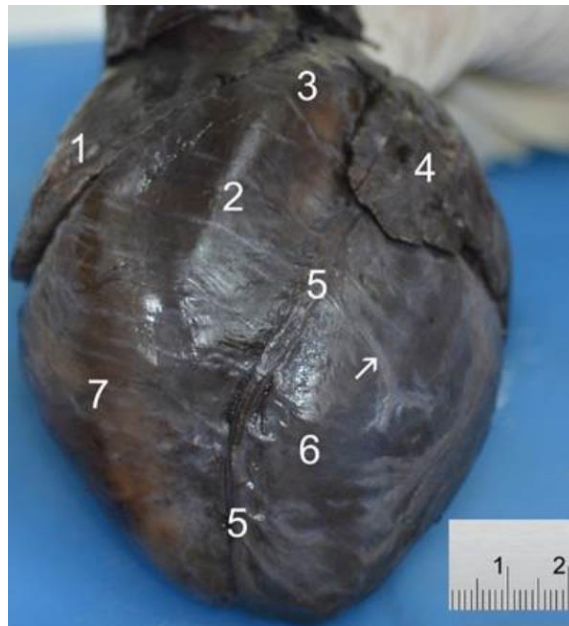
As far as the arterial supply of the heart is concerned, the left coronary artery arising from the left coronary sinus of the aorta is well developed, larger and more widely distributed than the right, being responsible for the irrigation of most of the myocardium. It runs in a caudolateral direction between the pulmonary trunk and the left atrium and bifurcates into two branches, the paraconal interventricular branch that descends in the paraconal interventricular sulcus and the circumflex branch that runs caudally in the coronary sulcus, not joining the right coronary artery. The circumflex branch irrigates the dorsal part of the left ventricle and the left atrium through several branches and continues as the subsinusal interventricular branch in the subsinusal interventricular groove, where it is accompanied by the middle cardiac vein. In proximity of the cardia capex the subsinusal interventricular branch runs cranially to irrigate the distal part of the right ventricle, and finally anastomosing with the paraconal interventricular branch originated from the left coronary artery. The paraconal interventricular branch, accompanied by the great cardiac vein, courses through the paraconal interventricular groove and ends on the right ventricular margin, anastomosing with the subsinusal interventricular branch coursing through same groove, and emitting an intermediate branch destined for the caudal part of the left ventricle (Magariños et al., 2018).

The right coronary artery, originating from the right coronary sinus of the aorta, is less developed than its left counterpart; it runs cranially between the pulmonary trunk and the right atrium and then ventrocaudally in the right coronary sulcus, without reaching the subsinusal interventricular groove. Along this path, it emits ascending branches towards the right atrium and descending branches towards the right ventricle (Magariños et al., 2018).

The presence of large anastomoses among the branches of the left coronary artery is noteworthy (Magariños et al., 2018).

In conclusion, the left coronary artery supplies a greater cardiac area than it does the right coronary artery (Sejín et al., 2003). The atresia of the right coronary artery has been documented

in capybara hearts (Tenani et al., 2010).



***Capybara heart***, auricular surface. 1: right auricle; 2: arterious cone; 3: pulmonary trunk; 4: left auricle; 5: interventricular paraconal sulcus; 6: left ventricle; 7: right ventricle; arrow: intermediate branch of the paraconal interventricular artery (from Magariños et al., 2018)

## Large arterial and venous vessels

### ***Cavia porcellus***

A unique feature of the circulatory system of the guinea pig is the presence of a caudal cerebral artery arising between the basilar and the internal carotid arteries (Hargaden and Singer, 2012). The small internal carotid arteries alone do not supply sufficient blood to the cerebral arterial vascularization and, therefore, the paired internal ophtalmic arteries provide a significant collateral input (Shively and Stump, 1974).

The basal and peak coronary blood flows of the guinea pigs are lower than in other rodents, such as the rat (Harkness et al., 2002). However, the guinea pig heart is characterized by a well-developed collateralization of the coronary arteries, making it difficult for a myocardial infarction by acute coronary artery occlusion to occur, in comparison to other species, such as humans, cats, dogs, pigs, and rats (Brewer and Cruise, 1994).

Another peculiarity of the guinea pig circulatory system, unlike the typical mammalian pattern, is the origin of the bronchoesophageal artery from the right costocervical, the right internal thoracic, or the brachiocephalic trunk instead of from the aorta (Shively and Stump, 1974).

In the thoracic region, there exist large dorsal scapular arteries partly distributed to the large fat pad of the dorsal cervical region of the guinea pig (Shively and Stump, 1974). Furthermore, each vertebral artery arises as two distinct rami anastomosing with each other a few millimeters from their origin (Shively and Stump, 1974).

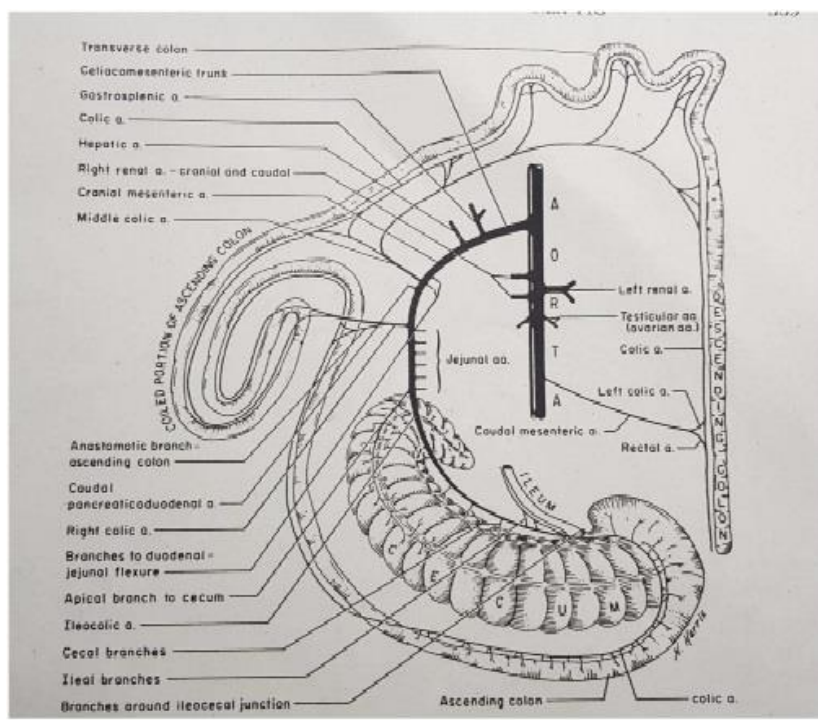
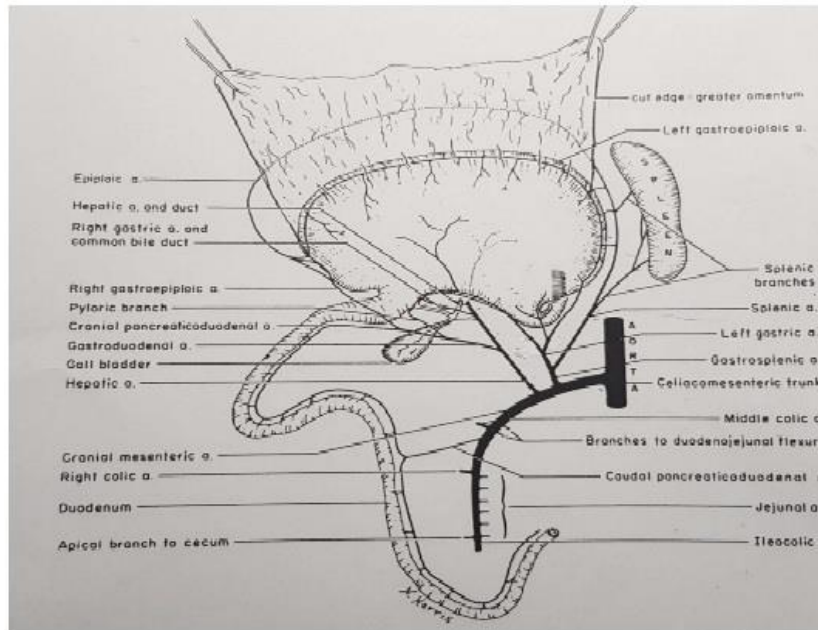
The guinea pig pulmonary trunk, unlike the aorta, is composed of short and irregular branching elastic fibers interspersed with smooth muscle and collagen, with the pulmonary artery and its branches being characterized by an abundant muscular component at the middle tunic level (Kay, 1983). The size of the lumen of the pulmonary arteries changes abruptly when

branching, due to the muscular organization that tends to form localized wellings that resembles the structure of sphincters (Kay, 1983). The tracheobronchial vasculature is characterized by frequent arterovenous anastomoses (Widdicombe, 1996). The pulmonary capillaries are fenestrated and smaller in size in their central portion in comparison with the periphery of the pulmonary lobule (Sekhon et al., 1995). The pulmonary veins also possess a well-developed smooth muscle component and present several dilatations (Kay, 1983). Histologically, the pulmonary vessels of the lung of the guinea pig commonly present an aggregation of lymphocytes in the adventitia in the form of perivascular nodules, whose role has not been clarified yet (Percy and Barthold, 2001). Unlike other rodents, the pulmonary veins in the lung of the guinea pig are not surrounded by cardiac muscle (Kramer and Marks, 1965).

The cranial vena cava in guinea pigs is single, unlike lagomorphs and other rodents (Orti et al., 2004). The azigos vein is more frequently located on the right side, instead of the left side as in other mammals (Orti et al., 2004).

The arterial distribution of the abdominal vessels of the guinea pigs resembles the typical mammalian pattern, with some exceptions (Barone, 2006a; Shively and Stump, 1975). Specifically, the guinea pig presents a single celiacomesenteric trunk, instead of separate celiac and cranial mesenteric arteries (Shively and Stump, 1975). The celiac components of the celiacomesenteric trunk can originate following five different patterns: 1) the celiacomesenteric trunk emits the gastrosplenic artery which, in turn, branches off into the splenic and left gastric arteries, and, subsequently, it emits the hepatic artery (Pernecky, 1969; Shively and Stump, 1975); 2) the celiacomesenteric trunk emits a celiac artery which subsequently bifurcates into the hepatic and gastrosplenic arteries (Pernecky, 1969; Shively and Stump, 1975); 3) the gastrosplenic artery detaches directly from the abdominal aorta, and the celiacomesenteric trunk gives off the hepatic artery (Shively and Stump, 1975); 4) the celiacomesenteric trunk emits, separately, the gastrosplenic and the hepatic arteries, with the gastrosplenic artery contracting an anastomosis with the aorta cranially to the origin of the celiacomesenteric trunk (Shively and Stump, 1975); 5) the celiacomesenteric trunk bifurcates into a gastrosplenic trunk, giving rise to the splenic and left gastric arteries, and a hepatomesenteric trunk, subdividing into the common hepatic artery and the cranial mesenteric artery (Bednářová e Malinovský, 1990).

Another common finding in guinea pigs is the presence of 2 pairs of renal arteries on either side, arising separately, and located cranially and caudally to each kidney (Shively and Stump, 1975). When two renal arteries are present bilaterally, the testicular arteries may arise from the renal arteries, from the aorta between the renal arteries, or caudally to the caudal renal artery (Favre, 1967; Shively and Stump, 1975). The ovarian artery, which perfuses the oviduct, the ovary and the uterus, usually originating from the aorta, may arise from the aorta between the double renal arteries or directly from the caudal renal artery (Mattei, 1966).



*Top: Schematic representation of the celiacomesenteric trunk and its collaterals in the guinea pig. Bottom: Distribution of the cranial and caudal mesenteric arteries in the guinea pig (from: Shively and Stump, 1975)*

***Hydrochoerus hydrochaeris***

From the aortic arch of the capybara originates, as only collateral branch, the brachiocephalic trunk (Culau et al., 2007). The brachiocephalic trunk in this species presents three different patterns of branching. The first reported pattern is the most frequently occurring and consists in the brachiocephalic trunk first emitting the left subclavian artery, followed by the left common carotid artery and finally by the brachio-carotid trunk which, in turn, emits the right common carotid artery and the right subclavian artery. The second pattern consists of the

brachiocephalic trunk giving rise to the left subclavian artery and then trifurcating into the right subclavian artery, the left common carotid artery and the right common carotid artery. The third observed pattern consists in the brachiocephalic trunk emitting, first, the left subclavian artery and, in sequence, the right subclavian artery and, finally, the bicarotid trunk giving origin to the right and left common carotid arteries (Culau et al., 2007).

The distribution of the arteries and veins of the abdomen of the capybara presents similarities with that described in other rodents, with some exceptions (Shively and Stump, 1975; Ibáñez Orihuela et al., 2019).

The diaphragm of the capybara is irrigated by the phrenic arteries, originating from the aorta (Ibáñez Orihuela et al., 2019). The short celiac artery of the capybara supplies the spleen, stomach, first half of the duodenum, liver, and pancreas. It originates from the ventral aspect of the abdominal aorta.

The celiac artery ends by emitting three branches: the splenic artery towards the left, the left gastric artery in the middle, and the hepatic artery, to the right. The splenic artery supplies the spleen, the fundus and the greater curvature of the stomach, and the left lobe of the pancreas (Ibáñez Orihuela et al., 2019). The splenic artery continues as left gastroepiploic artery in the greater omentum, runs along the greater curvature of the stomach, and then anastomose with the right gastroepiploic artery originating from the hepatic artery. The left gastric artery distributes through the lesser curvature of the stomach, as well as the parietal and visceral aspects of the stomach, and ends in proximity of the gastric incisure where it anastomoses with the right gastric artery. The hepatic artery vascularizes the liver, the body and right lobe of the pancreas, as well as the lesser curvature of the stomach (through the right gastric artery) and the first half of the duodenum (through the gastroduodenal artery). The gastroduodenal artery gives off the right gastroepiploic artery directed to the greater curvature of the stomach. The hepatic artery enters the hepatic portal accompanied by the portal vein, where it runs ventral to the vein and branches off in the liver in a right and a left hepatic artery destined to the liver.

The cranial mesenteric artery, originating on the ventral aspect of the aorta, caudal to the celiac artery, supplies most of the intestine, from the mid-duodenum to the beginning of the descending colon. Along its course through the pancreas, it emits the caudal pancreatic duodenal artery, which terminates by emitting a branch directed to the duodenojejunal flexure which anastomoses with the first of the jejunal arteries and continues following the duodenum retrogradely and anastomosing with the cranial pancreatic duodenal artery. The cranial mesenteric artery, along its distribution, branches by giving off, in order, the jejunal arteries followed by the ileal arteries; the ileocolic artery, whose branches are destined for the terminal part of the ileum, the cecum and the beginning of the ascending colon; and, finally, the right and middle colic arteries, destined to the ascending, descending and transverse colon, respectively (Ibáñez Orihuela et al., 2019).

The thinner and simpler caudal mesenteric artery supplies the large intestine from the middle of the transverse colon to the rectum; its origin from the ventral aspect of the termination of the aorta, is distant from that of the cranial mesenteric artery, and located at the level of the last lumbar vertebra. The caudal mesenteric artery bifurcates into the left colic artery, supplying most of the descending colon and anastomosing with the middle colic artery, and the cranial rectal artery, which ends by anastomosing with the caudal rectal artery (Ibáñez Orihuela et al., 2019).

Each adrenal gland is vascularized by the caudal phrenic artery, the renal artery and the aortic artery (Ibáñez Orihuela et al., 2019).

The paired and voluminous renal arteries of the capybara originate just caudal to the emission from the cranial mesenteric artery, with the right renal artery being located slightly more cranial than the left (Ibáñez Orihuela et al., 2019).

The paired and small testicular arteries, originating distal to the renal arteries in proximity



of the caudal mesenteric artery on the lateral aspect of the abdominal aorta, and presenting a tortuous course in its distal course towards the inguinal canal, where it gives off a branch that anastomoses with that of the vas deferens to supply the body of the epididymis. The homologous but larger ovarian arteries, with an analogous origin than the testicular arteries, penetrate through the broad uterine ligament and, with a sinuous course, supply the ovaries, the uterine tubes and the adjacent part of the uterus (Autino et al., 2019; Ibáñez Orihuela et al., 2019).

The abdominal walls are irrigated by the deep circumflex iliac arteries, originated from the external iliac arteries. Dorsal to the abdominal aorta originate six lumbar arteries, branching off into a muscular branch and a spinal branch, which enters the intervertebral foramen to supply the spinal cord; six lumbar satellite veins are present (Ibáñez Orihuela et al., 2019).

The veins of the abdomen are satellites to the arteries and join to form the cranial and caudal mesenteric veins, giving rise to the portal vein that enters the hepatic hilum. The splenic vein is tributary of the portal vein. The renal veins, satellites to the corresponding arteries, open into the caudal vena cava, and then, at the level of the liver, they receive the hepatic veins. The testicular veins make up a very complex and closely tangled pampiniform plexus, ultimately reducing to a single vein opening into the caudal vena cava. The caudal vena cava runs to the right of the aortic artery in the abdomen, passing through the caudal vena cava foramen of the diaphragm and emptying into the right atrium of the heart (Ibáñez Orihuela et al., 2019).

The abdominal aorta ends at the level of the last lumbar vertebrae, branching off into three uneven branches: from the dorsal surface of the aorta before its final bifurcation, it emits the unpaired sacral median artery, and, subsequently, cranially to the pelvic inlet, it emits the well-developed paired common iliac arteries. The small median sacral artery is located in the midline, at the level of the pelvic side of the sacrum and it runs dorsal to the rectum, accompanied by its satellite vein. Each common iliac trunk emits the uterine artery in the female and the umbilical arteries and then bifurcates into the external iliac arteries, with branches directed to the pelvic limb, and the internal iliac arteries, distributing to the pelvic cavity and wall (Autino et al., 2019). The uterine artery, running through the uterine broad ligament, gives off multiple branches to the uterine body and horns, then it reaches the uterine tube where it anastomoses with the ovarian artery. The common iliac trunk also emits the vestigial umbilical arteries, which give origin to the cranial vesical artery (Autino et al., 2019).

The short internal iliac artery ends at an acute angle by giving off the internal pudendal arteries and a common trunk emitting the caudal gluteal and the caudal rectal arteries. In the male, the internal pudendal artery gives off the artery of the vas deferens, the caudal vesical artery and a branch directed to the accessory sexual glands; it then continues as ventral perineal artery and gives rise to the penile artery and preputial branches. In the female, the internal pudendal artery emits the caudal vesical artery and continues as ventral perineal giving off branches for the clitoris, the vulva and the vaginal vestibule (Autino et al., 2019).

The external iliac artery irrigates the pelvic limb, the caudal abdominal wall, and the external genital organs. It gives rise, in sequence, to the following collaterals: the deep iliac circumflex artery, distributing to the muscles of the abdominal wall; the deep femoral artery directed ventrocaudally and passing cranial to the pubis between the muscles of the region; the pudendal-epigastric trunk, directed to the external genitalia and abdominal wall by giving off the middle vesical, the caudal epigastric directed to the internal oblique abdominal muscles and cremaster, and the external pudendal arteries, branching into the ventral scrotal artery, the ventral labialis and the mammary arteries (Autino et al., 2019).

The external iliac artery, after giving off the deep femoral artery, continues as femoral artery, which, in turn, gives rise to multiple collaterals: the superficial iliac circumflex artery, the lateral circumflex femoral artery, the well-developed saphenous artery directed medially in the thigh, the descending artery of the knee, the nutritious artery of the femur, and the caudal

femoral arteries. After the emission of the last caudal femoral artery, the femoral artery continues as popliteal artery directed to the distal femur and giving off the caudal and the well-developed cranial tibial arteries. The blood flow to the foot is supplied by the common, dorsal and plantar digital arteries, and by the dorsal and plantar metatarsal arteries (Autino et al., 2019).



*Ventral view of the abdominal aorta and its collaterals in the capybara. 1: Aorta; 2: testicular artery; 3: kidney; 4: caudal mesenteric artery (from Ibáñez Orihuela et al., 2019)*

## **Urogenital system**

### ***URINARY SYSTEM***

#### ***Cavia porcellus***

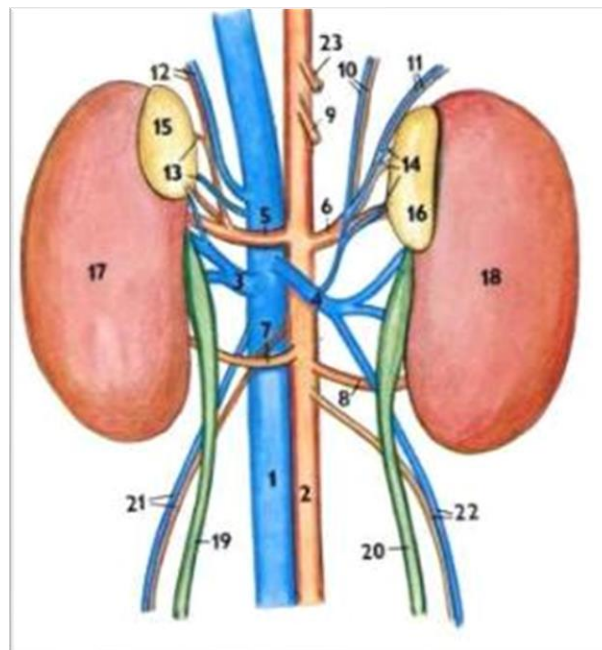
The kidneys of an adult guinea pig measure approximately 18 to 21 mm in length and 12 to 14 mm in diameter (Hargaden and Singer, 2012). The right kidney extends from the 12th intercostal space to the 3rd lumbar vertebra. The left kidney has a more caudal topography and extends from the 13th rib to the 4th lumbar vertebra (Cooper and Schiller, 1975a). Kidneys are located retroperitoneally and are not supported by a mesentery (Breazile and Brown, 1976). The guinea pig kidneys are characterized by a large renal pelvis with a single longitudinal renal papilla (Queesenberry et al., 2004; Cozzi et al., 2006). Short- and long-loop nephrons of the guinea pig kidney are equiparable in size, unlike rats, hamsters and gerbils, where one predominates over the other; specifically short-loop nephrons in rats and long-loop nephrons in hamsters and gerbils (Ichii et al., 2006a). Male guinea pigs present a higher ratio of total kidney weight to body weight in comparison to females (Ichii et al., 2006b). On the other hand, the diameter of the renal corpuscle is not significantly different between sexes, whereas female

guinea pigs present a greater number of PAS-positive granules in the proximal tubules (Ichii et al., 2006b).

The ureters measure approximately 80 mm in length and 2 mm in diameter (Hargaden and Singer, 2012). The pyriform-shaped urinary bladder of guinea pigs, when empty, is entirely located within the pelvic cavity; when distended, it extends above the margin of the pubis. Moreover, the trigone is absent in the urinary bladder of guinea pigs. The urine of guinea pigs is physiologically alkaline and cloudy containing numerous urinary crystals (Hargaden and Singer, 2012).

Microscopically, in the upper urinary tract of the guinea pigs, at the level of the pelvicalyceal junction to the kidney parenchyma, typical “pacemaker” smooth muscle cells generate pacemaker potentials in the proximal renal pelvis (Hargaden and Singer, 2012). Furthermore, within the lamina propria of the renal pelvis and pelvicalyceal junction, ICC (interstitial cells of Cajal)-like cells have been found which conduct pacemaker cellular signals to the smooth muscle cells of the renal pelvis and ureter (Klemm et al., 1999).

The ureters and bladder of the guinea pig present intramural ganglia which are associated with the muscular control of continence and micturition (Hargaden and Singer, 2012). The guinea pig urinary bladder contains 2000 to 2500 neurons that may be individual or grouped within ganglia of 40 neurons. These ganglia are more abundant on the dorsal wall of the bladder, especially at the level of the entrance of the ureters and urinary arteries into the bladder (Gabella, 1990).



**Guinea pig kidney and adrenal glands, ventral view.** 1: caudal vena cava; 2: aorta; 3: right renal vein; 4: left renal vein; 5: Right cranial renal artery; 6: Left cranial renal artery; 7: right caudal renal artery; 8: left caudal renal artery; 9: cranial mesenteric artery; 10: left caudal phrenic artery and vein; 11: left cranial abdominal a. and v.; 12: right cranial abdominal a. and v.; 13: right adrenal aa.e vv.; 14: left adrenal aa.e vv.; 15-16: right and left adrenal glands; 17-18: right and left kidneys; 19-20: right and left ureters; 21-22: right and left testicular a. and v.; 23: celiac a. (da: Popesko et al., 1992)

### ***Hydrochoerus hydrochaeris***

The capybara kidneys are located ventral to vertebrae T12 through L2, are elliptical in shape, with a smooth surface, and similar in size. The renal hilum is located ventral to the medial border, at the level of the first lumbar vertebra. The left kidney is in relation with the base of the spleen, whereas the right kidney is in communication with the dorsal border of the liver. The ureters and urinary bladder do not present differences with the other domestic species. The urinary meatus is an independent and ventral opening in the cavity shared by the digestive and genital tracts. The paired adrenal glands, similar in size and shape, are located medial to the kidneys and the right one is displaced cranially (Resoagli et al., 2009).

The capybara kidney is irrigated by a single renal artery originating from the aorta, caudal to the origin of the cranial mesenteric artery (Sejín et al., 2003). Once entering the renal hilum, it subdivides into several terminal branches directed towards the renal cortex where they form the interlobular arteries until the corticomedullary margin. The interlobular arteries end by forming the arcuate arteries, which emit the afferent vessels for the glomeruli. The efferent arteries from the glomeruli empty into the capillary networks surrounding the proximal and distal convoluted tubules located in the renal cortex. The veins, which closely accompany the corresponding arteries exit the renal hilum and empty into the cranial vena cava directed towards the right atrium, as in other mammals (Sisson, 1975; Sejín et al., 2003).



***Capybara kidney.*** Lateral view. Corrosion casts using polymethacrylic resins and methyl methacrylate of the renal arteries (red), renal veins (blue), and ureter (yellow) (from Sejín et al., 2003)

## **MALE GENITAL SYSTEM**

### ***Cavia porcellus***

The paired ovoid testes measure approximately 25 mm in length and 15 mm in width and are located within scrotal pouches (Cooper and Schiller, 1975a). The well-developed epididymis, composed of a head, a neck and a tail, is located on the dorso-lateral surface of the testis, and surrounded by fat tissue, with the tail giving rise to the ductus deferens (Breazile and Brown, 1976). The inguinal canals of the guinea pig, like in rabbits, are widely open throughout the life of the animal, so that testes can be retracted into the pelvic cavity (Hargaden and Singer, 2012; Stan, 2015).

The S-shaped penis measures approximately 50 mm in length and 5 mm in diameter and consists of a body and a glans with an associated intromittent sac (Cooper and Schiller, 1975a).

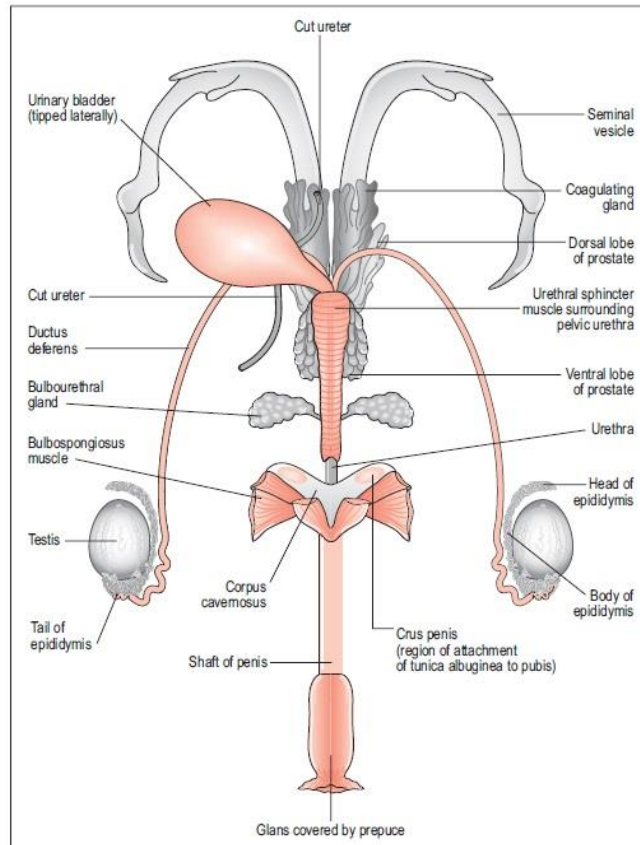
A unique feature of hystricomorphs is the presence of saw-toothed white spurs arranged on the cranial, lateral and ventral surfaces of the glans and extending in two parallel lines from

the urethral orifice to the glans. Guinea pigs present an os penis within the dorsal surface of the entire length of the glans (Cooper and Schiller, 1975a). The aforementioned intromittent sac is also a unique feature of hystricomorphs: during erection, thanks to the presence of inner longitudinal folds continuous with the corpus spongiosum and that of elastic retractor tendons attached to the base of the intromittent sac, the sac everts with two 3-5 mm-long horny styles that protrude externally. The functional role of the intromittent sac has yet to be clarified (Cooper and Schiller, 1975a).

The urethra is composed of a pelvic and a spongy portions. The pelvic part extends, with a straight cranio-caudal course, from the neck of the urinary bladder to the penis, passing through the pelvic canal, and it measures 15-25 mm in length and 4 mm in diameter (Brown and Mans, 2007). The spongy part of the urethra is 33-50 mm long and 3 mm wide and opens externally at the urethral orifice. The urethral sphincter is incomplete dorsally, except at the level of the prostate (Cooper and Schiller, 1975a).

As far as the musculature of the urogenital tract is concerned, the male guinea pig is characterized by a well-developed musculus sphincter vesicae (bladder outlet), a poorly-developed musculus sphincter urethrae, which surrounds the caudal urethra, a strong musculus sphincter urethrae transversostriatus partially surrounding the urethra dorsally, a strong ventral longitudinal urethral muscle (musculus dilatator urethrae) and a weak musculus ejaculatorius originating from the colliculum seminalis. Finally, unlike humans, guinea pigs have a dorsal longitudinal urethral muscle extending from the bladder sphincter to the colliculum seminalis (Neuhaus et al., 2001).

The accessory glands of the genital system of the male guinea pigs are four: the seminal or vesicular glands, the prostate gland, the coagulating glands and the bulbourethral glands (Queesenberry et al., 2004). The paired and well-developed seminal vesicles measure 100 mm in length and 6-9 mm in diameter; they appear as long and coiled, blind transparent sacs located ventral to the ureters and opening into the urethra by ducts caudodorsally to the ductus deferens (Cooper and Schiller, 1975a). The prostate gland is bilobed, with a smaller ventral lobe and a larger dorsal lobe connected by a transversal isthmus, located caudomedial to the coagulating glands and lateral to the base of the seminal vesicles (Cooper and Schiller, 1975a). The prostate and coagulating glands are at the base of the seminal vesicles and in close contact (Stan, 2015). The paired coagulating glands are closely related to the prostate, lobulated and pyramid-shaped, lying caudal to the urinary bladder (Cooper and Schiller, 1975a; Neuhaus et al., 2001). Finally, the small and oval bulbourethral glands are lobulated and each connected to the urethra by a single duct (Cooper and Schiller, 1975a; Stan, 2015).



**Guinea pig male genital system. Ventral view (from O'Malley, 2005)**



**Guinea pig male genital system. Dorsal view. Note the topography of bulbourethral glands caudally to the prostate and the well-developed seminal vesicles (from: Stan, 2015)**

### ***Hydrochoerus hydrochaeris***

The male capybara does not have a properly defined scrotum and the testes are located in the inguinal region subcutaneously (Paula and Walker, 2013). The average mass of capybara testes is 34.4 grams, with the two testes comprising 0.14% of body mass (Moreira et al., 1997).

The testicular layers are the same as those observed in other mammals, although the cremasteric tunic is significantly more developed, which, combined with a wide inguinal canal, allows testicular retraction into the abdominal cavity (Paula and Walker, 2013). The adult male

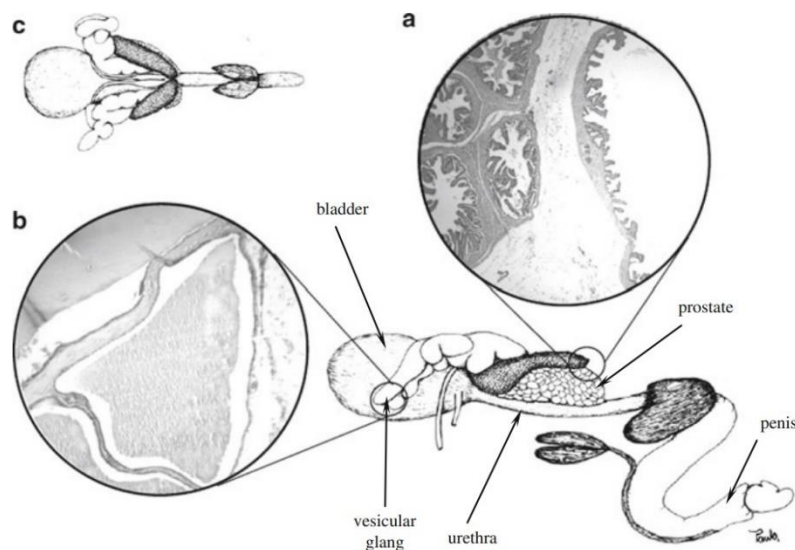
capibara is characterized by a wide anogenital invagination which is composed of the penis, the anus located dorsally and a pair of paranal scent glands, with the parallel anal sacs being covered with fur and oily secretions and used in both sexes for glandular marking (Macdonald and Herrera, 2012; Paula and Walker, 2013). The penis is flexed caudally: the base of the penis is directed cranially and the middle third presents a ventrocaudal curvature of 180°, with its distal extremity pointed caudally. The penile gland opens externally through a urethral sinus that has an inverted T shape and comprised of the external urethral ostium connected to the opening of the terminal invagination. The urethral sinus in capibara, unlike in equids (Dyce et al., 2015), is functionally related to penile erection (Paula and Walker, 2013), since the gland expands as a result of blood flow into the corpus spongiosum of the penis, promoting the reversal of the urethral sinus of the gland and the appearance of the so-called bulb of the gland, which causes the fixation of the penis in the female genital tract during copulation. To permit an increased rigidity of the penis, capibara have a penile bone, which originates from the ventral aspect of the coxal bone and occupies the distal third of the free part of the penis which lacks cavernous bodies. Well-developed ischiocavernosus muscles fixate the penis to the ischiatic arch (Paula and Walker, 2013).

The accessory genital glands of the capibara are the well-developed vesicular glands and the prostate, whereas bulbourethral glands have not been detected (Paula and Walker, 2013). The accessory glands are linked to seminal production and located dorsal to the long and thin pelvic urethra covered by the urethral muscle (Paula and Walker, 2013).

The ductus deferens of the capibara opens in the seminal colliculus in proximity to the ostium of the vesicular glands through two dilatations called ampoules of the ductus deferens (Ojasti, 1973). Histologically, the ampoules are lined with a pseudostratified epithelium without microvillousities. The mucosa lacks glands, whereas the muscular tunic is composed of an internal longitudinal layer, a middle circular layer and an external longitudinal layer (Paula and Walker, 2013). The paired and well-developed vesicular glands are located dorsal to the neck of the bladder and present digitiform projections, which range in number from 2 to 14 in each gland (Ojasti, 1973). The vesicular glands open in the seminal colliculus through an independent ostium. Histologically, the vesicular glands are composed of large acini containing abundant secretion. The epithelium is pseudostratified, with a well vascularized tunica propria. The muscular tunic consists of a circular internal and a longitudinal external layer of smooth muscle. The prostate gland is lobulated and coated with a layer of connective serosa. The lobules of the prostate, grouped into a dorsomedial and a ventrolateral portions, are located dorsal to the pelvic urethra. The lobes are lined internally by a simple cuboidal prismatic epithelium. The mucosa of the lobule lumen presents folds filled with vascularized loose connective tissue. The ventrolateral portion of the prostate is characterized by an accumulation of secretes, causing an increase in lumen and a distension of the foldings (Ojasti, 1973; Paula and Walker, 2013).

The architecture and structure of the capibara testicles is very similar to those observed in other species (Paula and Walker, 2013). The testicular albuginea, rich in blood and lymph vessels, penetrates the testis following an inverted trajectory from the efferent ducts, and it continues with the testicular mediastinum. Large connective septa deriving from the albuginea converge at the mediastinum and demarcate the lobes that contain the seminiferous tubules and a wide intertubular space. The testicular mediastinum occupies the central portion of the testis and is positioned in a longitudinal manner. The peculiarity of the histological analysis of adult capibara testes is the abundance of Leydig cells and the abundant network of lymphatic spaces in the intertubular compartment. The extensive lymphatic space is composed of a continuous parietal endothelial layer in contact with the seminiferous tubules, and of a visceral layer in contact with the Leydig cells and the blood vessels. This pattern is also seen in guinea pigs and chinchillas (Fawcett et al., 1973; Paula and Walker, 2013). Unlike canids and equids, for

instance (França and Russel, 1998), in male adult capybaras 50% of the testicular parenchyma volume is occupied by the intertubular compartment, which is mainly composed of Leydig cells (Paula and Walker, 2013).



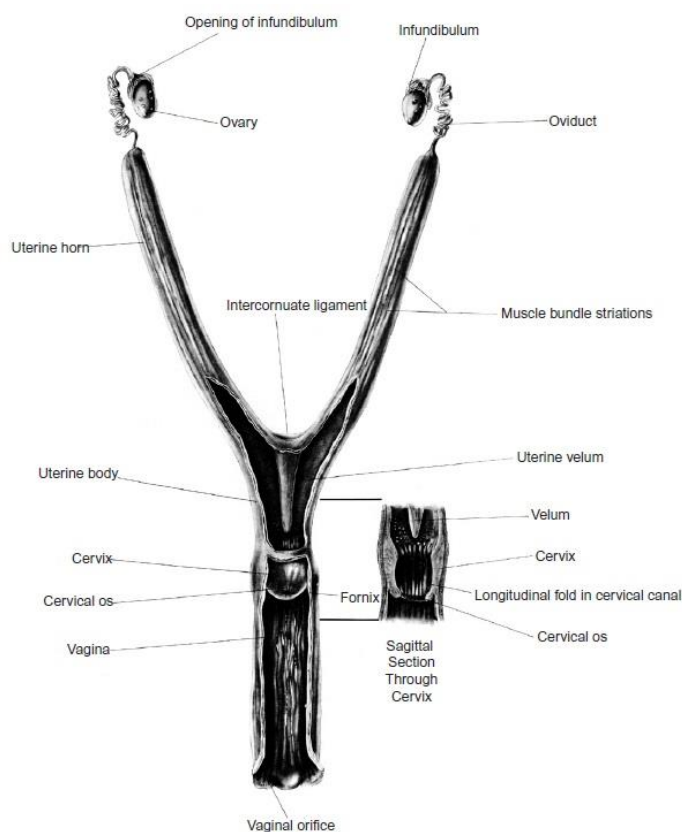
*Schematic representation of a left-side view of the bladder, genital glands and penis in adult capybaras. Histological sections of the vesicular gland acini (b) and of the prostate (a); c: dorsal view (from Moreira et al., 1997)*

## FEMALE GENITAL SYSTEM

### *Cavia porcellus*

The guinea pig ovaries measure approximately 3-6 mm in length by 2-4 mm in height by 2-3 mm in width. The right ovary is located caudolateral to the right kidney, whereas the left ovary is craniolateral to the left kidney. The oviducts measure 50-60 mm in length and 1 mm in diameter. The female guinea pig has a bicornate uterus consisting of paired uterine horns which measure 30-50 mm in length and 3 mm in diameter each, of a poorly-developed uterine body, measuring 12-20 mm in length and 6 mm in diameter, and of a single os cervix. The vagina is about 30-40 mm long and is composed of well-developed longitudinal ridges. The vagina lacks a vaginal vestibule (Cooper and Schiller, 1976). The external vaginal orifice is U-shaped and is covered by a membrane that opens only at estrus, parturition, and at around the 26th-27th day of gestation (Weir, 1974b). The pubic symphysis widens by 50 times during parturition. The paired mammary glands lie laterally to either side of the midline (Cooper and Schiller, 1976).





***Guinea pig female reproductive system. Ventral view (from: Cooper and Schiller, 1975a)***

### ***Hydrochoerus hydrochaeris***

The capybara ovaries are located in the sublumbar region, at the level of the third lumbar vertebra in contact with the caudal pole of the corresponding kidney, measuring approximately 2.2-3 cm in length, 2 cm in width and 0.5-0.8 cm in thickness. The ovaries are completely covered by the ovarian bursa, analogously to the bitch, and held by the meso-ovary (Pradere et al., 2006; Resoagli et al., 2009). The ovaries are ovoid in shape, have a smooth surface, yellowish-red in color and flattened dorso-ventrally (Resoagli et al., 2009). The two layers that make up the ovarian bursa (the mesosalpinx and the mesoovarium) continue caudally to the cranial end of the uterine horn (cornus uteri), thus forming the ovarian ligament (ligamentum ovarii proprium). Cranially, the two layers of the ovarian bursa extend to the inner aspect of the last rib, forming the suspensory ligament of the ovary (ligamentum suspensorium ovarium) (Pradere et al., 2006).

The uterine tubes have a sinuous trajectory, are in relation to the medial surface of the ovarian bursa, and are supported by the mesosalpynx, with the ovarian extremity (infundibulum) of greater diameter and the uterine extremity continuous with the uterine horn (Resoagli et al., 2009). The uterine extremity presents an approximate length of 12 cm, and a diameter of 3.5 mm in the region of the infundibulum (infundibulum tubae uterinae), of 2 mm at the tubouterine junction (pars uterina) (Pradere et al., 2006).

The uterus is located, for the most part, in the sublumbar region of the abdominal cavity, even though part of it extends into the pelvic cavity. The uterine horns are two long, rectilinear V-shaped horns with the caudal vertex at their junction with the uterine body, and from this point they diverge towards each of the kidneys. The body of the uterus (corpus uteri) is cylindrical, presenting an approximate length of 5 cm and is entirely located in the abdominal cavity. Externally, it appears as a single duct; internally, however, it presents a middle partition:

there exist two ducts throughout the body, which are the continuation of each of the horns. The neck or cervix of the uterus (cervix uteri) is located in the pelvic cavity. It has an approximate length of 4- 6 cm, with a transverse diameter of 3 cm and a dorsoventral diameter of 1.5 cm. Internally, the cranial portion of the cervix presents a double duct that represent the continuation of the two ducts present in the body. In the caudal third, the septum that separates them terminates, constituting a single duct that ends in the external uterine orifice and empties into the vagina (Pradere et al., 2006; Resoagli et al., 2009).

The vagina is a tubular organ, approximately 15 cm long with longitudinal folds caudally. The vulva is located dorsal to the urinary meatus and ventral to the anus; the clitoris is slightly conical and poorly-developed. The mammary gland is composed of 5 pairs of nipples: 1 axillary, 1 thoracic, 2 abdominal and 1 inguinal (Resoagli et al., 2009).

The structures that make up the female genital tract of the capybara are irrigated by the ovarian, the uterine and the vaginal arteries. The ovarian arteries originate from the ventral surface of the abdominal aorta, approximately 4 to 6 cm caudal to the origin of the respective renal arteries, the origin of the right artery being slightly caudal in relation to the left ovarian artery. Each artery has a straight course extending approximately 7cm, with the right obliquely crossing the ventral face of the caudal vena cava and the right psoas muscle, while the left crossing the left psoas muscle in the same manner. Each one gives rise to a branch that contributes to the irrigation of the uterine tubes (ramus tubarius). Following the origin of this branch, the course of the artery becomes tortuous and gives off a second collateral branch (ramus uterinus) that anastomoses with the terminal branches of the uterine artery. The final portion of the ovarian artery divides into small terminal branches that are distributed in the cranial third of the corresponding ovary and anastomose with one of the terminal branches of the uterine artery (Pradere et al., 2006).

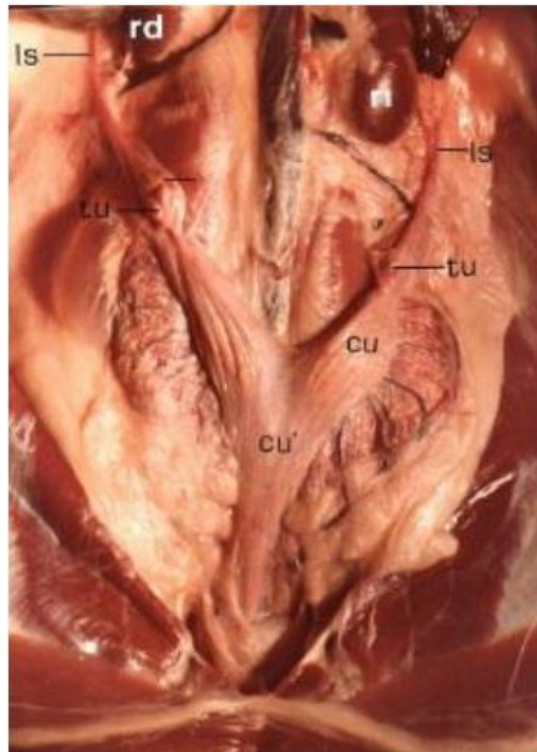
The uterine artery originates from the dorsal surface of the common iliac artery. In its initial course, the uterine artery is located between the common iliac vein and the medial iliac lymphnodes, then it turns around the vein and crosses the corresponding ureter, heading to the union of the uterine body with the cervix, and finally dividing into two branches. The cranial branch courses in the middle portion of the broad ligament of the uterus, emitting from its dorsal surface 5 to 6 small branches for the broad ligament. It then emits, from its ventral surface, 28 to 35 branches directed towards the uterine horns and body, included within the two sheets of the broad ligament, and taking in their initial portion a tortuous path, remaining either indivisible or further dividing into 2 to 5 arterial branches (Pradere et al., 2006).

The branches that irrigate the uterine horns are directed towards their mesometrium edge, each of them dividing into two branches that penetrate the wall of the uterine horns with a tortuous course, anastomosing in an arcade with the contralateral. The branches that supply the body of the uterus are directed towards its lateral margins, divide into several dorsal and ventral branches with a tortuous course through the wall, and anastomosing with their correspondent branches on the opposite side. The cranial branch gives rise to two terminal branches: one that goes towards the uterine tube, which contributes to its irrigation, anastomosing with the tubal branch deriving from the ovarian artery. The other branch supplies blood to the caudal two thirds of the ovary, dividing into two small vessels: one that irrigates the caudal one third of the ovary and the other that anastomoses with the terminal branch of the ovarian artery, contributing to irrigate the middle and cranial third of the ovary, emitting 4 branches that contribute to irrigate the ovarian sac (Pradere et al., 2006).

The caudal branch of the uterine artery runs parallel to the lateral margins of the body and cervix, distributing in the caudal portion of the body and cervix, further emitting dorsal and ventral branches that anastomose with those of the opposite side. The caudal continuation of this branch anastomoses with the cranial branches of the vaginal artery (Pradere et al., 2006).

In conclusion, the uterine artery represents the main arterial vessel to the ovary, sending

segmental branches to the uterine horns and body, branching off into vessels that penetrate into the walls of the uterus and anastomose with the opposite homologue vessels (Pradere et al., 2006).



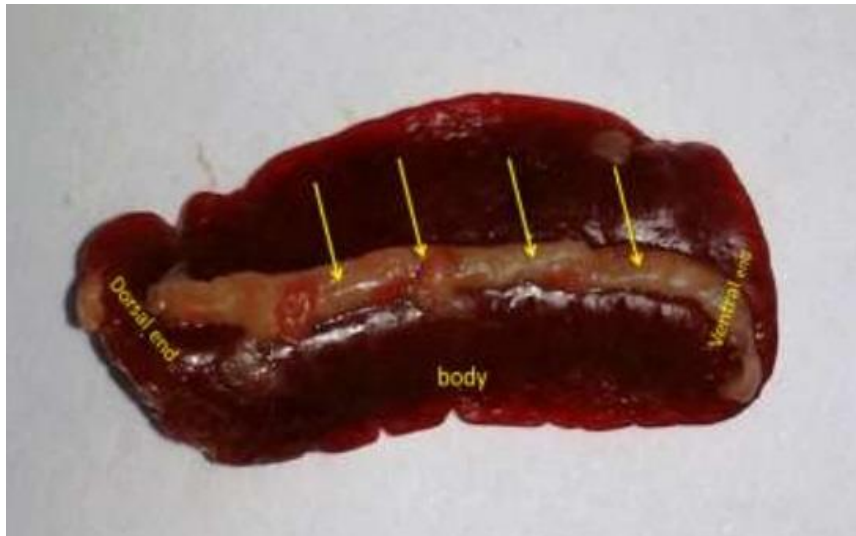
*Capybara in-situ female genital tract, ventral view. Cu: uterine horn; cu': uterine body; tu: uterine tube; ls; ovary suspensor ligament; rd: right kidney; ri: left kidney (from: Pradere et al., 2006)*

## Lymphatic system

### Spleen

#### *Cavia porcellus*

The spleen of guinea pigs is relatively large, broad and irregularly-shaped in comparison with other species such as most rodents and rabbits (O'Malley, 2005; Cozzi et al., 2006). It is quadrilateral in shape and narrowing towards the dorsal end, with the hilum extending along its entire surface (H Qasem et al., 2015) It measures approximately 26 mm in length and 13 mm in width, at its widest point (Breazile and Brown, 1976): It is red-brown in color, with a soft to firm consistency, and covered by a thin transparent capsule, the tunica serosa (Hargaden and Singer, 2012). It is composed of lymphatic tissue arranged around small-sized arteries (Cozzi et al., 2006). It is located in the left cranial abdomen, on the left lateral side of the greater curvature of the stomach and connected to it by the gastrosplenic or gastrolial ligament (Breazile and Brown, 1976). Moreover, its cranial portion is attached to the diaphragm through the phrenicosplenic ligament (Hargaden and Singer, 2012).

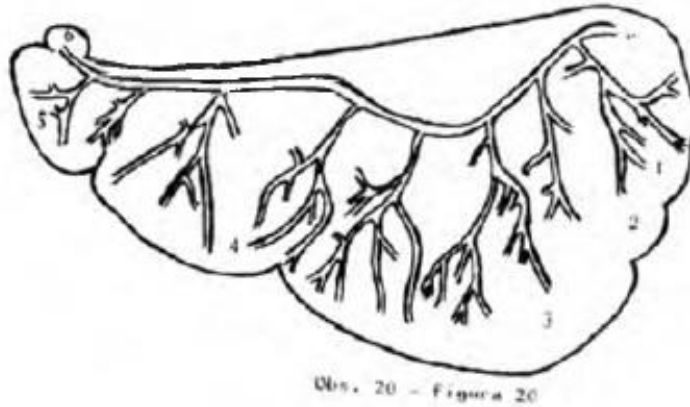


*Guinea pig spleen. Visceral surface. The hilus (yellow arrows) extends along the surface of the organ (from: H Qasem et al., 2015)*

### ***Hydrochoerus hydrochaeris***

The spleen of the capybara, externally, has a shape that resembles that found in equids, that is, slightly triangular, with a wider portion in the hilar region located cranially, where the splenic artery penetrates, and gradually decreasing in width in the caudal direction, as the splenic artery courses through it and emits branches directed to its parenchyma (Germinaro et al., 1997). According to Germinaro et al. (1997), the capybara spleen can either present continuous margins, without fissures, or, in the majority of cases, it can have a polylobated appearance, with incisures being located especially in the ventral and caudal margins of the organ. The capybara spleen can be composed of 3 to 7 splenic lobes total (Germinaro et al., 1997). In a minority of cases, an accessory splenic lobe completely separated from the splenic parenchyma can be found. The number of arterial segments branching from the splenic artery can vary from a minimum of 5 to a maximum of 16, with 10 being the most frequent occurrence. The arterial branches supplying different lobes often contract anastomoses. A significant positive correlation exists between the number of splenic lobes and the number of arterial segments (Germinaro et al., 1997).

According to Makita et al. (1998), on the other hand, the dorsal edge of the spleen of the capybara presents two sharp and deep sulci, so that two small portions are divided from the rest of the body of the spleen.

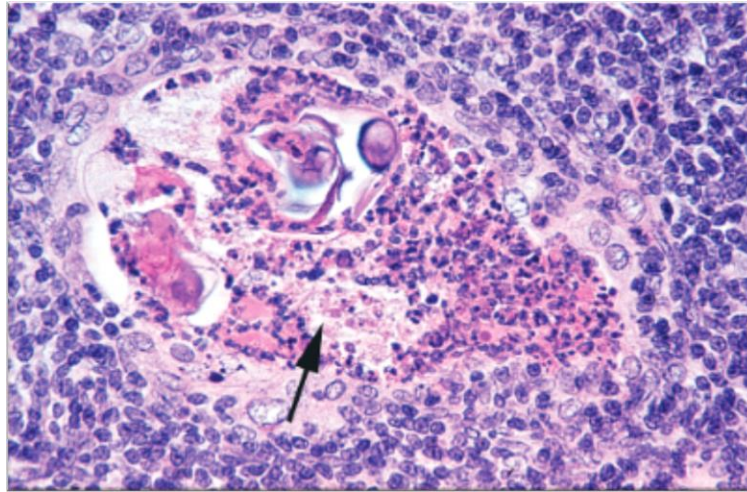


*Schematic representation of the capybara splenic artery branching through the spleen. Numbers from 1 to 6 indicate the splenic lobes (from: Germinaro et al., 1997)*

## Thymus

### *Cavia porcellus*

In immature subjects, the functional thymus lies in the cranial mediastinum and ventral cervical region, surrounding the trachea ventrally and laterally in the neck (O'Malley, 2005; Cozzi et al., 2006). It extends from the caudal angle of the mandible to halfway to the thoracic inlet; it is composed of two paired pink-tan elongated oval lobes with fat and fascia connecting the lobes and characterized by the absence of afferent lymphatic vessels (Ernström and Larsson, 1970; Cooper and Schiller, 1975a). Paired accessory thymic nodules are common, located near the parathyroid glands or even fused with them (Cooper and Schiller, 1975a; Cozzi et al., 2006). The superficial cervical thymus is located beneath the platysma and ventral to the infrahyoid muscles, triangular in shape and in contact with the parotid gland laterally and with the submandibular gland craniodorsally (Yamasaki, 1995). A so-called cranial thymic chain is often present, consisting in a string of lobules extending cranially from the cranial end of the thymus to cross over the hypoglossal nerve lateromedially (Yamasaki, 1995). The parathymus lymphnodes are found in proximity of the thymus (Cozzi et al., 2006). Hassall corpuscles within the thymus are physiological structures that contain desquamated epithelium, cellular debris and heterophils and are often associated with the degenerating thymic cells, which sometimes can evolve into cystic structures (Barthold et al., 2016). The thymus maximum weight occurs at birth. By 12 months of age, the thymus involutes and gets replaced by adipose tissue in the adult animal (Breazile and Brown, 1976, Harkness and Wagner, 1995). The superficial cervical thymus is irrigated by the superior and inferior superficial cervical thymic arteries. The superior superficial cervical thymic artery arises from the lingual artery, the superior laryngeal artery, the superior thyroid artery or the common carotid arteries, whereas the inferior superficial cervical thymic artery originates from the homologue superior (Yamasaki, 1995). Due to the accessible topography of the thymus in this species for removal, measurements and manipulations, the guinea pig has been often used as an animal model for immunology research studies (Hargaden and Singer, 2012). A peculiarity of the guinea pig is its resistance to the immunosuppressive effect of corticosteroid drugs: even after prolonged therapy cycles, guinea pigs do not show leukopenia, immunodepression or decreased thymic functionality (Sisk, 1976).



***Histological organization of a young guinea-pig thymus. Note a Hassall's corpuscle (arrow) containing desquamated epithelium, cellular debris and heterophiles (from: Barthold et al., 2016).***

## **Lymph nodes**

### ***Cavia porcellus***

The guinea-pig lymph nodes are red-brown, oval- or bean-shaped nodules located within the lymphatic vessels. They are capsulated, where the capsule is smooth and transparent, and present a small *hilus* for the entrance of blood vessels, nerves and lymphatic vessels.

The mandibular lymph nodes of the guinea pig are composed of 2 to 4 nodes located at the level of the mandible, along its ventral border (O'Malley, 2005). The cervical lymph nodes, 5 to 8 mm in diameter, are located cranial to the scapula and embedded in adipose tissue. The deep cervical lymph nodes lie between the internal and external jugular veins in proximity to the trachea, and covered by the thymus in juveniles (O'Malley, 2005).

### ***Hydrochoerus hydrochaeris***

The head and neck lymphocenters of the capybara comprise the mandibular, the parotid, the superficial cervical, and the cranial, caudal and middle deep cervical lymph nodes (Bode et al., 2009). The mandibular lymph nodes are 1 to 2 ovoid nodes, which measure approximately 20 mm in length and 15 in width and are located ventral to the intermandibular space, rostral to the mandibular gland, ventrally to the larynx and covered by the cutaneous facial muscle (Bode et al., 2009). The parotid lymph node is small and is located ventral to the temporomandibularis junction, on the caudal border of the mandible, covered by the parotid gland (Bode et al., 2009). The superficial cervical lymph nodes are two to three ovoid-shaped nodes, located proximal to the scapulo-humeral junction, over the cranial border of the prescapular pectoral muscle, covered by the brachiocephalic muscle, along the course of the superficial cervical vein (Bode et al., 2009). The cranial deep cervical lymph nodes are two small nodules located lateral to the larynx, covered by the caudal border of the parotid gland (Bode et al., 2009). The caudal deep cervical lymph nodes are two small nodules, located on the ventral aspect of the trachea, at the level of the 14th tracheal ring, covered by the sternohyoid and sternothyroid muscles. The middle deep cervical lymph nodes, larger than the cranial and caudal deep cervical lymph nodes, are two lymph nodes located on the sides of the trachea, at the level of the middle third of the neck, along the course of the common carotid artery (Bode et al., 2009). The lymphocenters identified in the capybara resemble those generally described in other species

such as the pig; however, in contrast to the pig (Getty, 1982), the retropharyngeal lymph nodes have not been identified in the capybara (Bode et al., 2009).

The lymphocenters of the thoracic cavity of the capybara comprise the left and right tracheobronchial lymph nodes, the dorsal bronchial and the sternal lymph nodes (Cao et al., 2011). The left tracheobronchial lymph node is an unpaired elliptical nodule located caudoventral to the aortic arch, dorsolateral to the tracheal bifurcation, in proximity of the left main bronchus. The right tracheobronchial lymph node, ovoid in shape, is located dorsal to the right main bronchus, and dorsomedial to the oesophagus. The dorsal or apical bronchial lymph node is located dorsal to the trachea, just caudal to its bifurcation. Finally, the elongated suprasternal or sternal lymph node, elongated is located dorsal to the first sternbrae, and cranial to the internal thoracic artery. Caudal mediastinal lymph nodes have not been identified in capybaras (Cao et al., 2011).

The lumbar lymphocenter of the capybara is located in the sublumbar region, extending from the first lumbar vertebra to the base of the sacrum and it comprises the abdominal phrenic, the celiac mesenteric, the renal, the lumbar aortic, and the medial and lateral iliac lymph nodes (Bode et al., 2008).

The abdominal phrenic lymph node is ovoid in shape and situated caudal to the pillars of the diaphragm, covered by the kidneys, ventral to L1 and in correspondence with the lateral border of the major psoas muscle, measuring 18 mm in length and 10 mm in width.

The celiac mesenteric lymph node is located caudal to the abdominal phrenic lymphnode, at the origin of the celiac and mesenteric arteries.

The renal lymph nodes are located at the renal hilum, located along the course of the renal arteries, and surrounded by adipose tissue. They are ovoid in shape, are in number of 5 to 6 (2 in the right kidney and 3–4 in the left), with an approximate length of 6 to 7 mm (Bode et al., 2008).

The lumbar aortic lymph nodes are 6 to 8 small lymph nodes, 9 to 32 mm long and 9 mm wide, located on both sides of the aorta and caudal vena cava, partly covered by adipose tissue, extending from the kidneys to the bifurcation of the aorta.

The medial iliac lymph nodes are 3 to 4 large ovoid nodes, located medial to the iliac artery, close to its origin. The lateral iliac lymph node is relatively large, 35 mm long by 5 mm wide and is located lateral to the course of the iliac artery, close to the aortic bifurcation (Bode et al., 2008).

The histoarchitecture of the lymph nodes of the capybara does not differ to that observed in other domestic mammals (Getty, 1982), with well-defined cortical and medullary regions (Bode et al., 2008).

## **Endocrine system**

### ***Adrenal glands***

#### ***Cavia porcellus***

The well-developed adrenal or suprarenal glands of the guinea pig are triangular/pyramidal in shape, bilobed, flattened, and grayish to yellowish-brown in color (O'Malley, 2005; Abass, 2017). The medial lobe of the adrenal gland is larger than the lateral lobe (Cozzi et al., 2006): the adrenal glands are much larger than those of other mammals, due to the expansion of their cortical portion (Cozzi et al., 2006). They are embedded in adipose tissue and in relation to the craniomedial surface of the corresponding kidney, within the retroperitoneal cavity (O'Malley, 2005; Abass, 2017). In cross-section, the adrenal gland

presents a yellowish outer cortex, which represents 80% to 90% of the organ, and a brownish inner medulla (Abass, 2017). The adrenal cortex has a uniform thickness, whereas the adrenal medulla is characterized by an irregular shape (Abass, 2017). The adrenal glands derive, embryologically, from the ectoderm and the mesoderm; specifically, the medulla originates from ectodermal neural crest cells and during their migration, they are surrounded by the mesodermal cells of the adrenal cortex, which derive from the intermediate mesoderm (Abass, 2017). Histologically, the adrenal gland is surrounded externally by a well-developed capsule of connective tissue which presents trabecular projections that penetrate into the cortex and medulla. The adrenal cortex is divided into three zones, which, from external to internal, are the zona glomerulosa, the zona fasciculata and the zona reticularis (Abass, 2017). The zona glomerulosa consists of thin and rounded or arched clusters of columnar cells, found near the capsule, and cuboidal cells found near the deeper layer. The broad but not well-defined zona fasciculata is three times thicker than the zona glomerulosa and consists of cells arranged in straight cords of one or two cells positioned at right angles towards the surface of the gland. The zona reticularis contains cells arranged in a reticular or net-like manner by forming cords. The medulla consists of cells that are loosely arranged into clusters and cords, and that secrete noradrenaline and adrenalin and appear more basophilic than the cellular population of the cortex; chromaffin cells are columnar in shape and basophilic when stained (Abass, 2017).

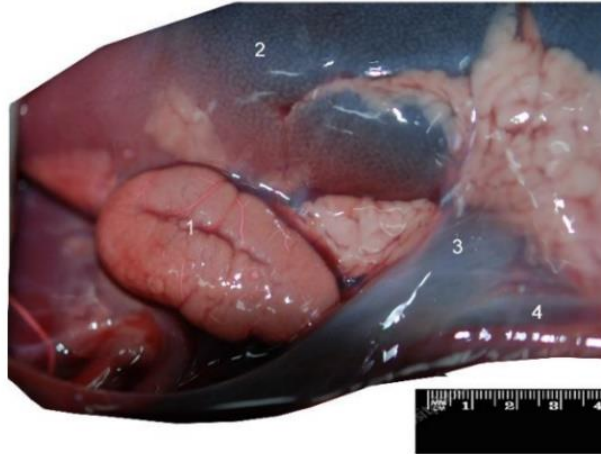


*Guinea pig adrenal gland, transversal section, showing the pale outer cortex and the darker inner medulla (from Abass, 2017)*

### ***Hydrochoerus hydrochaeris***

The paired adrenal glands of the capybara, similar in size and shape, are located medial to the kidneys and the right one is displaced cranially (Resoagli et al., 2009). Each adrenal gland is vascularized by the caudal phrenic artery, the renal artery and the aortic artery (Ibáñez Orihuela et al., 2019). A study has demonstrated the presence of Kurloff cells in several tissues of capybaras, such as the spleen, and the adrenal medulla (Jara et al., 2005). Kurloff cells have been extensively studied in guinea pigs (Eremin et al., 1980), where they are especially present in the peripheral blood of pregnant females. These cells are mononuclear cells with lymphocyte and monocyte properties, immune and natural killer activity, and anticancer properties (Eremin et al., 1980; Debout et al., 1984). Unlike guinea pigs, they are present in higher concentrations in tissues and organs, being particularly abundant in adrenal glands, rather than in circulating peripheral blood (Jara et al., 2005).





*Capybara adrenal gland. Medial view. 1: adrenal gland; 2: kidney; 3. renal vein; 4: caudal vena cava (from Ibanez Orihuela et al., 2019)*

## **Pineal gland**

### ***Cavia porcellus***

The pineal gland is a neuroendocrine gland that secretes the hormone melatonin (Møller and Baeres, 2002). Its embryological derivation is from the neural tube and it is located at the border between the mesencephalon and diencephalon and is described as part of the epithalamus (Møller and Baeres, 2002). The parenchyma of the pineal gland consists of cords of cells separated by capillaries and composed of wide perivascular spaces. Macroscopically, the rodent pineal gland is elongated and subdivided into a superficial gland located at the dorsal surface of the brain and a more innervated deep gland at the level of the brain stem, which are connected by the pineal stalk (Møller and Baeres, 2002). It is composed of five cell types: the pinealocytes which produces hormones and contain synaptic ribbons, the interstitial cells, the perivascular phagocytes, the neurons, and the peptidergic neuron-like cells (Møller and Baeres, 2002). Nerve fibers innervating the pineal gland originate from perikarya located in the sympathetic superior cervical ganglio, the parasympathetic sphenopalatine ganglion and the otic ganglion; in addition, nerve fibers originating from perikarya located in the brain also innervate the pineal gland via the pineal stalk (Møller and Baeres, 2002).

The pineal glands of the guinea pig contain numerous photoreceptor cells (Cozzi et al., 2006).

### ***Hydrochoerus hydrochaeris***

The pineal gland of capybaras is described as a small structure projecting dorsally from the diencephalon to the brainstem through an evagination of the roof of the third ventricle (Alves, 2019). It is located between the occipital brain lobes and the cerebellar vermis, on the roof of the third ventricle, in proximity to the rostral colliculus. It is whitish or brownish in color, it projects beyond the brain contour, it is elongated and composed of a base with two peduncles, a stem and an apex; the apex is surrounded by a menyngeal tent of dura mater and it contains a cavity (Branco et al., 1997). It measures approximately 1.3 mm, 1.2 mm and 2.0 mm in length at the base, stem and apex, respectively. It is covered by a vascularized capsule of connective tissue and the parenchyma shows pinealocytes, arranged in cords, intermingled with blood vessels, connective tissue and neuroglial cells, containing condensed nuclear granules (Branco et al., 1997).

The pineal gland of the capybara is vascularized by the terminal branches of the caudal choroidal artery and of the rostral tectal artery, both originating from the caudal cerebral artery (Reckziegel et al., 2017).

## **Thyroid gland**

### ***Cavia porcellus***

The thyroid gland of guinea pigs consists of paired lobes, appearing with a rounded cranial head and a slender tail (Yamasaki, 1995). The thyroid lobes are located along the caudal half of the larynx and trachea extending caudally to the 6th tracheal cartilage. A thyroid isthmus connecting the two lobes has been reported in a minority of cases (Yamasaki, 1995). The vascularization of the thyroid of guinea pigs has been seen to be more abundant and variable than that seen in humans (Yamasaki, 1995). The thyroid is vascularized most frequently by the superior thyroid artery originating from the external carotid artery, which then gives off the superior and inferior laryngeal arteries in addition to glandular rami (Yamasaki, 1995). A middle and an inferior thyroid arteries have also been described. The middle thyroid artery, arising from the external carotid artery or common carotid artery penetrates the gland cranially to then terminate in the inferior laryngeal artery. The inferior thyroid artery, arising from the common carotid artery reached the gland caudally to then end in the inferior laryngeal artery. Independent thyroid arteries have also been described arising from the lingual and the ascending pharyngeal arteries, suggesting that these represented the original thyroid arteries (Yamasaki, 1995).

### ***Hydrochoerus hydrochaeris***

The bibliography did not provide data on the thyroid gland in capybaras.

## **Parathyroid glands**

### ***Cavia porcellus***

Histomorphologically, parathyroid glands of guinea pigs consist of a fibrous capsule and a cellular parenchyma including chief and oxyphil cells (Tantawy et al., 2022). Ultrastructurally, parathyroid glands of adult guinea pigs contain several chief cells, fibroblasts and blood capillaries. Chief cells were of two types: granulated and vacuolated, with the granulated containing several organelles (mitochondria, golgi complex, lysosomes and RER), and variable-sized secretory granules and with the vacuolated cells containing few organelles and numerous vacuoles (Tantawy et al., 2022).

### ***Hydrochoerus hydrochaeris***

The bibliography did not provide data on the parathyroid gland in capybaras.

## **Pituitary gland**

### ***Cavia porcellus***

The pituitary gland is a complex endocrine gland, located at the base of the brain and lying in the sella turcica, a depression within the sphenoid bone. It in relation with the hypothalamus through a narrow stalk. Microscopically, it is composed of an epithelial component referred to as adenohypophysis and a nervous component called neurohypophysis.

Pars distalis consists of chromophilic cells, whereas pars intermedia consists of chromophobic and basophilic cells. The neurohypophysis presents nerve fibers interspersed with numerous pituicytes (Luay, 2016).

### ***Hydrochoerus hydrochaeris***

The pituitary gland is located immediately ventral to the diencephalon and is in relation with the hypothalamic tuber cinereum through the infundibulum (Alves, 2019).

Due to the prominent concavity of the pituitary fossa of the sella turcica, the hypophysis of capybaras is more developed and extended than that of other rodents and domestic mammals (Alves, 2019). It reveals focal areas of signal hyperintensity on MR images due to the abundance of neurotransmitters (Alves, 2019).

## **Central nervous system**

### ***Cavia porcellus***

The adult guinea-pig brain has an average weight of 4 g and the two cerebral hemispheres measure approximately 2.1 cm x 2.25 cm (Cooper and Schiller, 1975a). The brain is of the lissencephalic type, however characterized by the presence of few shallow sulci, which show some interindividual variation, with the larger dimples, however, tending to present a fixed topography (Cooper and Schiller, 1975a; Campos and Welker, 1976). The gross anatomical morphology of the cerebrum, ventricles, brain stem, cerebellum and spinal cord does not differ significantly from other rodents and mammals (Hargaden and Singer, 2012). The relative proportion of the cerebral cortex area occupied by sensory areas is similar to that of the capybara, whereas the forebrain structures of the guinea pig are relatively smaller than the capybara's (Campos and Welker, 1976).

A study of the sensory areas of the cerebral neocortex of guinea pigs and capybaras has shown that the representation of the buccal area (lip and perioral areas) in the main somatic sensory cortex (SI) is relatively large in the guinea pig, with the head representation constituting about 80% of the surface of the somatic sensory cortex of the mapped brain in both capybaras and guinea pigs (Campos and Welker, 1976).

The vascularization of the brain of the guinea pig is characterized by the presence of a caudal cerebral artery originating between the basilar and the internal carotid arteries (Hargaden and Singer, 2012). The small internal carotid arteries alone do not supply sufficient blood to the encephalon and a major collateral input is provided by the internal ophthalmic arteries (Shively and Stump, 1974).

The topographical anatomy of the guinea pig cerebellum has been studied in immunohistochemistry studies (Larouche et al., 2003) by using zebrin-II, a marker of compartmental cerebellar heterogeneity. A peculiarity that emerged from these studies is the complex expression pattern of zebrin II in the Purkinje cells, which show at least three levels of expression of this marker, as opposed to rats, where zebrin expression only distinguishes two classes of Purkinje cells (Larouche et al., 2003).

Moreover, the guinea-pig cerebellum presents a higher total Purkinje cell count (De Silva et al., 2021) in comparison with the rat (Sonmez et al., 2010).

The respiratory control is located in the dorsal respiratory group (DRG) and ventral respiratory group (VRG) at the medullar level. Unlike the rat and cat, however, the guinea-pig DRG is located just ventral to the tractus solitarius (Richerson and Getting, 1992).

A phylogenetic study investigating the evolution of the mammalian neocortex (Hof et al., 1999) has analyzed the immunohistochemical distribution and morphological characteristics of calcium binding proteins-immunoreactive neurons (inhibitory interneurons and pyramidal

neurons) in the neocortex of different mammalian species to help define taxon-specific patterns that can be used as phylogenetic traits. The study has set in light that calcium binding protein-containing neurons vary significantly among mammalian orders and that closely-related species show highly divergent patterns. A close phylogenetic relationship among primates, carnivores and rodents, including guinea pigs, has been identified (Hof et al., 1999).

### ***Hydrochoerus hydrochaeris***

The brain of an adult 30 kg capybara weighs around 52 grams and is more convoluted than that of the guinea pig; the cerebral neocortex of the capybara is also more fissured than that of the guinea pig (Campos and Welker, 1976).

The brain of the capybara has a greater degree of gyrification than in other rodents; it also presents a higher proportional degree of neocorticalization which implies a greater capacity of information processing in the neocortex, so as to establish complex social relationships (Ferreira et al., 2022). The capybara also displays prominent and irregularly-shaped olfactory bulbs, an elongated olfactory tract without a marked circular fissure, a marked temporal region, gyrencephaly, and conspicuous neocortical fissures (Ferreira et al., 2022).

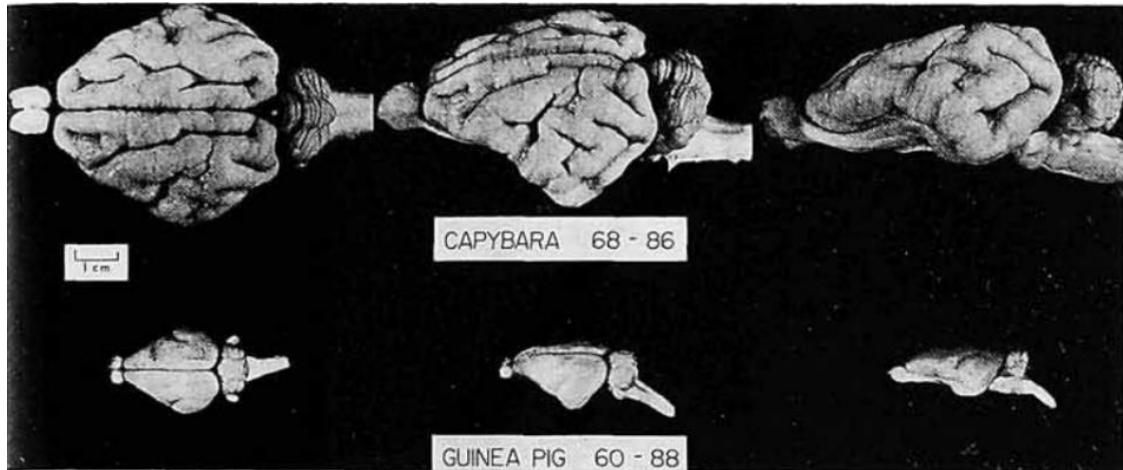
Analogously to the guinea pig, the representation of the perioral and intraoral buccal surfaces (buccal pad and mobile lip areas) in the main somatic sensory cortex (SI) is relatively large in the capybara, with the sizes of the receptive fields from these buccal parts being the smallest (Campos and Welker, 1976). Furthermore, this study showed that the head representation constitutes about 80% of the surface of the somatic sensory cortex of the mapped brain in both capybaras and guinea pigs (Campos and Welker, 1976). In the capybara, the different cortical projection areas are well-demarcated through several cortical fissures and sulci. The sulcal patterns show significant inter-individual variations; however, the deeper cortical fissures appear to be consistently situated in capybaras (Campos and Welker, 1976). All capybara forebrain structures are relatively larger than comparable guinea pig structures (Campos and Welker, 1976). Neuronal nuclei, variably-sized, especially at the cerebral cortex, are larger in the capybara, in comparison with guinea pigs (Campos and Welker, 1976). Furthermore, the proportion of surface area of the cerebral cortex occupied by the three sensory areas is similar in both capybara and guinea pig, meaning that the capybara brain does not have relatively greater amounts of nonsensory cortex, although being more fissured (Campos and Welker, 1976),

The brain base arteries, specifically the vertebro-basilar system and its derived branches for the encephalon, have been studied in the capybara (Reckziegel and Lindemann, 2017). The arterial vascularization to the encephalon derives solely from the vertebro-basilar system, as the internal carotid arteries are absent (atresic) in adult capybaras (Reckziegel and Lindemann, 2017). The right and left vertebral arteries anastomose ventral to the encephalon to form the basilar artery which gives off two collaterals, the caudal cerebellar and the middle cerebellar arteries. The basilar artery then bifurcates into right and left terminal branches, giving rise, in turn, to the rostral cerebellar arteries, the caudal cerebral arteries, the internal ophthalmic arteries and the middle cerebral artery. The basilar artery then terminates with the rostral cerebral arteries. The arterial circle closes rostrally and contracts anastomoses with the maxillary artery (Reckziegel and Lindemann, 2017).

The caudal cerebral artery irrigates the thalamus, the rostral and partially the caudal colliculum, the caudal portion of the pyriform lobe, the tentorial surface, and the dorsolateral face of the brain hemisphere, along the dorsal longitudinal and transversal fissures of the brain (Reckziegel et al., 2017). The caudal cerebral artery originates from the terminal branch of the basilar artery rostral to the root of the oculomotor nerve. After its emergence, it gives off the rostral tectal artery and crosses dorsally the cerebral peduncles to give rise to branches that irrigate the geniculate bodies and the pulvinar. Over the course of the hippocampal gyrus, it

branches into small hippocampal branches, the caudal choroidal artery rostrally, and cortical branches caudally. The caudal cerebral artery terminates by giving rise to branches for the splenium of the corpus callosum and the caudo-medial surface of the brain hemisphere (Reckziegel et al., 2017).

The cerebellum is small and compact, and its folia are arranged in a transverse pattern; the cerebellum also shows a large floccular lobe (Mones and Ojasti, 1986).



**Brains of adult capybara (top row) and guinea pig (bottom row). Dorsal, left dorsolateral and left lateral views (left to right) (from: Campos and Welker, 1976).**

## **SECOND PART**

## MATERIALS & METHODS

### Animals

The research project was partially developed at the Department of Veterinary Medical Sciences of the University of Bologna, Italy (for the study of guinea pigs) and at the Veterinary Faculty of the Universidad Nacional del Litoral of Santa Fe, Argentina (for the study of capybaras), and involved the macro- and microscopic anatomical study of the different systems. The macroscopic examination was carried out through the anatomical dissection of both species, by also making use of specific techniques, such as the execution of anatomical casts for the investigation of hollow organs.

#### *Cavia porcellus*

Thirty adult guinea pigs of both sexes, 10 for the histological study and 20 for the macroscopic anatomical study, weighing 340-600 grams, and aged 1-3 years, were used for our research purposes, following owners' permission. The animals did not present a history or clinical presentation of systemic disease.

The microscopic study involved the study of 50 tissue samples per animal, through the development of the classical histological technique.

Both macroscopic and microscopic investigations were accompanied by a photographic record. All actions were carried out in accordance with certified procedures according to ISO 9001: 2008 standards.

The entire study on guinea pigs was carried out at the Laboratory of Histology and at the Anatomical sector room of the Normal Veterinary Anatomy Unit (ANV) of the Anatomy and Physiology Service (ANFI) of the Department of Veterinary Medicine Sciences (DIMEVET) of the University of Bologna (UNIBO).

According to Directive 2010/63/EU of the European Parliament and of the 22 September 2010 Council on the protection of animals used for scientific purposes, the Italian legislation (D. Lgs. n. 26/2014) does not require any approval by competent authorities or ethical committees, as this research did not influence any therapeutic decisions.

#### *Hydrochoerus hydrochaeris*

All animals were obtained from a breeding farm of capybaras destined for meat consumption, located in the town of Chavarría, province of Corrientes, Argentina.

Six animals of both sexes were used, 4 adult breeders (2 males and 2 females) weighing between 30 and 50 kg, and two juveniles of approximately 6 months of age and weighing 20-25 kg. Prior to sacrifice, all the animals underwent sanitary control of the molecular presence/absence of *Trypanosoma evansi*, *Leptospira* spp., *Rickettsia belli*, *Ehrlichia* spp. and *Anaplasma platys*, in order to check the health status of the animals used. The parasitology analyses were carried out by the InnoVaT Laboratory (Agreements and Services of the InnoVaT

Foundation - CONICET Technological Linkage Unit, Santa Fe Delegation, Paraje El Pozo, Santa Fe).

The capybaras bred in captivity were slaughtered by the owners of the establishment with the authorization of the Directorate of Fauna, Flora and Ecology of the Secretary of Natural Resources of the province of Corrientes.

The research protocol was evaluated and approved by the Ethics Committee of the Faculty of Veterinary Sciences of the Universidad Nacional del Litoral.

The animals were processed in the aforementioned establishment, to obtain sampling of approximately 50 tissular samples per capybara for the microscopic study. The sampled tissues were transported in a fixative 37% formaldehyde carrier solution for the subsequent histological study.

Both the samples and the animals were transferred, in refrigerated form, to the Faculty of Veterinary Sciences of the UN, Esperanza, Santa Fe for further macroscopical and microscopical investigations. The tissues were processed following classical histology protocols at the Veterinary Pathology Laboratory of the Veterinary Faculty of UNL, whereas the cadavers were kept at -20°C at the Veterinary Anatomy pavilion of UNL until further processing.

## **Gross anatomy**

### **Dissection procedure**

The present study is based on the stratigraphic dissection of cadavers of 20 guinea pigs and 4 capybaras. Upon receipt, the subjects, who died from diseases not inherent to the cardiovascular, gastrointestinal or genitourinary systems, were either used fresh or immediately stored in a cold room at -20° C and thawed about two days before carrying out the dissection. Once thawed, the animals were placed on the anatomical table in right or left lateral decubitus, depending on the structures to be analyzed. An anatomical dissection by stratigraphic planes was carried out, to expose the organs to be analyzed, and the morphology, the topography and the relationships with the adjacent anatomical structures were evaluated. In case of the execution of anatomical casts of the thoracic, abdominal and pelvic cavities, the skin of the costo-abdominal region was removed, the left thoracic limb excised, and, at the level of the costal region, after having removed the skin and the more superficial muscles, the ribs were removed with a costotome, taking care to leave the diaphragm and its rib insertions intact. An access window to the abdominal cavity was then obtained by removing the skin and muscles of the left abdominal wall, in order to monitor the correct filling of the vessels of the abdominal and pelvic cavities during the execution of the polyurethane casts. Having thus obtained access to the thoracic and abdominal cavities, the course of the aorta was observed, its passage through the aortic hiatus and the course of the main arterial vessels was verified.

All the phases of the study, from the dissection of the various planes to the measurements of the anatomical structures such as blood vessels, were photographically documented using a digital camera (Fujifilm HS50) and the images were process using Adobe Photoshop CS.



## **Preparation technique of anatomical casts**

For the anatomotopographic analysis of the venous, arterial and bronchial systems of the lungs and splanchnic cavities, anatomical casts of the arteries of the abdominal, thoracic and pelvic cavities and their main branches were performed on all subjects, in order to carry out a morphometric and morphological survey of the aforementioned vessels.

For the execution of the anatomical cast, the method that involves the use of the polyurethane foam was adopted, as described by De Sordi et al. (2014).

After positioning the subjects in left lateral decubitus on the anatomical table, all the layers that make up the thoracic and abdominal wall were incised: skin, subcutis and the muscles of the costal and abdominal regions.

In order to obtain vascular and bronchial anatomical casts of the heart and lungs of guinea pigs and capybaras, to access the thoracic cavity and the mediastinal region, the ribs were removed using a costotome; subsequently, the greater vessels (aorta, cranial vena cava, caudal vena cava, right azigos vein, brachycephalic trunk and left subclavian) were cut, as were the trachea and esophagus. In order to isolate the two lungs and the heart, the mediastinal pleura was excised. Subsequently, in order to eliminate the clots and the residual blood inside the vessels, repeated washes were carried out inside a basin filled with water; small incisions had previously been made on the surface of the lungs to facilitate their perfusion. Subsequently, after having placed the samples in a plastic tray, the brachycephalic trunk, the first intercostal arteries originating from the aorta and the left subclavian artery were closed with the aid of Kocher-type surgical forceps. For the cast of the venous system, the injection of the foam occurred through the aorta and up to the left ventricle. As soon as the foam began to come out of the incisions previously made on the lung margins, the rubber extension was removed and the aorta closed with forceps. The arterial system was then filled with blue polyurethane foam. The right azigos and caudal veins were clamped with hemostatic forceps and the foam was injected into the cranial vena cava through a tube attached to a syringe. The infusion of the bronchial tree was carried out by injecting the polyurethane foam, added with yellow dye, through the trachea.

For the arterial cast of the arterial vessels of the abdominal and pelvic cavities, the thoracic aorta was incised, about halfway through its course, and a 22 or 24G-needle cannula was inserted, in relation to the size of the animal and the caliper of the aorta; the mandrel was then extracted and a 60 cc-syringe was connected to the cannula positioned in the vessel. The vessels were then repeatedly washed with spring water, after cutting the femoral artery, in order to create an outflow. When the water that came out of the femoral artery was devoid of blood, we continued blowing air, to free the vessels from any residues. When the subject was ready to be injected, the solution was prepared, according to the technique reported by De Sordi et al. (2014).

The polyurethane foam (diphenylmethane 4,4 diisocyanate; Soudafoam® -Soudal N V, Turnhout, Belgium) was diluted with acetone, in a ratio of about 4: 1. Red, blue or yellow nitro dye was added to the solution (PebeoCeramic®-Pebeo, Gemenos Cedex, France) for the arteries, veins and bronchi, respectively. Once the desired consistency and quantity was obtained, the mixture was poured into the previously-prepared syringe and we proceeded with the injection by acting on the plunger. In some cases, a silicone gun was used, which helped to exert greater pressure. As soon as the foam began to come out of the femoral artery, the previously-incised

femoral artery was clamped using a Klemmer haemostatic forceps. In this way, all the foam could be channelled into the main branches of the abdominal aorta, such as the celiac stem, the renal arteries, the testicular or ovarian arteries, and the caudal mesenteric artery, up to the bifurcation of the aorta into the common iliac arteries and their branches. During the execution of the injection, care was taken to check that there were no leaks of solution from accidentally-cut vessels. Once all the vessels of interest for the study were properly filled with foam, the injection was suspended, the cannula was removed and the thoracic aorta was immediately clamped with haemostatic forceps. The abdominal and pelvic viscera were covered with wet absorbent paper, in order to avoid dehydration. Finally, the subjects were placed at refrigeration temperature (4° C) for 24 hours, taking care to position them so as not to alter the topography of the vessels, to allow time for the polyurethane foam to expand and solidify. The next day we proceeded with the dissection of the soft tissues to highlight the vessels, with their analysis, and with their measurement *in situ* through the use of a digital caliper (Kennon Instruments; measuring range 150 mm, resolution 0.01 mm, accuracy  $\pm$  0.03 mm). The caliber of the vessels of interest and the distance between two successive arteries were measured at their point of origin. The point of origin of the main branches of the abdominal aorta was also observed and documented, expressed in terms of the vertebral body (thoracic or lumbar) at which level they originated. After measuring and observing the topography of the vessels, the gastrointestinal system was isolated, in order to assess its vascularization in detail.

As for the vascular and bronchial casts of the heart and lungs, after the injection and solidification of the casts, these were completely immersed in a 10% sodium solution for a week, in order to obtain the maceration and corrosion of the organic tissues. The casts were then carefully rinsed under running water to eliminate any residue of organic tissue. Subsequently, the casts were cleaned with the aid of tools such as surgical forceps, scissors, scalpels, needles and brushes, in order to highlight the main bronchial branches (main bronchi and lobar bronchi) and vascular branches. The cast was then analyzed to identify the first series of ramifications and the relationships of the bronchial tree with the arterial and venous trees. With the aid of a digital caliper (Kennon instruments; measuring range 150 mm, resolution 0.01 mm, accuracy  $\pm$  0.03 mm), the diameter of the bronchial branches and the corresponding satellite arteries and veins were measured. For the naming of the anatomical structures, the *Nomina Anatomica Veterinaria* (Schaller, 1999) and the indications given by Getty (1982), Barone (2003), Nickel et al. (2006) and Dyce et al. (2010) were used. For all those bronchial branches lacking specific denominations in the literature, they were defined according to their direction or on the basis of their reciprocal position.

All the data deriving from the study were processed using Microsoft Office Excel 2003 and photographs were acquired using a digital reflex camera (Fujifilm HS50) and processed using Adobe Photoshop Elements®.

# **Microscopic anatomy**

## **Classical histology techniques**

The preparation of the tissue samples for histological examination followed the classical histology procedure (Mazzi, 1977). Immediately after collection, the tissues were fixated by immersion in a 4% paraformaldehyde solution for a minimum of 48 hours. The 4% paraformaldehyde solution was obtained by a 50% dilution of a concentrated 8% paraformaldehyde solution with 0.2M sodium phosphate buffer, and stored at refrigerator temperature (+ 4° C). This solution, in addition to inactivating the autolytic enzymes and bacteria, confers the necessary structural stability to the cellular and extracellular chemical components of the samples.

The preparation of the samples for paraffin inclusion consists in the initial dehydration of the samples by placing them in alcoholic solutions at gradually increasing concentrations; specifically, the sample was immersed in 50° alcohol for 15 min, in 70° alcohol for 45 min, in 80° alcohol for 1h, in 90° alcohol for 1h, in 95° alcohol for 30 min, and, finally in 100° alcohol for 2 hours minimum. After dehydration, the samples were immersed for 30 minutes in a xylene solution, in order for the samples to clear. All the above steps were carried out employing a class-A extractor hood.

The paraffin inclusion procedure consisted in heating the solid paraffin tablets with a Bunsen burner until partial melting, except for the bottom layer which must remain semi-solid. Once the melted paraffin was poured into the molds, the sample was quickly immersed in the liquid paraffin inside the molds; subsequently, the blocks were allowed to solidify at room temperature for 24h minimum.

Microtomy was then performed by employing a rotary microtome, in order to obtain tissue sections. The slides used had been previously processed with specific substances to allow the adhesion of the tissue to the surface of the slide itself. Each slide was univocally identified by a progressive number and sample references. After having properly prepared the microtome with the disposable blade, the block was fixed on the special support and oriented towards the cutting surface, and successive sections of 8-10 µm thickness were obtained. The selected sections were collected with a small wet brush and placed on the surface of bidistilled water of the thermostatic bath to allow adequate distension of the sections. They were subsequently collected with a brush, spread out on the slide, and let dry in a specific oven overnight, before staining.

### **MASSON'S TRICHROMIC STAINING (Mazzi, 1977)**

Masson's trichrome stain is specifically designed to highlight the connective tissue. It is composed of hematoxylyn, which gives the nuclei a dark purple color, fuchsin acid which colors the cytoplasm in orange or red, and aniline blue which stains the connective tissue and mucus of a blue color. Masson's trichrome staining consists in the following procedure:

- Immersion of the slides in a xylene solution for at least 15 minutes for paraffin removal;
- rehydration of the sections with passages in alcohols at decreasing concentrations, from

100° passing through 95°, 90°, 80°, 70° and up to 50°;

- rinsing in double distilled water and immersion of the slides in Mayer's Hemalum for 5-10 minutes; two additional washes in water for 5 minutes each;
- immersion in Ponceau Red 2R stain for 5 minutes;
  - immersion in Orange G stain for 5 minutes;
- quick rinsing with 1% acetic acid solution;
- staining with Aniline Blue by immersion for 5 minutes;
- quick rinsing with 1% acetic acid;
- drying and successive passages in 100° alcohol for 2 minutes, and in xylene for at least 15 minutes;

Mounting of the slides with a coverslip and synthetic resin.

#### HEMATOXYLIN-EOSINE STAINING (Mazzi, 1977)

Hematoxylin-eosin staining is routinely used to generally highlight the morphology of the cellular structures in tissues. It is referred to as a combined or bichromic stain since it involves the combination of two dyes: hematoxylin and eosin. Staining depends on the pH value of the different cellular portions. Mayer's hematoxylin is largely composed of hematoxylin which, in itself, is not properly a dye: it is oxidized to hematoin which, in the presence of potassium alum, turns into a basic dye. As such, it colors the basophilic components (i.e. negatively charged) blue/purple. Eosin, prepared in slightly acidified water, is, unlike hematoxylin, an acid dye that colors acidophilic (positively charged) substances in red/pink. This stain allows to distinguish the different cellular components: nuclei are stained dark blue/purple, whereas cytoplasm, intracellular substances and muscle fibers appear pink/red. Lipids do not take on the stain, and fluids are weakly colored, appearing as large white spaces.

Hematoxylin-eosin staining is accomplished by performing the following steps:

- Removal of paraffin from sections by soaking the slides in xylene for at least 15 minutes;
- hydration of the sections with successive passages in alcohols at decreasing concentrations from 100°, 95°, 90°, 80°, 70° and 50° for 20 seconds each;
- washing in bidistilled water;
- immersion of the slides in Mayer's Hemalum for 5-10 minutes;
- two washes by immersion in water of 5-10 minutes each;
- staining with Eosin 1% for 30 seconds;
- dehydration with rapid passages in alcohols 70°- 80° and then in alcohols 90°-95°-100° for 5-10 seconds;
- immersion of the slides in Xylene for minimum 15 minutes;

Mounting of the slides with synthetic resin and a coverslip.

After obtaining the histological sections, they were observed by optical microscopy and images were digitally recorded with a Canon Coolpix P500® digital camera.

## CRESYL VIOLET (NISSL) STAINING (Mazzi, 1977)

The Cresyl Violet Acetate solution is used to stain the Nissl substance in the cytoplasm of neurons in paraformaldehyde-fixed or formalin-fixed tissue. The neuropil will be stained a granular purple-blue. This stain is commonly used to identify the neuronal structure in brain and spinal cord tissues.

The Cresyl Violet method uses basic aniline dye to stain RNA blue, and is used to highlight important structural features of neurons. The Nissl substance (rough endoplasmic reticulum) appears dark blue due to the staining of ribosomal RNA, giving the cytoplasm a mottled appearance. Individual granules of extra-nuclear RNA are named Nissl granules (ribosomes). DNA present in the nucleus stains a similar color.

### Method:

- Wash slides briefly in tap water to remove any residual salts.
- Immerse slides through 2x 3min changes of 100% ethanol.
- Defat the tissue: 15min in 100% xylene (2-3 changes as directed), then 10min in 100% ethanol.
- Rehydrate through alcohol (100% x 2) 3 min each.
- Wash in tap water.
- Stain in 0.1% Cresyl Violet 4-15min.
- Quick rinse in tap water to remove excess stain
- Wash in 70% ethanol (the stain will be removed by this method).
- If required, immerse sections for 2 min in Differentiation solution (2 drops glacial acetic acid in 95% ethanol) – check staining on microscope.
- Dehydrate through 2x3min changes of absolute ethanol.
- Clear in xylene x2 and mount in synthetic resin. Allow dry in the fume hood.

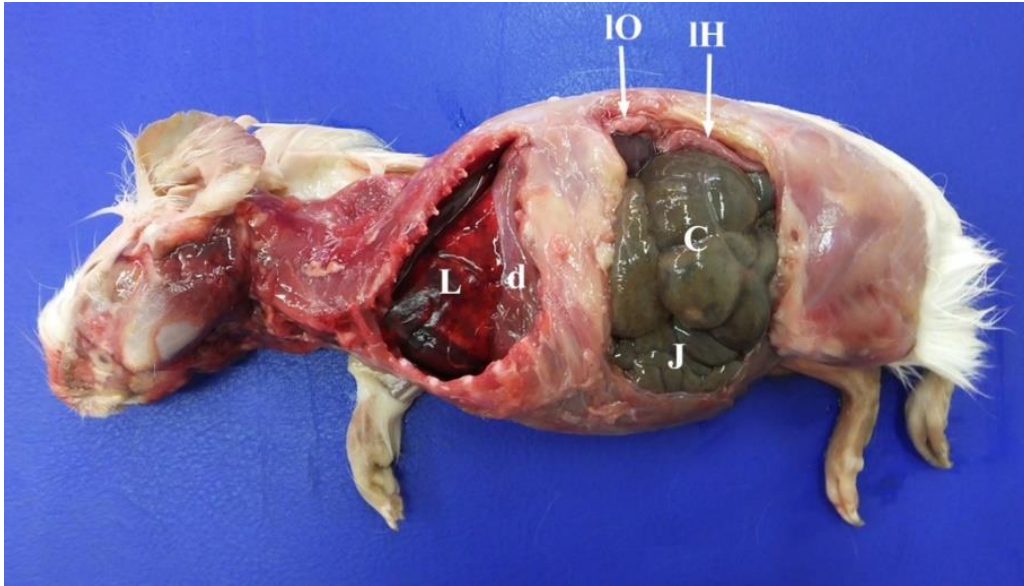
The thicker sections require exposure to each solution for longer to allow the diffusion of reagents.

## Statistics

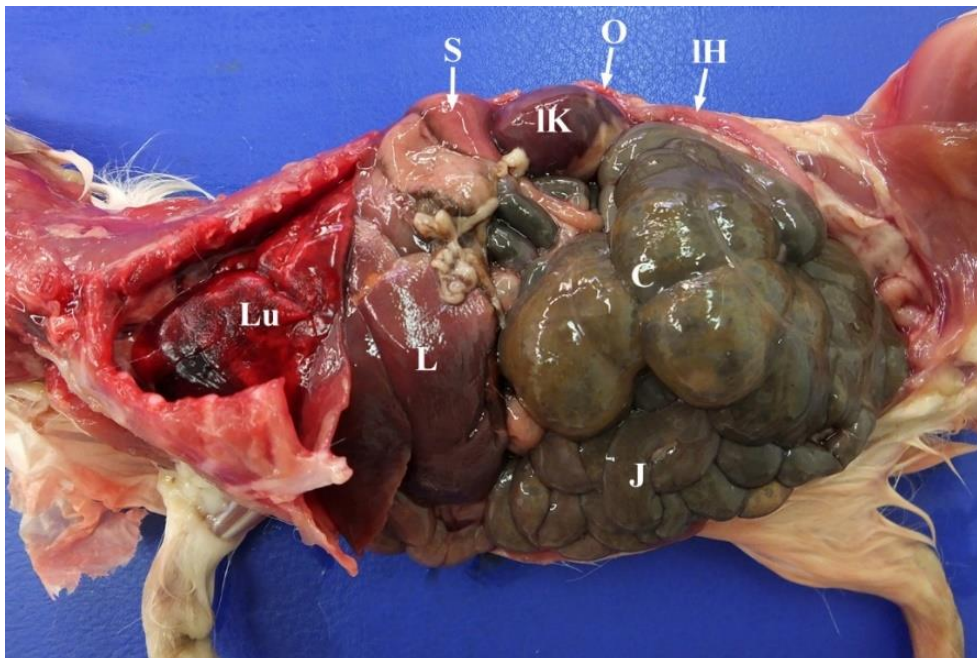
Statistical analyses were conducted using commercially available software (R Core Team 2020, version 4.0.2, R Foundation for Statistical Computing, Vienna, Austria; Excel: Microsoft Excel, Microsoft Office 2011, Microsoft Corporation, Bellevue, WA). Calculation of statistical indices (mean, standard deviation, median, range, distribution, variance) and creation of graphs were then performed using Microsoft Excel.

## RESULTS

### Atlas of gross anatomy



**Guinea pig splanchnic cavities** Splanchnic cavities of a female guinea pig seen from a left lateral view. C: cecum; d: diaphragm; J: jejunum; L: left lung; IH: left uterine horn; IO: left ovary.



**Guinea splanchnic cavities -** Splanchnic cavities of a female guinea pig seen from a ventral view. C: cecum; J: jejunum; L: liver; IH: left uterine horn; IK: left kidney; Lu: lung; O: left ovary; S: spleen.

## Respiratory system

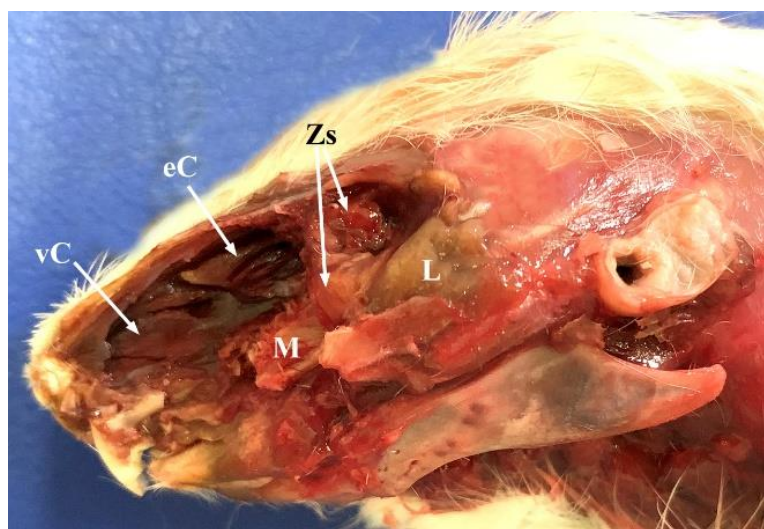
### Nasal cavities

#### *Cavia porcellus*

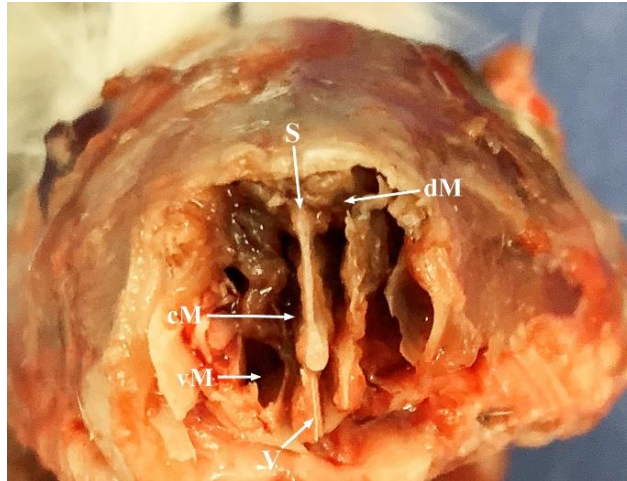
In the guinea pig skull, the complete zygomatic arch and infraorbital foramen were well-developed. Through these, a well-developed deep portion of the masseter passed medially, to insert on the incisor and maxillary bones, on the sides of the nasal bone. In the sagittal section of the nasal cavity, once the incomplete nasal septum was resected, well-developed ethmoturbinates, endoturbinates and a ventral concha were evidenced, subdividing the nasal cavity into a dorsal and a ventral meati. In the transversal section of the nasal cavities, the cartilaginous nasal septum subdivided the nasal cavity into right and left fossae, containing endoturbinates that delimited the dorsal, ventral and middle meati.



**Guinea pig nasal cavities** - Left lateral view. I: upper incisor; L: lacrimal gland; S: nasal septum; Zs: zygomatic salivary gland.



**Guinea nasal conchae** - Left lateral view. eC: ethmoid concha; L: lacrimal gland; M: maxillary bone; vC: ventral concha; Zs: zygomatic salivary gland.



**Guinea pig nasal cavities** - Guinea pig nasal cavities cut transversally. Rostral view.  
*cM: common meatus; dM: dorsal meatus; S: nasal septum; V: vomer; vM: ventral meatus.*

### ***Hydrochoerus hydrochaeris***

The female isolated capybara head had a weight of 3.9 kg. The skull was rectangular-shaped, elongated and flattened caudally, thinned in the nasal region and slightly convex in the parietal region. The zygomatic arch was well developed and wide, the orbit had a circular shape, and the infraorbital foramen was well developed; pterygoid fossae were deep and unperforated. The angular process of the mandible was not everted, and the masseteric crest was well-developed. The orbit and the temporal fossa were continuous.

The nasal septum was complete and well-developed. The well-developed endoturbinates delimited the dorsal and ventral nasal meatuses, in the longitudinal section of the head. In the transversal section of the nasal cavities, the nasal septum divided the nasal cavity into right and left fossae, and the well-developed endoturbinates delimited the dorsal, common (middle) and ventral meatuses.

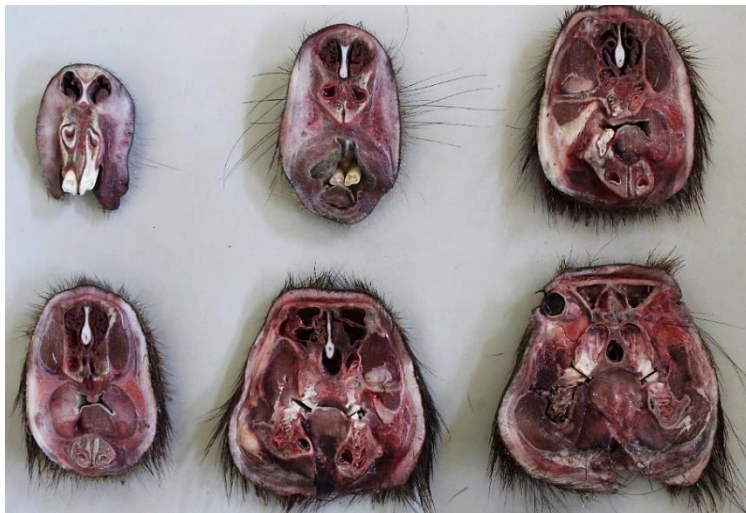


**Capybara nasal cavities** - Sagittal section of the capybara head (without mandible) after resection of the nasal septum. Note the well-developed endoturbinates and ethmoturbinates and ventral concha, delimiting the dorsal and ventral nasal meatuses, with the access to the maxillary recess. The ethmoidal concha with ethmoturbinates is visible, as well as the cranic cavity with the encephalon and casts of the cerebral vessels.





***Capybara nasal septum*** - Sagittal section of the capybara head (without mandible). Note the highly developed and complete nasal septum, the cranic cavity and the frontal sinus.



***Transversal sections of the capybara head*** from rostral to caudal, obtained at the following levels (from left to right). Front row: at the level of the upper incisors; between the upper and lower incisors, at the level of the lower incisors. Bottom row: at the level of the diastema; at the level of the first molars; at the level of the upper third molars.

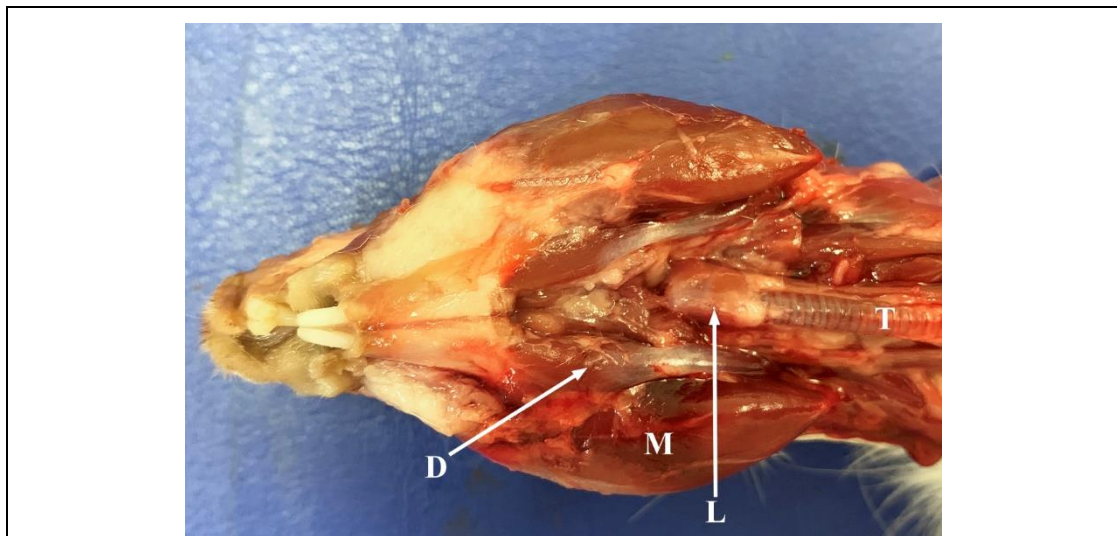


***Transversal section of a capybara's head*** at the level of the first inferior molars. Note the well-developed nasal septum dividing the nasal cavity into right and left portions, the choanae, and the spiral-shaped endo- and ecto-turbinates subdividing the nasal cavities into a dorsal, common, and a ventral meatus. The buccal vestibulus with tongue body, the mandible and the superficial masseter are visible.

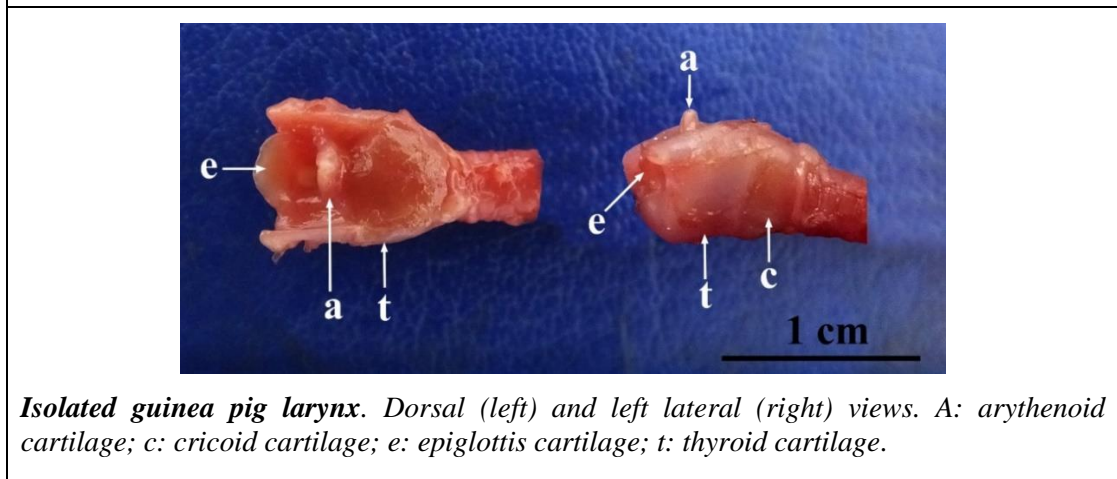
## Larynx

### *Cavia porcellus*

The larynx of the guinea pig was composed of four cartilages: the epiglottis, the arytenoids, the thyroid and the crycoid. The epiglottis was small and leaf-shaped; the arytenoids presented cranial and caudal processes; the thryoid was composed of a ventral body and lateral laminae and had a well-developed rostral horn; The crycoid was particularly voluminous and forming a complete ring around the caudal aspect of the larynx. The larynx measured 6.56 mm in length and 6.49 mm in width.



*In-situ guinea pig larynx. Ventral view. D: digastric muscle. L: larynx; M: superficial masseter; T: trachea.*


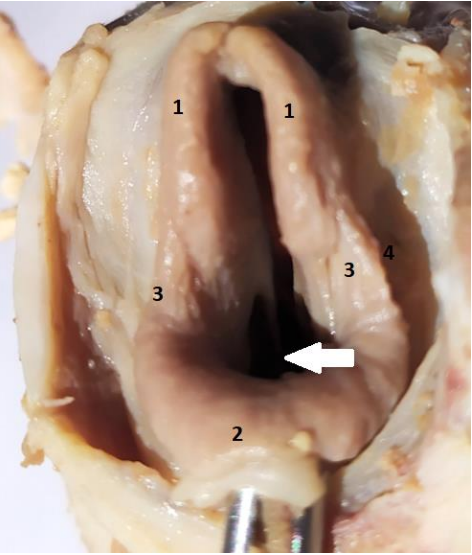
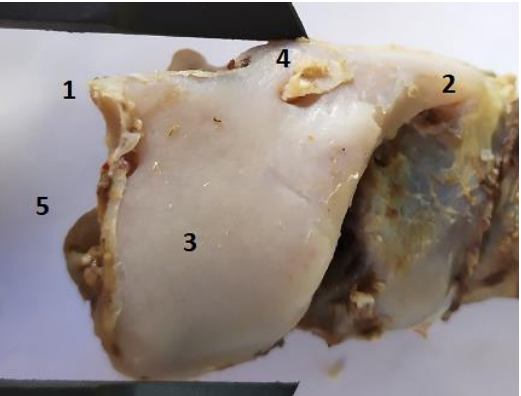


*Isolated guinea pig larynx. Dorsal (left) and left lateral (right) views. A: arythenoid cartilage; c: cricoid cartilage; e: epiglottis cartilage; t: thyroid cartilage.*

### *Hydrochoerus hydrochaeris*

The conical larynx of the capybara was composed of four cartilages: epiglottis, arytenoid, thryoid and the well-developed crycoid. Well developed vocal folds were also evidenced. The epiglottis was leaf-shaped and with a sharp rostral edge. The arytenoids were composed of corniculate and cuneiform processes. The thryoid was composed of a ventral body and lateral rectangular laminae. The crycoid was well developed and forming a ring on the caudal edge of

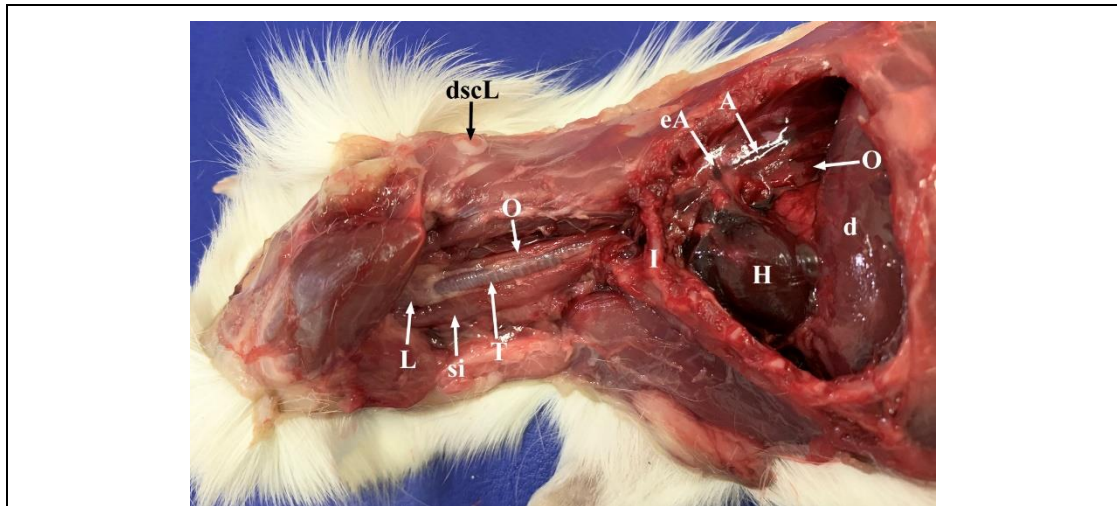
the larynx; it was broadened dorsally and narrowed ventrally. The mean total rostro-caudal length of the capybara larynx measured 3.4 cm.

	<p><b><i>Capybara larynx, lateral view.</i></b></p> <p>1. Hyoepiglottic ligament; 2. thyroid cartilage; 3. thyrohyoid; 4. stylohyoid; 5: cricoid cartilage; 6. trachea; 7: cricothyroid membrane; 8: cricotracheal membrane.</p>
	<p><b><i>Capybara larynx, rostral view.</i></b></p> <p>1. arythenoids; 2: epiglottis; 3: ariepiglottic fold; 4: laryngeal vallecula; Arrow: vocal cord.</p>
	<p><b><i>Capybara thyroid cartilage; lateral view.</i></b></p> <p>1. Rostral horn; 2; caudal horn; 3: lamina; 4: thyroid foramen; 5. thyroid fissure.</p>

## Trachoea

### *Cavia porcellus*

The guinea-pig trachea was seen to be composed, on average, by 35 incomplete tracheal rings. The tracheal rings were C-shaped and bridged dorsally by the trachealis muscle. The trachea of the guinea pig ended by bifurcating into the primary left and right bronchi at the level of the fourth to fifth rib. The diameter of the trachea was 3.56 mm.



**Guinea pig trachea.** Left lateral view.

*I: first rib; A: aorta; d: diaphragm; dscL: dorsal superficial cervical lymph node; eA: left hemiazygos; H: heart; L: larynx; si: sternohyoid muscle; O: esophagus. T: trachea.*

### *Hydrochoerus hydrochaeris*

The trachea of the capybara was composed of 40 tracheal rings, on average. The incomplete tracheal rings were U-shaped, with a mean external diameter of 1.8 cm, and joined dorsally by the trachealis muscle all throughout its length. The trachea of the capybara ended by bifurcating into the primary right and left bronchi.



**Capybara first tracheal ring.** Transversal section.

*Note the U-shaped cartilage joined dorsally by the trachealis muscle.*

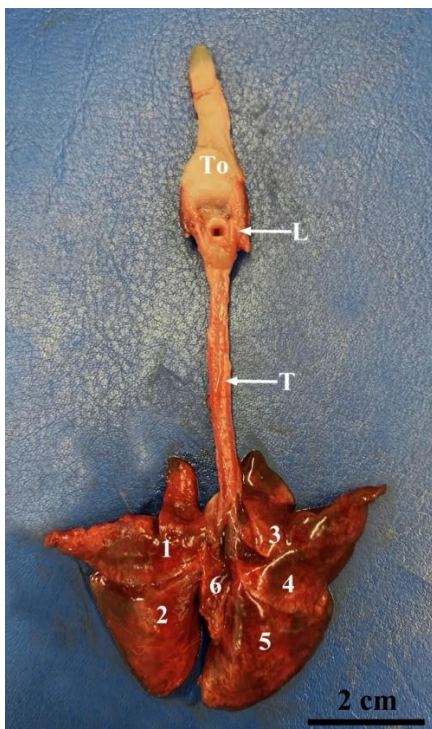


*Capybara larynx and trachea. Lateral view.*

## Lungs

### *Cavia porcellus*

From the macroscopical study of the guinea-pig lungs, it emerged that they were voluminous, divided into well-demarcated lobes, with sharp edges. The right lung was seen to be composed of four lobes: cranial, middle, caudal and accessory. The right cranial lobe was divided by a notch into cranial and caudal portions; the small middle lobe was seen to be partially fused to the large caudal lobe. The left accessory lobe was well developed and undivided. The left lung consisted of three lobes: a cranial lobe, divided into a smaller cranial and a larger caudal parts by a deep fissure, a caudal lobe, and an accessory lobe on the medial surface, which was smaller than the contralateral.



*Guinea pig lungs. Dorsal view.*

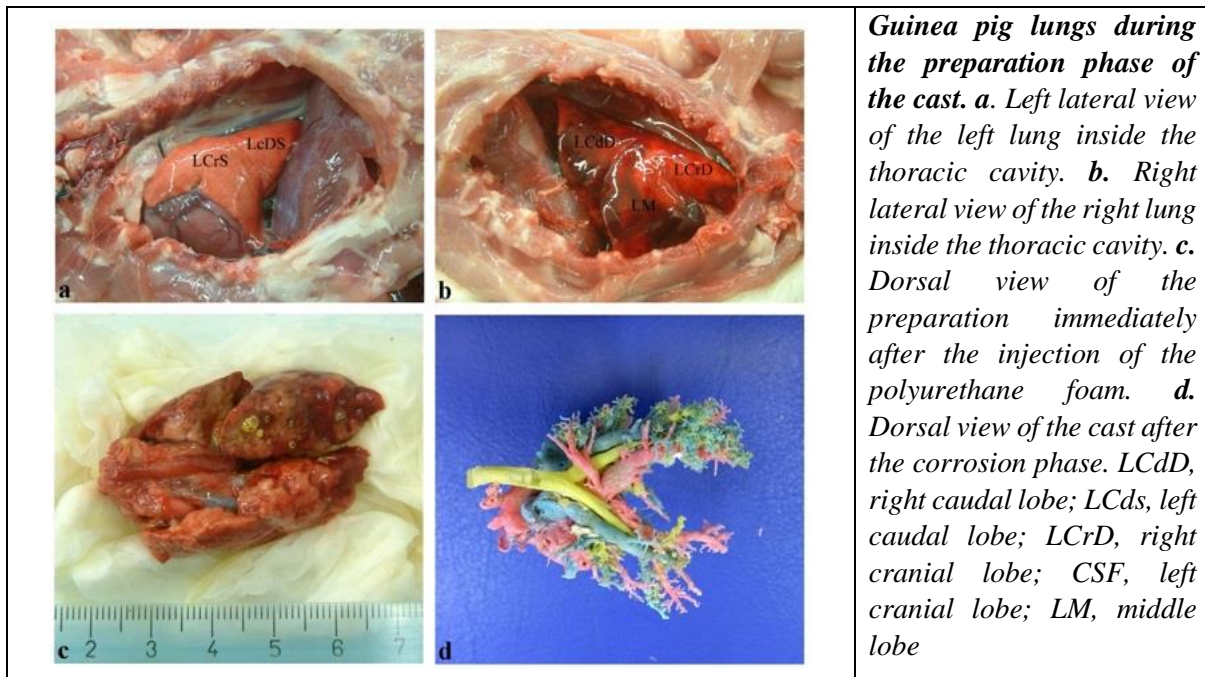
1: left cranial lobe; 2: left caudal lung lobe; 3: right cranial lung lobe; 4: right middle lung lobe; 5: right caudal lung lobe; 6: right accessory lobe. L: larynx; T: trachea; To: tongue.

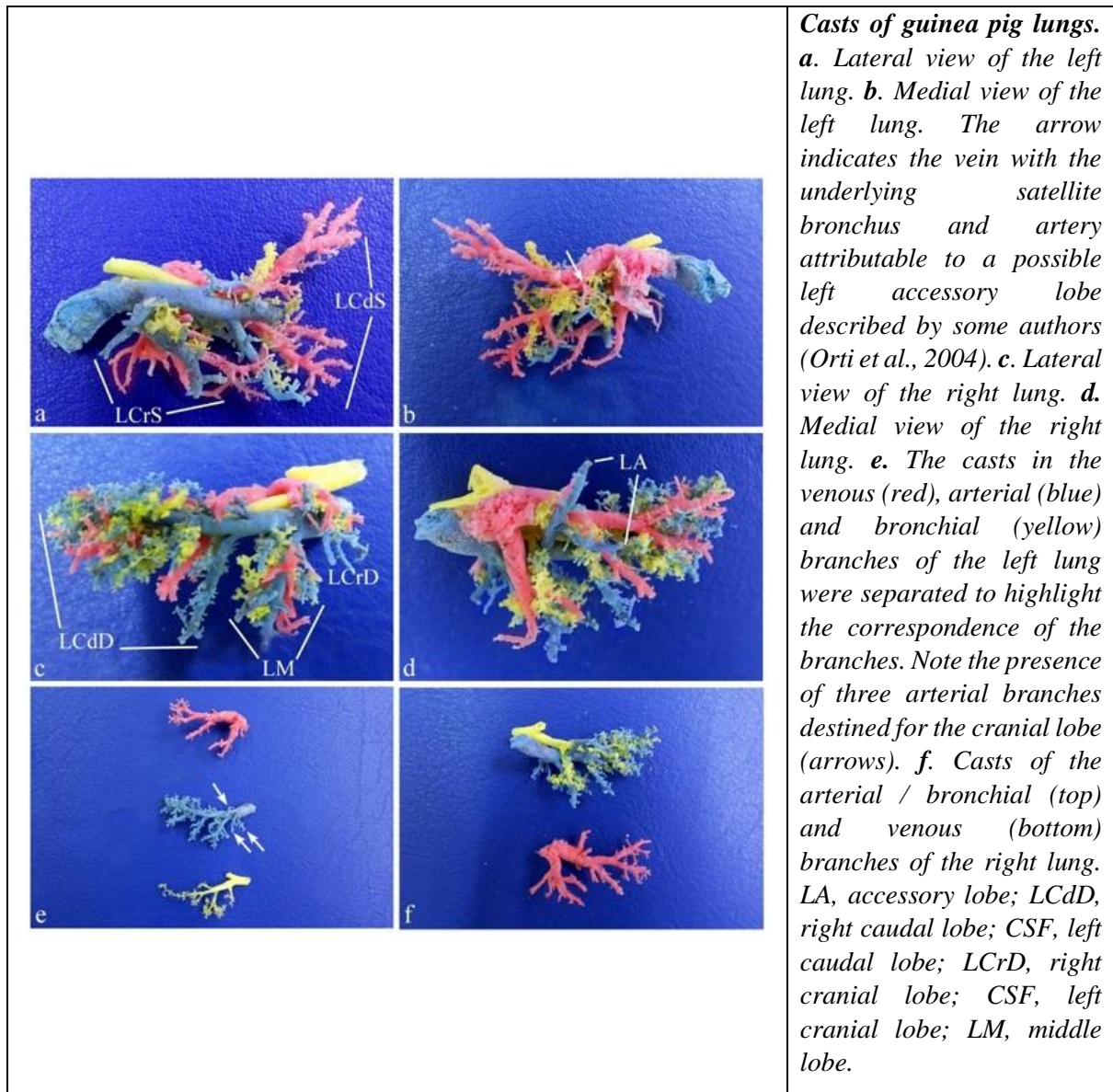
### *Hydrochoerus hydrochaeris*

The lungs of the capybara were voluminous and divided into well-defined lobes. The capybara right lung was composed of a cranial lobe, a middle lobe, a caudal lobe and an accessory lobe. The caudal lobe was the most developed. The right cranial lobe was subdivided by a deep fissure into two elongated cranial and caudal parts, with sharp edges. Interlobar fissures divided the cranial lobe from the middle lobe and the middle lobe from the caudal. The right accessory lobe, situated medially, was further divided by a shallow notch into a medial and a lateral portions. The left lung was composed of two lobes, a cranial and a caudal, with the left cranial lung lobe further divided, by the cranial intralobar fissure, into a cranial and a caudal portions.

### **Anatomotopographic and morphometric study of the main, lobar and segmental bronchi and their respective arterial and venous satellite vessels in the guinea pig and capybara**

#### *Cavia porcellus*





From the present study it emerged that the guinea pig has an articulated bronchial tree. The main right and left bronchi extend caudally into the right and left lungs, each accompanied by the corresponding pulmonary artery. The right main bronchus detaches, close to its origin the right cranial lobar bronchus and, at an average distance of 3.21 mm, the middle lobar bronchus. The accessory lobar bronchus originates from the right caudal lobar bronchus, being its direct continuation. The left main bronchus, shortly after the tracheal bifurcation, emits the left cranial lobar bronchus and continues as left caudal lobar bronchus.

The **right cranial lobar bronchus** (BLCrD) originates from the right main bronchus at an average distance of 2.5 mm from the tracheal bifurcation and, shortly after its origin, bifurcates into a cranial and a caudal branches. Numerous segmental branches originate from the BLCrD and from the cranial and caudal branches that originate from it. The arterial supply for the BLCrD derives from a single artery or a cranial and a caudal arteries, which originate from the right pulmonary artery. The right cranial lobe was found to be drained by a single or double venous vessel deriving from the confluence of three veins destined, two to the cranial bronchial branch

and another to the caudal bronchial branch. All veins were seen to flow medially to the corresponding bronchus, with the main vein ending in the right pulmonary vein.

The **middle lobar bronchus** (BLM) was seen to originate from the right main bronchus, and it ends, with a ventrocaudal direction, by bifurcating into a cranial and a caudal branch which then further bifurcates into two veins. During its course, it emits cranial and caudal segmental branches in alternating succession, in a variable number from 4 to 7. An arterial branch, originating from the right pulmonary artery and running cranio-laterally to the respective bronchus, is directed to the middle lobe and, about halfway along its length, it bifurcates into two vessels destined for the cranial and caudal bronchial branches, running laterally to them. A single pulmonary vein drains the middle lobe, originating from the confluence of two veins placed cranially and caudally to the BLM and running medially to it, finally ends in the left atrium.

The **accessory lobar bronchus** (BLA) arises from the right caudal lobar bronchus (BLCdD) and divides into a large ventromedial branch, which ends by bifurcating into a dorsal and a ventral branch, and into a caudal branch. The satellite artery of the BLA originates from the arterial branch of the BLCdD, with their ventromedial and caudal branches running laterally and close to the respective bronchi. A single venous vessel drains the accessory lobe, deriving from the confluence of a caudal and a ventromedial branches, running medially to the respective bronchial branches, and ends in the vein of the BLCdD.

The **right caudal lobar bronchus** is the direct continuation of the right main bronchus and, along its path, it emits two ventral branches and ends by bifurcating into a caudodorsal and a caudoventral branch. The right caudal lobe presents the most developed but also the most regular bronchial branching. The arterial branch of the right caudal lobe is the direct continuation of the right pulmonary artery, following closely the respective bronchus and each bronchial branch in a lateral position. A single right caudal pulmonary vein drains the right caudal lobe, it runs medially but not in close contact to the BLCdS and ends into the left atrium in an expansion to the right of the termination of the left caudal lobar vein.

The **left cranial lobar bronchus** (BLCrS) divides into a cranial branch, intended for the cranial part of the left cranial lobe, and a larger caudoventral branch, directed to the caudal part, which gives rise to several segmental cranial and caudal branches. A single or, in some cases, multiple arterial branches vascularize the left cranial lobe, running laterally and in close contact with the respective bronchi, and originates from the left pulmonary artery. As for the venous drainage, the left cranial lobe can be drained by a single venous branch deriving from the confluence of two venous branches destined to the caudoventral bronchial branch and to the cranial branch, respectively; in another case, two veins were found, a larger vein caudomedial to the bronchus and ending in the atrium and a smaller vein cranial to the bronchus and ending in the vein of the BLCdS. The veins were placed medially to the corresponding bronchi.

The **left caudal lobar bronchus** (BLCdS) is a direct continuation of the left main bronchus, with an identical course to the right caudal lobar bronchus: it emits two ventral branches, which in turn detach segmental cranial and caudal branches, and ends by bifurcating into a caudodorsal and a caudoventral branch. The artery of the left caudal lobe is the direct continuation of the left pulmonary artery, following closely the lateral aspect of the respective



bronchus and emitting collaterals the follow the course of the bronchi. A single venous vessel placed medially to the respective bronchus, while however remaining distant from it, was found, deriving from the confluence of a caudodorsal and caudoventral veins, receiving ventral venous vessels along its course, and ending directly in the left atrium.

From the anatomotopographic study of the principal, lobar and segmental bronchi of the guinea pig, it emerged that the arteries, unlike the veins, mantain a closely connected relationship with the corresponding bronchial branches throughout their course. The arteries are generally located laterally to the respective bronchus. The veins, on the other hand, tend to be located on the medial side of the bronchi, without however maintaing a close relationship with them. From the morphometric study, it emerged that there is no clear prevalence between the calibers of the bronchi and the satellite vessels in the right lung, whereas in the left, the bronchi have a smaller caliber than the respective vessels. In addition, the arteries were found to be larger than the veins in the right lung, but smaller in the left lung. The morphometric study of the diameters of the bronchi, has set in light that the parent bronchial branch is 1.5X larger in diameter than the daughter branch; moreover, a ratio of 1.66 between the diameter of the major daughter branch and the minor daughter branch. In conclusion, from the study emerged that the bronchial tree exhibits irregular dichotomous branching, that is the parent bronchus diving into two daugther branches slightly differing in diameter and branching angle (Schlesinger and McFadden, 1981).

#### ***Hydrochoerus hydrochaeris***

From the anatomotopographic and morphometric study of the principal, lobar and segmental bronchi and their satellite arteries and veins in the capybara, it emerged that the arteries, unlike the veins, mantain a close relationship with the corresponding bronchial branches throughout their course. The arteries are generally located dorsolaterally to the respective bronchus. The veins, on the other hand, tend to be located on the ventromedial side of the bronchi, without however maintaing a close relationship with them.

<b>DIRAMATION (diameters expressed in mm)</b>	<b>Guinea pig</b>	<b>Capybara</b>
Trachea	3.24	13.21
Primary left bronchus	2.37	8.9
Left pulmonary artery	2.87	14.10
Primary right bronchus	2.55	10.1
Right pulmonary artery	3.30	14.31

The **left cranial lobar bronchus** (BLCrS) has only dorsal and ventral segmental bronchi. Its satellite vein, on the other hand, divides into a dorsal branch (4.5 mm) and a ventral branch (5.0 mm). Its satellite artery is twofold: it has a dorsal branch (3.30 mm), and a ventral branch (5.25 mm).

The **left caudal lobar bronchus** (BLCdS) emits smaller dorsal segmental branches and larger ventral segmental branches and ends by bifurcating into a lateral and a medial branches.

<b>DIRAMATION (diameters expressed in mm)</b>	<b>Guinea pig</b>	<b>Capybara</b>
<b>BLCrS</b>	<b>1.94</b>	<b>5.23</b>
Satellite artery	2.09	Double: 5.25 3.30
Satellite vein	2.13	7.02
<b>Cranial branch of the BLCrS</b>	<b>0.74</b>	
Satellite artery	0.84	
Satellite vein	1.25	
<b>Caudovertral branch of the BLCrS</b>	<b>1.05</b>	
Satellite artery	1.63	
Satellite vein	1.45	
<b>BLCdS</b>	<b>2.23</b>	<b>8.58</b>
Satellite artery	2.38	11.81
Satellite vein	2.30	11.79
<b>I ventral branch of the BLCdS</b>	<b>0.86</b>	<b>3.76</b>
Satellite artery	0.99	4.91
Satellite vein	1.19	6.90
<b>II ventral branch of the BLCdS</b>	<b>0.75</b>	<b>6.36</b>
Satellite artery	0.79	5.97
Satellite vein	0.68	5.26
<b>Caudodorsal branch of the BLCdS</b>	<b>0.85</b>	<b>Lateral branch 4.25</b>
Satellite artery	Non misurabile	4.84
Satellite vein	0.93	4.87
<b>Caudovertral branch of the BLCdS</b>	<b>0.72</b>	<b>Medial branch 3.98</b>
Satellite artery	Non misurabile	4.34
Satellite vein	0.71	4.45

The **right cranial lobar bronchus** (BLCrD) has only dorsal and ventral segmental bronchi; the satellite vein flows into a common trunk, with a branch coming from the middle lobe.

The **middle lobar bronchus** (BLM) has only segmental branches and is accompanied by two satellite veins: the first, larger, flows into a common trunk together with the vein coming from the cranial lobe; the second, smaller, flows into a vein (6.70 mm) which also receives the first ventral branch of the BLCdD. Two satellite arteries are also present.

The **accessory lobar bronchus** (BLA) does not have a satellite vein, because the veins following the caudal and ventromedial branches of the BLA do not converge into a common vessel but, instead, open separately into the right caudal lobar vein.

The **right caudal lobar bronchus** (BLCdD), after detaching some segmental bronchi of which the two ventral ones are the largest, ends by bifurcating into two branches, caudodorsal and caudoventral. The satellite veins of the second ventral branch and the caudoventral branch converge into a common vein that flows into the right caudal lobar vein.

The substantial difference between the two species lies in the cranial lobar bronchus which, in the capybara, presents a segmental division, while in the guinea pig, it bifurcates.

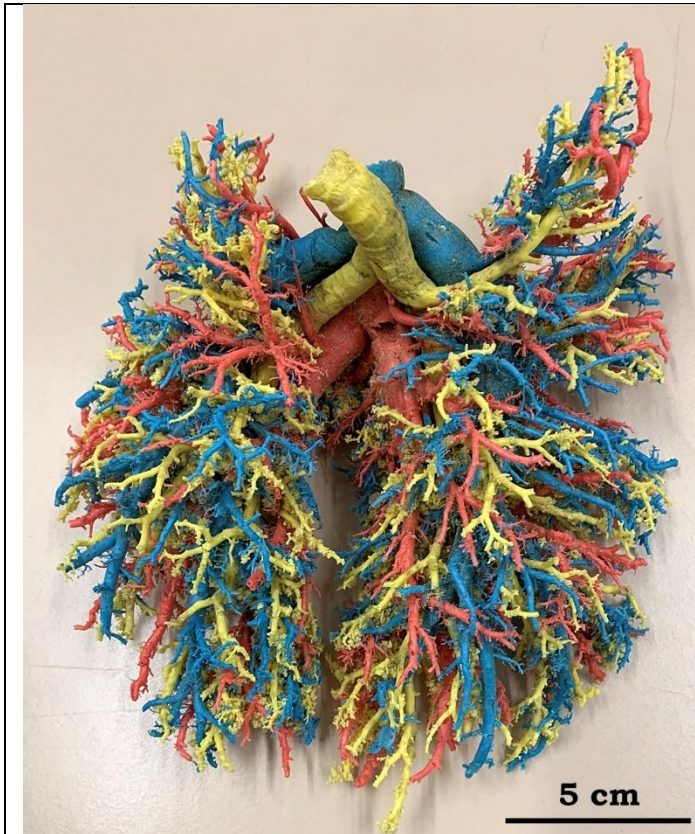
<b>DIRAMATION (diameters expressed in mm)</b>	<b>Guinea pig</b>	<b>Capybara</b>
<b>BLCrD</b>	<b>1.06</b>	<b>5.59</b>
Satellite artery	1.34	5.75
Satellite vein	1.98	5.85
<b>Cranial branch of the BLCrD</b>	<b>1.00</b>	
Satellite artery	0.81	
Satellite vein	0.72	
<b>Caudal branch of the BLCrD</b>	<b>0.55</b>	
Satellite artery	0.44	
Satellite vein	0.85	
<b>BLM</b>	<b>0.80</b>	<b>5.95</b>
Satellite artery	1.48	Double: 5.70 3.68
Satellite vein	1.84	Double: 4.55 3.96
<b>BLA</b>	<b>1.32</b>	<b>4.66</b>
Satellite artery	1.29	5.10
Satellite vein	-	-
<b>Caudal branch of the BLA</b>	<b>0.71</b>	<b>2.66</b>
Satellite artery	0.79	2.80
Satellite vein	1.08	3.02
<b>Ventromedial branch of the BLA</b>	<b>1.03</b>	<b>3.33</b>
Satellite artery	1.06	3.81
Satellite vein	1.05	4.00
<b>BLCdD</b>	<b>1.88</b>	<b>9.05</b>
Satellite artery	2.67	10.97
Satellite vein	2.55	10.44
<b>I ventral branch of the BLCdD</b>	<b>1.12</b>	<b>4.85</b>
Satellite artery	1.11	4.63

Satellite vein	0.94	4.04
<b>II ventral branch of the BLCdD</b>	<b>1.30</b>	<b>3.60</b>
Satellite artery	1.02	3.50
Satellite vein	0.93	2.52
<b>Caudodorsal branch of the BLCdD</b>	<b>1.15</b>	<b>5.80</b>
Satellite artery	1.14	6.65
Satellite vein	0.81	6.40
<b>Caudoventral branch of the BLCdD</b>	<b>1.01</b>	<b>4.75</b>
Satellite artery	0.93	5.05
Satellite vein	0.68	4.60

From the morphometric study, it emerged that, in the capybara, there is no clear prevalence between the calibers of the bronchi and the satellite vessels in the right lung, whereas in the left, the bronchi have a smaller caliber than the respective vessels. In addition, the arteries were found to be larger than the veins in the right lung, but smaller in the left lung. The morphometric study of the diameters of the bronchi has set in light that the parent bronchial branch is 1.7 times larger in diameter than the daughter branch; moreover, a ratio of 1.52 between the diameter of the major daughter branch and the minor daughter branch. Therefore, from the study emerged that the bronchial tree of the capybara exhibits dichotomous branching, with the peculiarity of the segmental branching of the cranial lobar bronchi.

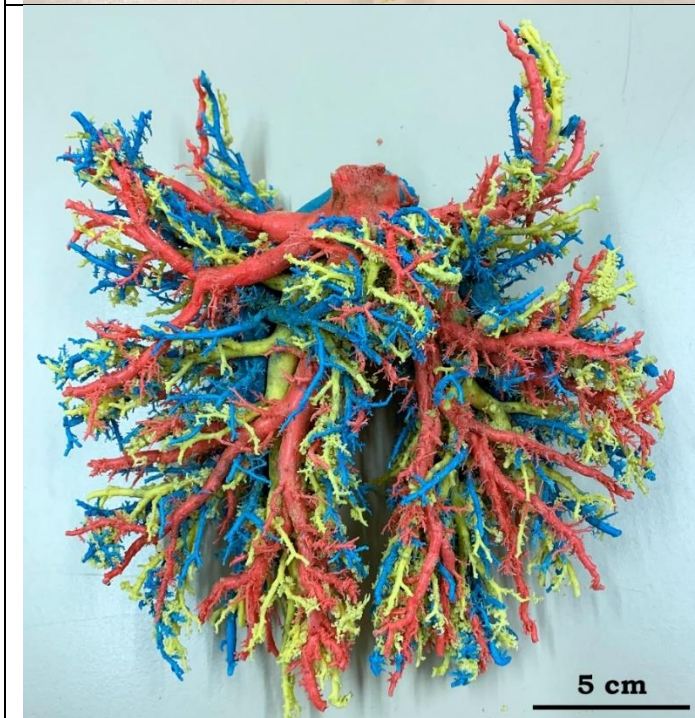


**Capybara right lung.** Ventral view (left), Dorsal view right). The right lung is composed of a cranial lobe, a middle lobe, a caudal lobe and an accessory lobe. The caudal lobe is the largest one. An interlobar notch is present between the cranial and middle lobes, and an interlobar fissure divides the right middle lobe from the caudal.



*Cast of the capybara lungs.  
Dorsal view.*

*In blue, the arterial branching,  
in red the venous branching  
and, in yellow, the bronchial  
branching.*



*Cast of the capybara lungs.  
Ventral view.*

*In blue, the arterial branching,  
in red, the venous branching  
and, in yellow, the bronchial  
branching.*

## Gastrointestinal system

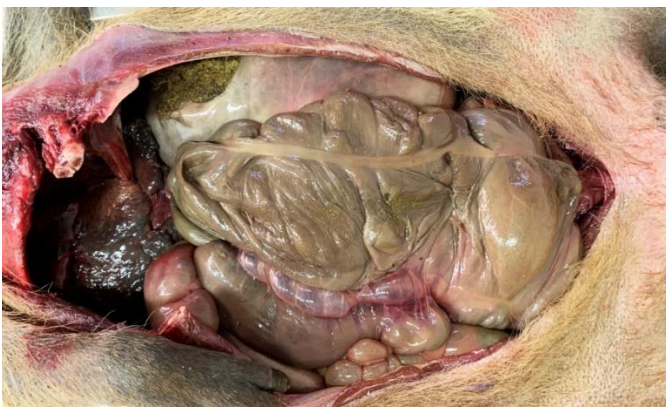
### *Cavia porcellus*



**Guinea pig splanchnic cavities.**  
*In-situ ventral view of the thoracic and abdominal cavities.*

*Note the voluminous cecum occupying a large portion of the abdominal cavity.*

### *Hydrochoerus hydrochaeris*



**Capybara abdominal cavity.** *View of the organs in situ.*

*The voluminous cecum occupied a large portion of the abdominal cavity.*

## Teeth

### *Cavia porcellus*

The guinea pig had 20 teeth total. In each hemiarch, 1 incisor, 1 premolar and 3 molars. A large diastema divided the incisors from the molariforms. The incisors were white and sharp; the maxillary molariforms were oriented laterally, whereas the mandibular molariforms had a medially-directed orientation, towards the tongue. The premolar and molar teeth are indistinguishable, with roughly the same shape and dimensions, with particularly large occlusal surfaces for efficient antero-posterior grinding masticatory movements.

As for the masticatory muscles of the guinea pig, these included the well-developed masseter, composed of superficial and deep portions, the temporalis, the digastric, and the lateral and medial pterygoid muscles. A peculiarity that was observed in this species is the high development of the deep (medial) portion of the masseter muscle, which passed through the large infraorbital foramina to insert anteriorly to the zygomatic arch, at the level of the incisor and

maxillary bones and the lateral edges of the nasal bones. Note the presence, in the photo, of the emergence of the infraorbital nerves from the infraorbital foramen, alongside the deep masseter. Another peculiarity that was observed was the presence of a voluminous zygomatic (orbital) salivary gland that occupied the entire floor of the orbit. Caudoventral to it, a well-developed lacrimal gland was observed.



*Guinea pig maxillary (top) and mandibular (bottom) teeth.*

*LI: lower incisors; LM: lower molars; LP: lower premolar; UI: upper incisors; UM; upper molars; UP: upper premolar teeth.*



*Guinea pig head structures seen in left lateral view.*

*dM: deep masseter; I: infraorbital nerves; L: lacrimal gland; M: superficial masseter; Zs: zygomatic salivary gland.*

### ***Hydrochoerus hydrochaeris***

The capybara dental formula was composed of 20 teeth total. Each hemiarch presented 1 incisor, no canine teeth, 1 premolar and 3 molars. A large diastema was present between the incisors and the cheek teeth. The mandibular molariforms had a slightly medially-oriented direction, as opposed to the maxillary molariforms, which were more laterally oriented. The incisors were broad, white and sharp-edged. The premolars and molars were all similar in shape and dimension, with the exception of the maxillary third molar, which had a particularly wide

occlusal surface. The condylar and angular processes of the mandible were well-developed and bulging.



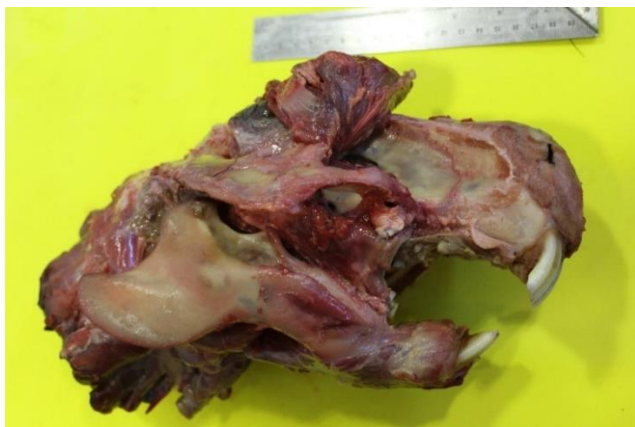
***Capybara mandible with mandibular incisor and molariform teeth. Dorso-lateral view.***

*Note the bulging condylar process and the elongated angular process of the mandible, as well as the uniformity of the cheek teeth with their large occlusal surfaces.*

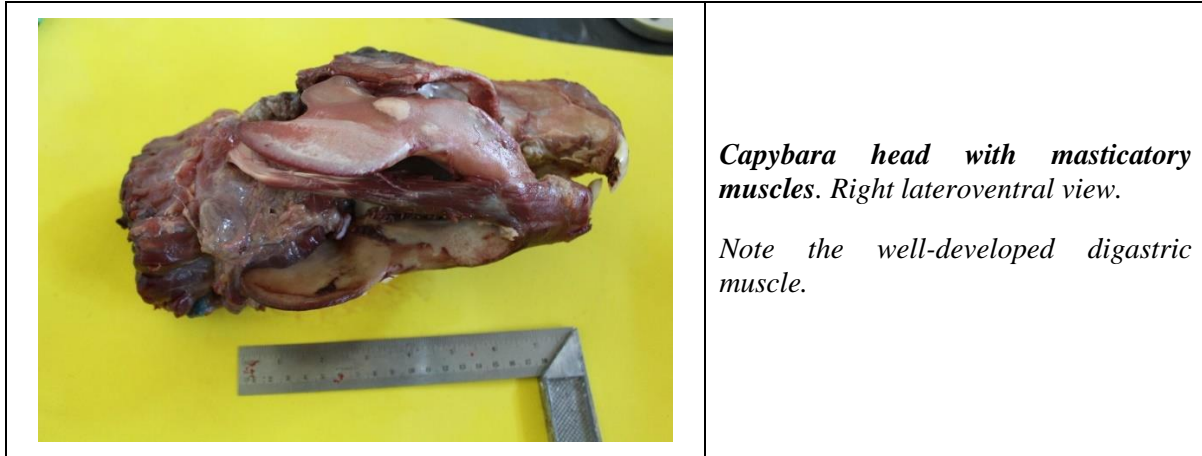


***Capybara head and masticatory muscles. Right lateral view.***

*Note the well-developed everted deep portion of the masseter muscle, showing its medial origin, its passage through the infraorbital foramen, and its point of insertion, anteriorly to the zygomatic arch, at the level of the incisor and maxillary bones.*







The masticatory muscles of the Capybara included the masseter, composed of superficial, and deep portions, the temporalis, divided into lateral and medial portions, the lateral (external) and medial (internal) pterygoideus, the digastric muscle and the zygomatic muscle. The masseter muscle was particularly developed, its deep portion passed through the large infraorbital foramina to insert anteriorly to the zygomatic arch, on the sides of the nasal bone, at the level of the incisor and maxillary bones.

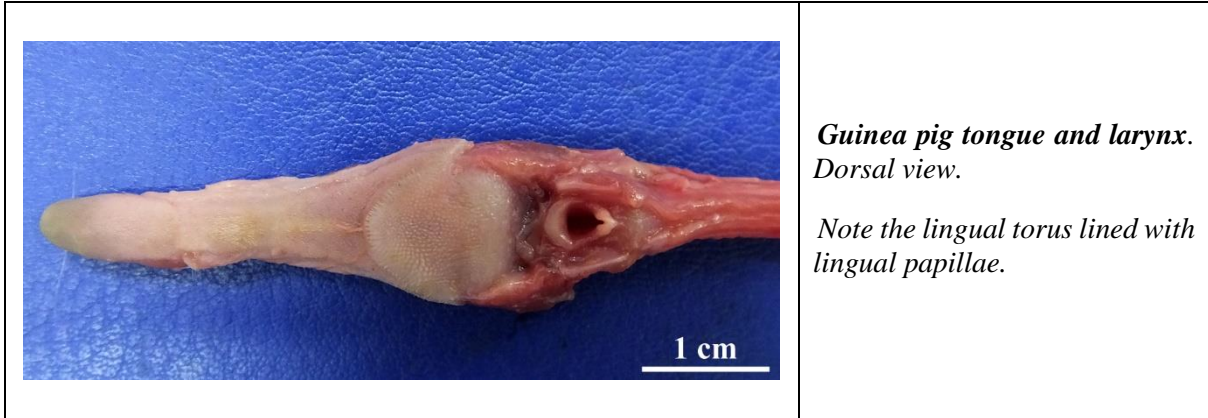
A particular orientation of the masseter muscles was observed, with the superficial masseter horizontally oriented and extended backward, and the *m. masseter medialis pars zygomaticomandibularis* was characterized by originating on the zygomatic bone medially to the zygomatic muscle, passing through the infraorbital foramen through short and vertically-oriented fibers which inserted onto the upper lateral surface of the mandible. The elongated angular process of the mandible was associated with the internal pterygoid muscles and with the superficial masseter. The masseter muscle and the internal pterygoideus joined through a median rafe on the ventral border of the mandible. Also note the well-developed digastric muscle, with its right and left portions fused ventrally to the incisive part of the mandible.

## **Tongue**

### ***Cavia porcellus***

The guinea pig tongue (dorsal view) was narrow and particularly elongated. It measured 3.2 cm in length, and 1 cm in width at its base. It was composed of a narrow apex and body, whereas its root was characterized by a broad and elevated torus (radix), covered with lingual papillae.

Note, in the photo, the opened oropharynx caudodorsally to the glottis and continuing into the esophagus.



***Hydrochoerus hydrochaeris***

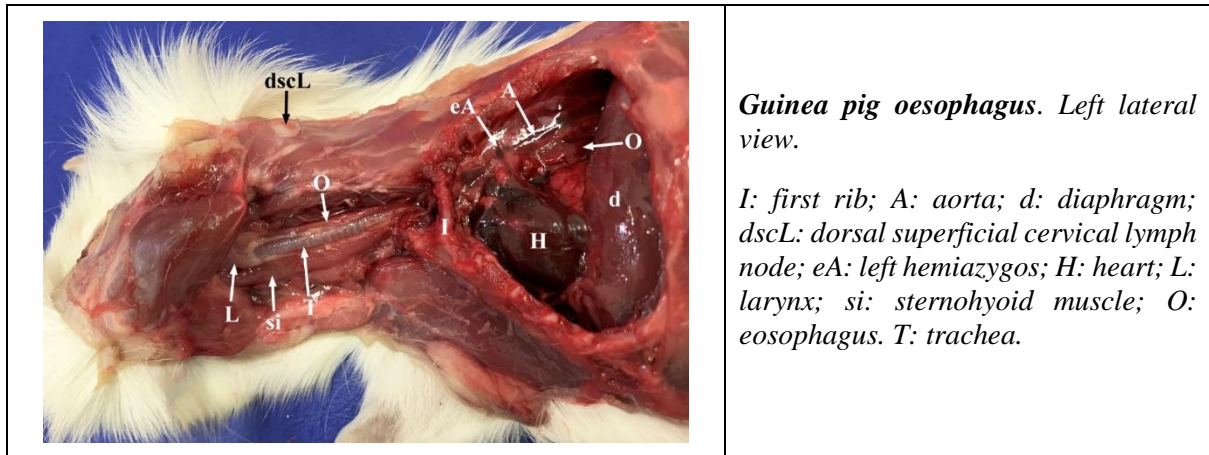


The tongue of the capybara measured 14 cm in length and weighed, on average, 77 grams. It was narrow and elongated along its antero-posterior axis and rounded at the anterior extremity. The anterior part is narrower, whereas the posterior part is broader, and covered by a pair of circumvallate papillae.

**Oesophagus**

***Cavia porcellus***

The oesophagus of the guinea pig ran in close contact and dorsal to the trachea in the neck region, and was displaced dorsolaterally to its left at the entrance of the thorax. It entered the stomach through the cardias near the lesser curvature at an oblique angle, forming an angular notch with the stomach.



**Guinea pig oesophagus.** Left lateral view.

*I: first rib; A: aorta; d: diaphragm; dscL: dorsal superficial cervical lymph node; eA: left hemiazygos; H: heart; L: larynx; si: sternohyoid muscle; O: oesophagus. T: trachea.*

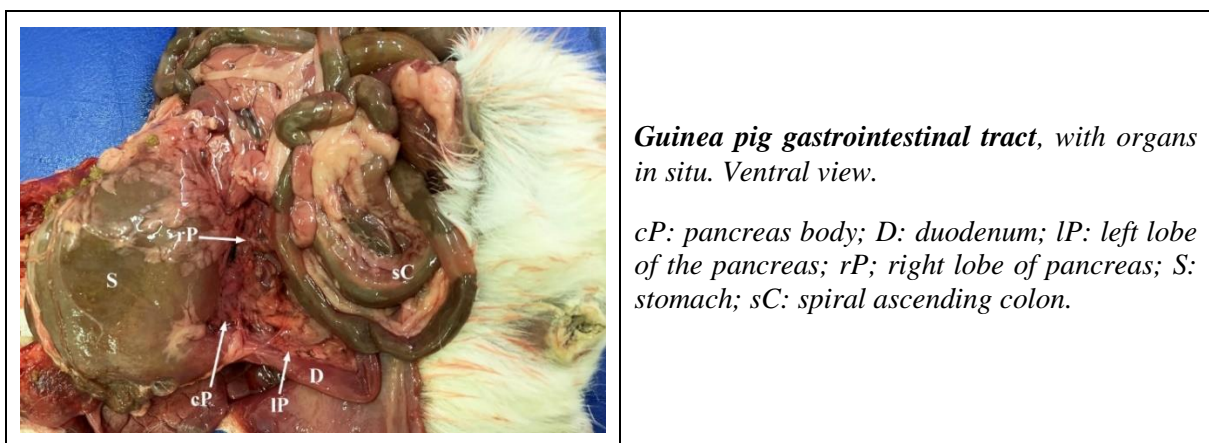
***Hydrochoerus hydrochaeris***

The esophagus of the capybara ran dorsally to the trachea in the neck, whereas in the thorax it ran dorsolaterally to its left. Its terminal portion entered the stomach near the lesser curvature, by forming with the gastric fundus a visible cardiac incisure.

**Stomach**

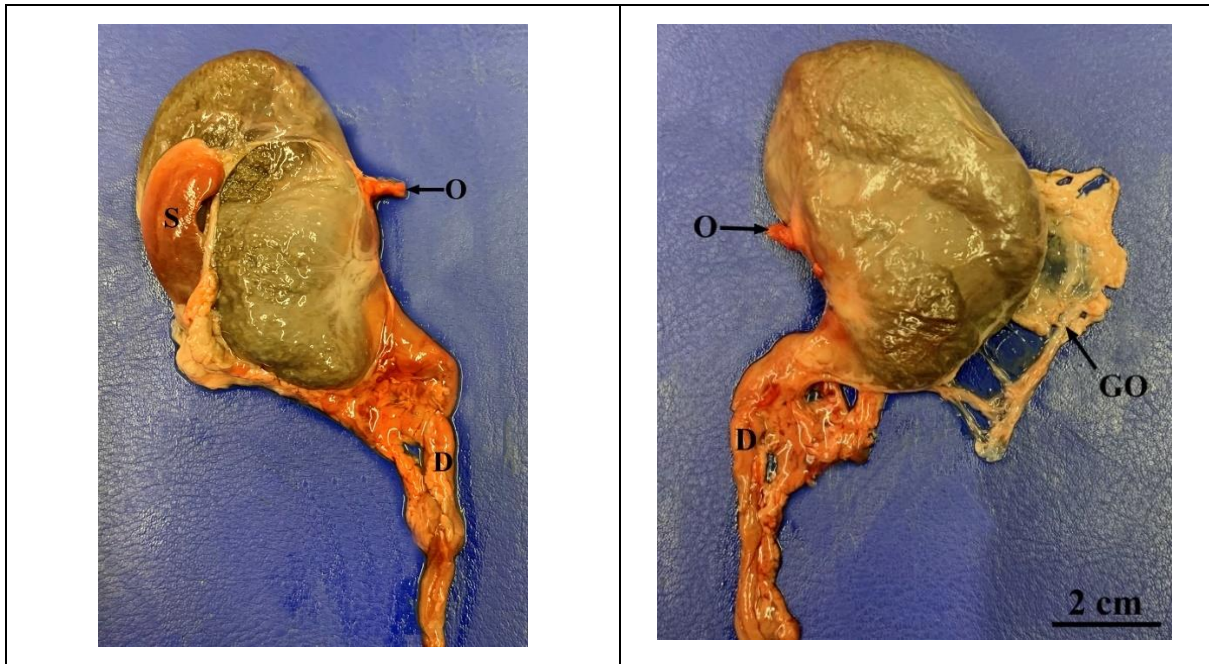
***Cavia porcellus***

The stomach of the guinea pig was topographically located in the left cranial abdomen. It was composed of the cardias, with an angular incisure in its lesser curvature formed by the union with the oesophagus, by a large fundus with a cranial expanded diverticulum, the body and the pylorus. The lesser curvature, giving attachment to the lesser omentum, was poorly developed. Its internal mucosa appeared smooth.



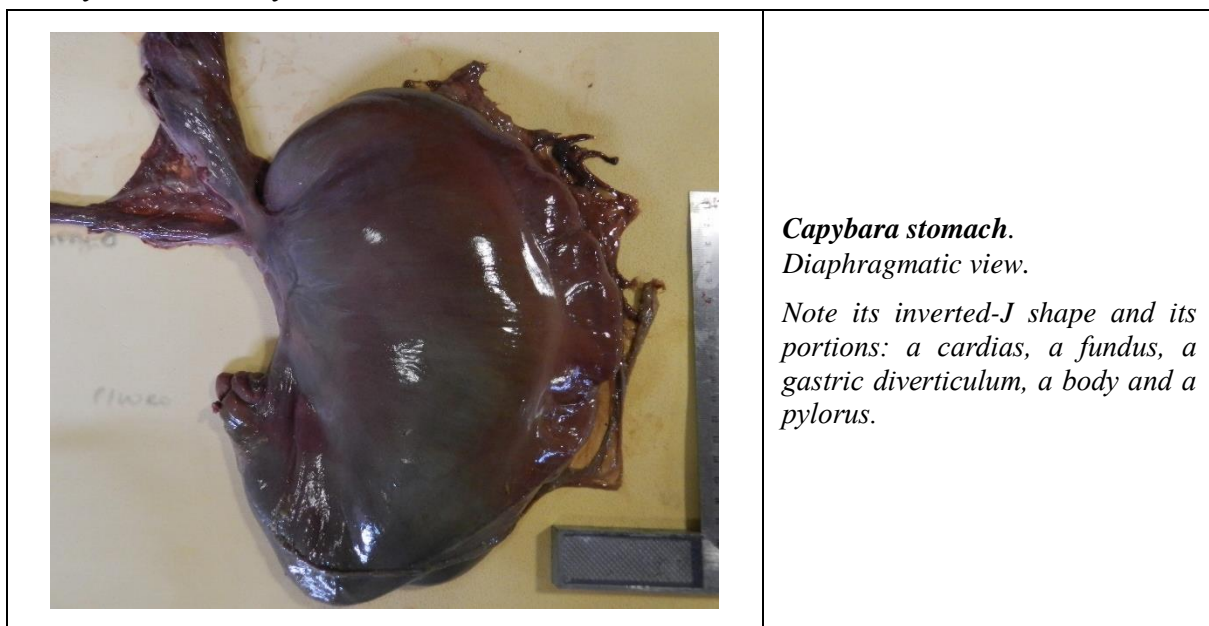
**Guinea pig gastrointestinal tract, with organs in situ.** Ventral view.

*cP: pancreas body; D: duodenum; IP: left lobe of the pancreas; rP; right lobe of pancreas; S: stomach; sC: spiral ascending colon.*



**Guinea pig isolated stomach.** Left: visceral view; right: diaphragmatic view.  
*D: duodenum; GO: greater omentum; O: oesophagus; S: spleen.*

***Hydrochoerus hydrochaeris***



***Capybara stomach.***  
*Diaphragmatic view.*

*Note its inverted-J shape and its portions: a cardias, a fundus, a gastric diverticulum, a body and a pylorus.*

Macroscopically, the stomach of the capybara consisted of 5 well-demarcated portions: a cardias, a fundus, a gastric diverticulum (a cranial expansion of the fundus), a body and a pylorus.

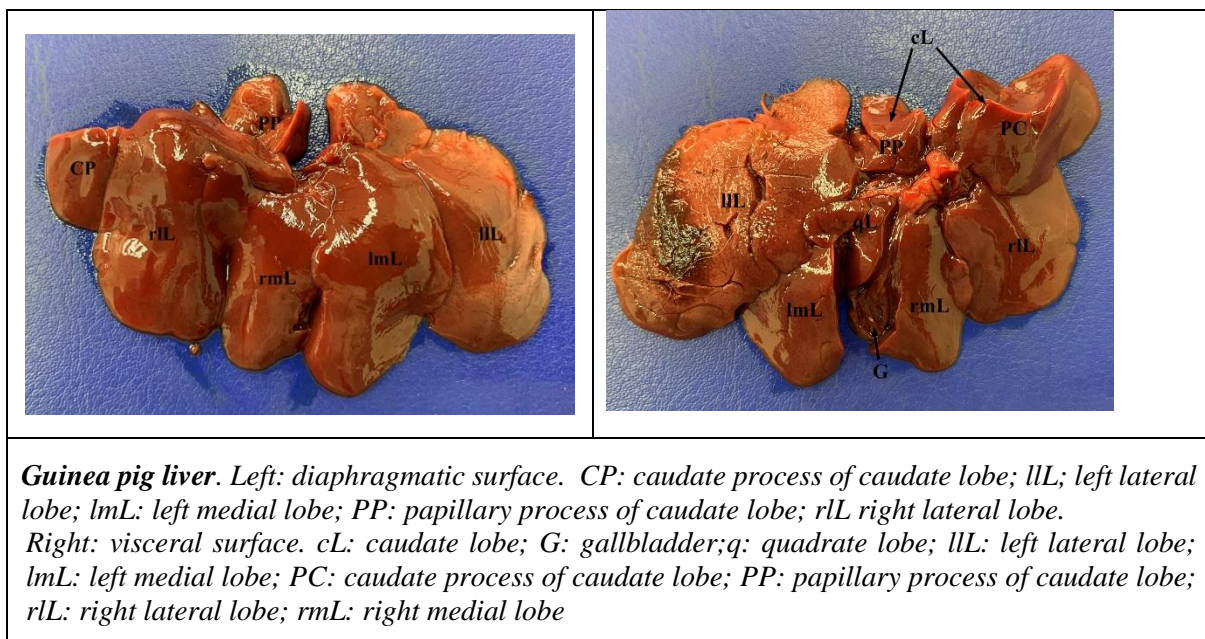
It had the shape of an inverted J, presenting a greater and a lesser curvatures. Externally, it was characterized by the presence of 2 gastric teniae located on the parietal face and on the visceral face in proximity of the greater curvature. Two incisures were also observed: the cardiac incisure, located at the union with the oesophagus, and an angular incisure, at the level of the lesser curvature in proximity of the pyloric antrum.

The capybara stomach had a total longitudinal diameter of 250 mm and a transversal width, at the level of the fundus, of 108 mm. The caliber of the cardias was 12 mm and that of the pylorus 23.2 mm.

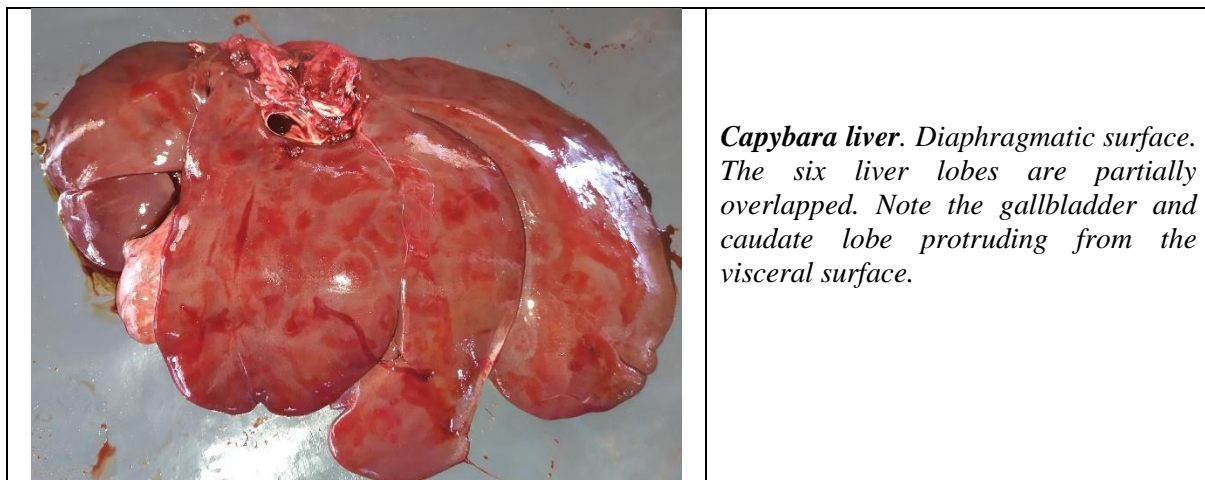
## Liver

### *Cavia porcellus*

The large guinea-pig liver was dark red-brown in color, with a smooth surface and sharp edges, and it consisted of six well-demarcated and partially overlapping lobes: left lateral, left medial, right medial, right lateral, quadrate and caudate. A well developed, thin-walled oval gallbladder lied in the fossa of the quadrate liver lobe on its medial aspect.

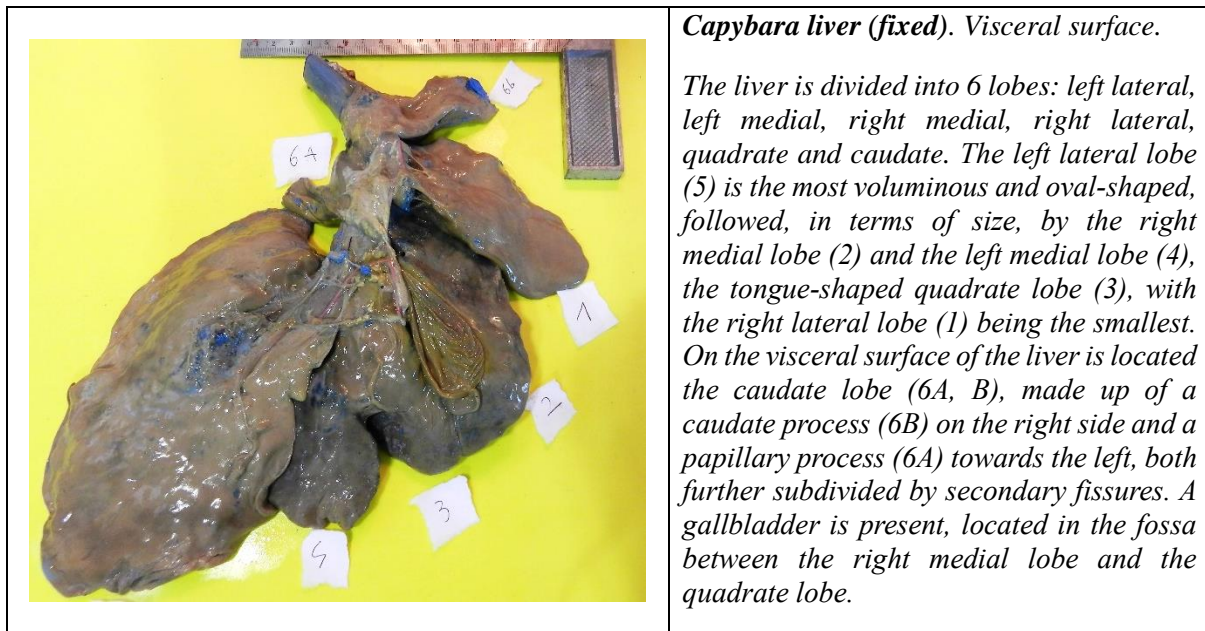


### *Hydrochoerus hydrochaeris*



The capybara liver weighed on average 611.5 grams and measured 26 cm in length, 18 cm in width and 3.54 cm in height. Macroscopically, the liver of the capybara consisted of 6

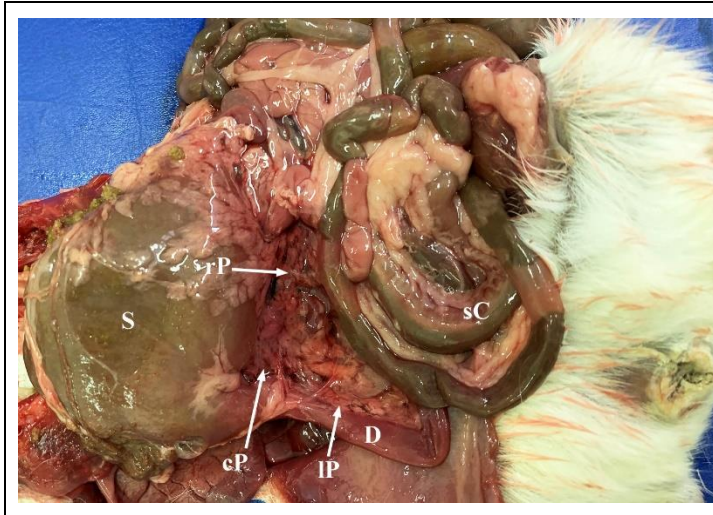
lobes, which overlap each other: left lateral (the most voluminous), left medial, right medial, right lateral, quadrate and caudate. The caudate lobe, located on the visceral surface was divided by secondary fissures into a caudate process and a papillary process. The liver of the capybara had thinned sharp margins, with well-demarcated lobes separated by deep fissures, except for the shallow fissure located between the left medial lobe and the quadrate lobe. A well-developed gallbladder was present on the visceral surface, located in the fossa between the right medial lobe and the quadrate lobe. The diaphragmatic surface of the liver appeared convex and smooth. On the visceral surface, a deep visible oesophageal impression was present.



## **Pancreas**

### ***Cavia porcellus***

The guinea pig pancreas was diffuse and included in the mesoduodenum and it was dark pink in color. It had a triangular shape and was composed of a left lobe, lying transversally between the stomach and the spiral colon, a body in contact with the cranial curvature of the duodenum, and a right lobe lying along the descending duodenum.



**Guinea pig gastrointestinal tract, with organs in situ. Ventral view.**

*cP*: pancreas body; *D*: duodenum; *lP*: left lobe of the pancreas; *rP*: right lobe of pancreas; *S*: stomach; *sC*: spiral ascending colon.

### ***Hydrochoerus hydrochaeris***



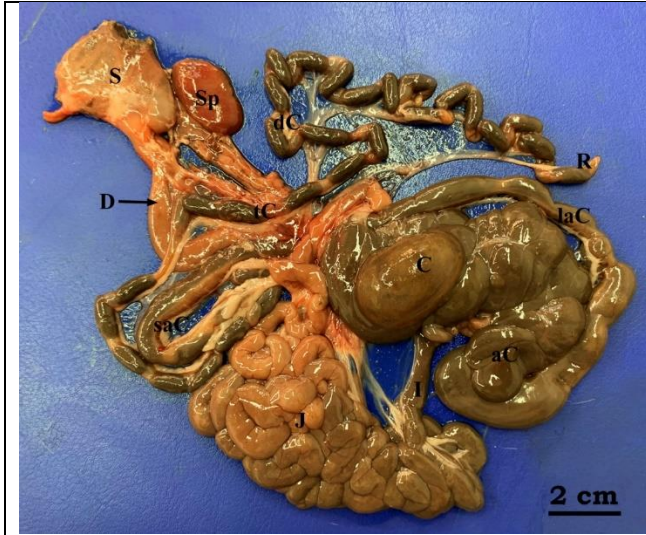
***Capybara pancreas. Head (left), body, and tail (right).***

The capybara pancreas weighed 9 grams, and measured 13 cm in length, 33.6 mm in width, and 7 mm in height. It lied in contact with the descending duodenum, incorporated in the mesoduodeum. It presented an elongated and irregular prismatic shape, and was divided into a head, a body and a tail, which appeared polylobed. It was seen to be irrigated by several pancreatic arteries originating from the celiac and cranial mesenteric arteries; specifically, it received blood from the pancreatic branches of the hepatic artery, the gastroduodenal and gastroepiploic arteries, the splenic artery and the cranial and caudal pancreaticoduodenal arteries.

## **Small intestine**

### ***Cavia porcellus***

The small intestine of the guinea pig was the longest portion of the alimentary tract and lied on the right side of the abdominal cavity. The duodenum, the jejunum and the ileum were not well-distinguishable macroscopically.



***Guinea-pig isolated gastrointestinal tract.***  
*aC: apex of the cecum; C: cecum body; D: duodenum; dC: descending colon; I: ileum; J: jejunum; laC: left ascending colon; R: rectum; S: stomach; SaC: spiral ascending colon; Sp: spleen; tC: transverse colon.*

***Hydrochoerus hydrochaeris***



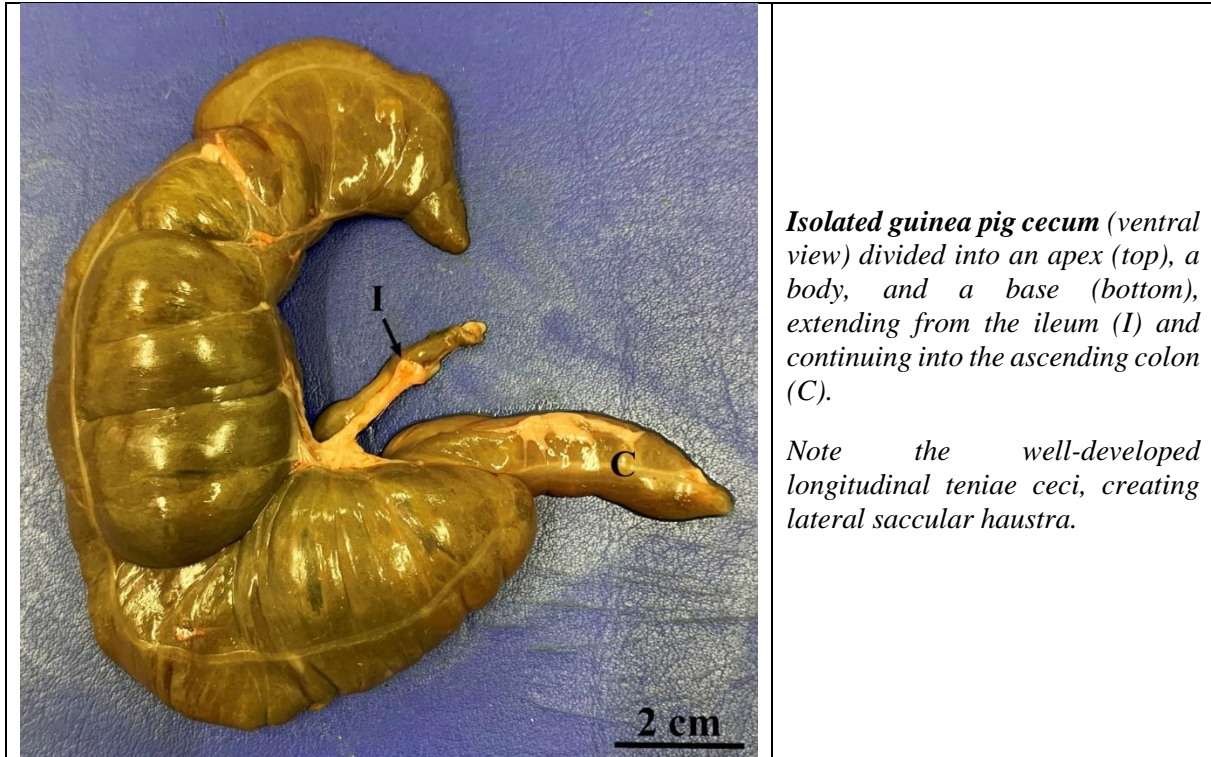
***Capybara isolated and distended small intestine (duodenum, jejunum, ileum).***

The small intestine of the capybara had a total length of 4 meters, of which the duodenum measuring approximately 27 cm, the ileum 32 cm and the jejunum 3.80 meters. The three portions were not distinguishable macroscopically.



## Large intestine

### *Cavia porcellus*



The large intestine of the guinea pig extended from the ileocecal valve and ended with the anus.

The cecum was very voluminous and developed, with a thin wall and occupying most of the guinea pig abdominal cavity and it was composed by a body, a base and an apex. It lacked a cecal appendix. On its outer surface, it presented three white longitudinal teniae ceci, which created lateral saccular haustra.

The colon was dark green in color and divided into an ascending, a transverse, and a descending portions, with the ascending portion being composed of a well-developed spiral colon composed of a centrifugal and a centripetal gyri.

*Hydrochoerus hydrochaeris*



*Isolated capybara cecum, divided into an apex (right), a body, and a base (left), continuing into the proximal ascending colon. Note the terminal portion of the ileum joining the cecum (forceps). Note the abundant vascularization of the cecum and the termination of the ileocolic artery into branches dedicated to the base of the cecum.*



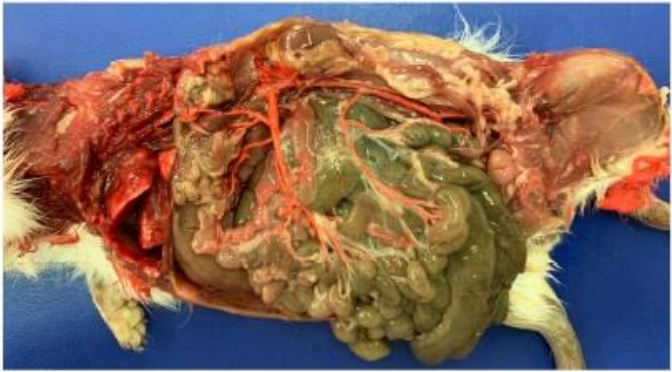
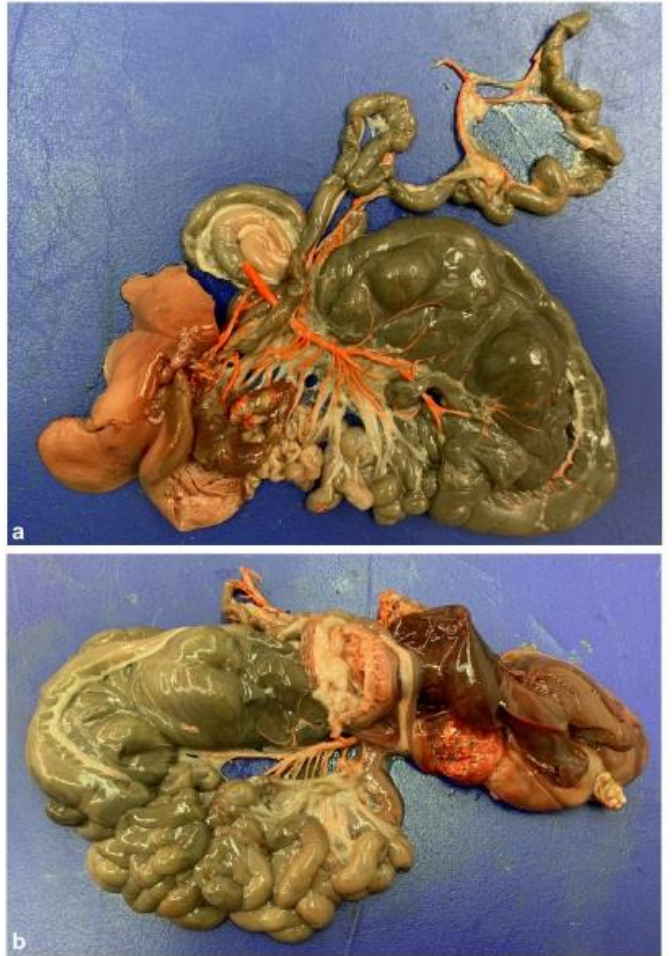
*Capybara isolated large intestine showing the casts of the cranial mesenteric artery and its collaterals*

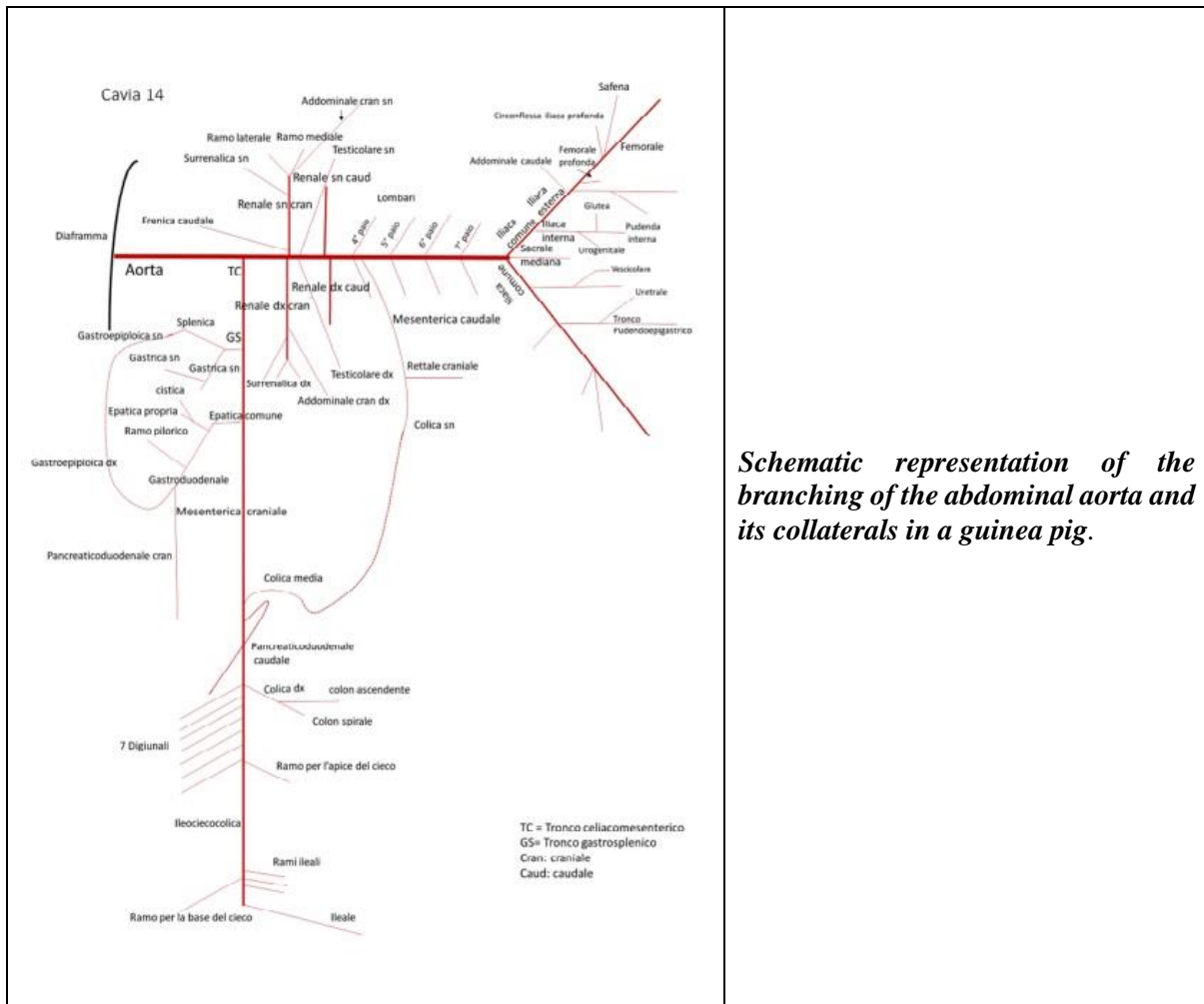
The capybara large intestine was composed of a voluminous cecum, which measured approximately 91 cm in length and was characterized by a base, a body and an apex, an ascending colon, divided into a proximal ansa and a distal or spiral ansa (45 cm long, distended), characterized by a centrifugal and a centripetal gyri, the transverse colon, the descending colon,

and the rectum. Four large dorsal and ventral teniae crossed the external surface of the cecum.

## **Anatomical morphological and morphometric study of the abdominal aorta and its collaterals in the guinea pig and capybara**

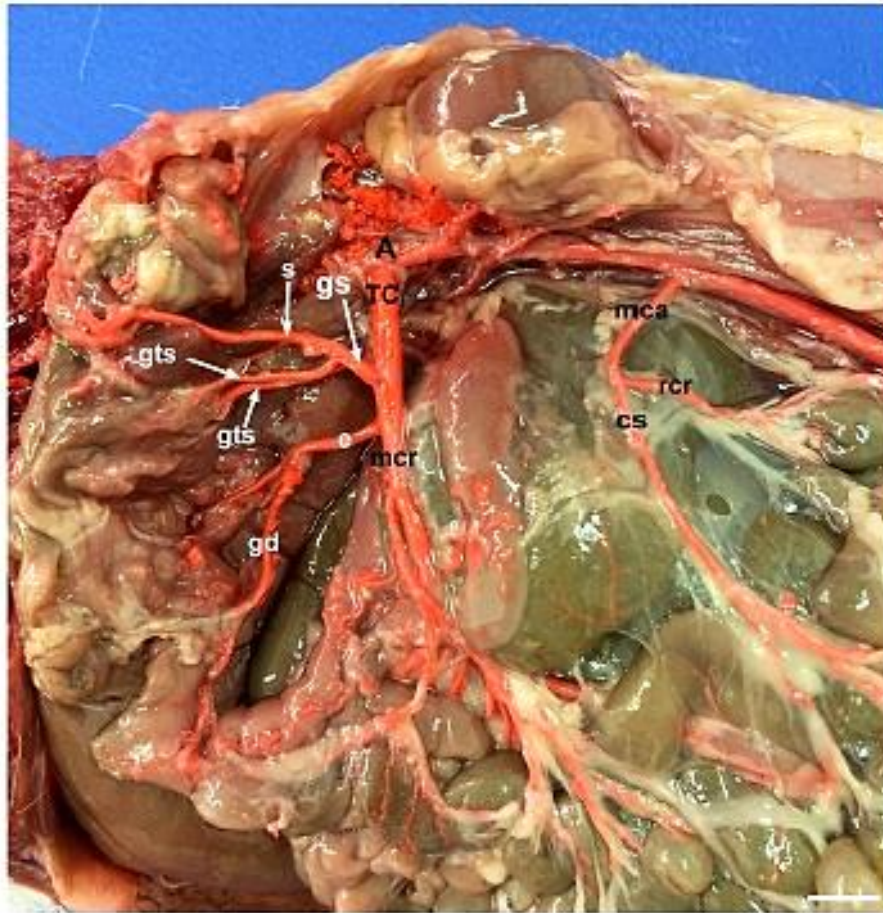
### *Cavia porcellus*

 A photograph showing the abdominal cavity of a guinea pig during a surgical procedure. The abdominal wall is open, and the internal organs, including the liver, stomach, and intestines, are visible. The abdominal aorta and its branches are highlighted in red, indicating the phase of isolation of the vessels.	<p><i>Guinea pig abdominal cavity. Phase of isolation of the abdominal and pelvic arterial vessels.</i></p> <p><i>The complete opening of the abdominal and pelvic cavities allowed the highlighting of the vessels under study.</i></p>
 Two photographs showing the isolated gastrointestinal tract of a guinea pig. The top photograph (a) shows the left lateral view, and the bottom photograph (b) shows the right lateral view. The organs are arranged in a complex, branching pattern, with the abdominal aorta and its branches clearly visible. The vessels are highlighted in red, allowing for detailed observation and measurement.	<p><i>Guinea pig isolated gastrointestinal tract. The viscera of the abdominal cavity in left (a) and right (b) lateral view after isolation. This phase made it possible to observe and measure the arteries in detail.</i></p>



*Schematic representation of the branching of the abdominal aorta and its collaterals in a guinea pig.*

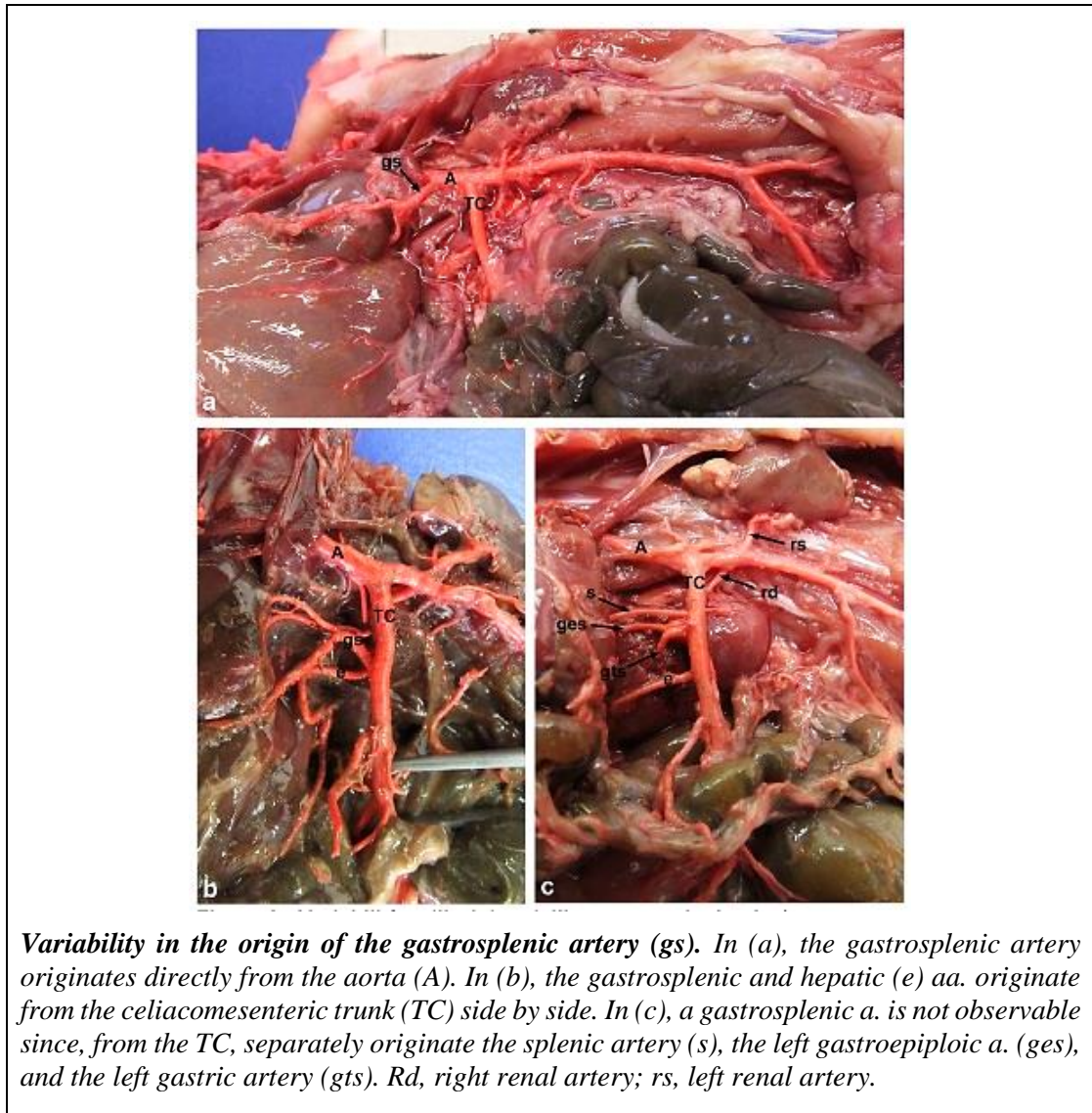
In all the guinea pigs studied, a **celiacomesenteric trunk (CT)** was evidenced, instead of separate celiac and cranial mesenteric arteries, as seen in most mammals. The celiacomesenteric trunk originated from the abdominal aorta at an average distance from the diaphragm of 5.15 mm and presented an average diameter of 2.39 mm, occurring in correspondence of the first lumbar vertebra (13.3%), between the first and second lumbar vertebrae (6.7%), at the level of the second lumbar vertebra (6.7%), or between the twelfth thoracic vertebra and the first lumbar vertebra (6.7%). Five different modes of branching of the celiac component of the celiacomesenteric trunk were observed: 1) in most cases, the CT first emitted the gastrosplenic artery, which gave rise to the left gastric and splenic arteries, and, subsequently, detached the hepatic artery; 2) the gastrosplenic artery originating from the CT contracted an anastomosis with the abdominal aorta cranially to the origin of the CT; 3) the gastrosplenic artery originated from the abdominal aorta, whereas the CT emitted the hepatic artery; 4) the gastrosplenic and hepatic arteries originated from the confluence of a common trunk detached from the CT; 5) the gastrosplenic artery was absent: the CT gave rise first to the splenic artery and, subsequently, it emitted a common trunk which, in turn, gave rise to the left gastroepiploic and the left gastric arteries.



***Origin of the celiacomesenteric trunk (CT) from the aorta (A).***

*The TC emits: the gastrosplenic artery (gs), the hepatic artery (e) and the cranial mesenteric artery (mcr). Cs, left colic a.; gd, gastroduodenal a.; gts, left gastric a.; mca, caudal mesenteric a.; rcr, cranial rectal a.; s, splenic a. Scale bar = 1 cm.*

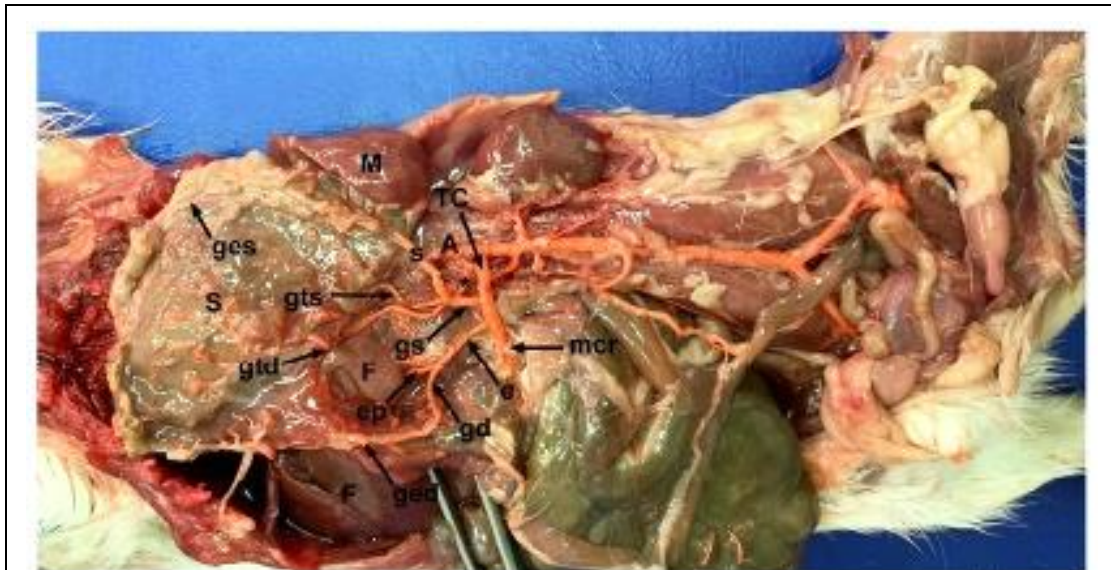
As for the division patterns of the **gastrosplenic artery**, a large variability was encountered in the animals studied: 1) in the majority of cases, the gastrosplenic artery divided into the left gastric artery and the splenic artery; 2) it trifurcated into the left gastric, the left gastroepiploic, and the splenic arteries; 3) it gave rise to two left gastric arteries and, subsequently, it emitted the splenic artery which continued as the left gastroepiploic artery; 4) it emitted, simultaneously, two left gastric arteries and the splenic artery; 5) it emitted the left gastric artery, which in turn gave rise to a second left gastric artery, and then emitted the splenic artery; 6) it emitted, in succession, the right gastric and the left gastric arteries, whose branches anastomosed at the small curvature of the stomach, and, subsequently, provided the splenic artery which continued as the left gastroepiploic artery; 7) it emitted the left gastric artery, and, subsequently, the splenic artery that continued as left gastroepiploic; 8) it first emitted the gastrosplenic artery, then the left gastric, and, finally, the splenic artery; 9) it first emitted the left gastric artery, then the central gastric artery and, finally, the splenic artery, which continued as left gastroepiploic.



The **hepatic artery**, originating from the CT independently, or, in one case, from a common trunk with the gastrosplenic artery, was observed showing the following branching pattern:

In the majority of cases, the common hepatic artery emitted the cystic artery, followed by the proper hepatic artery, the right gastric artery, and continued as gastroduodenal artery. The right gastric artery was not always highlighted. In a minority of cases, the right gastric artery originated from the common hepatic artery before the emission of the cystic artery. In a single subject, the common hepatic artery emitted simultaneously the cystic and proper hepatic arteries.

In all the subjects, the gastroduodenal artery terminated by bifurcating into an ascending branch, the right gastroepiploic artery, and into a descending branch, the cranial pancreaticoduodenal artery. The right gastroepiploic artery ran at the level of the greater curvature of the stomach where it anastomosed with its homologue from the left. The cranial pancreaticoduodenal artery, destined to the right lobe of the pancreas and the lesser curvature of the duodenum, anastomosed with its caudal homologous originating from the cranial mesenteric artery.



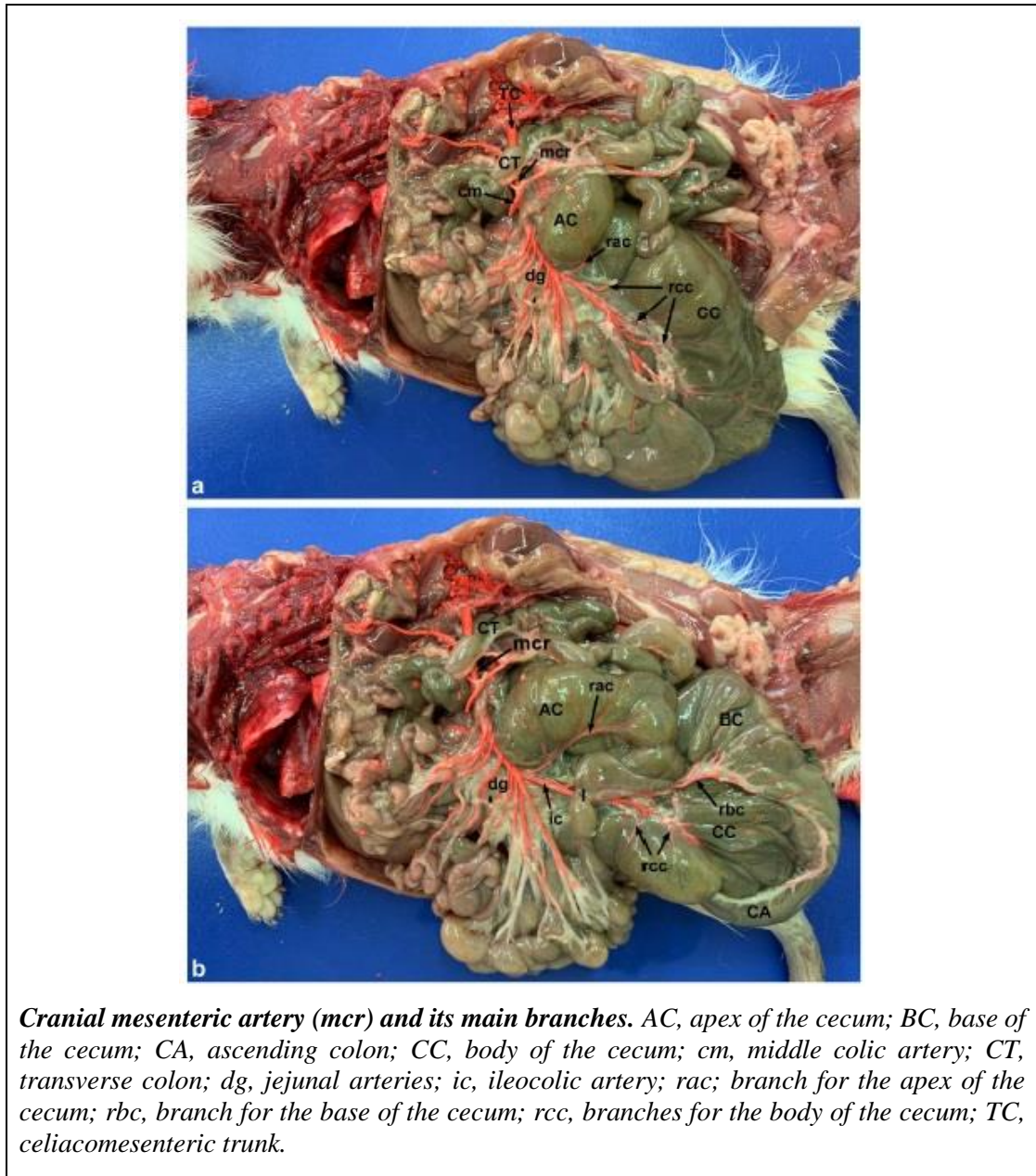
***Division of the gastrosplenic (gs) and hepatic (e) arteries.***

*From the gastrosplenic artery originate: the splenic artery (s), which in turn continues into the left gastroepiploic artery (ges), the left gastric artery (gts) and the right gastric artery (gtd). The common hepatic a. bifurcates into the hepatic a. (ep) and gastrooduodenal a. (gd). The latter emits the right gastroepiploic a. (ged). The asterisk indicates an anastomosis between the gs a. and the aorta (A). F, liver; M, spleen; mcr; cranial mesenteric a.; S, stomach; TC, celiacomesenteric trunk.*

The CT, after having emitted the hepatic artery, continued as the **cranial mesenteric artery**, which runs along the right side of the abdomen following the body of the pancreas. The **middle colic artery**, originated from the cranial mesenteric artery at an average distance of 18.8 mm from the aorta, was directed towards the ascending, spiral and transverse colon, and anastomosed with the left colic artery, originating from the caudal mesenteric artery, at the level of the descending colon.

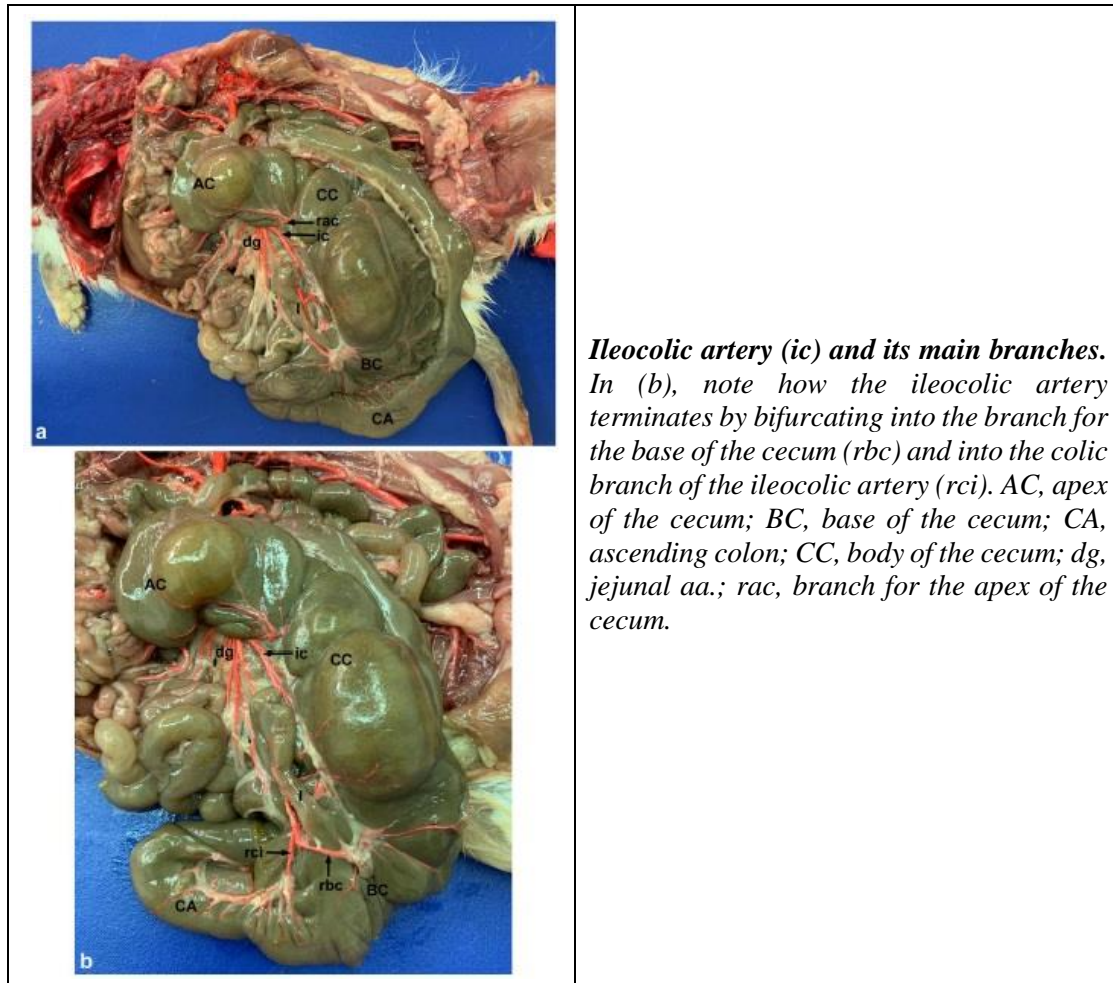
The cranial mesenteric artery originated, subsequently, the **caudal pancreaticoduodenal artery**, which ran in the mesoduodenum to supply the right lobe of the pancreas and the proximal duodenum, to then anastomose with its cranial homologue. In two guinea pigs, the caudal pancreaticoduodenal artery originated from the first jejunal artery.

The cranial mesenteric artery then detached the **right colic artery**, directed to the ascending colon. In two subjects, the right colic artery appeared to be double. The right colic artery originated from the cranial mesenteric artery at the level of the first jejunal artery in the majority of cases, or at the level of the second or third jejunal artery. In one subject it originated before the emission of the first jejunal artery. The cranial mesenteric artery gave rise to a number of **jejunal arteries** that ranged from a minimum of 5 to a maximum of 10, 7 being the average number of branches.



The cranial mesenteric artery, after detaching the jejunal arteries, continued as **ileocolic artery** destined for the large intestine. The ileocolic artery provided several branches for the apex, body and base of the caecum. It then detached several ileal branches and ended by bifurcating into the branch for the base of the cecum and the colic branch of the ileocolic artery, destined for the initial part of the ascending colon.



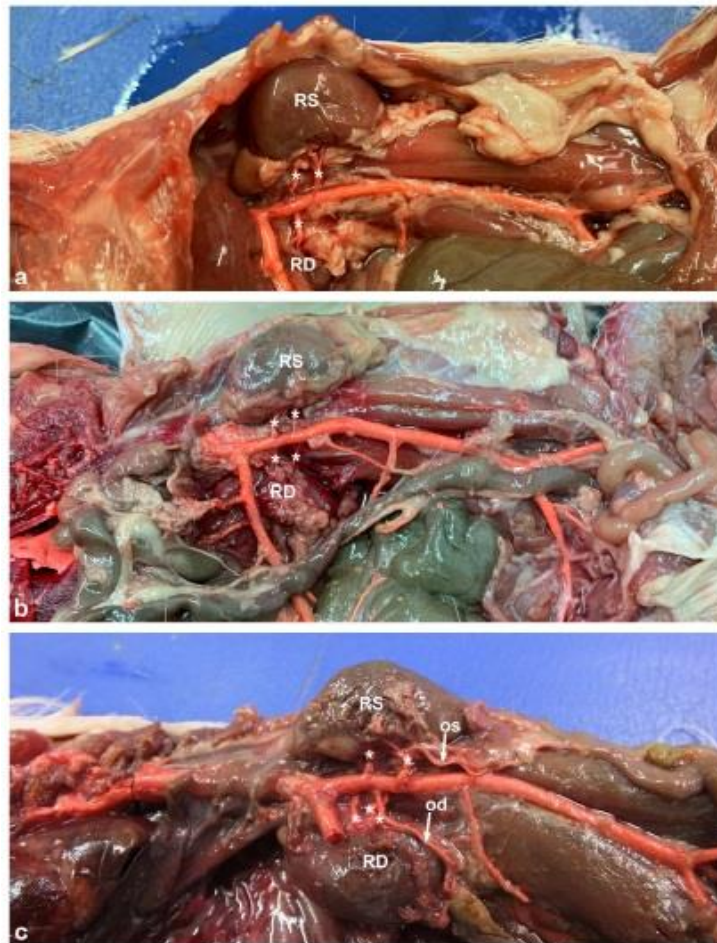


The right and left adrenal glands were perfused by the **adrenal arteries** of the corresponding side. These on each side, detached from the corresponding renal artery at various levels, from its point of origin, to the renal hilum. In one case, the adrenal artery originated from the cranial abdominal artery originating from the renal artery; in some cases, it originated from the caudal phrenic artery, emitted by the ipsilateral renal artery or directly by the abdominal aorta cranial to the renal arteries; in one case, it originated directly from the abdominal aorta cranial to the origin of the renal arteries. In presence of double renal arteries, the adrenal originated from the cranial renal artery. In addition, in a minority of subjects, a ureteral artery directed to the initial part of the ureter and emitted from the ipsilateral renal artery in proximity of the renal hilum, was found.

The **renal arteries** were found to be single, double or even triple in the guinea pigs studied. 1) In the majority of animals (57.1%) the renal arteries were single on both sides; 2) 14.3% of subjects had double right renal arteries; 3) 14.3% had double renal arteries on both sides; 4) 9.5% had double left renal arteries; 4) in one specimen, three renal arteries were observed on the right: a cranial and two caudal renal arteries, and double renal arteries, cranial and caudal, on the left side.

Each renal artery divided into a lateral and a medial branch at the level of the organ hilum. The left renal arteries were found to be, on average, larger in diameter than the corresponding right ones, and, in case of double renal arteries, the cranial branch was always larger than the

caudal. Moreover, the right renal artery originated more cranially than the left renal artery. In general, the renal arteries originated in correspondence of the second/third lumbar vertebrae.



*Numerical variability of the renal arteries. In addition to the presence of single renal arteries on both sides (see Fig. 5c), other patterns that can be found are: double renal arteries on one side (a), double renal arteries on both sides (b), and triple renal arteries on one side and double on the other (c). In the latter case, note the origin of the ovarian arteries from one of the renal aa. The renal arteries are indicated by an asterisk. Od, right ovarian a.; os, left ovarian a.; RD, right kidney; RS, left kidney.*

The paired **caudal phrenic arteries**, intended for the abdominal face of the pillars and the tendinous center of the diaphragm, originated directly from the abdominal aorta, cranial or caudal to the CT in the majority of cases; in a minority of instances, they originated directly from the cranial renal artery of the corresponding side.

The **cranial abdominal arteries**, directed to the muscles of the abdominal wall, took origin, in all guinea pigs, from the corresponding renal artery, or from the cranial renal artery in case of double renal arteries.

The paired **ovarian arteries** originated, symmetrically, from the sides of the abdominal aorta caudal to the renal arteries in the majority of females; in one instance, the right ovarian artery originated between the right cranial and caudal renal arteries, and, in another case, both

ovarian arteries originated from the caudal renal arteries. The ovarian arteries originated at the level of the third lumbar vertebra. In a guinea pig, it was possible to highlight the anastomosis, at the level of the broad ligament of the uterus, between the uterine branch of the ovarian artery and the uterine artery.



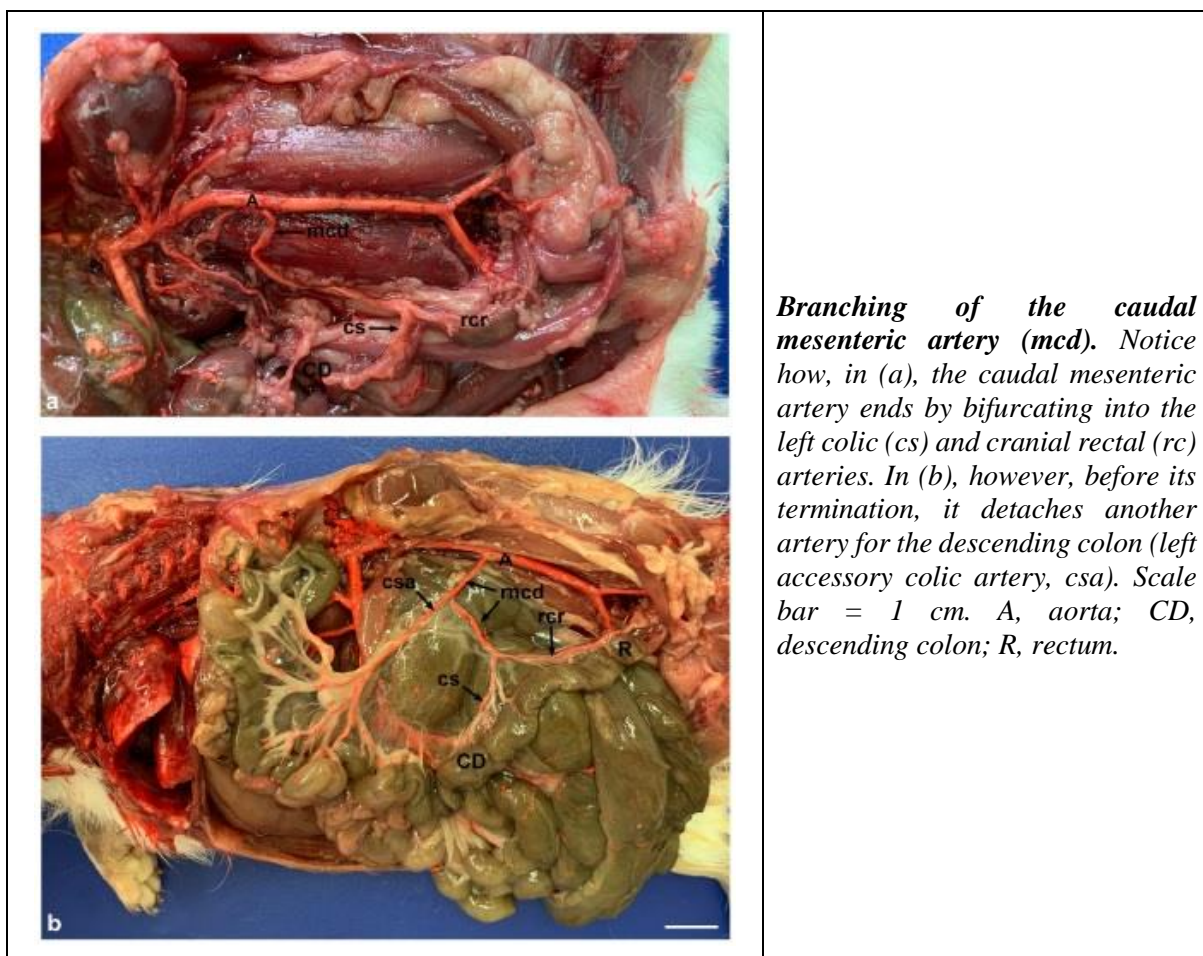
**Arterial vascularization of the female reproductive system.** A, aorta; CU, body of the uterus; CUD, right uterine horn; ilc, common iliac artery; ile, external iliac a.; ili, internal iliac a.; od, right ovarian a.; OD, right ovary; RD, right kidney; ug, urogenital a.; ut, uterine a.; V, bladder.

The paired **testicular arteries**, in the majority of specimens, originated from the abdominal aorta, caudally to the renal arteries, and terminated at the testicular level by passing through the respective inguinal canals. In two specimens, the left testicular artery originated cranially to the corresponding renal artery, and, in another animal, both testicular arteries originated cranial to the ipsilateral caudal renal arteries.



**Origin and course of the testicular artery.** A, aorta; aca, caudal abdominal artery; acr, cranial abdominal artery; cip, deep iliac circumflex artery; ilc, common iliac artery; RS, left kidney; ts, testicular artery; VS, seminal vesicles.

The unpaired **caudal mesenteric artery**, with a mean diameter of 0.9 mm, originated from the ventral aspect of the aorta, at an average distance of 20.4 mm from the emission of the CT, and headed caudally to supply the descending colon and rectum. The caudal mesenteric artery ended by bifurcating into the **left colic artery**, destined for the descending colon, and a **cranial rectal artery**, directed to the rectum. The left colic artery ended by anastomosing, at the level of the descending and transverse colon, with the middle colic artery, deriving from the cranial mesenteric artery. In one subject, a double left colic artery was evidenced. The caudal mesenteric artery emerged at the level of the fourth lumbar vertebra (42.9%), between the fourth and fifth lumbar vertebra (35.7%), at the level of the fifth lumbar vertebra (14.3%), or between the third and fourth lumbar vertebrae (7.1%).



The abdominal aorta, at an average distance of 25.9 mm from the caudal mesenteric artery, terminated by bifurcating into the right and left **common iliac arteries**, which, in turn divided into an internal and an external iliac artery. The **median sacral artery** originated at the level of the aortic bifurcation into the common iliac arteries, from its dorsal aspect. The bifurcation of the aorta into the common iliac arteries occurred at the level of the seventh lumbar vertebra (36.4%), between the seventh lumbar and first sacral vertebrae (36.4%), or at the level of the first sacral vertebra (27.3%).

Each **internal iliac artery** ran caudally towards the dorsal part of the pelvic cavity, and,

after emitting the urogenital artery, it continued as internal pudendal artery.

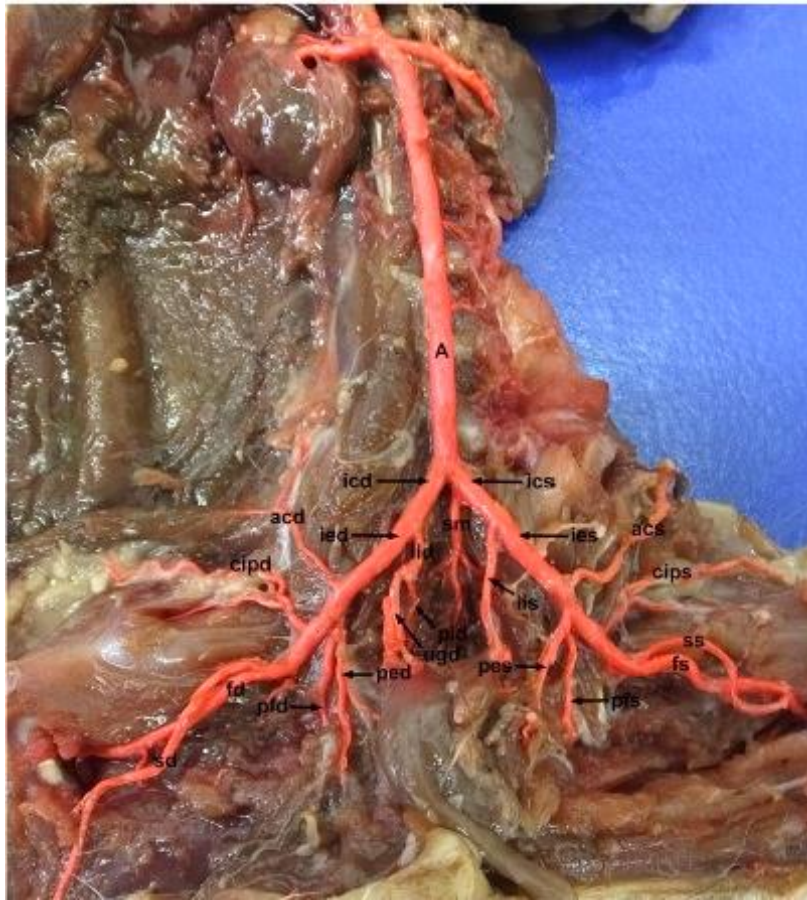
The right and left **urogenital arteries**, in females, where they irrigated the urinary tract, uterus, ovary and vagina, emitted the right and left uterine arteries, respectively. In males, the urogenital arteries, which irrigate the urinary tract and accessory sexual glands, emitted the vesicular arteries, destined to supply the guinea-pig well-developed seminal vesicles.

The **internal pudendal artery**, emitted, a few millimeters after its origin from the internal iliac artery, the gluteal artery directed to the muscles of the thigh.

The **external iliac artery** emitted, in succession, the caudal abdominal artery, the pudendal epigastric trunk, the deep artery of the femur, and the deep circumflex iliac or ileolumbar artery. The external iliac artery then continued as femoral artery, which then gave rise to the saphenous artery.

The **caudal abdominal artery**, originating from the external iliac, ran ventrocranially over the deep face of the internal oblique abdominal muscle, parallel to the lateral border of the rectus abdominis muscle. The **pudendal epigastric trunk** emitted a urethral branch destined to the urethra, and, in the male, to the prostate. The **deep artery of the femur** originated at the termination of the external iliac artery, immediately before the emission of the femoral artery, and ran in a ventrocaudal direction passing cranially to the pubis between the iliopsoas and pectineus muscles. The **deep circumflex iliac artery** originated from the dorsal aspect of the external iliac artery and ran laterally between the peritoneum and the iliac fascia, ran along the ventral face of the psoas muscles up to the ventrocranial iliac spine and, finally, ended by crossing the transverse abdominal muscles and the internal oblique abdominal muscles.

The external iliac artery continued as **femoral artery** to vascularize the region of the thigh. The **saphenous artery**, originating from the femoral, was well-developed and played an important role in the vascularization of the foot.



**Termination of the aorta (A).** The aorta, after having emitted the right (icd) and left (ics) common iliac arteries, continues as the median sacral artery (sm). acd, right caudal abdominal a.; acs, left caudal abdominal a.; cipd, right deep circumflex iliac a.; fs, left femoral a.; ied, right external iliac a.; ies, left external iliac a.; iid, right internal iliac a.; iis, left internal iliac a.; ped, right epigastric pudendal trunk; pes, left epigastric pudendal trunk; pfd, right deep a. of the femur; pfs, left deep a. of the femur; pid, right internal pudendal a.; sd, right saphenous a.; ss, left saphenous a.; ugd, right urogenital a.

### ***Hydrochoerus hydrochaeris***

The irrigation of the diaphragm and adrenal glands came from the paired **caudal phrenic arteries**, directly branching from the abdominal aorta cranially to the origin of the celiac artery.

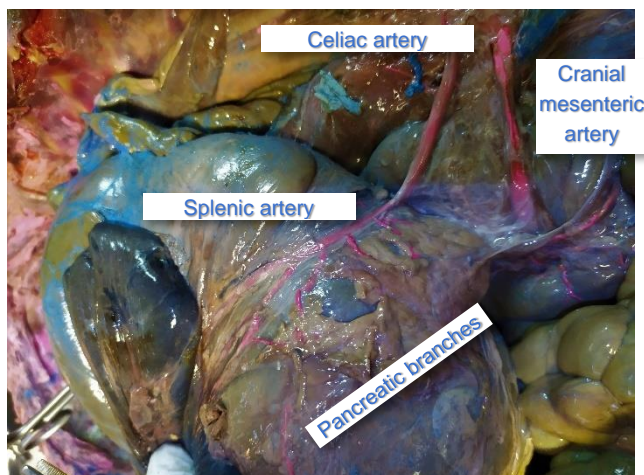
The capybara, unlike the guinea pig, had separate celiac and cranial mesenteric arteries.

The **celiac artery** was short and voluminous, with an average diameter of 5.8 mm, and originated from the ventral aspect of the abdominal aorta, at an average distance of 13 cm from the diaphragm: it supplied the spleen, the stomach, the first part of the duodenum, the liver and the pancreas.

The celiac artery was seen to divide into three branches: the splenic artery, to the left, the left gastric artery, in the middle, and the hepatic artery, to the right.



*Capybara celiac artery and its collaterals.*

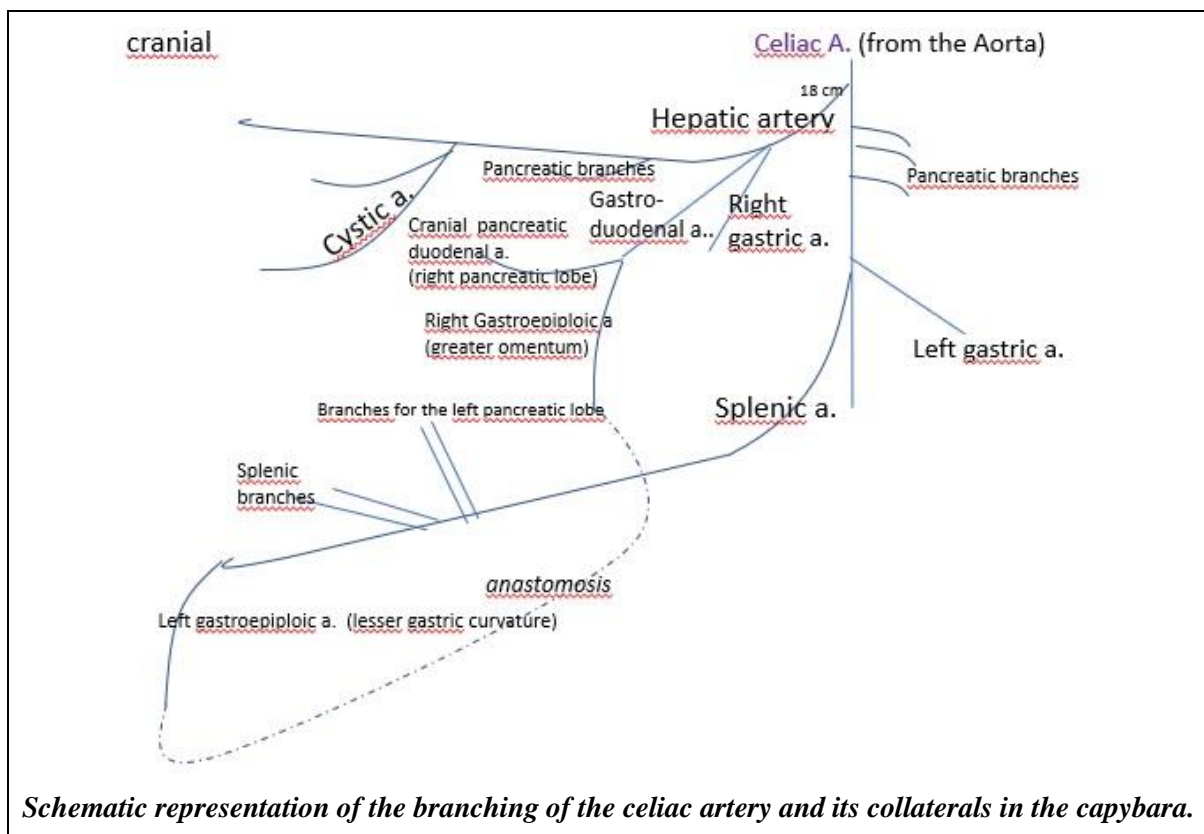


The **splenic artery**, measuring 17.9 mm in length, supplied the spleen, the fundus and greater curvature of the stomach, as well as adjacent parts of the stomach wall, and the left lobe of the pancreas; it continued in the greater omentum along the greater curvature of the stomach as **left gastroepiploic artery**, which anastomosed with the right gastroepiploic artery originating from the hepatic artery.

The **left gastric artery** distributed to the lesser curvature of the stomach up to the visceral aspect of this organ. It finally ends near the gastric incisure where it anastomosed with the **right gastric artery**. The latter is made up of small branches that are directed towards the anterior or parietal face of the stomach.

The **hepatic artery** supplied the liver and gave off branches for the right lobe of the pancreas (pancreatic arteries), a branch for the lesser curvature of the stomach (**right gastric artery**), and a branch to the first half of the duodenum (**gastrooduodenal artery**). The gastrooduodenal artery gave off the **right gastroepiploic artery** directed to the greater curvature of the stomach, to finally anastomose with the left gastroepiploic artery.

The **hepatic artery** reached the hepatic hilum together with the portal vein, and then branched off inside the hepatic parenchyma. The right and left hepatic branches distributed to the corresponding portions of the liver. In its passage through the pancreas, the initial part of the hepatic artery gave off the **cranial pancreatic duodenal artery**. The latter sent a branch directed to the duodeno-jejunal flexure, anastomosed with the first jejunal arteries, and continued in the opposite direction following the duodenum retrogradely to anastomose with its caudal counterpart.



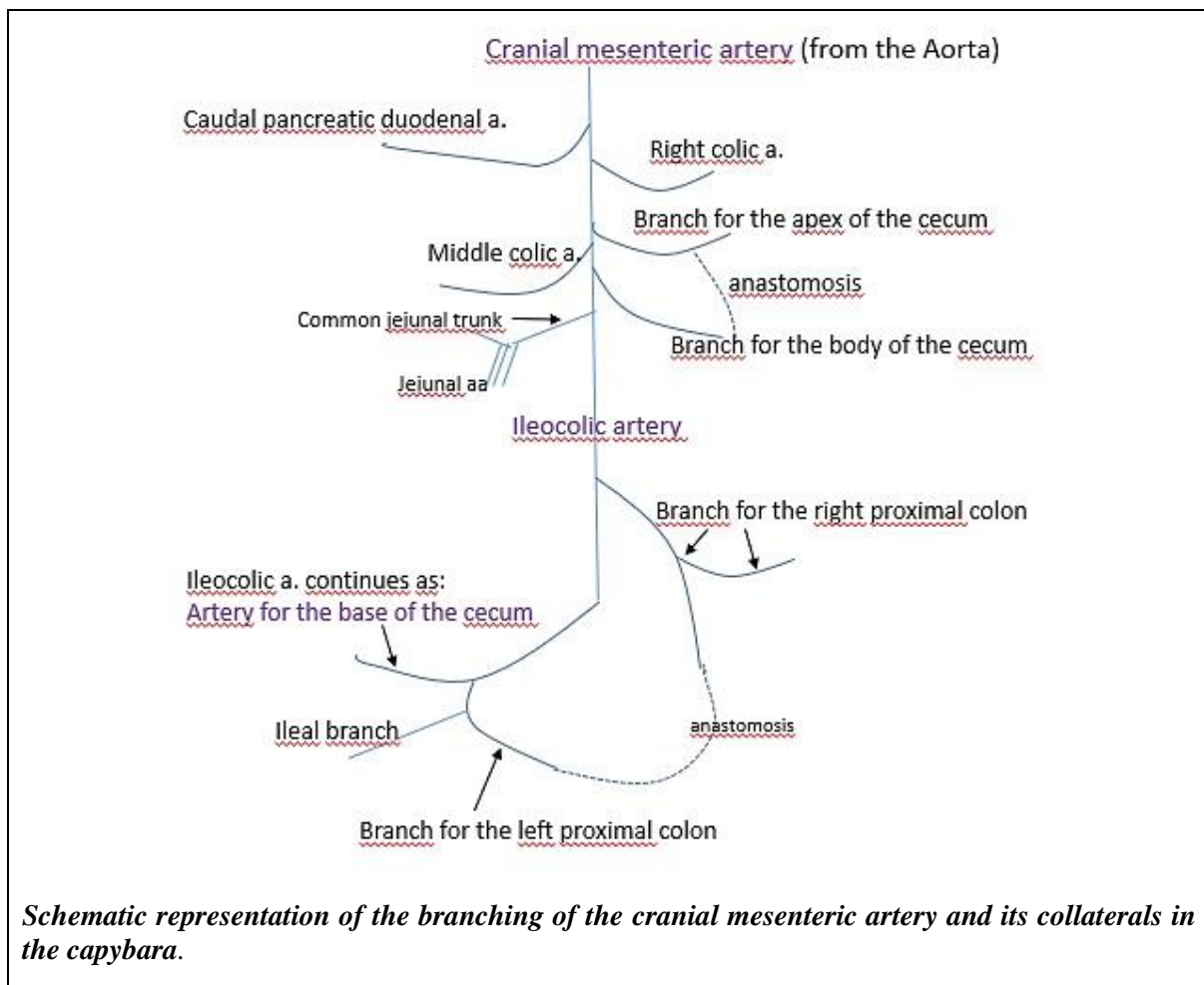
The **cranial mesenteric artery** originated from the aorta, at an average distance of 14.8 mm from the emission of the celiac artery. The cranial mesenteric artery supplies most of the intestine, from the posterior half of the duodenum to the beginning of the descending colon.

The cranial mesenteric artery, measuring on average 77.3 mm in length and 7.8 mm in diameter, gives off the **caudal pancreatic duodenal artery**, which anastomosed with the homonymus from the left; subsequently it gave off the the **right colic artery** destined for the ascending and spiral colon. Subsequently, it emitted the **middle colic artery**, destined for the descending and transverse colon, and two **cecal branches** destined for the apex and body of the



cecum, which contracted anastomosis with each other. It then detached a common jejunal trunk, which gave rise to multiple **jejunal arteries**.

The cranial mesenteric artery then continued as ileocolic artery, measuring on average 38.4 mm and destined for the termination of the ileum, the cecum, and the beginning of the ascending colon. The **ileocolic artery** gave off a branch for the right proximal colon, and terminated by bifurcating into an ileal artery, which gave rise to a branch for the left proximal colon which anastomosed with the homologous from the right, and a **cecal artery** destined for the base of the cecum. The cecum was richly irrigated by numerous branches dedicated to its apex, body and base. The termination of the ileocolic artery occurred with a voluminous terminal artery dedicated to the cecum.



The **renal arteries** were very voluminous and they divided into a medial and lateral branches before entering the hilum of the organ. They originated from the abdominal aorta about 14 mm caudally to the emission of the cranial mesenteric artery, and had an average diameter of 6.7 mm. Unlike the guinea pig, they were found to be single on both sides in all the animals studied. The right renal artery was located more cranially than its left counterpart.

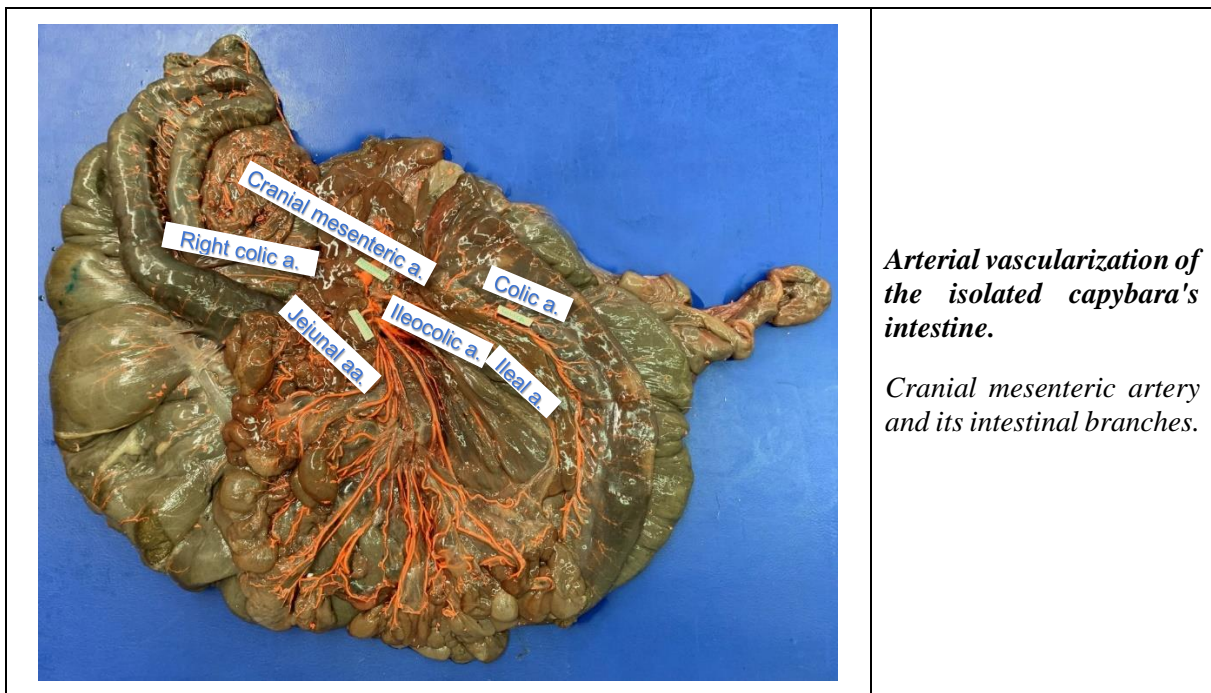
The renal veins closely accompany the corresponding arteries and open into the caudal vena cava; they were short and voluminous and entered the renal hilum caudally to the

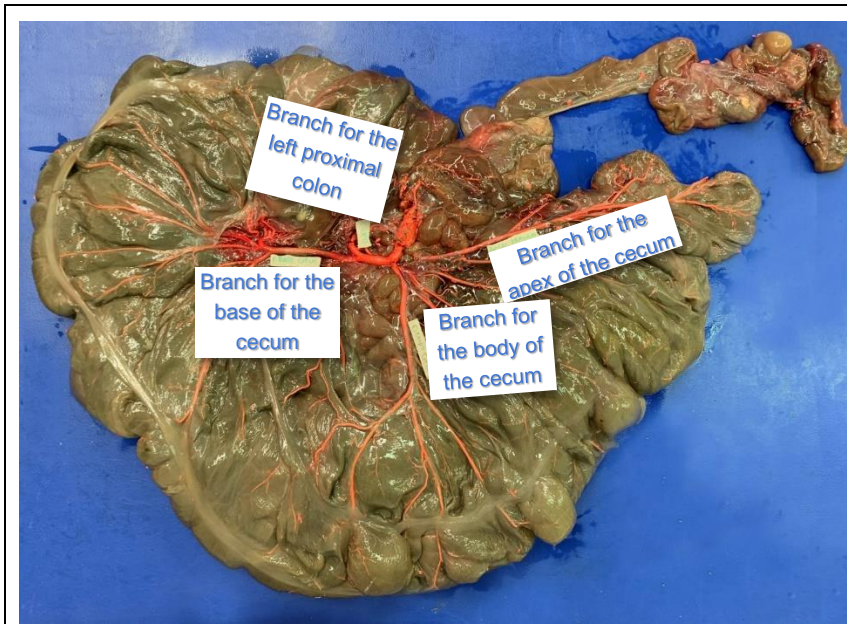
corresponding arteries, but cranially to the ureters.

The paired **testicular arteries** have a small caliber (1.9 mm) and originate on the sides of the aorta, 26 mm caudally to the emission of the renal arteries and 42 mm cranially to the emission of the caudal mesenteric artery; they follow their course towards the vaginal ring to join the components of the spermatic cord. The distal portion of the testicular artery is very tortuous. In females, **the ovarian arteries** irrigate the ovary and then, through uterine branches they are directed towards the horns, body and cervix of the uterus to finally anastomose with the branches of the caudal uterine artery originating from the internal iliac artery.

The **caudal mesenteric artery**, with an average diameter of 3.9 mm, supplied the colon, from the middle of the transverse colon, to the rectum. It originated from the ventral aspect of the aorta, approximately 42 mm caudally to the emission of the testicular or ovarian arteries, and gave off the following main branches: the left colic artery, directed to the descending colon, and the cranial rectal artery. The caudal mesenteric artery supplies the colon from the middle third of the transverse colon to the rectum; it is thinner and with a simpler distribution than the cranial mesenteric artery.

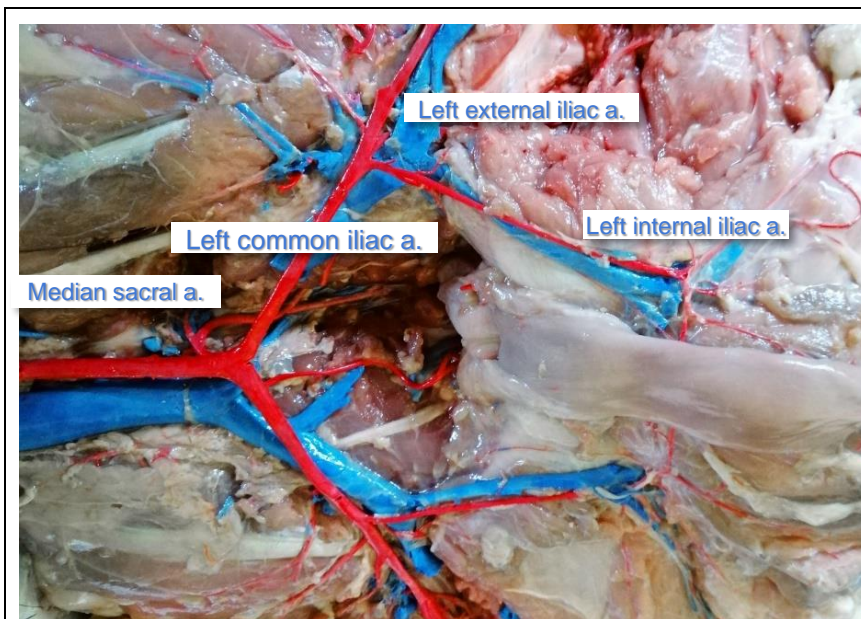
The **left colic artery** supplied most of the descending colon and the left curvature of the colon, anastomosing with the middle colic artery. The **cranial rectal artery** anastomosed with the caudal rectal artery.





*Arterial vascularization of the isolated capybara's intestine. Termination of the ileocolic artery into a colic, and ileal, and cecal arteries*

The vascularization of the pelvis originated from the right and left **common iliac arteries**, which divided into **external and internal iliac arteries**. The terminal bifurcation of the abdominal aorta into the right and left common iliac arteries occurred about 55 mm caudally to the emission of the caudal mesenteric artery. After approximately 30 mm, each common iliac artery bifurcated into the external and internal iliac arteries. The external iliac artery had a mean diameter of 8.5 mm, whereas the internal of 2 mm. The abdominal walls received the blood supply mainly from the **deep circumflex iliac arteries**, deriving from the external iliac artery. The **median sacral artery** arose from the dorsal surface of the aorta before its bifurcation into the common iliac arteries.



*Termination of the abdominal aorta in the capybara. Bifurcation into the right and left common iliac arteries, dividing into external and internal iliac arteries. Note the dorso-cranial origin of the median sacral artery.*

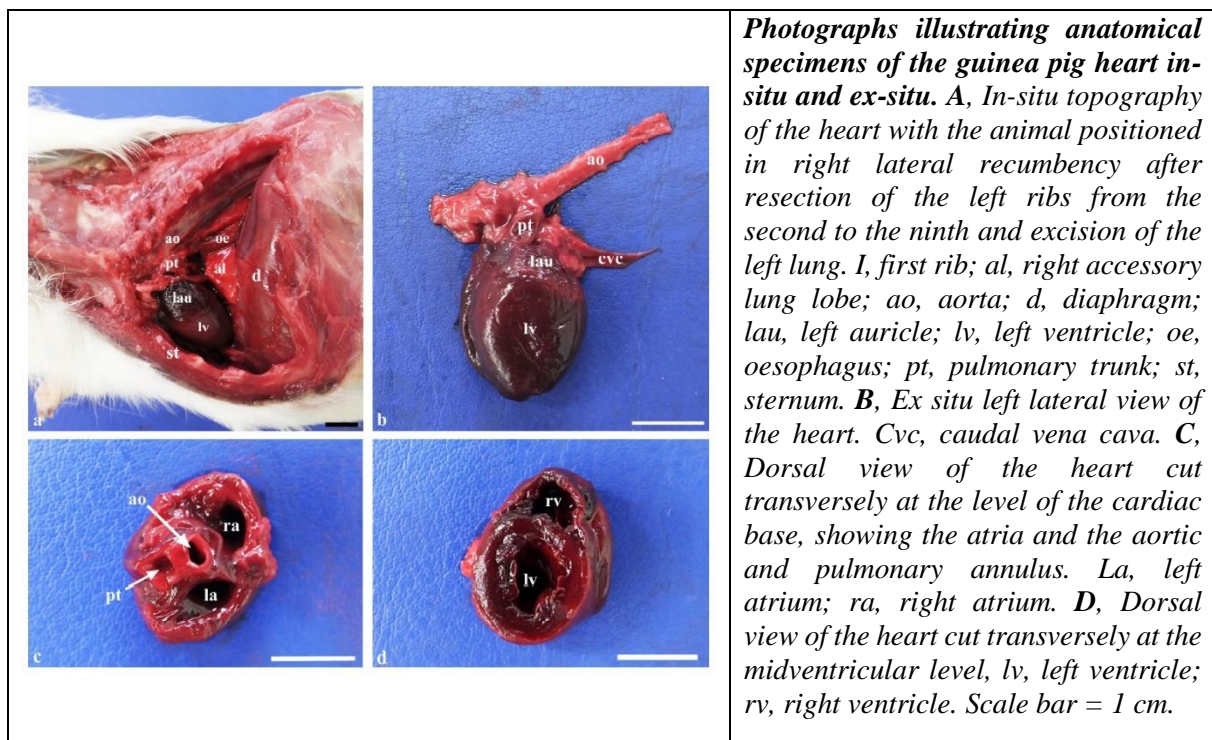
# Cardiovascular system

## Heart and large vessels

### *Cavia porcellus*

The guinea-pig heart, weighing a mean 1.54 grams, had a globoid and laterally-flattened appearance, it occupied a large portion of the thoracic cavity, and extended from the second rib to the fifth intercostal space, the fifth rib, or the fourth intercostal space. In left lateral recumbency, the heart had a more cranial topography, extending from the second to the fourth ribs or the fourth intercostal space. It lied in the midline, with a ventro-caudal inclination over the sternum, to which was anchored by the sternum-pericardial ligament.

It had four cardiac chambers and surrounded by a pericardium. Externally, the atria were separated from the ventricles by a deep coronary sulcus for the passage of the coronary arteries and veins. Internally, the atrial septum separated the atria, and a particularly thick interventricular septum separated the ventricles. In the right ventricular lumen, a large septomarginal trabecula was evidenced in all animals, whereas it was evidenced in the left ventricular lumen in a minority of animals.





*Guinea pig heart cut longitudinally, showing the right and left ventricles, the interventricular septum and the aortic emergence.*

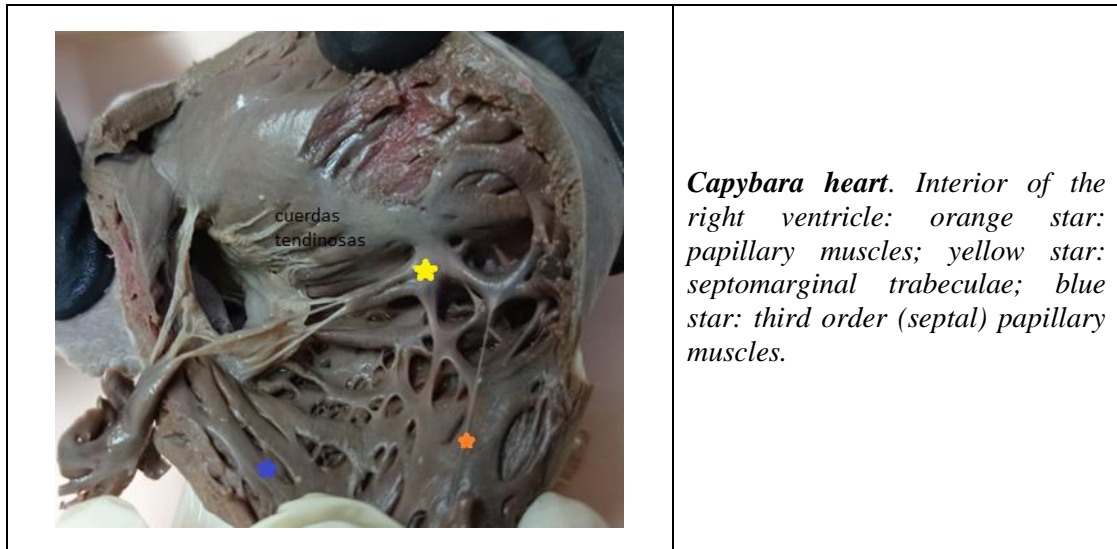
From the morphometric study of the guinea pig heart emerged that the cardiac long axis, measured from apex to the emergence of the large vessels, measured on average 21.9 mm, whereas the short axis, measured at the level of the maximum craniocaudal length, was 17 mm. The left atrial diameter was 5 mm, the aortic diameter 2.6 mm, with a ratio of 1.6. The left ventricular internal diameter measured 7 mm on average, whereas the right ventricular internal diameter measured 3.7 mm. The interventricular septum had a thickness of 2.5 mm, and the left ventricular posterior wall thickness measured 2.8 mm.

The guinea pigs studied presented a right azygos vein opening into the cranial vena cava. A minority of animals also presented a left hemi-azygos directly opening into the venous sinus of the heart.

### ***Hydrochoerus hydrochaeris***

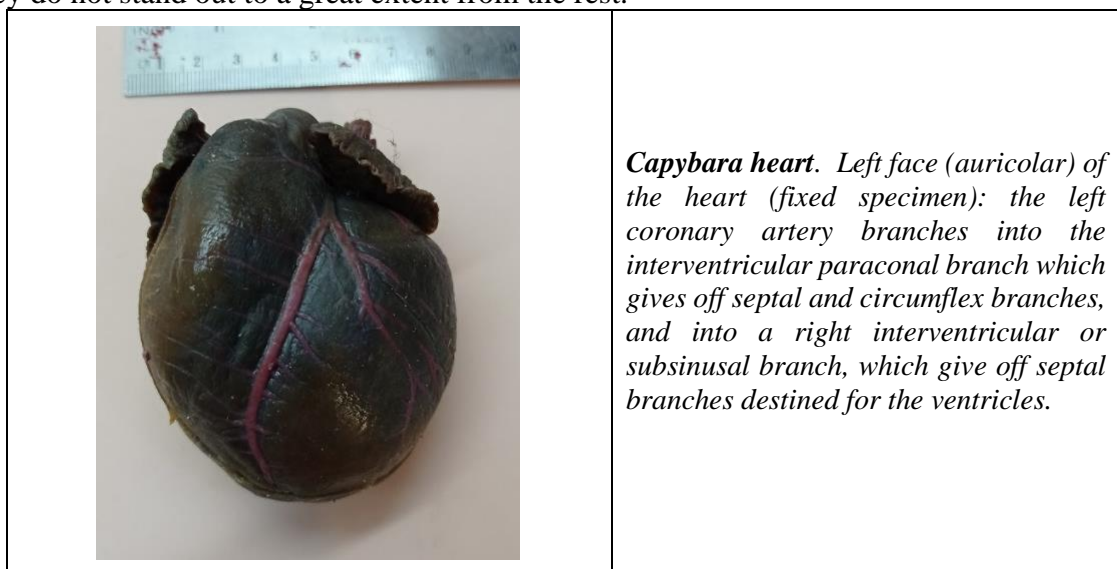


*Capybara heart (fixed). Left auricular surface, with the branching of the left coronary artery and its collaterals evidenced by the polyurethane casts.*



The capybara heart had a globoid appearance and weighed 126 grams on average. It extended from the second to the fifth intercostal spaces. The overall length, apex to base, of the capybara heart measured approximately 92.1 mm, whereas the length from the coronary sulcus to the apex 75.6 mm. The maximum cranio-caudal width of the ventricles measured on average 80.8 mm. The latero-lateral width of the heart at midventricular height was 68.4 mm. The cranio-caudal width of the right atrium was 50.7 mm, whereas that of the left atrium 43.6 mm.

The peculiarity of the capybara heart stands in the fact that the endocardial musculature of the ventricles resembles that of the pectinate muscles usually seen in the atria. The endocardial muscles are very reticular in appearance and the papillary muscles are arranged so that they do not stand out to a great extent from the rest.





*Capybara heart. Right (atrial) view of the capybara heart (fixed specimen): Note the circumflex branch of the left coronary artery (blue arrow), which gives off the right interventricular or subsinular branch (red arrow).*

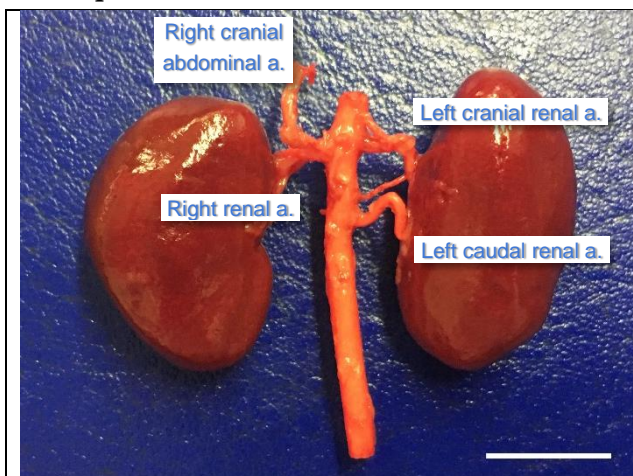
As for the intrinsic vascularization of the heart, the **left coronary artery** gives off the interventricular paraconal branch which then bifurcates into a branch directed to the left paraconal sulcus and a branch directed to the left ventricle. It then emits a muscular branch for the left ventricle, and runs caudally towards the caudal margin and continues as circumflex branch which gives off a muscular branch for the right ventricle and the right interventricular or subsinular branch.

The **right coronary artery** was absent in all the animals studied.

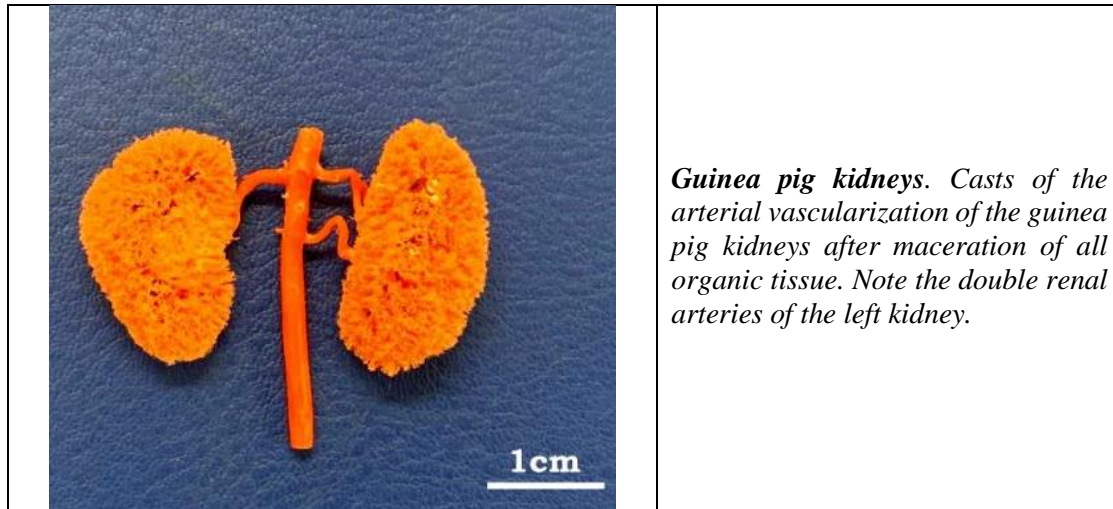
## Urogenital system

### Urinary system

#### *Cavia porcellus*



*Guinea pig kidneys. Corrosion cast of the kidneys vessels. Arterial vascularization of the guinea pig kidney. Note the double renal arteries of the left kidney, and the right cranial abdominal artery originating from the right renal artery instead of the aorta.*



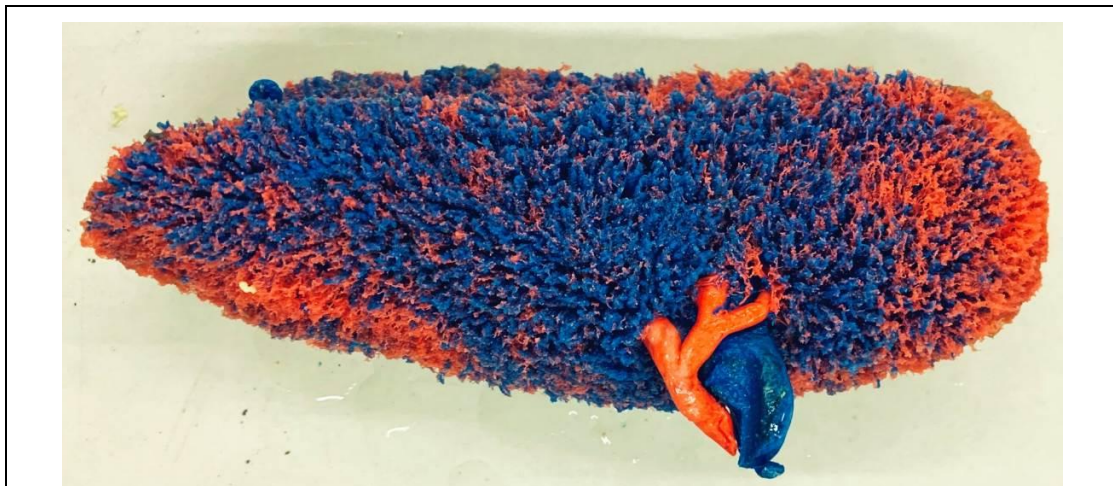
**Guinea pig kidneys.** Casts of the arterial vascularization of the guinea pig kidneys after maceration of all organic tissue. Note the double renal arteries of the left kidney.

The right guinea pig kidney measured, on average, 20 mm in length, 12.6 mm in width, and 9.7 mm in height (thickness). The left kidney had a mean length of 20.3 mm, a mean width of 12.8 mm, and a mean height of 9.7 mm. They presented an elongated oval shape. They were retroperitoneal and located at the level of the second and third lumbar vertebrae, with the right kidney having a more cranial topography. Their structure was unipapillar, simple and smooth and containing papillae fused into a single continuous renal crest.

The renal arteries of the guinea pig were found to be single, double or even triple on either side and originated from the abdominal aorta. Each cranial abdominal artery originated from the abdominal aorta. The well-developed adrenal glands were located cranio-medially to each kidney, at the level of the cranial pole.

The urinary bladder of guinea pigs was pyriform-shaped when empty, and entirely located within the pelvic cavity. It was composed of an apex, a body and a neck. Two lateral and one median vesical ligaments fixed it to the pelvic cavity. A vesical trigone was not evidenced.

### ***Hydrochoerus hydrochaeris***



**Capybara kidney.** Corrosion casts of the kidney's vessels. Arterial (red) and venous (blue) vascular irrigation, and renal pelvis (yellow), of the capybara's kidney after maceration of all organic tissue. The renal artery and vein, single, divide into a medial and a lateral branches right before penetrating the hilum of the organ.





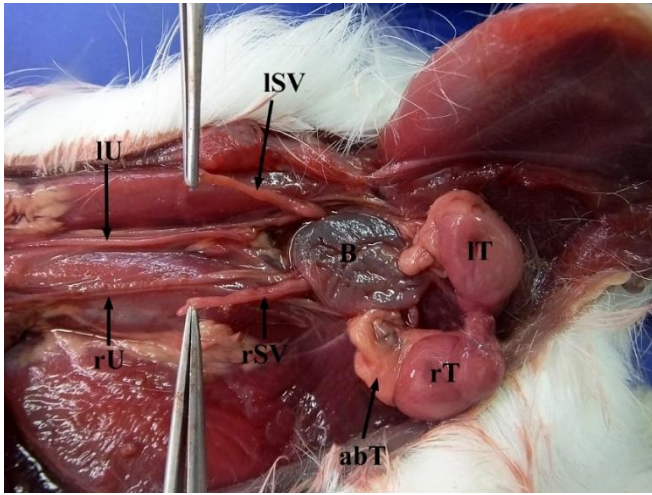
*Capybara kidneys ex-situ (left) and in-situ (right). Visceral (medial) surface, showing the voluminous adrenal gland located medial to the organ and cranially to the renal vessels.*

The capybara right kidney weighed on average 67 grams and measured approximately 115.6 mm in craniocaudal length, 48.9.5 mm in laterolateral width, and 26.2 mm in height. The left kidney had a mean weight of 85 grams and measured approximately 122.9 mm in length, 52.5 mm in width, and 26.9 mm in height. The capybara kidneys were elongated with an irregularly-elliptical shape, and were located retroperitoneally at the level of the first lumbar vertebrae. The capybara kidneys were simple, smooth, unipapillar with papillae that are fused into a single renal crest that empties into the renal pelvis. The renal arteries of the capybara were found to be single in all the animals studied. The well-developed adrenal glands were located craniomedially to the respective kidney. The ureters and the oval-shaped urinary bladder did not present differences with the other domestic species.

## Male genital system

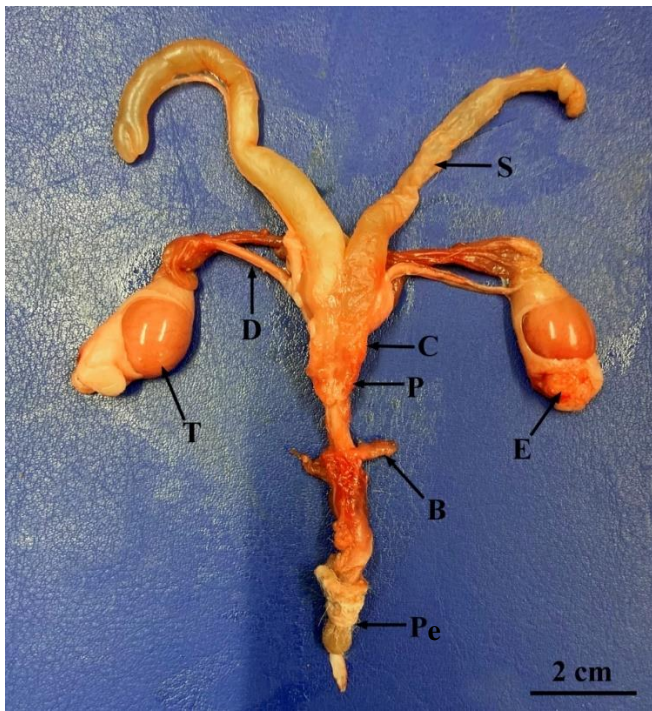
### *Cavia porcellus*

The guinea pig testes were located inside externally-visible scrotal pouches, and surrounded by abundant adipose tissue. The epididymis, composed of a head, a body and a tail, was located dorsolaterally on the testicular surface. The inguinal canals were open in all animals studied. The penis was sigmoid (S-shaped) with white spurs on the surface of the glans and of the intromittent sac, and presented an os penis. Two cartilaginous and sharp-edged horny styles, characterized by an irregular and rough surface, were evidenced inside the lumen of the intromittent sac. Four accessory sexual glands were evidenced in the majority of animals: the paired and well-developed seminal vesicles which appeared as coiled and elongated blind and transparent sacs, the bilobed prostate gland and the coagulating glands at the base of the seminal vesicles and the paired bulbourethral glands located caudally to the prostate.



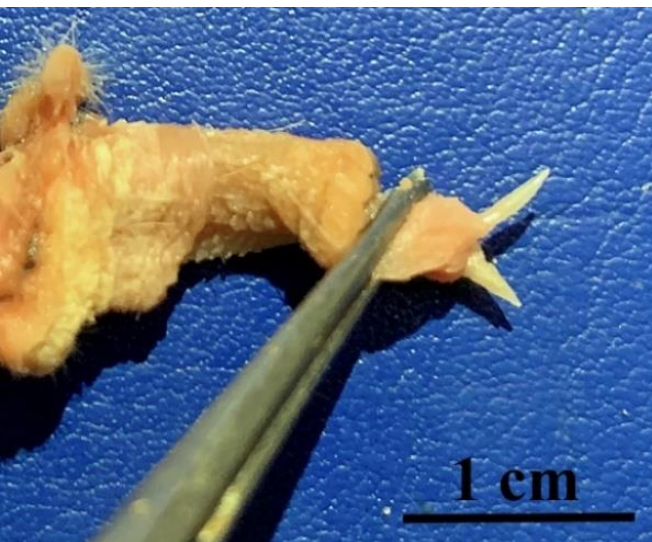
**Guinea pig in-situ male genital system. Ventral view.**

*abT: adipose tissue; B: urinary bladder; ISV: left seminal vesicle; IT: left testis; IU: left ureter; rSV: right seminal vesicle; rT: right testis; rU: right ureter*



**Guinea pig isolated male genital system. Dorsal view.**

*B: bulbourethral glands; C: coagulating glands; D: deferens duct; E: epididymis; P: prostate gland; Pe: penis; S: seminal vesicle; T: testis.*



**Guinea pig penis. Dorsal view.**

*Note the characteristic paired horny styles everted outwards from the inner lumen of the intromittent sac.*

***Hydrochoerus hydrochaeris***

The capybara testes were located subcutaneously, in the inguinal region, within a poorly-defined scrotum. The penis was flexed ventrocaudally and presented an os penis. The horny styles seen in the guinea pig were not observed within the capybara penis. The male capybara had two well-developed accessory sexual glands: the paired and well-developed seminal vesicles and the prostate. The inguinal canals were open, allowing the retraction of the testes into the pelvic cavity.



***Capybara in-situ male genital system.*** Ventral view. Note the testes, located subcutaneously within the pelvic cavity, due to the open inguinal canals.

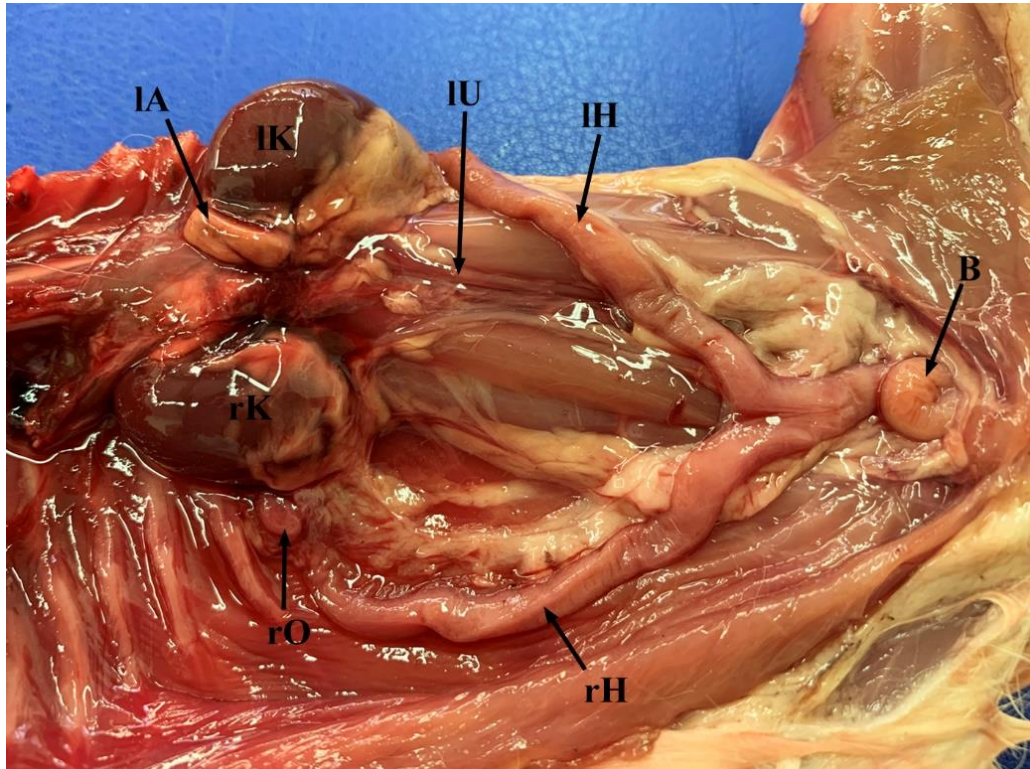


***Capybara penis*** everted outwards from the urethral opening. Note the sigmoid structure of the penis.

## Female genital system

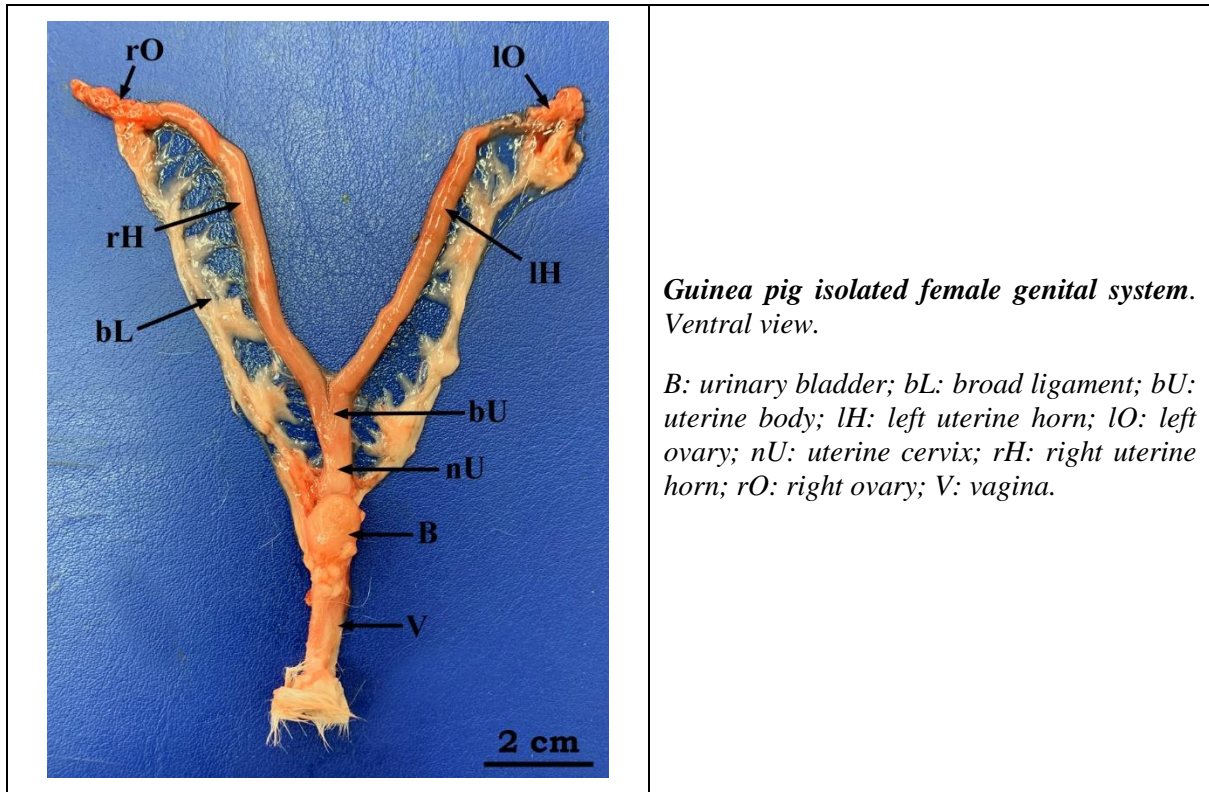
### *Cavia porcellus*

The female guinea pig had a simple bicornate uterus, consisting of paired well-developed and elongated V-shaped uterine horns, a short uterine body, and a single uterine cervix. The oval-shaped ovaries were located caudolaterally to the corresponding kidney, were dark pink in color and flattened dorsoventrally. The ovaries were completely covered by the ovarian bursa. Internally, the vagina presented longitudinal folds. The external vaginal orifice was U-shaped. The paired mammary glands were located lateral to the midline.



**Guinea pig. In-situ female genital system. Ventral view.**

*B: urinary bladder; IA: left adrenal gland; IH: left uterine horn; LK: left kidney; IU: left ureter; rH; right uterine horn; rK; right kidney; rO: right ovary.*



### ***Hydrochoerus hydrochaeris***

The oval-shaped capybara ovaries were located in the sublumbar region, and in contact with the caudal pole of the corresponding kidney. They were smooth, reddish in color and flattened dorso-ventrally.

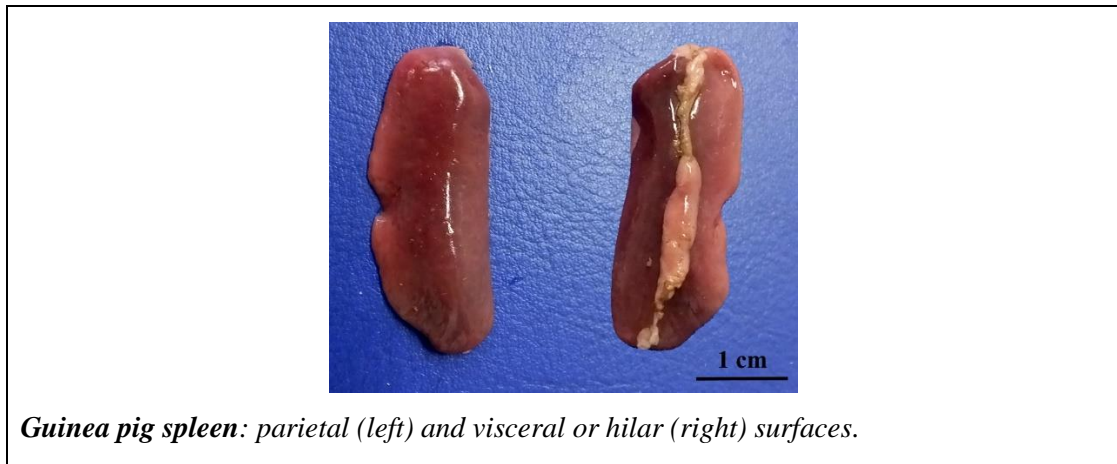
The double bicornate uterus of the capybara was composed of two long V-shaped horns, with a double cervix with a single opening into the vagina. The body of the uterus was cylindrical in shape and located in the abdominal cavity. Internally, it was bipartite into two separate ducts, that are the continuation of the horns. The cervix, located in the pelvic cavity, was internally divided into two ducts until its caudal third, where it presented a single duct opening into the vagina, which was characterized by longitudinal folds lining the mucosa of its most caudal part. The female capybara presented 5 pairs of mammary glands: axillary, thoracic, double abdominal and inguinal.

## Lymphatic system

### Spleen

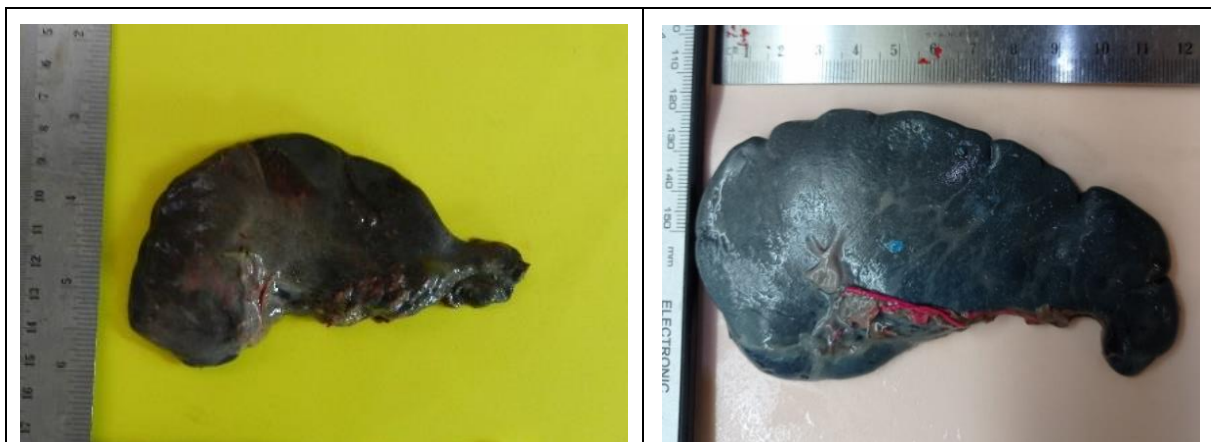
#### *Cavia porcellus*

The spleen of guinea pigs was relatively large, elongated and oval-shaped, with a smooth surface and red-brown in color. It was located in the left cranial abdomen, on the left lateral side of the greater curvature of the stomach and connected to it by the gastrosplenic ligament. It was attached to the diaphragm through the phrenicosplenic ligament.



#### *Hydrochoerus hydrochaeris*

The capybara spleen measured 120 mm in length, 50 mm in width, and 10.2 mm in height.



**Capybara spleen.** Visceral surface (top), Parietal surface (bottom). The spleen has a slightly triangular shape, with a wider portion in the hilar region located cranially, where the splenic artery penetrates, and gradually decreasing in width in the caudal direction. The capybara spleen presented fissured margins, specifically three to seven sulci, of variable depth, located on its dorsal edge, dividing it into multiple lobes.

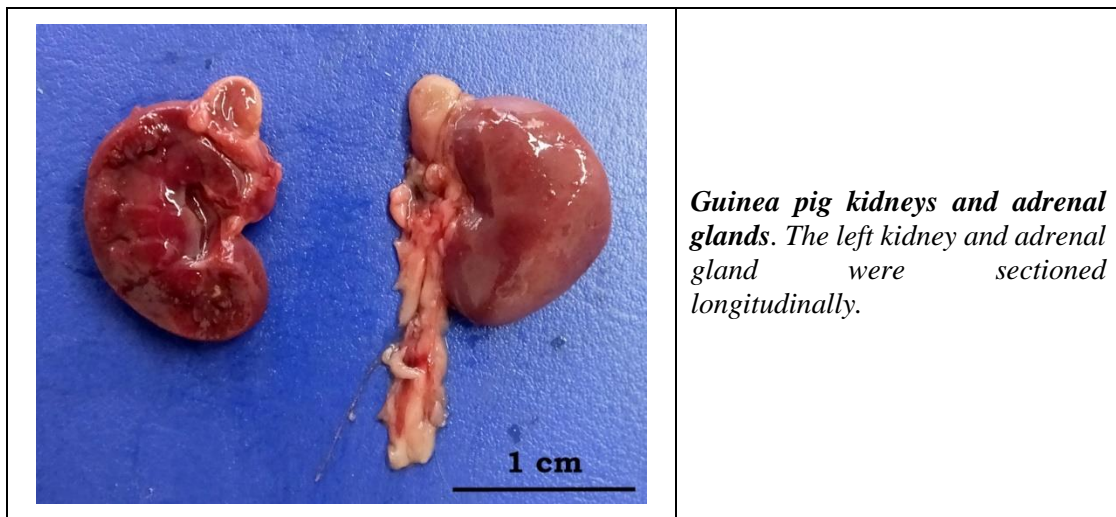
It had an irregularly triangular shape, wider cranially near the organ hilum, and narrowed down caudally. It presented fissured margins, specifically 3 to 7 shallow marginal sulci were identified on its dorsal edge, giving it a polylobed appearance.

## Endocrine system

### Adrenal glands

#### *Cavia porcellus*

The paired adrenal glands of the guinea pig were well-developed. They were pyramidally-shaped and yellowish-brown in color. They were proportionally voluminous, in relation to the size of the kidney, in comparison with those usually observed in other domestic mammals. They were embedded in adipose tissue and located craniomedially to the corresponding kidney, retroperitoneally. In cross section, the more-developed lighter outer cortex was distinguishable from the darker inner medulla.



#### *Hydrochoerus hydrochaeris*

The paired adrenal glands of the capybara were particularly voluminous and located medially to each kidney. They were yellowish-brown in color and characterized by an irregularly-triangular shape. They were embedded in adipose tissue. In cross-section the lighter outer cortex was distinguishable from the darker inner adrenal medulla.

### Thyroid gland

#### *Cavia porcellus*

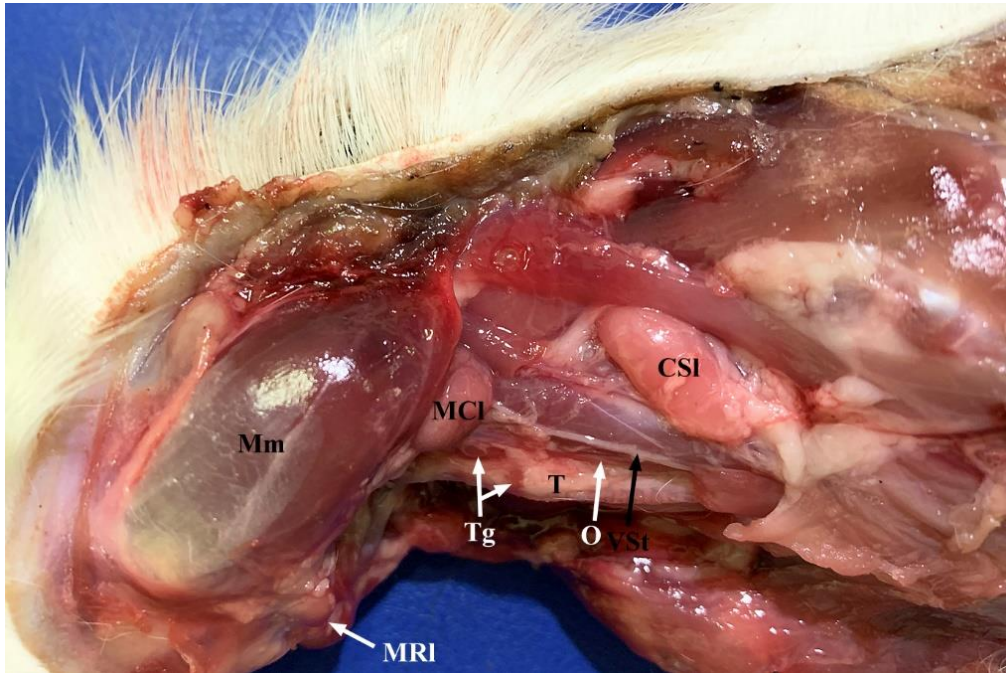
The thyroid gland of guinea pigs consisted of a right and a left lobe, with a smooth surface and dark red in color, joined by a glandular and well-developed ventral isthmus (measuring 0.9

mm in width). The right and left thyroid lobes were red-pink in color, oval-shaped and elongated, measuring 9.3 mm and 8.1 mm in length, respectively and surrounded by adipose tissue. The cranial end of the thyroid lobes was located in contact with the caudal edge of the cricoid cartilage of the larynx and surrounded the tracheal rings ventrolaterally, extending caudally to the 5th-8th tracheal ring, in the region of the neck medially to the mandible. The thyroid gland is in relation with the following surrounding structures of the neck, in rostrocaudal order: the rostral and caudal mandibular lymph nodes, the sublingual salivary glands, the mandibular salivary glands, the parotid salivary glands and the ventral superficial cervical lymph nodes. An internal parathyroid gland was not evidenced within the thyroid parenchyma.



**Guinea pig. Left lateral view of the superficial neck structures.** CSI: Ventral superficial cervical lymph node; MCl: Caudal mandibular lymph node; Mg: Mandibular salivary gland; Mm: Masseter muscle; Pg: Parotid gland; T: Trachea; Zg: zygomatic gland.





**Guinea pig. Left lateral view of the deep neck structures.** CSI: Ventral superficial cervical lymph node; MCI: Caudal mandibular lymph node; Mm: Masseter muscle; MRI: Rostral mandibular lymph node; O: Oesophagus; T: Trachea; Tg: Thyroid gland; VSt: Vagosympathetic trunk.



**Guinea pig. Ventral view of the neck structures, showing the right and left lobes of the thyroid gland (Tg) connected by a ventral isthmus, surrounding the ventral surface of the trachea (T) and located just caudally to the laryngeal cartilages.** Ca: Common carotid artery; CSI: Ventral superficial cervical lymph node; Mg: Mandibular salivary gland; MRI: Rostral mandibular lymph node; Sg: Sublingual gland; VSt: Vagosympathetic trunk.



*Isolated guinea pig thyroid gland (ventral view) showing the right and left paired lobes and the ventral isthmus that connects the two.*

## ***Thymus***

### ***Cavia porcellus***

The guinea pig thymus, in prepubertal subjects, lies in the cranial mediastinum cranial to the heart and in the ventral cervical region, surrounding the trachea lateroventrally near the thoracic inlet. It is pink-tan in color and elongated, and it is intermingled with adipose tissue and fascia.

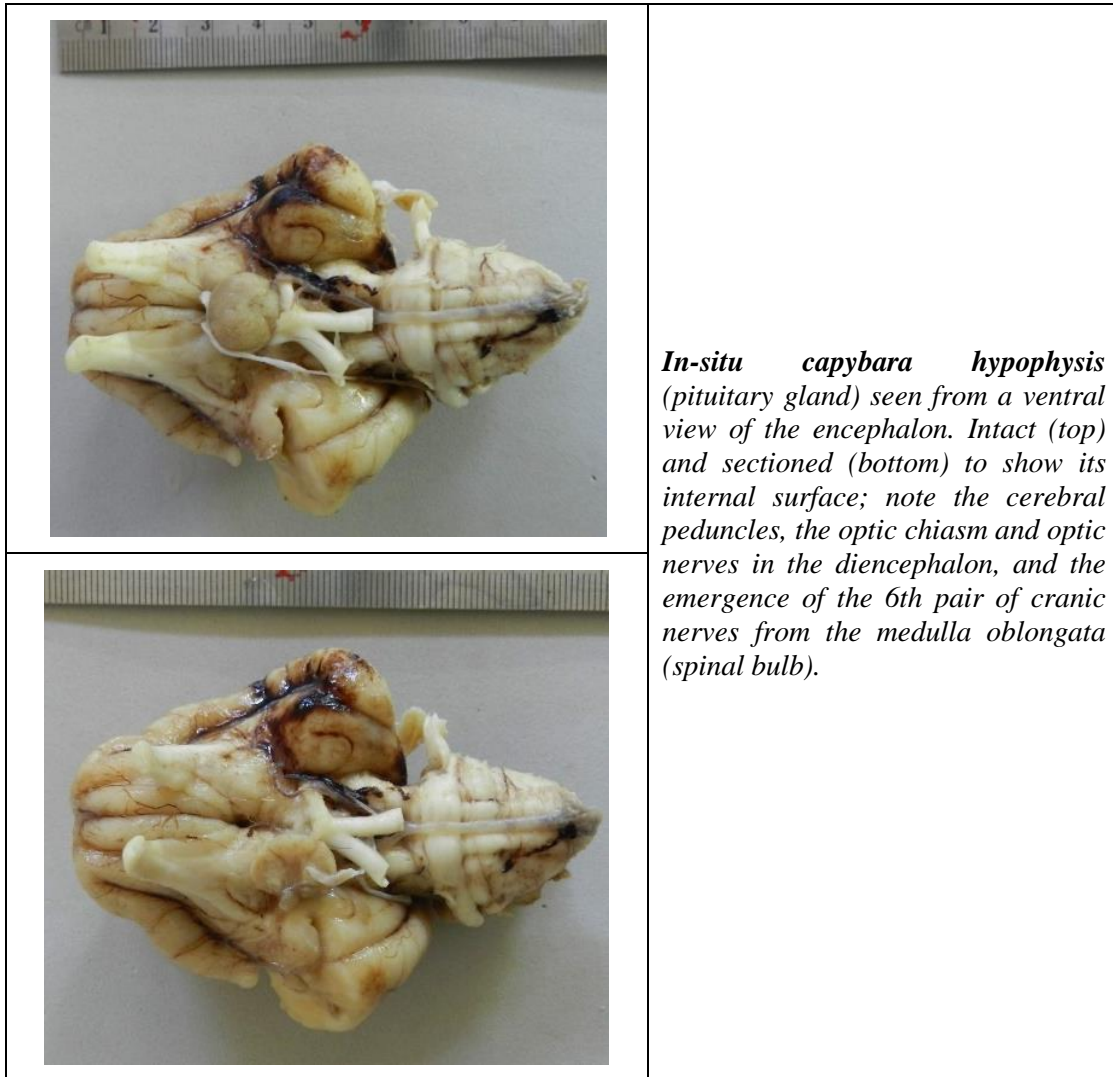
## **Pituitary gland**

### ***Cavia porcellus***



*In-situ guinea pig hypophysis (pituitary gland) seen from a ventral view of the encephalon. Note the cerebral peduncles, the optic chiasm and optic nerves in the diencephalon.*

*Hydrochoerus hydrochaeris*



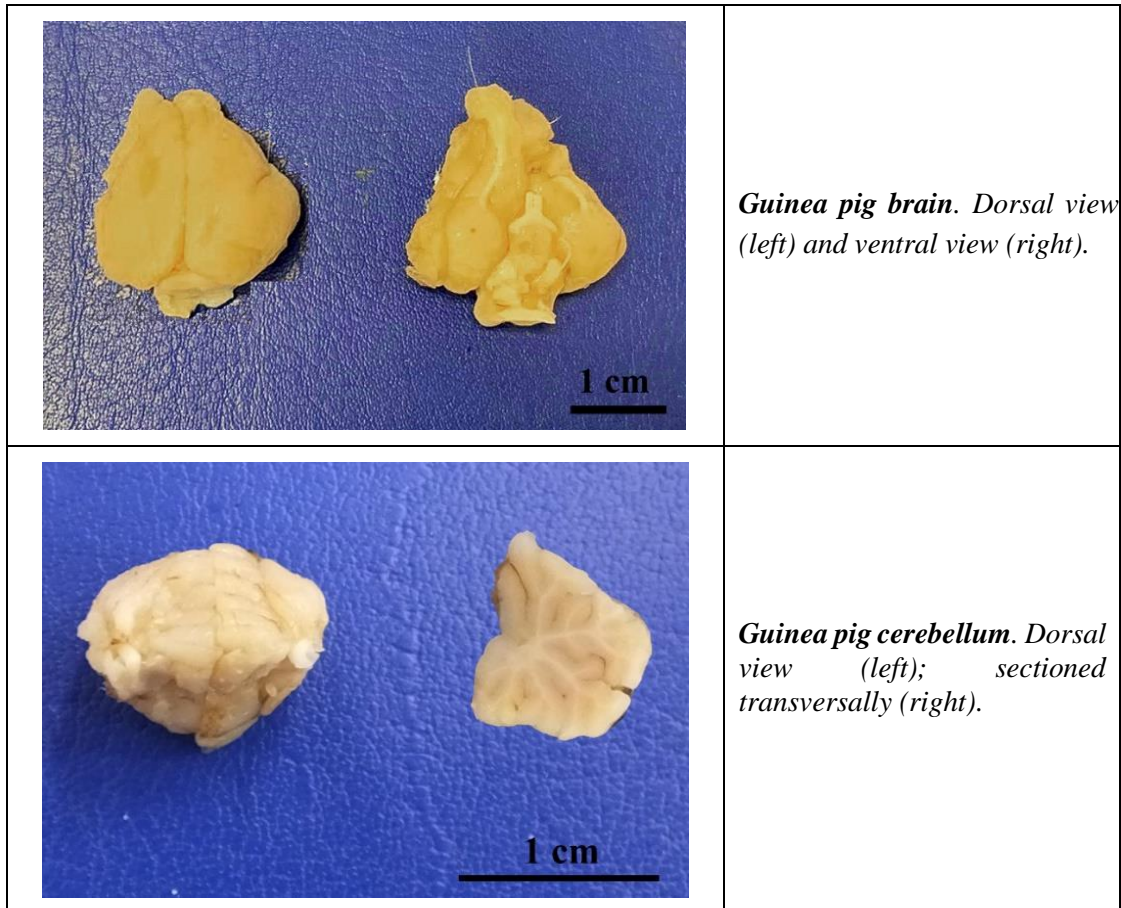
The pituitary gland, located immediately ventral to the diencephalon, in the deep pituitary fossa of the sella turcica, between the optic chiasm and the mammillary body, was particularly developed and extended in the capybara, in comparison to the guinea pig's.

## Central nervous system

### *Cavia porcellus*

The guinea pig brain was lissencephalic and characterized by the presence of few gyri and shallow sulci. The guinea pig brain weighed 2.9 grams on average, and measured 22.82 mm in length by 22.9 mm in width, and 12.85 mm in height. The guinea pig cerebellum weighed 0.6 grams and measured 9.66 mm in length, 10.82 mm in width, and 7.60 mm in height.

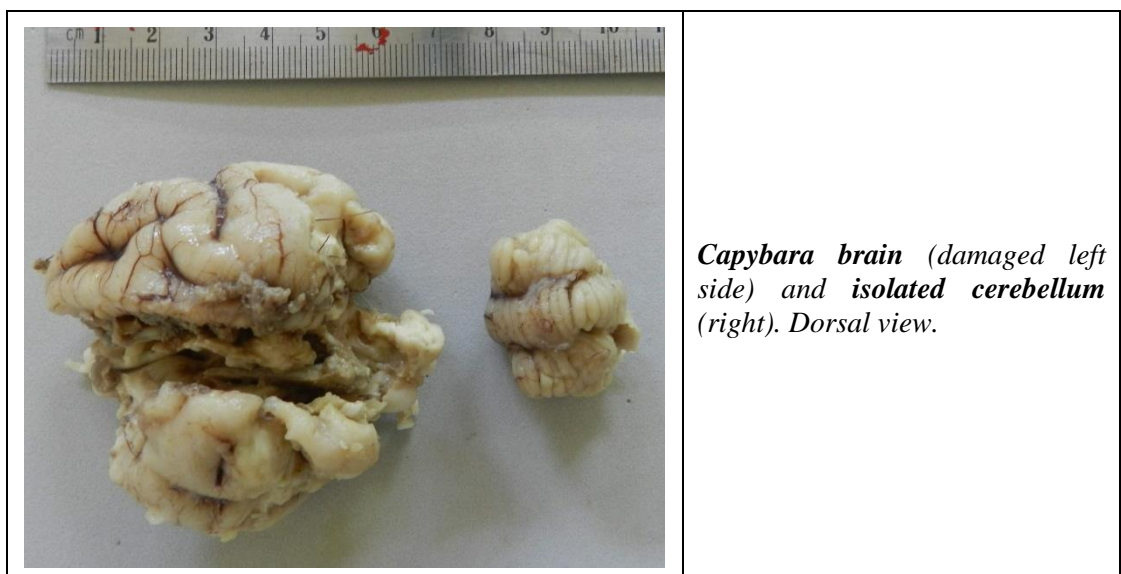
The cerebellum was small and compact, and its folia were arranged in a transverse pattern; the vermis slightly towered over the adjacent cerebellar hemispheres. In longitudinal section, the white matter of the cerebellum presented an arborescent ramification.

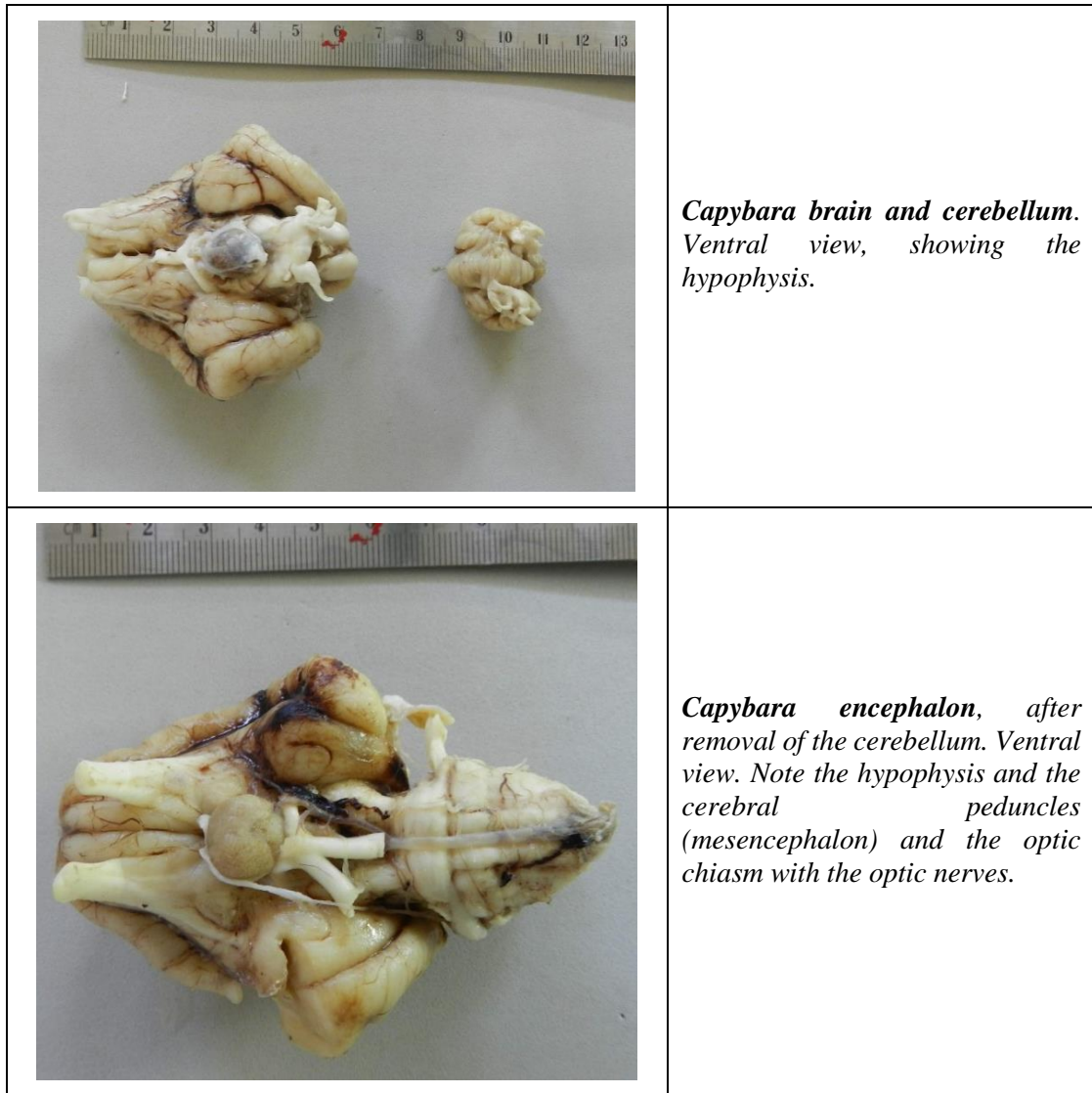


***Hydrochoerus hydrochaeris***

The capybara brain was gyrencephalic and with a more convoluted cerebral cortex than the guinea-pig's. It was characterized by conspicuous neocortical fissures, and prominent olfactory bulbs and with a greater degree of gyrification than the guinea pig's encephalon.

The cerebellum was small and compact, and its folia were arranged in a transverse pattern; a large floccular lobe was evidenced.





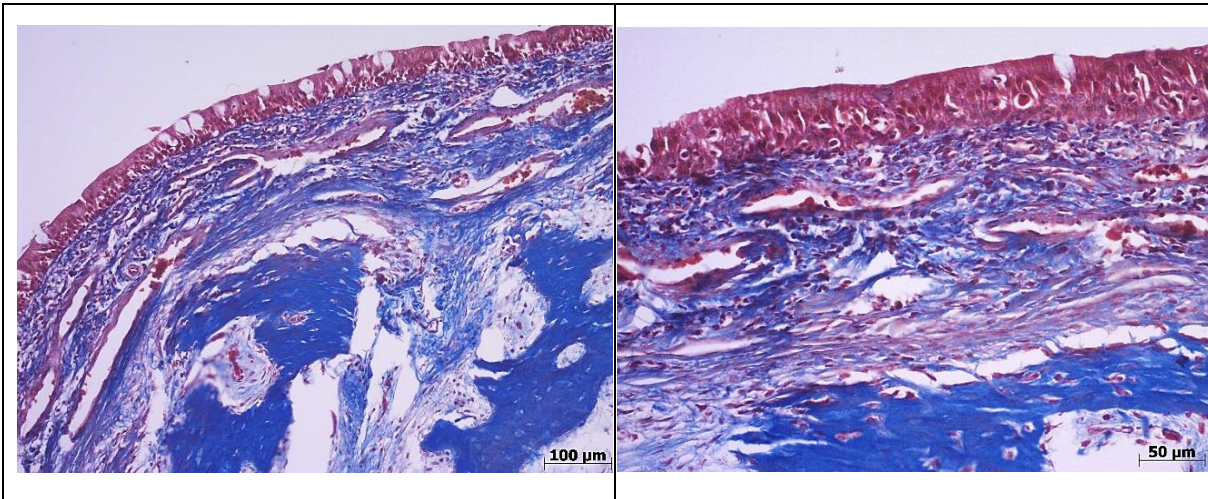
The weight of a male capybara encephalon was 56.5 grams, of which the brain 50 grams and the cerebellum 6.5 grams. The male capybara brain measured 55.3 mm in length by 58.5 in width, whereas the cerebellum was 23.8 mm long by 26.3 mm wide. The well-developed hypophysis measured 11.6 mm in width by 9.9 in length. The weight of a female capybara encephalon was 52 grams total, of which the brain weighing 47 grams and the cerebellum 4 grams. The female capybara brain measured 59 mm in length by 57.8 in width, whereas the cerebellum was 25 mm long by 24.6 mm wide. The well-developed hypophysis measured 11.4 mm in width by 10.3 mm in length.

# Atlas of microscopic anatomy

## Respiratory system

### Nasal cavities

#### *Hydrochoerus hydrochaeris*

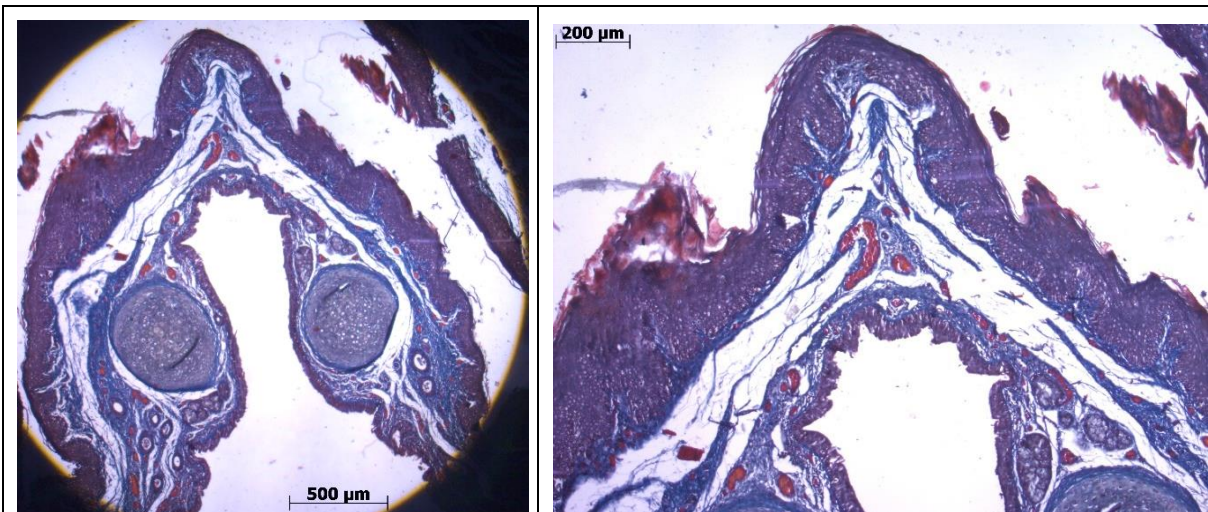


*Capybara nasal cavity.* Ciliated pseudostratified columnar epithelium with goblet, ciliated and basal cells lining the respiratory epithelium of the nasal cavity. Nasal gland acini occupy the connective tissue between the veins of the cavernous stratum of the respiratory mucosa.

Masson's Trichrome stain. 10x (left); 20x (right)

## Larynx

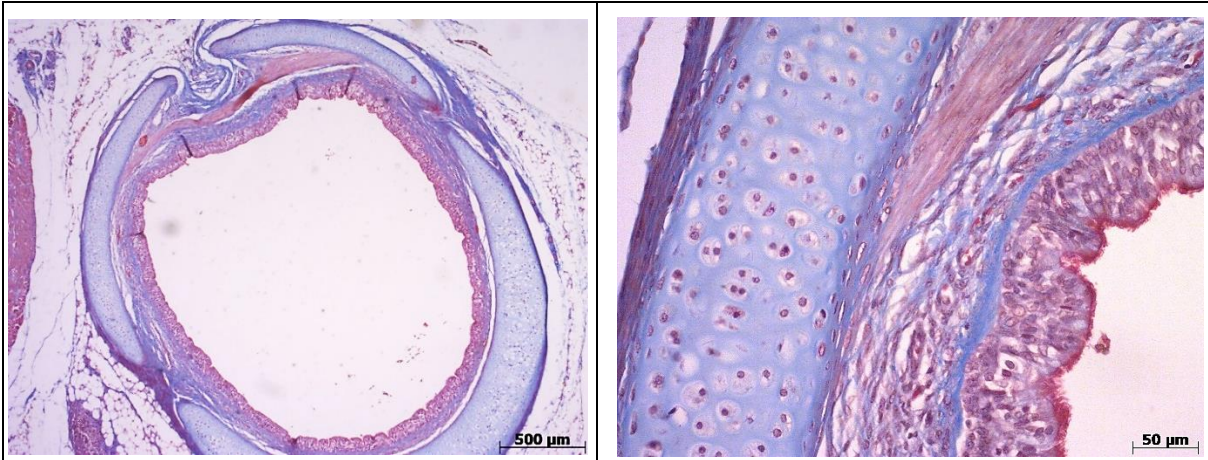
### *Cavia porcellus*



*Horizontal section through a guinea pig larynx.* The epithelium lying the epiglottis is nonkeratinized stratified squamous; the propria-submucosa beneath it is a dense-irregular connective tissue and glandular tissue. Note the epiglottis cartilage, vestibular folds, thyroid cartilage, cricoid cartilage, and thyrohyoid bone. Masson's Trichrome stain. 2.5x (left); 5x (right)

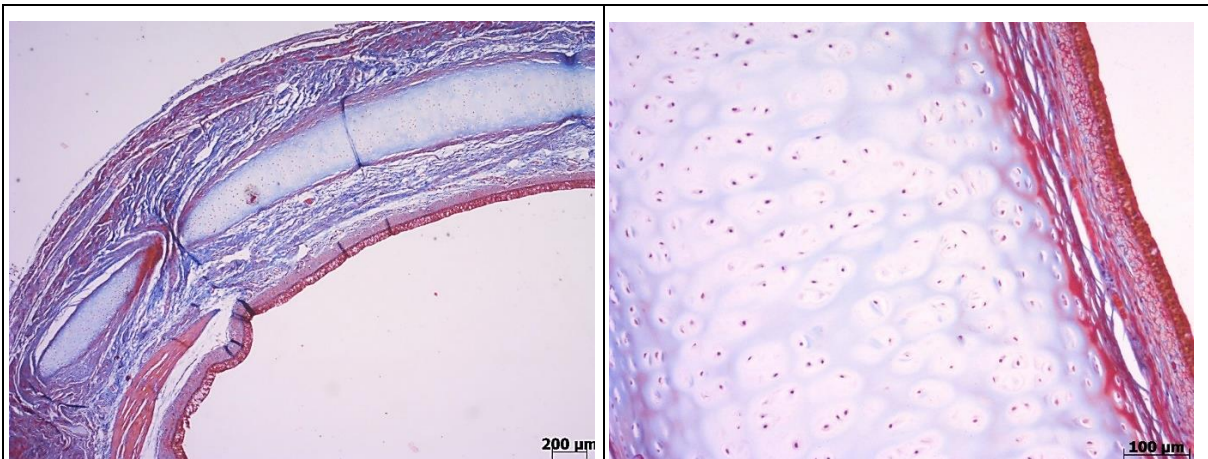
## Trachoea

### *Cavia porcellus*



**Guinea pig trachoea.** Cross-section. Note the respiratory epithelium, containing ciliated, brush, secretory (goblet), and basal cells, and the presence of the U-shaped separate rings of hyaline cartilage. The dorsal free edge of the cartilages is bridged by the trachealis muscles, a band of smooth muscle. Masson's Trichrome stain. 2.5x (left); 20x (right)

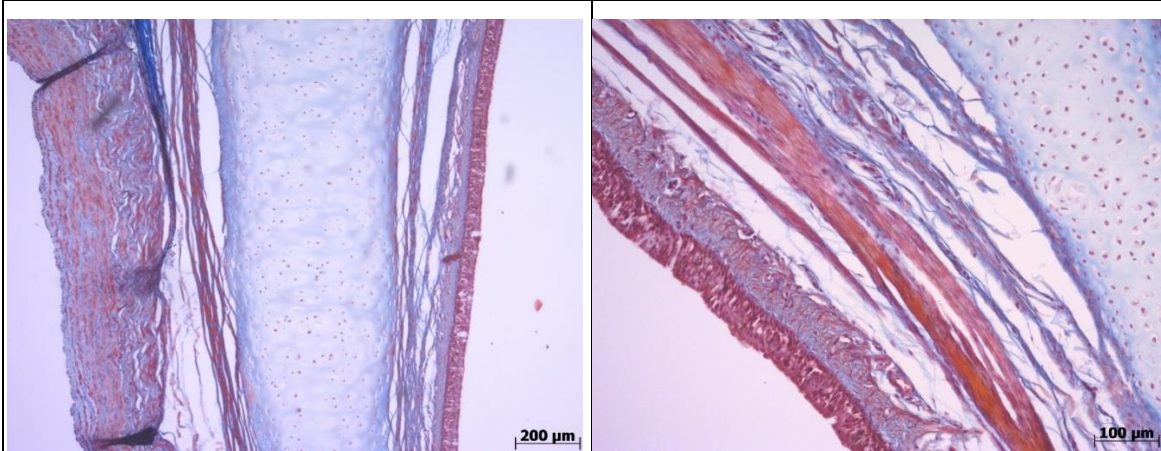
### *Hydrochoerus hydrochaeris*



**Capybara trachoea.** Cross-section. Note the respiratory epithelium, and the glandular density in the submucosa. The dorsal free edge of the hyaline cartilages is bridged by the trachealis muscles, a band of smooth muscle. Masson's Trichrome stain. 2.5x (left); 10x (right)

## Primary bronchus

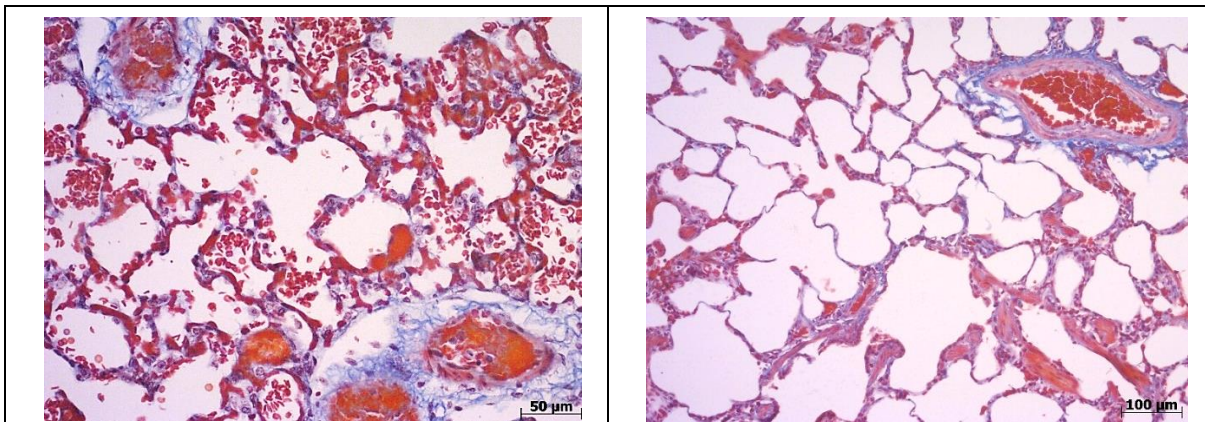
### *Hydrochoerus hydrochaeris*



**Capybara primary bronchus.** Cross-section. Note the respiratory epithelium, containing ciliated, brush, secretory and basal cells and the submucosa containing bronchial glands. The hyaline cartilage is in the form of irregular plates, instead of rings, as in the trachea.  
Masson's Trichrome stain. 5x (left); 10x (right)

## Lungs

### *Cavia porcellus*



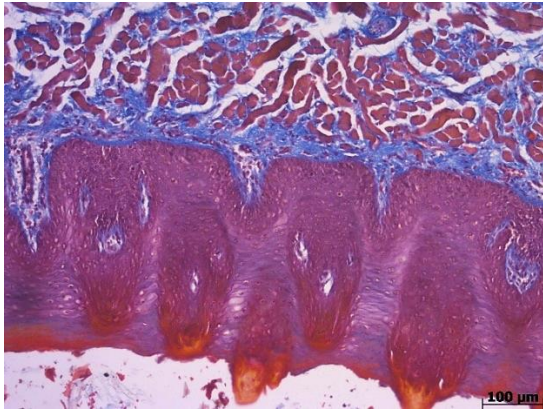
**Guinea pig lung parenchyma.** Alveoli lined by simple squamous epithelium and surrounded by alveolar septa. Note the vascular-connective tissue.  
Masson's Trichrome stain. 20x

**Capybara lung parenchyma** with alveoli lined by simple squamous epithelium and surrounded by alveolar septa. Note the vascular and connective tissue and the presence of a respiratory bronchiole lined by a simple cuboidal epithelium, followed by a thin layer of smooth muscle and surrounded by dense connective tissue.  
Masson's Trichrome stain. 10x



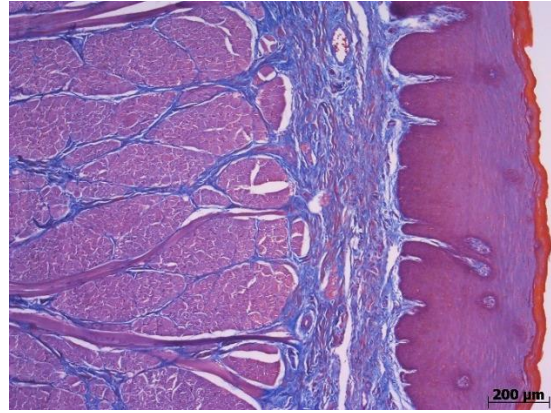
## Digestive system

### Tongue



**Guinea pig tongue.** Stratified squamous epithelium. Note the presence of filiform papillae projecting above the surface of the tongue and covered by a keratinized stratified squamous epithelium with a thick stratum corneum, and having a core of dense irregular connective tissue. Note the submucosa propria, beneath which abundant skeletal muscle is present.

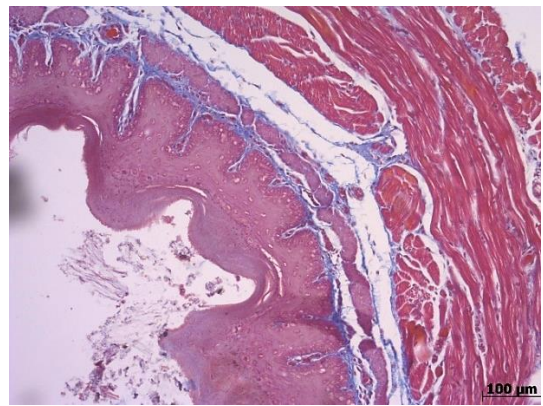
Masson's Trichrome stain. 10x



**Capybara tongue** lined with keratinized stratified squamous epithelium and having a core of dense irregular connective tissue. Note the underlying submucosa propria, beneath which abundant skeletal muscle is present.

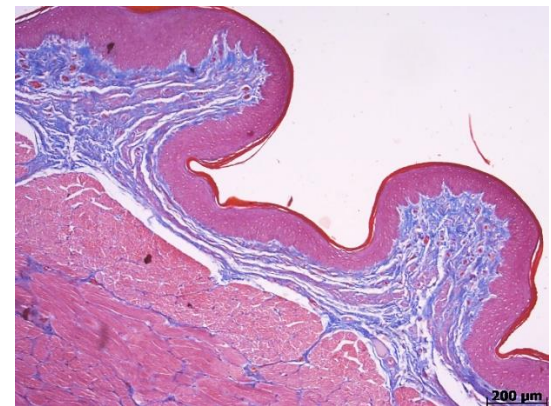
Masson's Trichrome stain. 5x

### Oesophagus



**Guinea pig oesophagus.** The epithelium is nonkeratinized stratified squamous, the lamina propria layer is composed of dense connective tissue, the well-developed lamina muscularis is made up of longitudinally-oriented smooth muscle bundles, the submucosa containing loose connective tissue with several vessels, and the highly developed striated tunica muscularis with an inner circular layer and an outer longitudinal layer. No glands were noted in the submucosa.

Masson's Trichrome stain. 10x

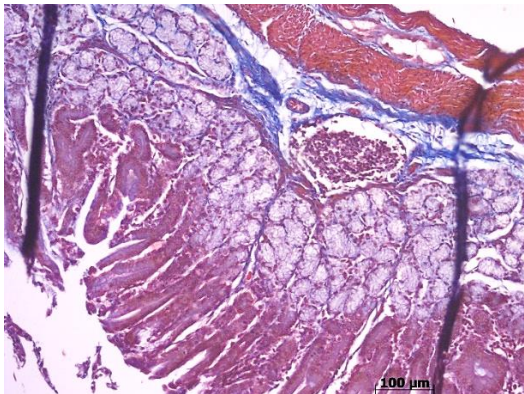
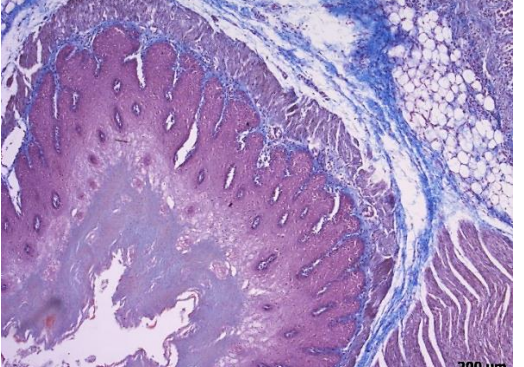
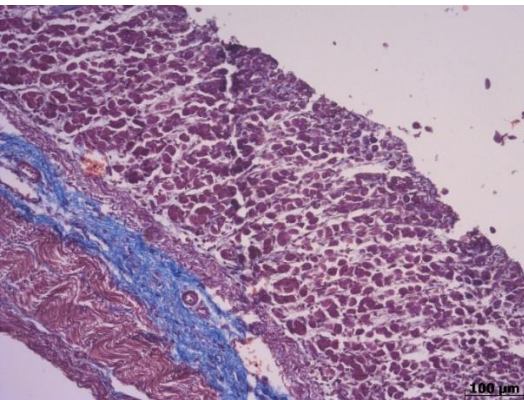


**Capybara oesophagus.** Note the highly keratinized stratified squamous epithelium, the lamina propria layer with dense connective tissue, the submucosa containing arteries and veins, and the highly developed striated tunica muscularis with an inner circular layer and an outer longitudinal layer. The lamina muscularis is absent.

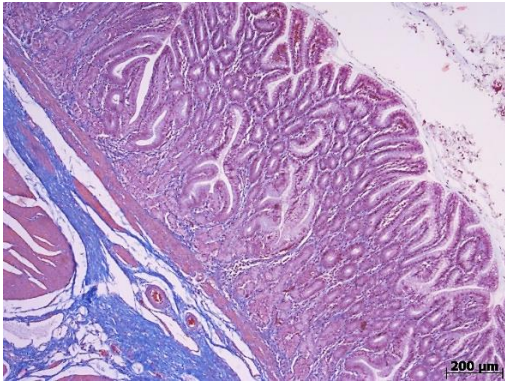
Masson's Trichrome stain. 5x

## Stomach

### *Cavia porcellus*

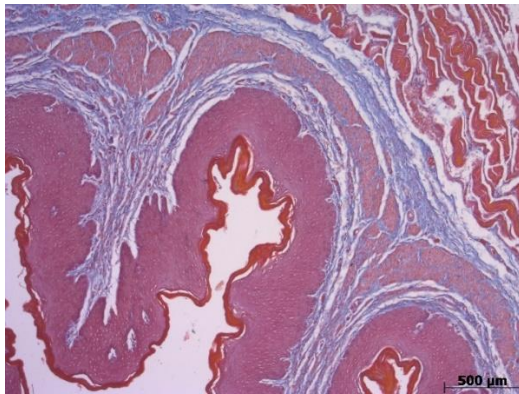
	<p><b>Guinea pig stomach (pylorus).</b> The guinea pig stomach is entirely glandular, therefore the mucosa is lined with tall simple columnar epithelial cells. Note the deep gastric pits which are continuous with the pyloric glands, characterized by flat basal nuclei and lightly stained apical cytoplasm, the lamina propria with loose connective tissue, and the thick circular muscular layer of the tunica muscularis. Note the presence of a lymphatic nodule in the submucosa.</p> <p>Masson's Trichrome stain. 10x</p>
	<p><b>Guinea pig stomach (cardias).</b> The non-glandular cardiac gastric region is lined with nonkeratinized stratified squamous epithelium, similar to that observed in the oesophagus. The lamina propria layer is composed of loose connective tissue, the well-developed lamina muscularis is made up of longitudinally-oriented smooth muscle bundles, the submucosa containing loose connective tissue with several vessels, and the highly developed striated tunica muscularis.</p> <p>Masson's Trichrome stain. 5x</p>
	<p><b>Guinea pig stomach (fundus).</b> The guinea pig stomach is entirely glandular, therefore the mucosa is lined with tall simple columnar epithelial cells. Note the deep gastric pits which are continuous with the proper gastric (fundic) glands, the lamina propria with loose connective tissue, the lamina muscularis with smooth muscle cells, the submucosa with vessels, and the thick tunica muscularis.</p> <p>Masson's Trichrome stain. 10x</p>

***Hydrochoerus hydrochaeris***



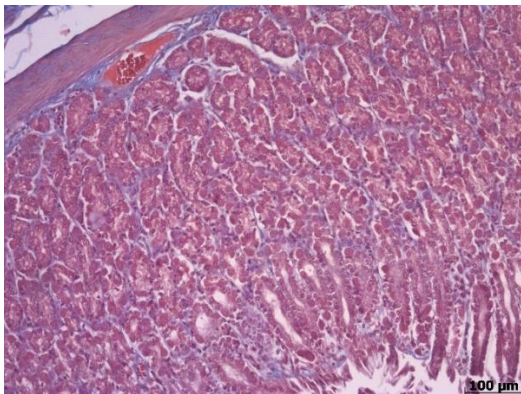
***Capybara stomach (pylorus).*** The pyloric glandular region of the stomach is lined with tall simple columnar epithelial cells. Note the deep gastric pits which are continuous with the pyloric glands, characterized by flat basal nuclei and lightly stained apical cytoplasm, the lamina propria with loose connective tissue, the lamina muscularis, the abundant submucosa containing blood vessels, and the tunica muscularis.

*Masson's Trichrome stain. 5x*



***Capybara stomach (cardias).*** The non-glandular cardiac gastric region is lined with keratinized stratified squamous epithelium, similar to that observed in the oesophagus. The lamina propria layer is composed of loose connective tissue, the highly-developed lamina muscularis is made up of longitudinally-oriented smooth muscle bundles, the submucosa containing loose connective tissue with several vessels, and the highly developed striated tunica muscularis

*Masson's Trichrome stain. 5x*

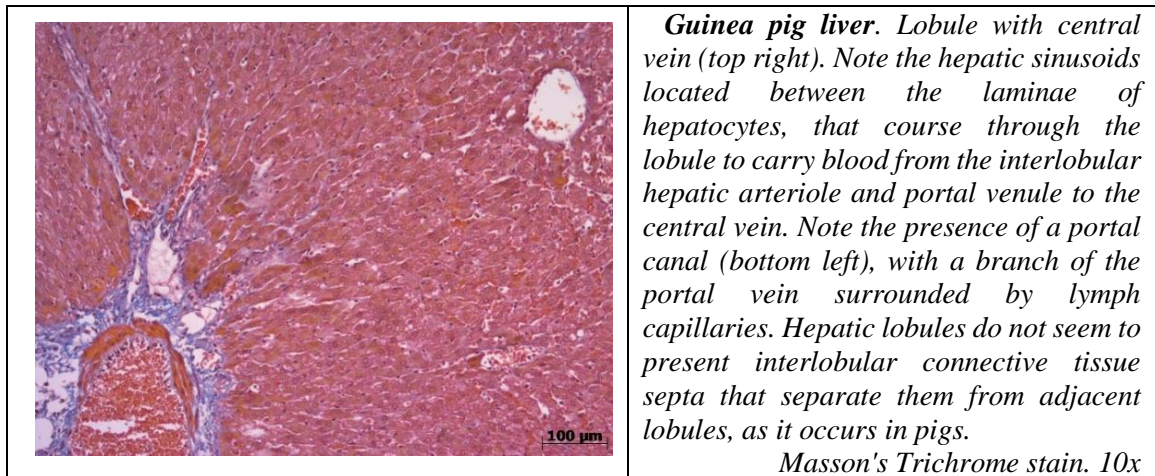


***Capybara stomach (fundus).*** The fundic glandular region is lined with simple columnar epithelium. Note the deep gastric pits which are continuous with the proper gastric (fundic) glands divided into mucous neck cells and chief cells, the lamina propria with loose connective tissue and the lamina muscularis with smooth muscle cells.

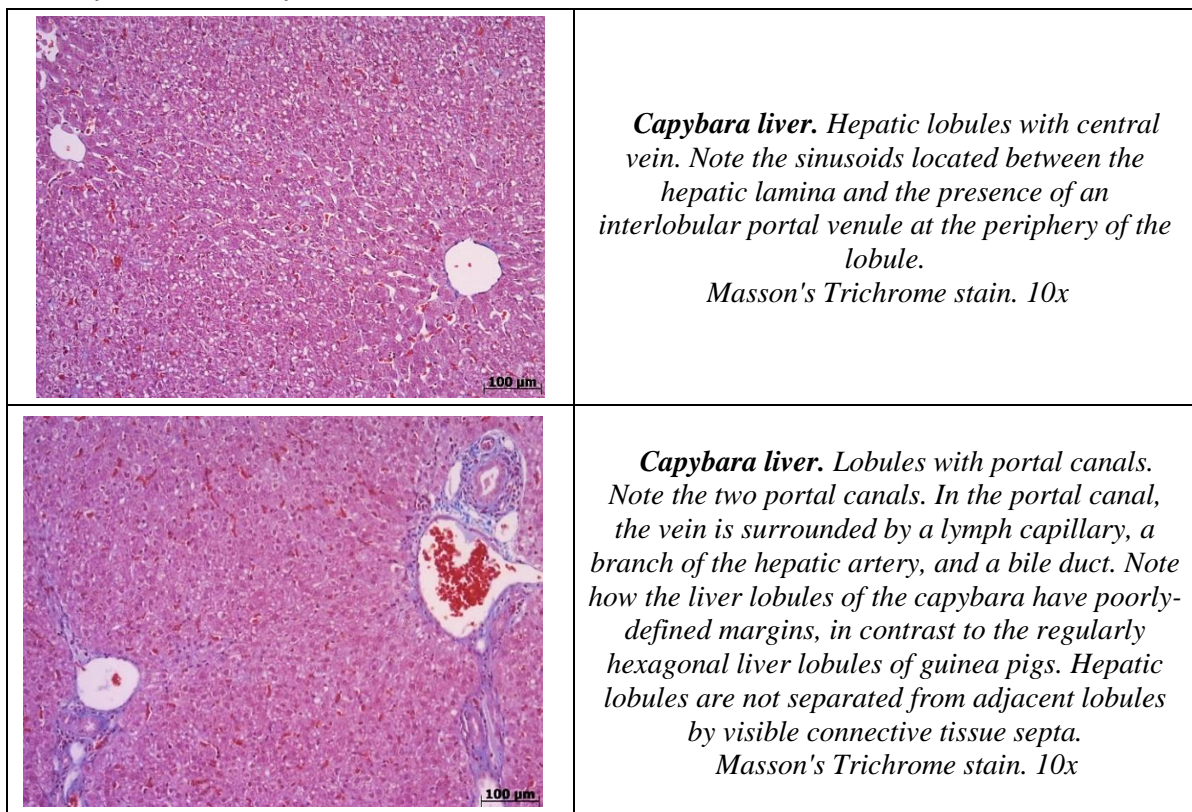
*Masson's Trichrome stain. 10x*

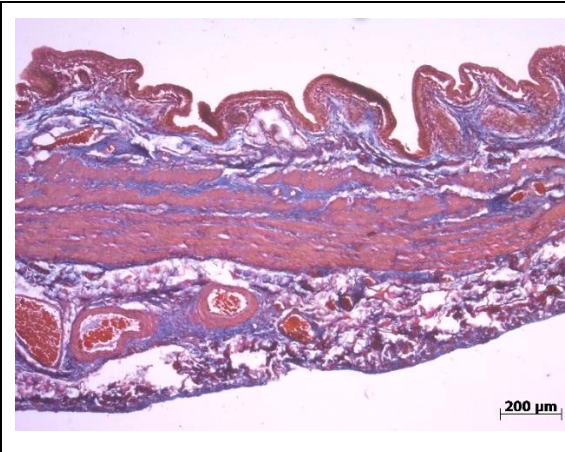
## Liver

### *Cavia porcellus*



### *Hydrochoerus hydrochaeris*

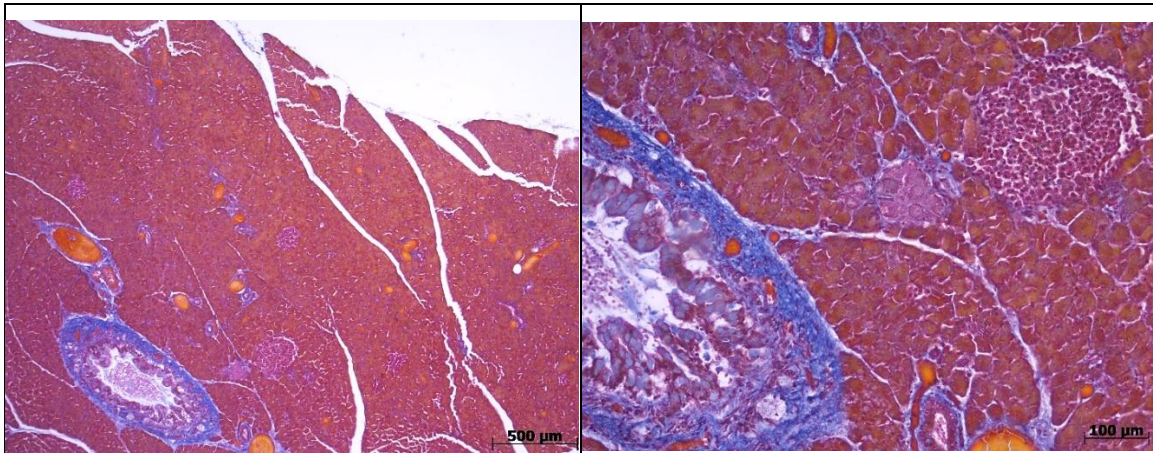




***Capybara gallbladder.*** The gallbladder is lined with a tall simple columnar epithelium containing goblet cells, and which extends into epithelial diverticula, the mucosal crypts in the lamina propria. Note how the mucosa is characterized by numerous plicae. The lamina muscularis is absent, the submucosa is composed of loose connective tissue containing also lymphatic tissue. The abundant tunica muscularis consists of thin bundles of smooth cells. The tunica serosa is thick and vascularized. Masson's Trichrome stain. 5x

## Pancreas

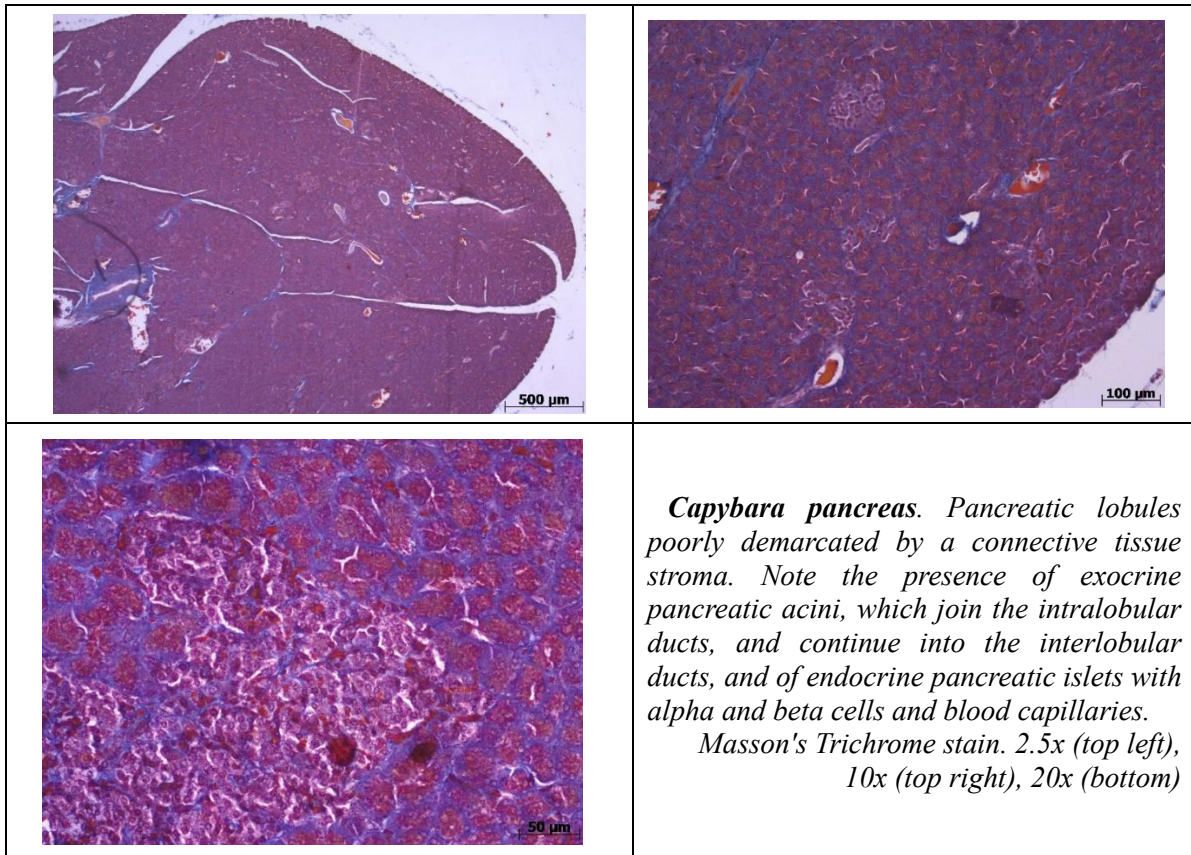
### *Cavia porcellus*



***Guinea pig pancreas.*** The parenchyma of the pancreas is separated into distinct lobules by a connective tissue stroma. The exocrine pancreas is composed of the tubuloacinar pancreatic acini with pyramid shaped glandular epithelial cells, which join the intralobular ducts, lined by simple cuboidal epithelium, which continue into the interlobular ducts, lined by simple columnar epithelium. Note the presence of endocrine pancreatic islets with alpha and beta cells.

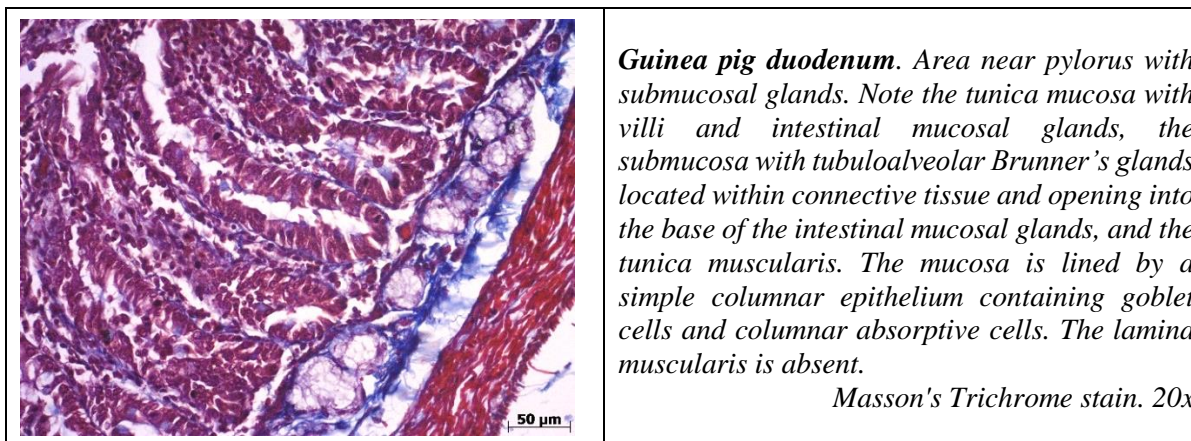
Masson's Trichrome stain. 2.5x (left), 10x (right)

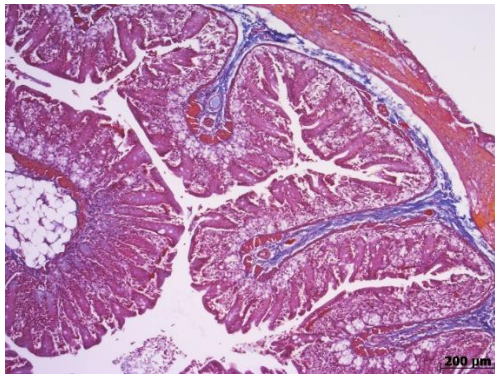
*Hydrochoerus hydrochaeris*



Small intestine

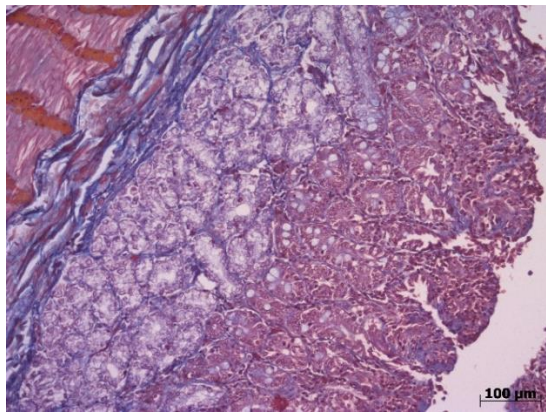
*Cavia porcellus*





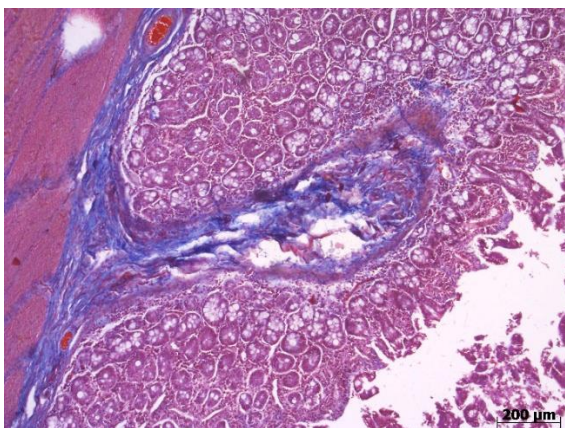
**Guinea pig ileum.** Note the tunica mucosa lined by simple columnar epithelium, with villi and intestinal mucosal glands, the lamina muscularis, the submucosa without glands, and the tunica muscularis.  
Masson's Trichrome stain. 5x (left), 10x (right)

### ***Hydrochoerus hydrochaeris***



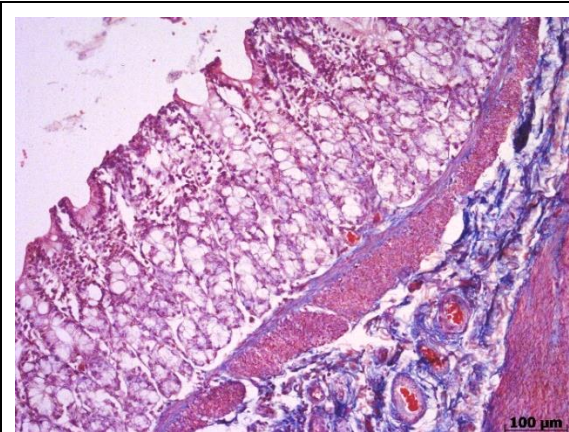
**Capybara duodenum.** Area near pylorus with submucosal glands. Note the tunica mucosa with villi and intestinal mucosal glands, the submucosa with tubuloalveolar Brunner's glands located within connective tissue and opening into the base of the intestinal mucosal glands, and the tunica muscularis. The mucosa is lined by a simple columnar epithelium containing goblet cells and columnar absorptive cells. The lamina muscularis is absent.

Masson's Trichrome stain. 10x



**Capybara jejunum.** Note the tunica mucosa lined by simple columnar epithelium, with villi and intestinal mucosal glands, crypts of Lieberkühn, the submucosa without glands, and the tunica muscularis.

Masson's Trichrome stain. 5x

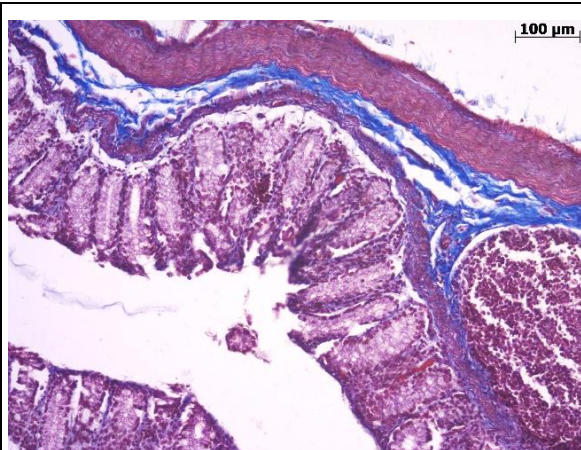


***Capybara ileum.*** Note the tunica mucosa lined by simple columnar epithelium, with villi and intestinal mucosal tubular glands, the crypts of Lieberkühn, the well-developed lamina muscularis, the submucosa without glands, and the tunica muscularis. No Peyer's patches have been evidenced.

*Masson's Trichrome stain. 10x*

Large intestine

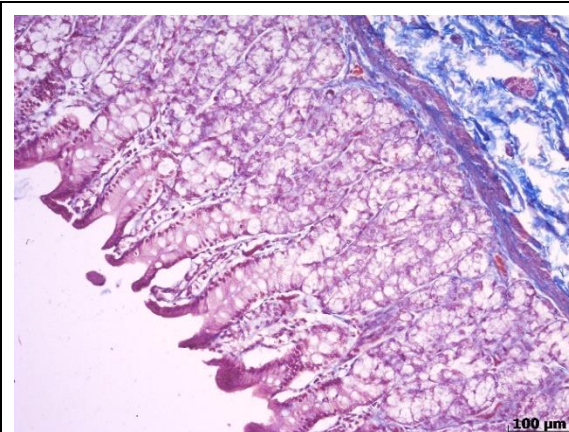
***Cavia porcellus***



***Guinea pig descending colon.*** The colon is characterized by the absence of villi, the presence of simple tubular intestinal glands with many goblet cells, and an increased number of submucosal lymphatic nodules. The mucosa is thick with longer intestinal glands (simple tubular) containing numerous goblet cells. Note the presence of a well-developed lamina muscularis and of a large lymphatic nodule in the submucosa. The outer longitudinal layer of the tunica muscularis forms a large flat muscle band with elastic fibers, corresponding to the taenia coli.

*Masson's Trichrome stain. 10x*

***Hydrochoerus hydrochaeris***



***Capybara ascending colon.*** Note the thick tunica mucosa lined with simple cylindrical epithelium without villi, containing an abundance of simple tubular intestinal glands containing numerous goblet cells. A lamina muscularis is present, as well as a small lymphatic nodule in the submucosa.

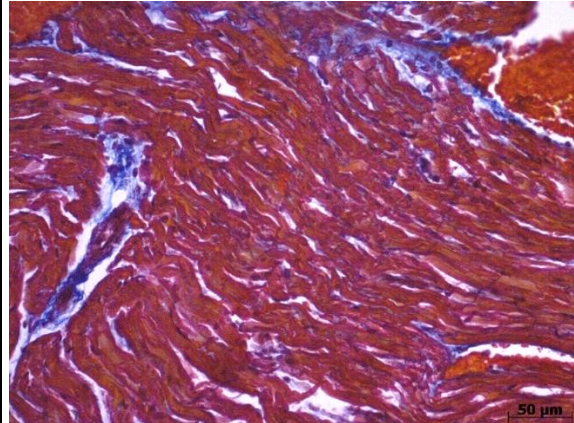
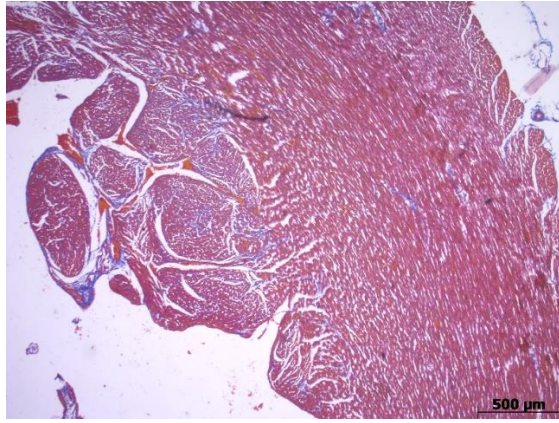
*Masson's Trichrome stain. 10x*



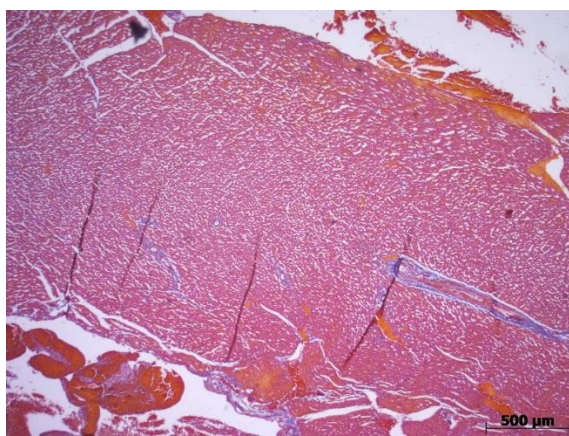
# Cardiovascular system

## Heart

### *Cavia porcellus*

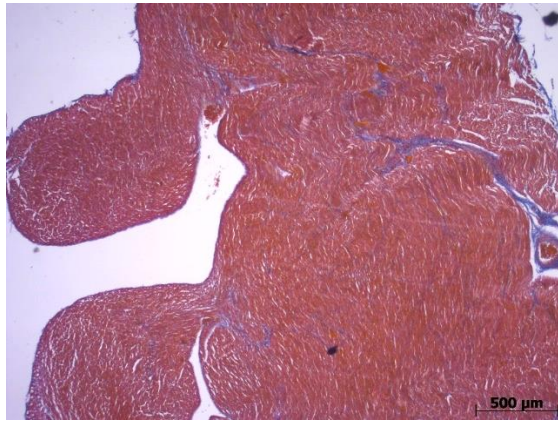


**Guinea pig heart.** Left ventricle free wall. Sagittal section. The myocardium is composed of bundles of cardiac muscle cells embedded in loose connective tissue containing a dense capillary network and lymph vessels. The innermost layer of the heart, including the ventricles, is formed by the endothelium, the subendothelium and the subendocardial layer continuous with the myocardium, composed of loosely arranged collagen and elastic fibers. Note the papillary muscle protruding towards the lumen of the left ventricle (left) and lined with endocardium and myocardium. Masson's Trichrome stain. 2.5x (left), 20x (right).



**Guinea pig heart.** Interventricular septum, sagittal section. Note the connective tissue containing vascular vessels, interspersed among the cardiac muscle cells of the myocardium. The fibrous part of the interventricular septum makes up the cardiac skeleton and consists of collagen fiber bundles. Masson's Trichrome stain. 2.5x

***Hydrochoerus hydrochaeris***

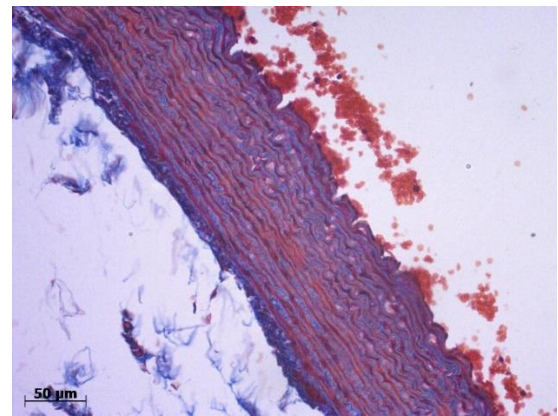


***Capybara heart.*** Right ventricle free wall. Sagittal section. Note the connective tissue containing vascular vessels, interspersed among the cardiac muscle cells of the myocardium. The endothelium lines the lumen of the ventricles, including the papillary muscles. Here, two papillary muscles protrude towards the lumen of the right ventricle and are lined with endocardium and myocardium. Also note that the ventricular wall is covered externally by the epicardium, made up of loose connective tissue rich in elastic fibers.

*Masson's Trichrome stain. 2.5x*

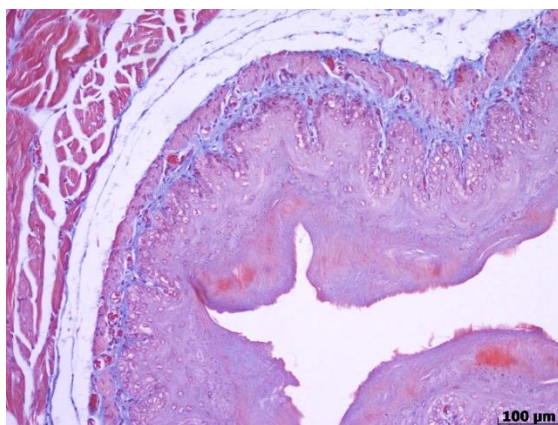
**Large arterial and venous vessels**

***Cavia porcellus***



***Guinea pig aorta.*** Cross-section of the aortic wall. The relatively-thick tunica interna (intima) is lined with a simple squamous epithelium (endothelium), a thick subendothelial layer of collagen, longitudinal elastic fibers and smooth muscle cells, and a prominent internal elastic membrane. The tunica media is composed of several layers of smooth muscle cells interspersed with abundant elastic laminae that predominate. The tunica externa (adventitia) consists in in collagen and elastic fibers.

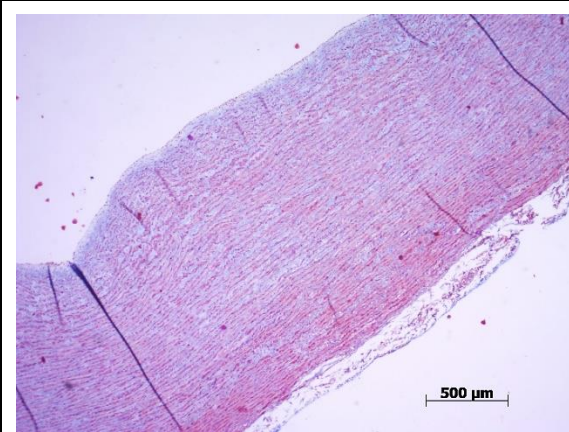
*Masson's Trichrome stain. 20x*



***Guinea pig caudal vena cava.*** Cross-section through part of the vein wall. The tunica interna is lined with endothelium with a thick underlying subendothelial layer composed of collagen and a prominent, thick internal elastic membrane. The tunica media is thin and consists of bundles of elastic fibers and few smooth muscle cells. The tunica externa is the most prominent layer and contains many bundles of longitudinally-oriented smooth muscle, together with elastic fibers.

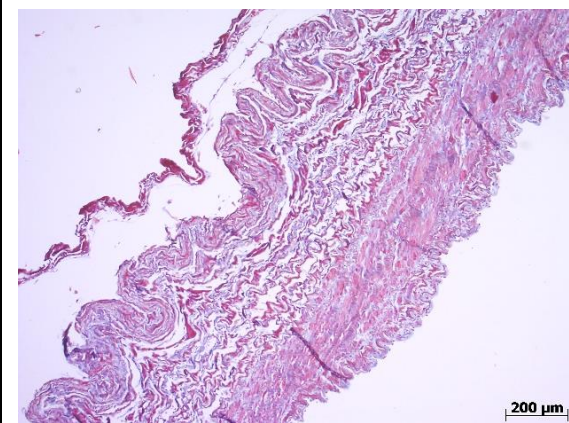
*Masson's Trichrome stain. 10x*

***Hydrochoerus hydrochaeris***



**Capybara aorta.** Cross-section of the aortic wall. The aorta, being an elastic artery, has a prominent tunica interna (intima) with a thick subendothelial layer of collagen, longitudinal elastic fibers and smooth muscle cells, but the thickest tunic is the tunica media, composed of several layers of smooth muscle cells interspersed with abundant elastic laminae that predominate. The tunica externa (adventitia) consists in longitudinally-arranged bundles of collagen and elastic fibers.

Masson's Trichrome stain. 2.5x



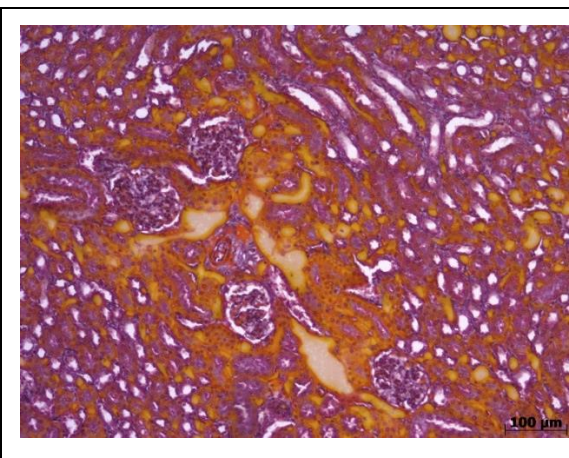
**Capybara caudal vena cava.** Cross-section. The tunica interna is lined with endothelium with a thick underlying subendothelial layer composed of elastic fibers and a prominent internal elastic membrane. The tunica media is thin and consists of bundles of elastic fibers and few smooth muscle cells. The tunica externa is the most prominent layer and contains many bundles of longitudinally and spirally-oriented smooth muscle, together with elastic fibers.

Masson's Trichrome stain. 5X

## Urogenital system

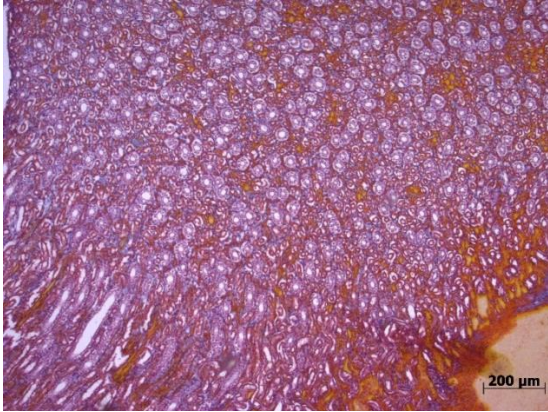
### Urinary system

#### *Cavia porcellus*

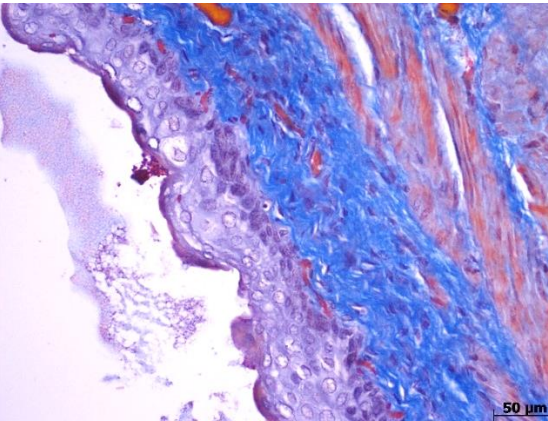


**Guinea pig kidney.** Cortical labyrinth. Four renal corpuscles among numerous proximal and distal convoluted tubules cut in cross section or longitudinally are well visible. Note the macula densa located in the vascular pole of the renal corpuscle.

Masson's Trichrome stain. 10x

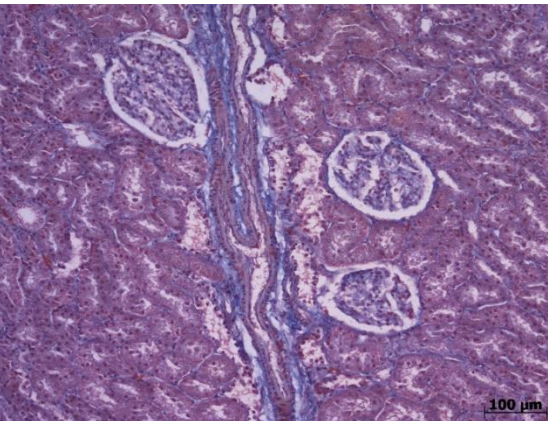


**Guinea pig kidney.** Inner medulla. The inner medullary collecting ducts, cut transversally or longitudinally, show a tall cuboidal epithelium. In addition, numerous capillaries are present.  
Masson's Trichrome stain. 20x

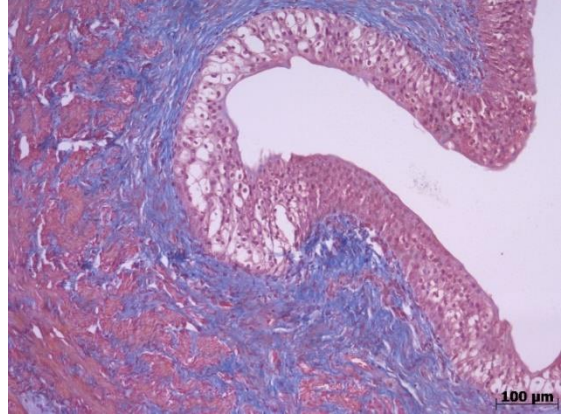
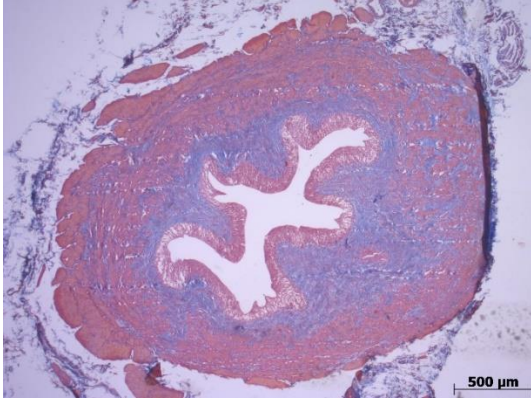


**Guinea pig urinary bladder.** The mucosa, not particularly folded and lined with a flattened transitional epithelium, and the submucosa are thick. Here, two (inner longitudinal and middle circular) of the three layers of the tunica muscularis are identifiable. The superficial cells of the transitional epithelium line the lumen. No lamina muscularis was identified.  
Masson's Trichrome stain. 20x

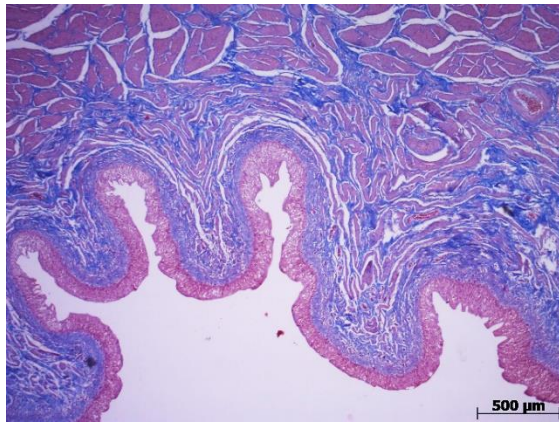
***Hydrochoerus hydrochaeris***



**Capybara kidney.** Cortex. Cortical labyrinth and medullary rays. Three renal corpuscles among numerous proximal and distal convoluted tubules cut transversally or longitudinally are well visible in the cortex. In the renal corpuscle, the glomerulus is surrounded by the glomerular capsule and presents a macula densa of the juxtaglomerular apparatus located at the vascular pole of the renal corpuscle. Note the medullary rays containing long straight tubules.  
Masson's Trichrome stain. 10x



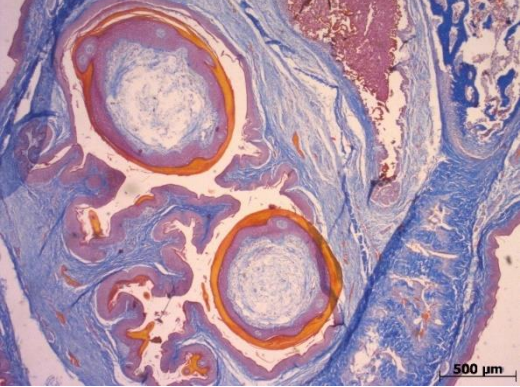
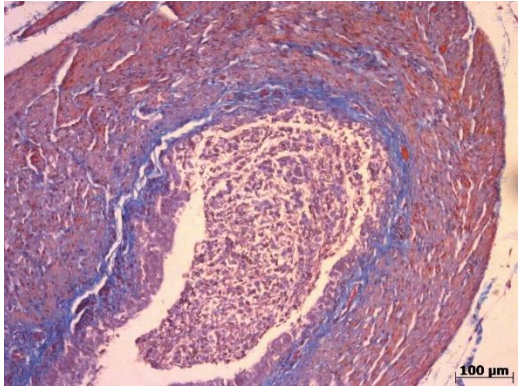
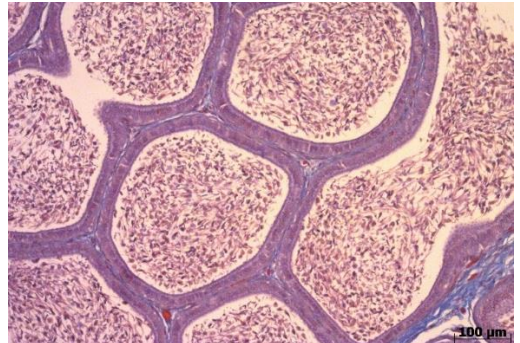
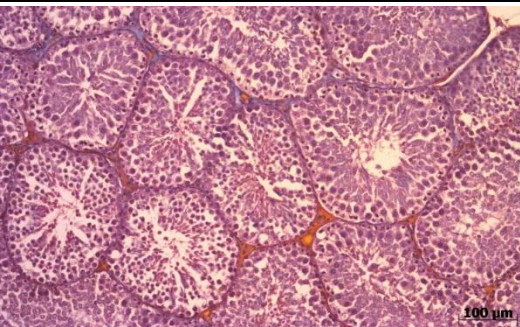
***Capybara ureter.*** Longitudinal mucosal folds give the lumen a stellate-shaped appearance. The mucosa is lined with a transitional epithelium, the underlying submucosa consists of loose connective tissue, the tunica muscularis consists of an inner longitudinal, a middle circular and an outer longitudinal layers, and an adventitia composed of loose connective tissue are well distinguishable. Masson's trichrome stain. 2.5x (left), 10x (right)

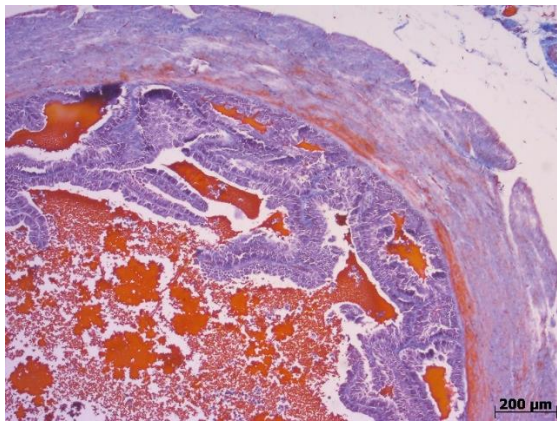


***Capybara urinary bladder.*** The mucosa, extensively folded and lined with transitional epithelium, is well-developed, analogously to the submucosa. The layers of the tunica muscularis are not well-defined and identifiable. The superficial cells of the transitional epithelium line the lumen. A lamina muscularis was not identified. Masson's Trichrome stain. 2.5x

## Male genital system

### *Cavia porcellus*

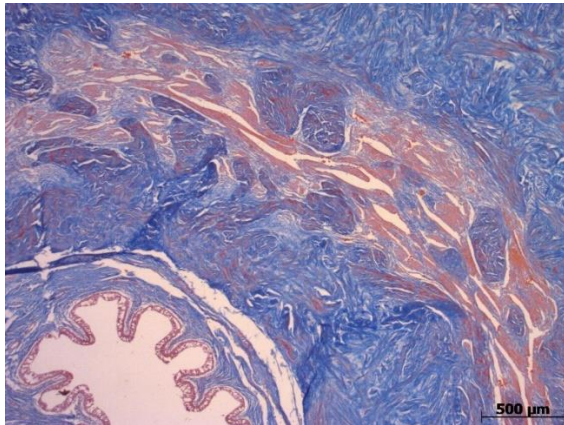
 <p>A low-magnification histological section of the guinea pig glans penis. The image shows the urethral mucosa with its characteristic folds (plicae) and a thick layer of connective tissue. Two prominent cartilaginous cores are visible, lined by a highly keratinized epithelium. The surrounding tissue is stained with Masson's Trichrome, showing blue collagen fibers and red muscle fibers. A scale bar in the bottom right corner indicates 500 μm.</p>	<p><b>Guinea pig glans penis.</b> The urethral mucosa is folded into plicae and is lined with a transitional epithelium. The submucosa consists of loose connective tissue with many elastic fibers and sparse lymph nodules. The urethra is surrounded by little subepithelial erectile tissue and a thick connective tissue layer. The glans is surrounded by a tunica albuginea rich in elastic fibers containing cavernous spaces typical of the erectile tissue. Note the two structures lined by a highly keratinized epithelium surrounding a cartilaginous core that are present in the urethral lumen, which are most likely ascribable to the guinea-pig typical horny stiles that protrude externally when the intromittent sacs everts during erection. Masson's Trichrome stain. 2.5x</p>
 <p>A cross-section of the guinea pig deferent duct. The duct is lined by a pseudostratified columnar epithelium with short microvilli. The submucosa is highly vascularized and contains a dense network of elastic fibers. The tunica muscularis is composed of intermingled longitudinal, oblique, and circular layers. The ductal lumen is filled with maturing spermatozoa. The image is stained with Masson's Trichrome. A scale bar in the bottom right corner indicates 100 μm.</p>	<p><b>Guinea pig deferent duct.</b> Cross-section. The mucosa of the ductus deferens is lined by a pseudostratified columnar epithelium that contains a higher amount of basal cells, in comparison with the epididymis, with the columnar cells having short microvilli. The loose connective tissue of the submucosa is highly vascularized and contains a dense network of elastic fibers. The tunica muscularis is composed of intermingled longitudinal, oblique and circular layers. The ductal lumen is filled with maturing spermatozoa. Masson's Trichrome stain. 10x</p>
 <p>A section through the wall of the epididymis body. The ductules are lined by a pseudostratified columnar epithelium characterized by columnar principal cells and small polygonal basal cells. The apical surface of the columnar cells bears microvilli. The ductules are surrounded by a small amount of loose connective tissue and poorly developed muscular coat, and their lumen is filled with maturing spermatozoa. The image is stained with Masson's Trichrome. A scale bar in the bottom right corner indicates 100 μm.</p>	<p><b>Guinea pig epididymis.</b> Section through the wall of the epididymis body. The ductules are lined by a pseudostratified columnar epithelium which is characterized by columnar principal cells and small polygonal basal cells: the apical surface of the columnar cells bear microvilli. The ductules are surrounded by a small amount of loose connective tissue and poorly developed muscular coat, and their lumen is filled with maturing spermatozoa. Masson's Trichrome stain. 10x</p>
 <p>A section of the adult guinea pig testis showing seminiferous tubules and intertubular tissue. The convoluted seminiferous tubules are lined with the stratified spermatogenic epithelium (germinal epithelium), and are surrounded by a lamina propria. They are also characterized by Sertoli cells and spermatogenic cells. The intertubular spaces contain loose connective tissue, vascular and lymph vessels. The image is stained with Masson's Trichrome. A scale bar in the bottom right corner indicates 100 μm.</p>	<p><b>Adult guinea pig testis.</b> Seminiferous tubules and intertubular tissue. The convoluted seminiferous tubules are lined with the stratified spermatogenic epithelium (germinal epithelium), and are surrounded by a lamina propria. They are also characterized by Sertoli cells and spermatogenic cells. The intertubular spaces contain loose connective tissue, vascular and lymph vessels. Masson's Trichrome stain. 10x</p>



**Guinea pig seminal vesicle.** Cross-section. The glandular epithelium is pseudostratified with columnar cells. Epithelial folds project into the secretory alveoli. The tunica muscularis, composed of intermingled circular and longitudinal muscle layers, is well developed.

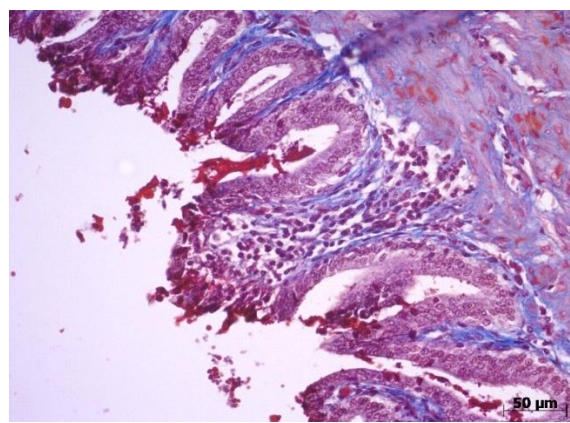
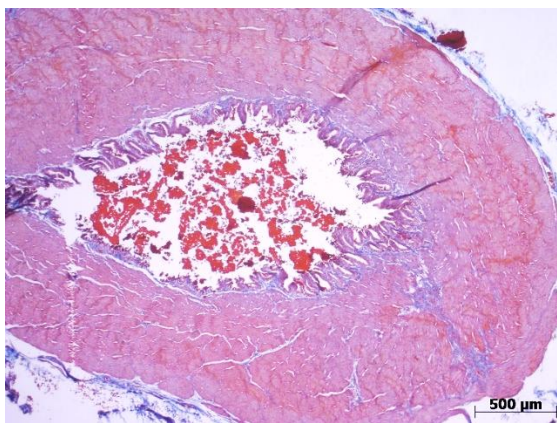
Masson's Trichrome stain. 5x

### ***Hydrochoerus hydrochaeris***



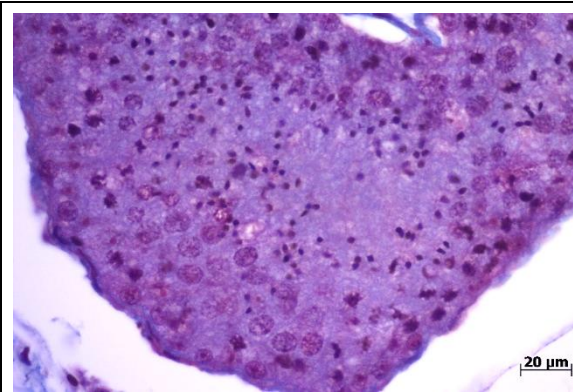
**Capybara penis.** Cross section through the penile urethra and corpus cavernosum. The urethral mucosa is folded into plicae and is lined with a transitional epithelium. The submucosa consists of loose connective tissue with many elastic fibers and sparse lymph nodules and vessels. The urethra is surrounded by little subepithelial erectile tissue and a thick connective tissue layer. The corpora cavernosa are surrounded by the tunica albuginea, a thick layer of dense irregular connective tissue containing elastic fibers and smooth muscle cells. The spaces between the tunica albuginea and the trabeculae originating from it are filled with erectile tissue. Bundles of smooth muscle are present in the connective-tissue trabeculae between the cavernous spaces.

Masson's Trichrome stain. 2.5x



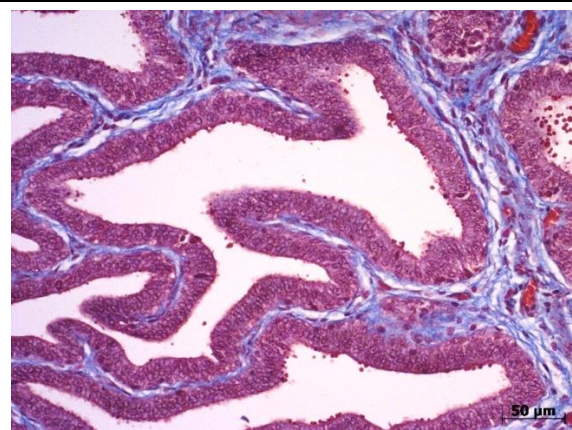
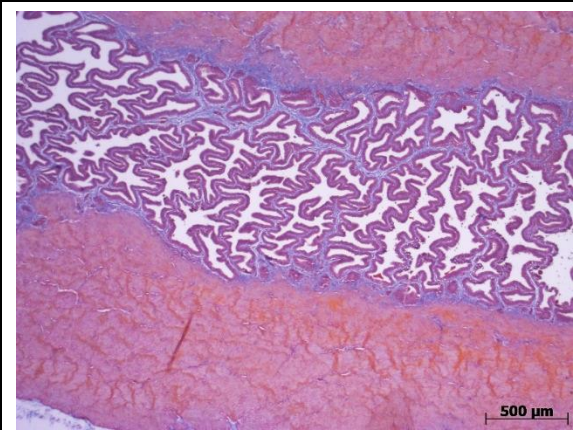
**Capybara deferent duct.** Cross-section. The highly-folded mucosa of the ductus deferens is lined by a pseudostratified columnar epithelium that contain a higher amount of basal cells, in comparison with the epididymis, with the columnar cells having short microvilli. The loose connective tissue of the submucosa is highly vascularized and contains a dense network of elastic fibers and fibroblasts. The tunica muscularis is composed of intermingled longitudinal, oblique and circular layers.

Masson's Trichrome stain. 2.5x (left), 20x (right)



**Testis of a prepubertal Capybara. Seminiferous tubule.** The convoluted seminiferous tubule is lined with the stratified spermatogenic epithelium (germinal epithelium), and is surrounded by a lamina propria. They are also characterized by Sertoli cells and spermatogenic cells. The intertubular spaces contain loose connective tissue, and vascular vessels. The lumen contains immature spherical primary spermatids.

Masson's Trichrome stain. 40x

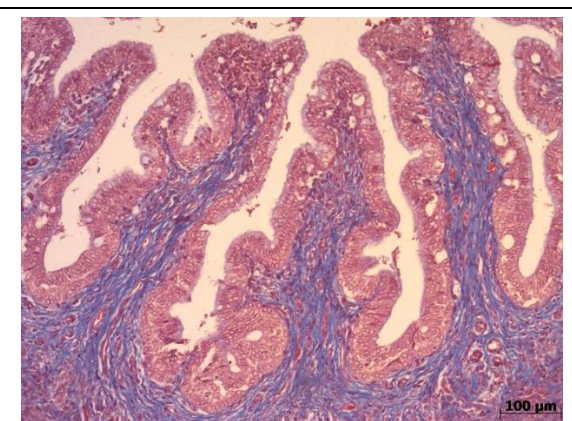
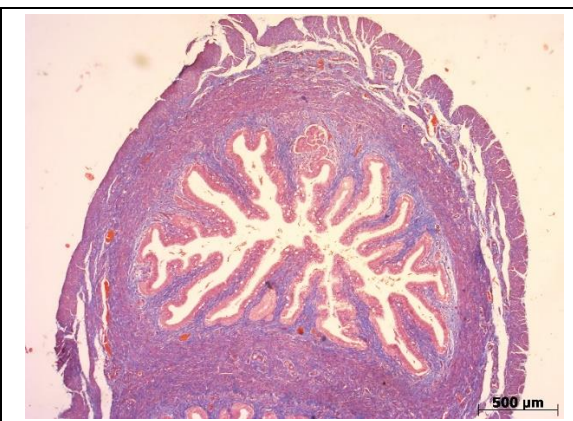


**Capybara seminal vesicle (vesicular gland).** The glandular epithelium is pseudostratified with columnar cells. The organ is subdivided into lobes and lobules by trabeculae, characterized by dense connective tissue that is continuous with the highly-vascularized loose connective tissue of the submucosa. Epithelial folds project into the secretory alveoli. The tunica muscularis is well developed.

Masson's Trichrome stain. 2.5x (left), 20x (right)

## Female genital system

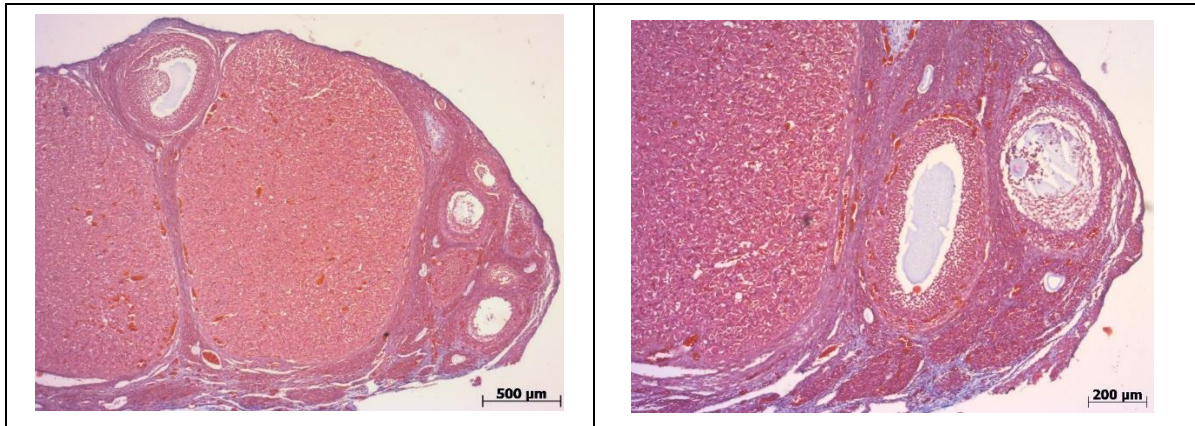
### *Cavia porcellus*



**Guinea pig uterus (horns). Cross-section.** The epithelium of the endometrium is pseudostratified columnar, whereas the subepithelial layer is composed of a richly vascular loose connective tissue, progressively less cellular in its deeper part. The endometrium forms several mucosal folds, and it presents numerous uterine tubular glands. The myometrium is composed of two muscular layers separated by an intermediate vascular zone.

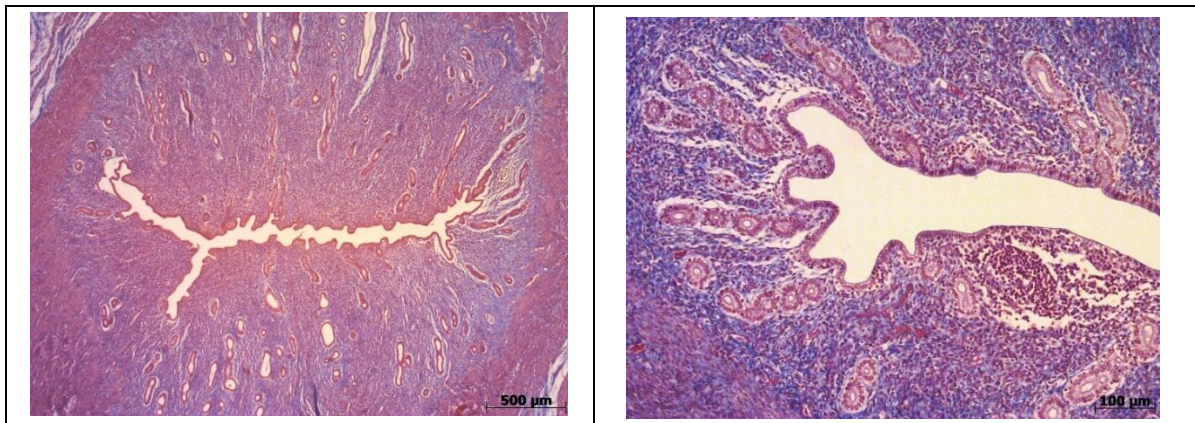
Masson's Trichrome stain. 2.5x (left), 10x (right)



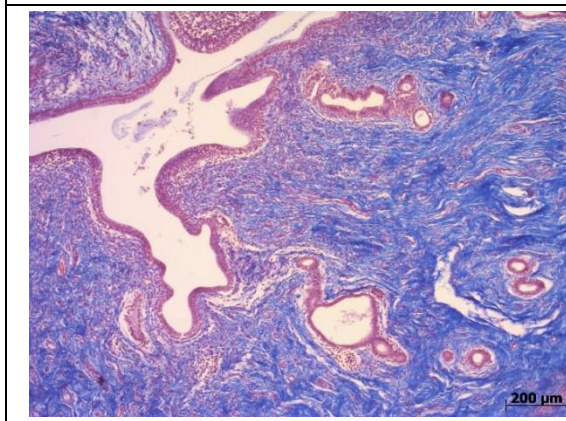


**Guinea pig ovary** showing the different stages of development and regression of follicles and corpora lutea in the ovarian cortex. Note the presence of two large corpora lutea, occupying most of the parenchyma, several tertiary follicles, in one case containing an oocyte within the cumulus oophorus and some primary follicles. The cuboidal surface epithelium is surrounded by a thick tunica albuginea of connective tissue. Masson's Trichrome stain. 2.5x (left), 5x (right)

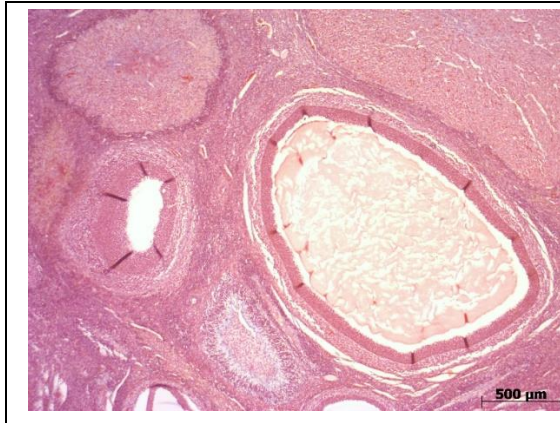
### ***Hydrochoerus hydrochaeris***



**Capybara uterus.** Cross-section of the uterine body (left) and of the uterine horn (right). The epithelium of the endometrium is simple columnar, whereas the subepithelial layer is composed of a richly vascular loose connective tissue, that is highly cellular and also contains lymph tissue. The endometrium forms several mucosal folds, and it presents abundant uterine tubular glands. The myometrium is composed of two muscular layers, with a vascular zone within the inner layer. Masson's Trichrome stain. 2.5x (left), 10x (right)



**Capybara uterine cervix.** Cross section of a large primary mucosa-submucosal fold. The mucosa of the cervix forms several primary and secondary folds. The epithelium is simple columnar and contains goblet cells, whereas the submucosa layer is composed of a dense irregular connective tissue and presents several venous plexuses. Note the mucus in the cervical lumen, demonstrating the mucous secretory activity of the epithelial cells. Masson's Trichrome stain. 5x



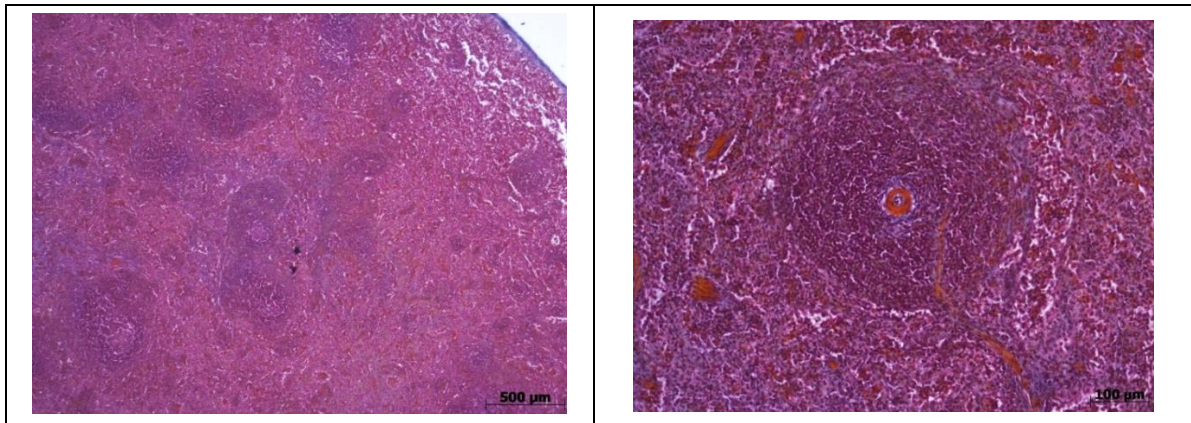
***Capybara ovary*** showing the different stages of development and regression of follicles and corpora lutea in the ovarian cortex. Note the presence of a corpus luteum (top right), two tertiary follicles, an atretic tertiary follicle, and a corpus regressivum.

*Hematoxylin-eosin stain. 2.5x*

## Lymphatic system

### Spleen

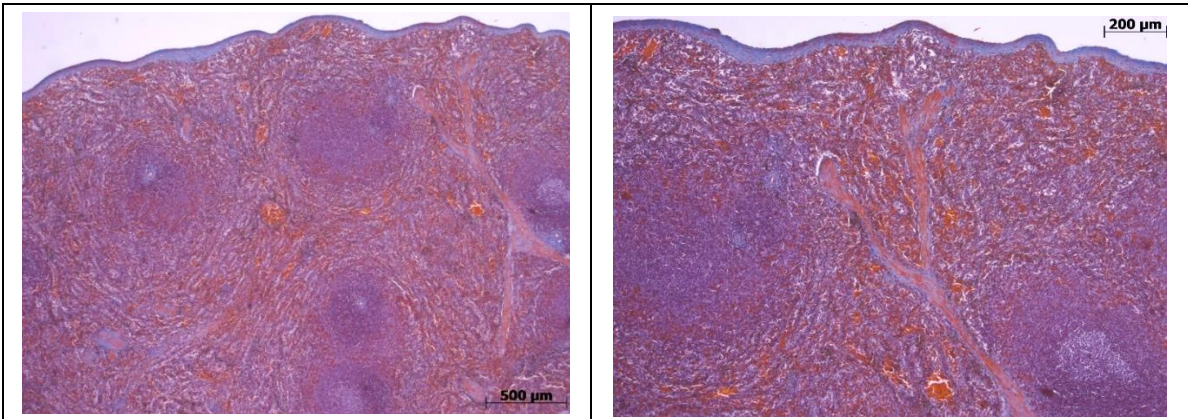
#### *Cavia porcellus*



***Guinea pig spleen.*** Most of the splenic parenchyma consists of the red pulp, composed of venous sinuses and splenic cords situated between them to form the reticular network. The white pulp is composed of lymphatic tissue. The marginal zone lies between the white and red pulp. Note the artery and the nodule of the white pulp, each embedded within the lymphocytes that constitute the periarterial lymphatic sheath, comprised of lymphatic nodules and diffuse lymphatic tissue.

*Masson's Trichrome stain. 2.5x (left), 10x (right)*

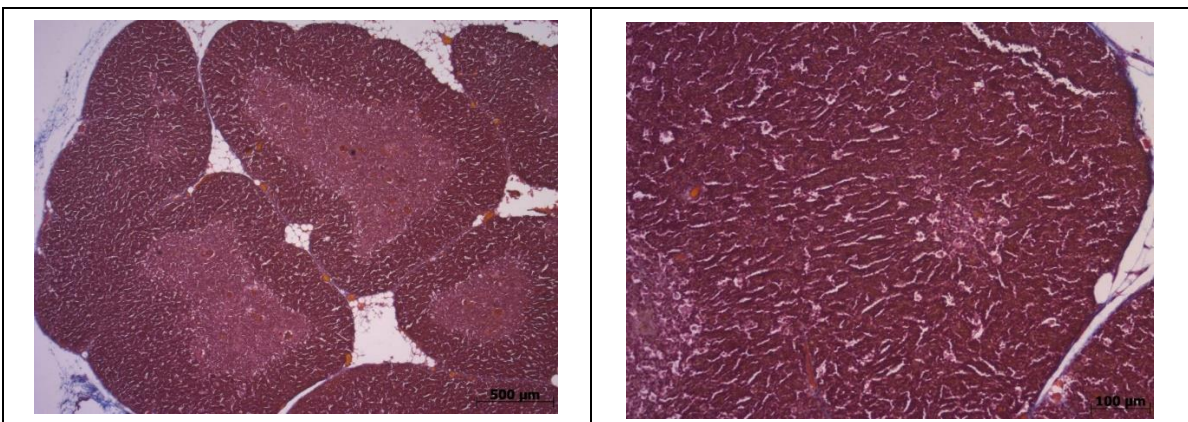
***Hydrochoerus hydrochaeris***



***Capybara spleen.*** Most of the splenic parenchyma consists of red pulp, composed of venous sinuses and splenic cords situated between them to form the reticular network. The white pulp is composed of lymphatic tissue. The marginal zone lies between the white and red pulp. Note the artery and nodule of the white pulp embedded within the periaarterial lymphatic sheath, comprised of lymphatic nodules and diffuse lymphatic tissue. Also note the venous sinus adjacent to the PALS. Masson's Trichrome stain. 2.5x (left), 5x (right)

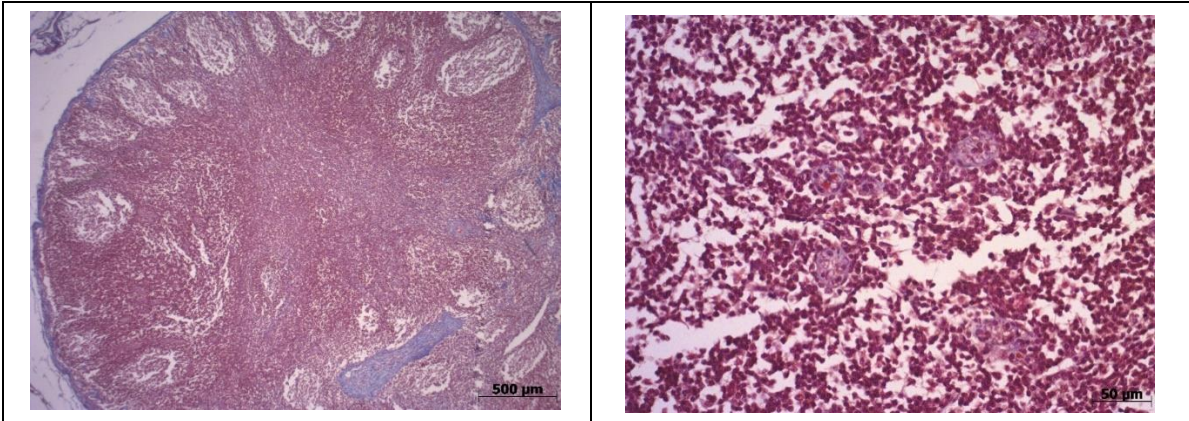
Lymph nodes

***Cavia porcellus***



***Guinea pig lymph node.*** The darker cortex with lymphatic nodules is clearly distinguishable from the lighter medulla. The cortex consists of lymphatic nodules separated by diffuse lymphatic tissue. The medulla contains medullary cords of lymphatic tissue, separated by the medullary sinuses, that derive from the trabecular septae coming from the cortex. Lymph nodes are surrounded by a capsule of connective tissue. Masson's Trichrome stain. 2.5x (left), 10x (right)

### *Hydrochoerus hydrochaeris*

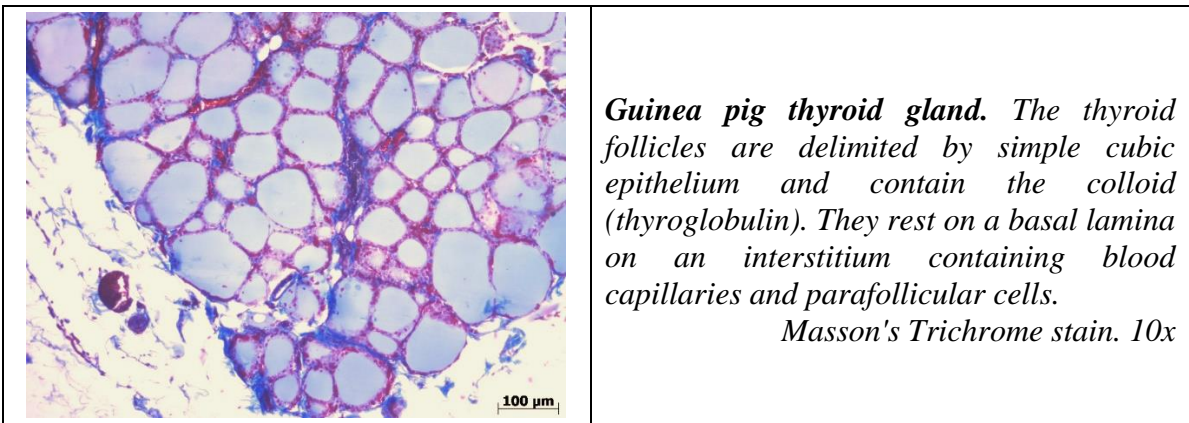


***Capybara lymph node.*** The darker cortex with lymphatic nodules is clearly distinguishable from the lighter interior medulla. The cortex consists of lymphatic nodules separated by diffuse lymphatic tissue. The medulla contains medullary cords of lymphatic tissue, separated by the medullary sinuses, that derive from the trabecular septae coming from the cortex. Lymph nodes are surrounded by a capsule of dense irregular connective tissue.

*Masson's Trichrome stain. 2.5x (left), 20x (right)*

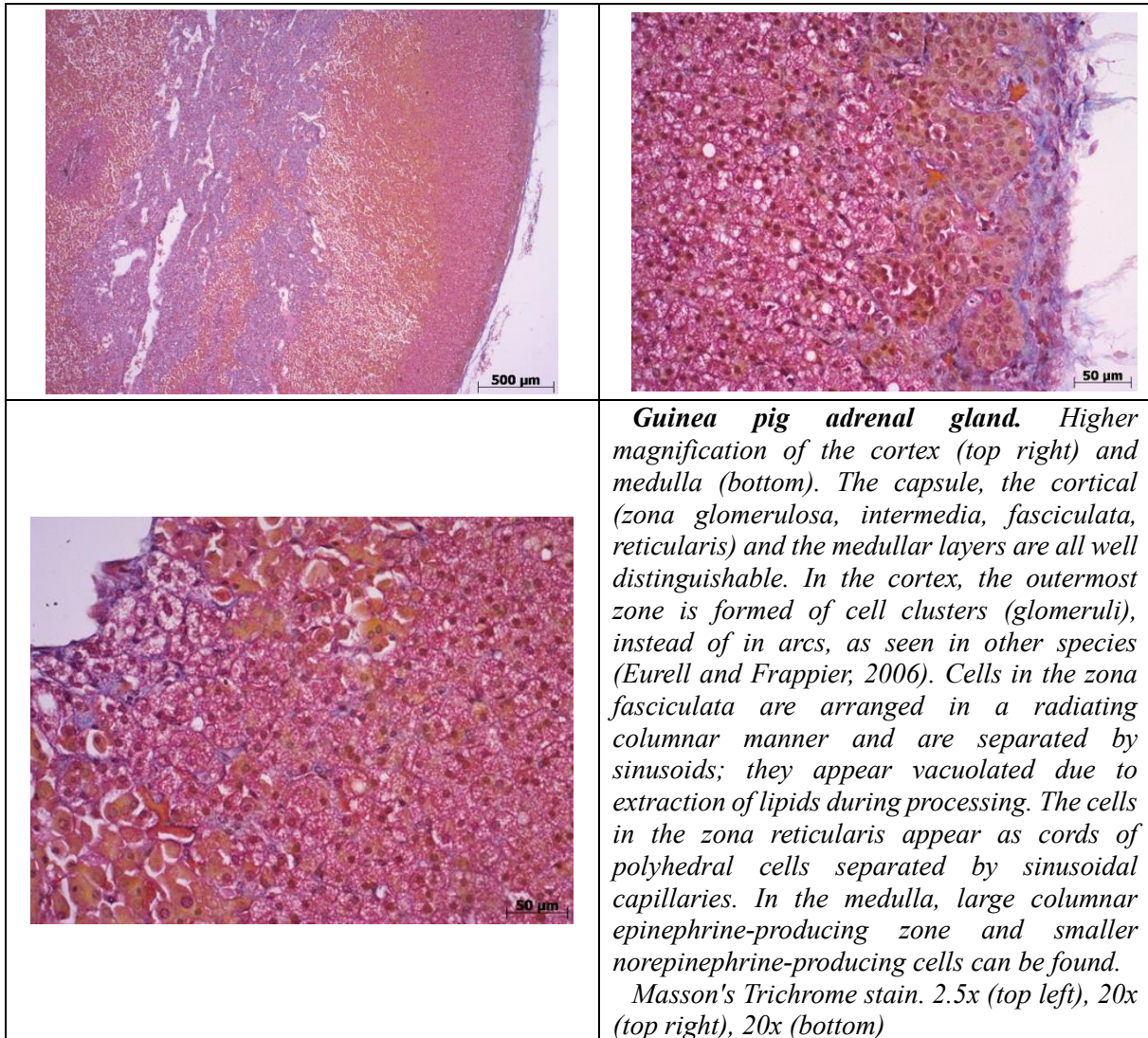
## Endocrine system

### *Cavia porcellus*

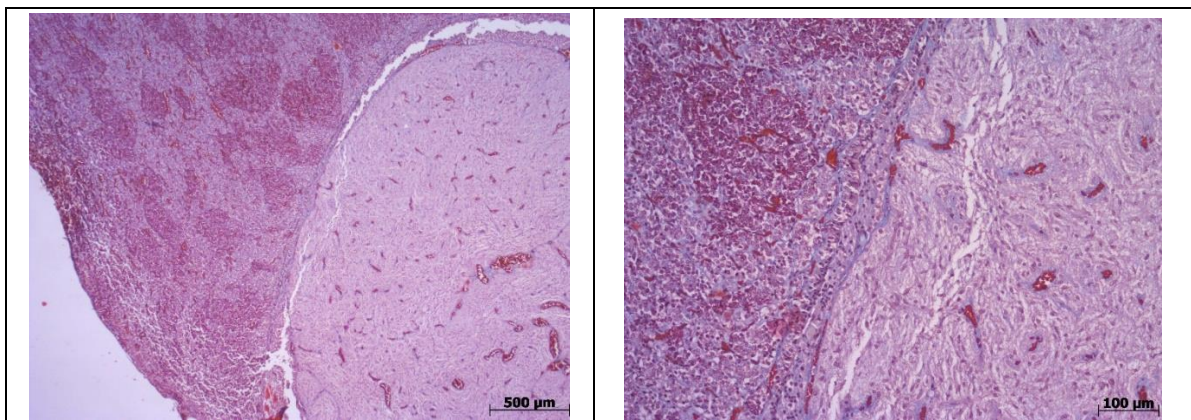


***Guinea pig thyroid gland.*** The thyroid follicles are delimited by simple cubic epithelium and contain the colloid (thyroglobulin). They rest on a basal lamina on an interstitium containing blood capillaries and parafollicular cells.

*Masson's Trichrome stain. 10x*



***Hydrochoerus hydrochaeris***


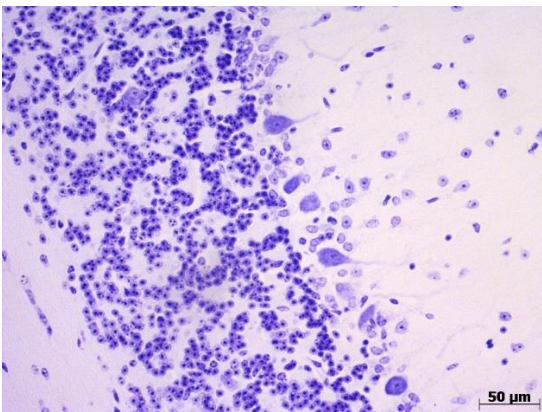


***Capybara hypophysis (pituitary gland).*** The pituitary gland is composed of the adenohypophysis consisting of glandular epithelial tissue, and the neurohypophysis consisting of secretory nervous tissue. The hypophysis is surrounded by a connectival capsule. The pars distalis (left) of the adenohypophysis stains more intensively due to the presence of chromophile cells; at higher magnification acidophilic, basophilic and chromophobe cells that are arranged in cords, are visible. The pars intermedia is located between the pars distalis and the pars nervosa and it contains

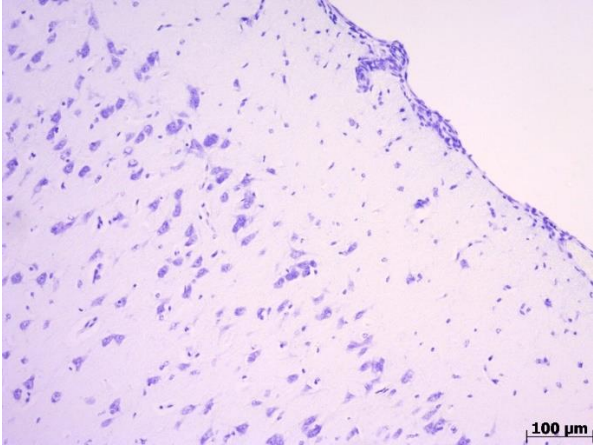
colloid-filled cavities (Rathke cysts) lined with follicular cells. The pars nervosa (right) of the neurohypophysis contains neurosecretory axons, pituicytes and capillaries, with a richly vascularized connective stroma and is more lightly stained. Note the typical Herring's bodies, which are dilatations of the nervous fibers that form focal accumulations of secretory vesicles.  
 Masson's Trichrome stain. 2.5x (left), 10x (right)

## Central nervous system

### *Cavia porcellus*

	<p><b>Guinea pig cerebellum.</b> Cross-section through the cortex and white matter. The white matter extends into the center of a cerebellar folium. The cortex covering the white matter presents a densely cellular layer and a poorly-cellular outer one. Specifically, it is composed of a deeper granular layer, an intermediate piriform cell layer, and the outer molecular layer. The Pia mater covers the cerebellar surface and extends into the sulci that separate folia.      Nissl Stain. 2.5x</p>
	<p><b>Guinea pig cerebellum.</b> Higher magnification of the cerebellar cortex. From left to right: white matter, granular layer, piriform layer (Purkinje cells), and molecular layer.      Nissl Stain. 20x</p>

### *Hydrochoerus hydrochaeris*

	<p><b>Capybara occipital cerebral cortex.</b> Note the neuron cell bodies in the VI different layers of the cerebral cortex. From right to left: tangentially-oriented neuropil (molecular layer); small interneurons (external granular layer); small and medium pyramidal neurons (external pyramidal layer); small stellate neurons (internal granular layer); medium to large pyramidal neurons that send axons into the white matter (internal pyramidal); spindle-shaped neurons that send axons into the white matter (fusiform layer). Underneath the cortex, the white matter is visible, composed of nerve fibers going to and coming from the cortex.      Nissl Stain. 10x</p>
---	--

# DISCUSSION

## RESPIRATORY SYSTEM

From the macroscopic anatomical study on the **nasal cavities** of the capybara, it emerged that the nasal plane, in this species, lies in a dorsal position, due to the adaptation of this species to a semi-aquatic life (Moreto et al., 2017), unlike guinea pigs, which are mainly terrestrial. The well-developed nasal septum of the capybara, which was complete and joined the dorsal surface of the hard palate, divided the nasal cavity into right and left cavities, and, cranially, it divided the rostral end into right and left vestibules through paired cartilages, in accordance with what had been reported for this species by Moreto et al. (2017). Conversely, in the guinea pig, the nasal septum, which also divided the nasal cavity into right and left nasal fossae, was found to be fenestrated, allowing the communication between the two nasal fossae, in accordance with previous reports by Cooper and Schiller (1975). Each nasal fossa, in both species, communicates caudally with the nasopharynx through the choanae. The nasal cavity, in cross-section, appeared increasingly T-shaped in both species, progressively broadening dorsally, and narrowing down ventrally, while moving in the caudal direction. The right and left nasal cavities of the capybara and guinea pig were occupied by highly developed and spiral-shaped endoturbinates and ethmoturbinates, dividing each nasal cavity into dorsal, middle and ventral meatuses. The literature regarding the anatomy of the nasal cavities in both species is scarce. Our macroscopical findings are in line with previous reports in the rat (Cozzi et al., 2006) and other domestic mammals (Barone, 2006b; König and Liebich, 2011). The nasal cavities, on histology, were lined with ciliated pseudostratified columnar epithelium with goblet cells and ciliated cells; nasal gland acini were also identified in the cavernous stratum of the respiratory mucosa, involved in the olfactory function. The histological appearance of the epithelium of the nasal cavity of the capybara is in accordance with what has been reported for other domestic mammals (Eurell and Frappier, 2006) and for the guinea pig (Breazile and Brown, 1976). In both species, the caudodorsal wall of the nasal cavities contains a developed olfactory epithelium, whereas a vomeronasal organ is located in the ventral portion of the nasal septum for the detection of pheromones (Breazile and Brown, 1976; Eurell and Frappier, 2006; Moreto et al., 2017). A peculiarity of all hystricomorph rodents is the presence of a well-developed system of paranasal sinuses, which are pneumatic cavities, in the frontal, maxillary, and lacrimal sinuses of the capybara and guinea pig; these latter, however, lack a frontal sinus (Ferreira et al., 2022). A frontal sinus, on the other hand, was evidenced in the capybaras of the present study, in accordance with a previous study in this species (Ferreira et al., 2022). The paranasal sinuses, histologically, contain a ciliated pseudostratified columnar epithelium, which functions in the transportation of mucus through the cilia (Eurell and Frappier, 2006).

The macroscopical investigation of the **larynx** of the guinea pig and the capybara, has set in light that this organ, in both species, has the typical macroscopical and microscopical structure seen in other mammals (Barone, 2006b). In the guinea pig, it has a more squared shape, whereas, in the capybara it is more conical. In both animals it is composed of four cartilages: the cricoid, the thyroid, the arythenoids with cuneiform and corniculate processes, and the epiglottis. Guinea pigs, however, lack a laryngeal ventricle (Cooper and Schiller, 1975a). As observed in the histological sections of the guinea-pig larynx, the laryngeal cartilages are predominantly hyaline, with the exception of the cricoid, composed of elastic fibers. The histological appearance of the laryngeal cartilages is in line with previous reports in the capybara, as well (Moreto et al., 2017). Macroscopically, the epiglottic cartilage of the capybara and guinea pig's larynx was sharp and leaf-shaped, inserted onto the thyroid cartilage

at its base. The thyroid cartilage was composed of a ventral body and two lateral rectangular laminae in both species; it presented poorly-developed rostral and caudal horns in the capybara, whereas in the guinea pig the rostral horn was well-developed. The arytenoid was composed of a cranial corniculate process and a caudal cuneiform process in both species. Finally, the cricoid formed a complete ring around the caudal portion of the larynx; in both species, the cricoid cartilage was particularly voluminous, it was broadened dorsally and narrowed ventrally. These data are in line with a previous anatomical study carried out in capybaras (Moreto et al., 2017). Moreover, the capybara presented well-developed vocal cords and laryngeal ventricles, whereas, in the guinea pig the laryngeal ventricle was absent and the vocal cords poorly developed; this finding is in line with previous reports in the guinea pig (Cooper and Schiller, 1975a).

From the macroscopical study of the **trachea** of the guinea pig and capybara, it emerged that, in both cases the tracheal cartilages formed incomplete rings, bridged dorsally and on their inner side, by a well-developed trachealis smooth muscle. In the guinea pig, the rings were more C-shaped, whereas in the capybara, they were more flattened in the laterolateral direction, resulting in a U-shaped appearance; moreover, tracheal rings were connected throughout the entire length of the trachea from the cricoid cartilage of the larynx to tracheal bifurcation, by dorsal annular ligaments; these macroscopical descriptions are in line with previous reports in both the guinea pig (Cooper and Schiller, 1975a) and the capybara (Moreto et al., 2017). The guinea-pig trachea was composed, on average, by 35 tracheal rings in the animals studied; in the capybara, the mean number of rings was 40; the number of rings counted in the two species fall within the ranges previously reported for each species, that is, 35 to 40 tracheal rings in the guinea pig (Cooper and Schiller, 1975a), and 35 to 46 rings in the capybara (Moreto et al., 2017). In both species, the trachea ended by bifurcating into the left and right primary bronchi, in accordance with data previously reported in these species (Cooper and Schiller, 1975a; Moreto et al., 2017), and species such as the cat (Coccolini, 2013) and the rabbit (Tagliavia, 2014); in the dog (Nenzi et al., 2008; Venturoli, 2008) and ferret (Tagliavia, 2014), on the other hand, a tracheal trifurcation occurs, due to the origin of the right cranial lobar bronchus directly from the trachea. The trachea of the guinea pig bifurcated at the level of the second to fourth rib, which is in line with previous studies (Breazile and Brown, 1976). Histologically, the tracheal mucosa is lined with respiratory epithelium, containing numerous ciliated, and goblet cells. In the, capybara, the submucosa was particularly glandular. The tracheal cartilage was of hyaline nature, and the trachea was covered by an adventitious layer of connective tissue. The histological and macroscopical findings were comparable in the two species. Histologically, the trachea had the typical structure seen in most other domestic mammals (Eurell and Frappier, 2006). Macroscopically, its gross structure in both species resembled that of the pig (König and Liebich, 2011), due to the C shape of their tracheal ring and internal arrangement of the trachealis muscle.

Histologically, the **bronchi** were characterized by the same epithelium as the trachea, but with an inferior amount of ciliated cells; however, the hyaline cartilage was arranged in the form of plates, instead of rings, as normally seen in the other domestic mammals, as well (Eurell and Frappier, 2006; König and Liebich, 2011).

In both species, the **lungs** were voluminous and polylobed and had an macroscopical structure, that is in line with previous reports in these species (Cooper and Schiller, 1975a; Moreto et al., 2017) and with the typical structure present in other domestic mammal species (Barone, 2006b), with a few exceptions. The **right lung** of the guinea pig and the capybara consisted of four lobes: cranial, middle, accessory and caudal lobes, separated by deep fissures, with the caudal lobe the being the most voluminous and having a concave diaphragmatic



surface. The right middle lobe presented a medial cardiac impression. The accessory lobe had an irregular shape and presented a ventral incisure for the caudal vena cava. In the capybara, the accessory lobe was further divided, by an accessory intralobar fissure, into a medial and a lateral portions.

The **left lung**, not as developed as the right, was composed of three lobes in the guinea pig, whereas it was composed of two lobes in the capybara. In the guinea pig, it consisted of a cranial lobe, divided into smaller cranial and larger caudal portions, an accessory lobe and a caudal lobe. The description of the macroscopic lobature of the left lung of the guinea pig seems to be contrasting: Orti et al. (2004) reported that the guinea pig lung is composed of a cranial lobe, divided by a deep fissure into a cranial and a caudal part, a caudal lobe and a small accessory lobe; this report is in line with our findings in the guinea pig. Cozzi et al. (2006), on the other hand, reported that it is composed of a cranial, a middle and a caudal. From our study emerged that the guinea pig left lung, in all the subjects, presented a bipartite cranial lobe, a caudal lobe and a small accessory lobe. In the capybara, the left lung was composed of a bipartite cranial lobe, divided into a cranial and a caudal parts, and a caudal lobe. In both species, the left cranial lobe had a cardiac impression on its medial surface. The small left accessory lobe of the guinea pig had a medial oesophageal notch and was partially covered by the large left caudal lobe. The lobar architecture of the capybara lungs resembles that of most other domestic species, with the exception of the horse, which does not present a middle right lobe and the cranial left lobe is not bipartite (König and Liebich, 2011). The presence of an accessory lobe in the left lung of the guinea pig, already reported in the literature for this species (Breazile and Brown, 1976, O'Malley, 2005), is peculiar of this species and is not found in most other domestic mammals and rodents (Cozzi et al., 2006; Barone et al., 2007, König and Liebich, 2011).

Histologically, the lung parenchyma, it is characterized in both species by alveoli lined by simple squamous epithelium and surrounded by alveolar septa of vascular connective tissue, endothelial cells at the level of the pulmonary capillary bed, interstitial cells, and macrophages. The histological structure of the lungs in the two species does not differ from the traditional description provided for the guinea pig (Brewer and Cruise, 1997), the capybara (Moreto et al., 2017), and most other mammal species (Eurell and Frappier, 2006).

From the anatomotopographic and morphometric study of the guinea-pig and capybara **primary, lobar and segmental bronchi and their satellite arteries and veins**, the method that employs the polyurethane foam technique, as described by De Sordi et al. (2014), was utilized. Several analogies and differences were evidenced between the two species. In both species, the literature was found to be lacking in data regarding the bronchial branching and the relationship with the satellite vessels.

The study carried out in the guinea pig lungs confirmed the data previously provided for this species by Tagliavia (2014), showing an articulated bronchial tree, as opposed to the more simplified bronchial tree of the capybara. For instance, the right and left cranial lobar bronchi bifurcate into cranial and caudal branches, which in turn, provide numerous segmental branches. In the capybara, on the other hand, the right and left cranial lobar bronchi have only dorsal and ventral segmental branches that originate from them. The present study showed that the highly articulated bronchial tree of the guinea pig, analogously to other species such as the rabbit, the ferret, and the dog (Nenzi et al., 2008; Venturoli, 2008) and the cat (Coccolini, 2013), had an almost identical structure to that identified in the rabbit (Tagliava, 2014). In both the guinea pig and the capybaras of the present study, the main bronchi extended caudally into the right and left lung, respectively, each accompanied by the corresponding pulmonary artery. The right main bronchus detached, very close to its origin, the right cranial lobar bronchus and, at a short

distance, the middle lobar bronchus. Therefore, in the guinea pig and capybara, analogously to other species such as the cat (Coccolini, 2013) and the rabbit (Tagliavia, 2014), the trachea was seen to bifurcate into the two primary bronchi, whereas in the dog (Nenzi et al., 2008; Venturoli, 2008) and in the ferret (Tagliavia, 2014), a tracheal trifurcation takes places, since the right cranial lobar bronchus originates directly from the trachea at its bifurcation. In line with previous studies in the dog (Nenzi et al., 2008; Venturoli, 2008) and in the cat (Coccolini, 2013), but also in the rabbit, ferret and guinea pig (Tagliavia, 2014), the accessory lobar bronchus of both the guinea pig and capybara did not originate from the right main bronchus, as argued by Ishaq (1980) and Getty (1982), but instead from the right caudal lobar bronchus, which represents its direct continuation. The left main bronchus, on the other hand, shortly after the tracheal bifurcation, in both species, always emitted the left cranial lobar bronchus and then continued as the left caudal lobar bronchus, as already observed by Tagliavia (2014) in the guinea pig.

In both species, the veins, unlike the arteries, did not maintain a close relationship with the corresponding bronchial branches throughout their course. In the capybara, the arteries were generally located dorso-laterally to the respective bronchus, whereas the veins tended to be located on the ventromedial side of the bronchi. In the guinea pig, similarly, the arteries were located laterally to the respective bronchus, whereas the veins were located medially to the corresponding bronchus.

Specifically, the bronchial architecture in the two species, was as follows:

As for the right lung, in the guinea pig, the right **right cranial lobar bronchus** (BLCrD), originating from the right main bronchus, immediately bifurcates into a cranial branch and a caudal branch, which, in turn, give rise to numerous segmental branches. In the capybara, on the other hand, the **right cranial lobar bronchus** (BLCrD) was seen to have only dorsal and ventral segmental bronchi.

In the guinea pig, the **middle lobar bronchus** (BLM) was seen to originate from the right main bronchus, and it ended, with a ventrocaudal direction, by bifurcating into a cranial and a caudal branch which then further bifurcated. During its course, it emitted cranial and caudal segmental branches in alternating succession, in a variable number from 4 to 7. In the capybara, the **middle lobar bronchus** (BLM), on the other hand, as for the cranial lobar bronchi, presented only dorsal and ventral segmental branches.

In the guinea pig, the **accessory lobar bronchus** (BLA) arose from the right caudal lobar bronchus (BLCdD) and divided into a large ventromedial branch, which ended by bifurcating into a dorsal and a ventral branch, and into a caudal branch. In the capybara, analogously, the **accessory lobar bronchus** (BLA) divided into a caudal and a ventromedial branch. Furthermore, in this species, it did not present a satellite vein, because the veins following the caudal and ventromedial branches of the BLA did not converge into a common vessel but, instead, opened separately into the right caudal lobar vein.

In the guinea pig, the **right caudal lobar bronchus** was the direct continuation of the right main bronchus and, along its path, it emitted two ventral branches and ended by bifurcating into a caudodorsal and a caudoventral branch. The right caudal lobe presented the most developed but also the most regular bronchial branching. In the capybara, the **right caudal lobar bronchus** (BLCdD), after detaching some segmental bronchi of which the two ventral ones being the largest, ended by bifurcating into two branches, caudodorsal and caudoventral, analogously to the guinea pig.

The anatomical descriptions of the macroscopic lobature of the left lung of the guinea pig

in the literature seem to be contrasting. In particular, Orti et al. (2004) reported that the guinea pig lung is composed of a cranial lobe, divided by a deep fissure into a cranial and a caudal part, a caudal lobe and a small accessory lobe. Cozzi et al. (2006), on the other hand, reported that it is composed of a cranial, a middle and an accessory lobe. Tagliavia (2014), on the other hand, reported the existence of two lobes only: a bipartite cranial lobe and a caudal lobe; they, however found the presence of a left caudomedial branch, originating from the caudal lobar bronchus and specular to the right BLA, which suggested the existence of a left accessory lobe. Our findings confirm this hypothesis as well as being in line with Orti et al. (2004)'s macroscopical description of the lung lobature in this species: Indeed, in all the guinea pigs studied, the left lung was composed of a bipartite cranial lobe, a caudal lobe and a small accessory lobe on the medial surface.

As for the left lung, in the guinea pig, the **left cranial lobar bronchus** (BLCrS) divided into a cranial branch, intended for the cranial part of the left cranial lobe, and a larger caudoventral branch, directed to the caudal part, which gave rise to several segmental cranial and caudal branches. In the capybara, the **left cranial lobar bronchus** (BLCrS), similarly to the right cranial lobar bronchus, had only dorsal and ventral segmental bronchi.

In the guinea pig, the **left caudal lobar bronchus** (BLCdS) was a direct continuation of the left main bronchus, with an identical course to the right caudal lobar bronchus: it emitted two ventral branches, which in turn detached segmental cranial and caudal branches, and ended by bifurcating into a caudodorsal and a caudoventral branch. In the capybara, in contrast with our findings in the guinea pig, the **left caudal lobar bronchus** (BLCdS) emitted smaller dorsal segmental branches and larger ventral segmental branches and ended by bifurcating into a lateral and a medial branch.

From the morphometric study, emerged that, in both species, there was no clear prevalence between the calibers of the bronchi and the satellite vessels in the right lung, whereas, in the left, the bronchi tended to have, generally, a smaller caliber than the respective vessels. This finding is in contrast with previous reports regarding the ferret (Horsfield, 1986), the dog (Nenzi et al., 2008; Venturoli, 2008), and the cat (Coccolini, 2013), which found that the bronchi have a larger diameter than the respective vessels. However, it is in line with findings in the rabbit (Tagliavia, 2014), in which the vessels are larger than the bronchi in both lungs.

In addition, the arteries were found to be larger than the veins in the right lung, but usually smaller in the left lung in both species. In the ferret, on the other hand, the opposite is generally true (Tagliavia, 2014); in the dog, the calibers of arteries and veins are similar (Nenzi et al., 2008; Venturoli, 2008), whereas in the cat, the arteries tend to be larger than the satellite veins (Coccolini, 2013) and, in the rabbit, the veins always have a greater caliber than the arteries (Tagliavia, 2014).

From the morphometric study of the diameters of the bronchi, it emerged that, in the guinea pig, the parent bronchial branch was 1.5X larger in diameter than the daughter branch, 1.7X in the capybara. These numerical data are in accordance with reports in the cat (Coccolini, 2013), but differ from the rabbit and ferret, in which the parent branch is twice as large, and the dog, in which the major daughter branch is only slightly smaller than the parent (Nenzi et al., 2008; Venturoli, 2008).

A calculated ratio of 1.66 was found between the diameter of the major daughter branch and that of the minor daughter branch in the guinea pig; in the capybara, the ratio was 1.52. These values are similar to those reported for the dog (1.73) (Nenzi et al., 2008; Venturoli, 2008) but greater than those reported for the rabbit (1.26) and the cat (1.32) (Coccolini, 2013), however inferior to the cutoff of 2 in any case. Therefore, in light of these findings, from the

study emerged that the bronchial tree of both the guinea pig and the capybara exhibits dichotomous branching.

## GASTROINTESTINAL SYSTEM

In both species, the opening of the **oral cavity** was seen to be proportionally narrower than in other domestic species such as carnivores (Legendre, 2016); this finding is in line with previous studies in the guinea pig and capybara (Mones and Ojasti, 1986; Cooper and Schiller, 1975a). The guinea pig and capybara had a common dental formula (20: I 1/1, C0/0, P1/1, M3/3), and all **teeth** were seen to be elodont and aradicular; these characteristics, together with the high development and particular orientation of the deep masseter muscle that was observed in both species, are shared by all caviomorpha, including the chinchilla (O'Malley, 2005). In both species, the maxillary molariforms were laterally oriented, whereas the mandibular molariforms were medially-oriented; the oblique arching of cheek teeth was more obvious in guinea pigs. The development and typical orientation of the deep masseter, passing through the large infraorbital foramina to insert anteriorly to the complete zygomatic arch on the incisor and maxillary bones, which has been reported to serve for gnawing efficiency (O'Malley, 2005; Herrera, 2013), was observed in both species, and is in line with previous studies in these species (Cooper and Schiller, 1975a; O'Malley, 2005; Herrera, 2013). Other than the strong mandibular musculature, and the trapezoidal shape of the mandible with developed angular and condylar processes, another adaptation of these species to a herbivorous and more abrasive diet consisted in the large occlusal surfaces, composed of lamellar prisms, of the molariform teeth seen in both species; moreover, the large dimension of the upper third molars in comparison with the other molariform teeth that was seen in the capybara only, was reported to play a role in masticatory function; all these findings are in accordance with what had been reported in the literature ( O'Malley, 2005; Pereira et al., 2020).

All five types of **salivary glands** reported in the literature for the guinea pig (Queesenberry et al., 2004, O'Malley, 2005), namely parotid, mandibular, zygomatic and major and minor sublingual glands were evidenced in the animals studied; the parotid and mandibular were particularly developed, as previously reported (O'Malley, 2005, Popesko et al., 1992); moreover, guinea pigs were seen to have a typical salivary gland that is not found in other species such as the rabbit and rat (Cozzi et al., 2006), the zygomatic or orbital gland, that was not observed in the capybara. The peculiarity of this gland in the guinea pig is the fact that it is voluminous and it occupies the entire floor of the orbit; this finding has been previously reported by few authors (Popesko et al., 1992). No previous studies regarding the salivary glands of the capybara were found in the literature.

Both the capybara and guinea pig had a particularly narrow and elongated **tongue** rounded at its free edge, composed of an apex, a body and a root, as previously reported by other authors for both species (Mones and Ojasti, 1986; O'Malley, 2005). In the capybara, the width of the tongue broadens moving towards its root, as previously reported (Cienas et al., 2019), whereas in the guinea pig, the apex and body had a similar width, with the root being thicker and broader. In the guinea pig, the root consisted in a well-developed, broad and thick torus, covered with lingual papillae, as previously described (Popesko et al., 1992). The rostrocaudal length of the guinea pig measured in this study (3.2 cm) is in line with the 3.5 cm reported by previous

authors (Cienas et al., 2019). The capybara tongue in this study was 14 cm long; no morphometric data regarding the tongue in this species were found in the literature. Histologically, the guinea pig tongue was lined with a stratified squamous epithelium with extensive and highly keratinized filiform papillae projecting above the surface of the mucosa, with abundant skeletal muscle beneath the submucosa; the abundant musculature present seen macroscopically on the ventral surface of the tongue in this species, confirms this finding. The histological aspect of the tongue of the guinea pig is in line with what Cienas et al. (2017) reported, according to whom filiform papillae are the most abundant throughout the entire extension of the tongue surface. It has been reported that the dorsal mucosa of the capybara tongue, with the exception of the root, is covered by extensive lingual papillae of all four types, filiform, fungiform, vallate and foliate (Watanabe et al., 2013). In the histological sections analysed in this study, however, no lingual papillae were evidenced in the capybara tongue; it is therefore likely that the sampled section was collected at the level of the tongue root. The capybara tongue, however, had the same histological structure as the guinea pig's, with a highly keratinized squamous epithelium, having a core of dense irregular connective tissue, and was outlined by abundant skeletal muscle, in accordance with previous histological descriptions of the tongue in this species (Watanabe et al., 2013).

The **oesophagus** of both the guinea pig and capybara had the same topography as that described in other domestic mammals (Barone, 2006b), running dorsally to the trachea in the cervical region, and being displaced dorsolaterally to its left side at the entrance of the thorax. In both species, its terminal portion entered the fundus of the stomach near the lesser curvature and forming with it an angular or cardiac incisure, in accordance with what had been previously described in these species (O'Malley, 2005; de Barros Moraes et al., 2002). The histological appearance of the oesophagus in the capybara was characterized by a highly keratinized stratified squamous epithelium composed of an evident stratum granulosum, with a well-developed striated tunica muscularis composed of a circular inner layer and an outer longitudinal layers; this description is in line with previous reports in this species (Carrascal Velasquez et al., 2016) and with the histological aspect of this organ seen in horses, pigs, and ruminants, all characterized by the presence of a keratinized squamous epithelium (Eurell and Frappier, 2006). Unlike the capybara oesophagus, in the guinea pig, on the other hand, the mucosa of the oesophagus was lined with a nonkeratinized stratified squamous epithelium with a well-developed lamina muscularis and a highly developed tunica muscularis with an inner circular layer and an outer longitudinal layer. This finding is in line with previous reports in this species (Cooper and Schiller, 1975b; O'Malley, 2005); it is noteworthy how the histological aspect of the guinea pig oesophagus, which is an herbivorous species, is analogous to the typical histological aspect normally seen in the oesophagus of carnivores, such as dogs and cats (Eurell and Frappier, 2006).

The topography, in the left cranial abdomen, and the subdivision into a cardiac, a fundic, a body and a pylorus of the **stomach** of both species are identical to what has been classically described in other domestic mammals (Barone, 2006b); however, in the capybara, the stomach had a typical inverted J-shaped appearance, with well-developed greater and lesser curvatures, that was not seen in the more simple stomach of guinea pigs with a poorly-developed lesser curvature. Moreover, both species presented a cranial expansion of the fundic part, especially in the capybara where it formed the so-called gastric diverticulum, as previously described (Cooper and Schiller, 1975b; de Barros Moraes et al., 2002). Externally, the stomach of the capybara presented 2 large gastric *teniae* that delimited haustras on its surface, as already described (de Barros Moraes et al., 2002); these *teniae* were not found in the guinea pig stomach. The stomach of both species is entirely glandular, unlike that of other rodents (Harkness et al., 2002; de Barros Moraes et al., 2002; O'Malley, 2005). Histologically, it was

observed that the fundic and pyloric regions of the stomach were lined by a well-developed glandular epithelium with tall simple columnar epithelial cells; the cardiac region in both species, on the other hand, was non-glandular. This finding has not been previously reported in the literature for these species, for which, usually, the stomach is described to be as entirely glandular (de Barros Moraes et al., 2002; O'Malley, 2005); however, in all other domestic species of veterinary interest, such as carnivores, pigs and horses, the cardiac region is lined with a nonglandular mucosa characterized by a nonkeratinized stratified squamous epithelium, analogous to the observed in the oesophagus (Eurell and Frappier, 2006). In the capybara, however, the nonglandular cardiac gastric region was lined with a keratinized stratified squamous epithelium, similar to that observed in the oesophagus of this species. These data have not been previously reported in the literature for the capybara. In both the capybara and guinea pig fundic and pyloric regions of the stomach, deep gastric pits continuous with gastric glands were observed on histology. These data are in line with what has been reported for the glandular gastric regions of the stomach of other domestic species (Eurell and Frappier, 2006). In the guinea pig gastric pylorus, a thick circular muscular layer of the tunica muscularis was observed; this finding is in line with previous reports stating that the major muscular component of the guinea pig stomach is a continuous layer of circular muscle, with the external longitudinal layer being absent in the region of the lesser curvature (de Barros Moraes et al., 2005).

The capybara and guinea-pig **small intestine** represented the longest portion of the alimentary tract, measuring up to 6 meters in the capybara, in accordance with what had been reported by de Freitas et al. (2008), which is an intermediate value between the canine and swine small intestinal lengths (Nickel et al., 1979). The gross anatomy of the small intestine of these species did not differ significantly from that of other domestic mammals, such as dogs and pigs (Nickel et al., 1979), where the three portions of the small intestine are not markedly distinguishable macroscopically, except for the long and convoluted jejunum. Histologically, the duodenum in both species was characterized by a tunica mucosa lined by a simple columnar epithelium with villi and intestinal mucosal glands, with submucosal (Brunner's) glands opening into the base of the intestinal mucosal glands. Our findings are in contrast with previous studies which reported the absence of glands in the submucosa of the small intestine of the capybara (de Freitas et al., 2008); the presence of submucosal glands in the duodenum of both species might be ascribable to the fact that the sampled area was very close to the pylorus, which usually occurs in other domestic species (Eurell and Frappier, 2006). In confirmation of this fact, both the ileum and jejunum of these species were characterized by the presence of villi and intestinal mucosal glands (crypts of Lieberkühn), and by the absence of submucosal glands. According to Hargaden and Singer (2012), the lamina propria of the small intestinal mucosa contains numerous Peyer lymphoid patches, especially in the ileum of guinea pigs. In our histological sections, no Peyer's patches were evidenced, however. Lymphatic nodules were noted in the submucosa of the guinea pig stomach, at pyloric level.

As for the **large intestine**, the cecum of both species was particularly voluminous and developed; it had thin wall and occupied most of the abdominal cavity and it was composed by a body, a base and an apex. It lacked a cecal appendix in both species, unlike the rabbit (O'Malley, 2005). On its outer surface, it presented three (in the guinea pig) or four (in the capybara) white longitudinal teniae ceci, which created lateral saccular haustra, as previously reported (Cooper and Schiller, 1975b; Vazquez et al., 2012).

In both species, the colon was dark green in colour and divided into an ascending, a transverse, and a descending portions, with the ascending portion being composed of a well-developed distal ansa, the spiral colon, composed of a centripetal gyrus, a central flexure, and a centrifugal gyrus. The colon of the capybara, with the exception of the spiral colon, presents outer haustras along its entirety (Cooper and Schiller, 1975b; Vazquez et al., 2012). These

findings are in line with previous reports (O'malley, 2005). In the guinea pig, the colon is functionally divided into a shorter proximal portion, which separates the digesta into the cecotrophs and the fecal pellets, and into a larger distal portion (O'Malley, 2005) since this species, unlike the capybara, exhibits coprophagy.

The colon of the capybara, with the exception of the spiral colon, presents outer haustras along its entirety (Cooper and Schiller, 1975b; Vazquez et al., 2012); these were not macroscopically observed in the guinea pig; however, in the histological section of the descending colon, a well-developed longitudinal layer of the tunica muscularis formed a large flat muscular band with elastic fibers, likely corresponding to a taenia coli. Histologically, the colon in both species was characterized by the presence of a simple cylindrical epithelium without villi, containing an abundance of simple tubular intestinal glands containing numerous goblet cells. Lymphatic nodules were observed in the submucosa of the colon of both species. The histological findings regarding the large intestine are in line with what has been previously reported in the literature for the capybara (Carrascal Velazquez, 2017) and for the other domestic mammals of veterinary interest (Eurell and Frappier, 2006).

The **liver**, in both species, was large, dark red-brown in color, with a smooth surface and sharp edges, and consisted of six lobes divided by fissures of variable depth: the left lateral, the left medial, the right medial, the right lateral, the quadrate and the caudate lobe, further divided into a caudate and a papillary processes. In the guinea pig, the lobes were poorly-demarcated and tended to blend with each other, as previously reported (O'Malley, 2005), whereas, in the capybara, in line with previous reports in this species (Cao et al., 2017), the lobes were well-demarcated by deep fissures, and they were partially overlapping. The visceral surface presented, in both species, a deep esophageal impression. In both species, a well-developed, thin-walled oval gallbladder, lied on the medial aspect of the quadrate lobe, in the guinea pig, or between the left medial lobe and the quadrate lobe, in the capybara. The macroscopic aspect of the liver, in comparison with that of the other domestic mammals of veterinary interest, resembled more that of carnivorous species such as the dog and cat, which present the same lobature (König and Liebich, 2011). The macroscopic lobature of the guinea pig and capybara liver also differed from that of other rodents, such as the rat and chinchilla, which only present four lobes (left lateral, median, right and caudate) and from that of the rabbit, which has five lobes, with an undivided right lobe (Stan, 2018). Moreover, unlike the guinea pig and capybara, the rat liver does not present a gallbladder (Cozzi et al., 2006). In both the guinea pig and capybara, the left lateral lobe of the liver resulted to be the most voluminous; this also applies to the liver of the rabbit (Stan, 2018), and that of the dog and cat (König and Liebich, 2011). The histological organization of the liver parenchyma resembled that reported for most domestic mammals and experimental rodents (Eurell and Frappier, 2006; Cao et al., 2017). It presented, in both species, the hepatic lobules with the sinusoids located among the laminae of hepatocytes, the central veins, the portal canals surrounded by lymph capillaries and the bile canaliculi. Hepatic lobules, in both species, were not separated from adjacent lobules by connective tissue septa, as it commonly occurs in pigs (Eurell and Frappier, 2006).

The liver lobules of the capybara had poorly-defined margins, in comparison with the hexagonal liver lobules of the guinea pig. This histological difference had been previously reported in the literature (Bhattacharjya et al., 2003; Cao et al., 2017)

The guinea-pig **pancreas**, unlike the capybara's, had a diffuse appearance and was widely distributed within the mesoduodenum. It was well-developed, triangular-shaped, and composed of a left lobe, lying transversally between the stomach and the spiral colon, a body in contact with the cranial curvature of the duodenum, and a right lobe lying along the descending duodenum. The classical U-shape of the pancreas of the guinea pig is similar to that seen in

dogs and cats (König and Liebich, 2011). These findings are also in line with previous descriptions of this organ in the guinea pig (Breazile and Brown, 1976; O'Malley, 2005), but in contrast with a study from which it emerged that the guinea-pig pancreas consists of only two lobes, a cranial and a caudal lobe (Cozzi et al., 2006). The capybara pancreas, on the other hand, although still being incorporated in the mesoduodenum in contact with the greater gastric curvature, duodenal cranial curvature and descending duodenum, had better-defined margins, had a more compact appearance, and was divided into a head, a body and a tail. The opening of the pancreas into the duodenum in the two species has not been evaluated in this study; according to the consulted literature, however, the guinea pig pancreatic duct either joins the common bile duct (Breazile and Brown, 1976), or, according to other authors (Cooper and Schiller, 1975b; Cozzi et al., 2006), it drains separately in the duodenum distally to the common bile duct. In the capybara, the pancreatic duct has been reported to empty into the duodenum through a distinctive papilla of the common bile duct, below its opening (Percegon et al., 2004).

Histologically, the pancreatic lobules, separated by connective tissue stroma, was composed of exocrine acini, with pancreatic intralobular ducts lined by a cuboidal epithelium, and of endocrine Langerhans islets, with poorly delimited borders, analogously to other domestic species (König and Liebich, 2011). The pancreatic lobules were more distinctly demarcated by connective tissue in the guinea pig than they were in the capybara. The histological findings in the capybara are in accordance with previous studies carried out in this species (Percegon et al., 2004), whereas the literature regarding the histological organization of the guinea-pig pancreas is scarce.

The anatomical morphological and morphometric study of the **abdominal aorta** and its collaterals in the guinea pig and capybara was conducted by employing the polyurethane foam casting technique, developed at the Veterinary Normal Anatomy Unit of the Department of Veterinary Medical Sciences of the University of Bologna (De Sordi et al., 2014) and might prove useful as a basic anatomical aid to various clinical branches regarding these exotics mammals of increasing veterinary interest, such as clinical medicine, surgery, diagnostic imaging and pathological anatomy. In the literature, similar anatomical studies were found; however, they are dated, often conflicting or incomplete, and lacking morphometric data (Potter et al., 1958; Perneczky, 1969; Shively and Stump, 1975; Shively and Stump, 1976; Maženský and Flešarova, 2017; Ibáñez Orihuela et al., 2019); moreover, a comparative anatomical study between the two species has not been carried out yet.

The distribution of the abdominal and pelvic arteries of the guinea pig and capybara showed some similarities with that of other domestic mammals, however with some exceptions.

In all the guinea pigs studied, in accordance with reports by Shively and Stump (1975) and Bednářová and Malinovský (1990), a celiacomesenteric trunk was observed, whereas the celiac and cranial mesenteric arteries originated separately in the capybara, in accordance with a previous study by Ibáñez Orihuela et al. (2019). Contrary to what happens in the guinea pig, the celiac and cranial mesenteric arteries have separate origins in most domestic mammals, such as carnivores, equidae, ruminants and pigs (Schaller, 1999; Barone, 2006b), but also in other exotic mammals such as the chinchilla (Özdemir et al., 2013), which also is a hystricomorph rodent, and the rabbit (Abidu-Figueiredo et al., 2008). Similarly, to the guinea pig, the presence of a celiacomesenteric trunk is also found in other species such as cetaceans, some bats and some insectivores like the hedgehog (Barone, 2006b). Furthermore, other reports indicate the frequent finding (40%) of a celiacomesenteric trunk in the sheep (Langenfeld and Patea, 1977), and a single described case of the presence of a celiacomesenteric trunk in humans (Çiçekcibaşı et al., 2005).



The guinea-pig **celiacomesenteric trunk** originated from the abdominal aorta at an average distance from the diaphragm of 5.15 mm in correspondence of T12 to L2, whereas the celiac artery and the cranial mesenteric artery of the capybara originated from the ventral aspect of the abdominal aorta about 13 cm and 14.5 cm, respectively, behind the diaphragm. As for the origin of the celiacomesenteric trunk, Bednářová and Malinovský (1990) roughly bring it back to the level of the stomach, whereas other authors do not report this data (Shively and Stump, 1975). No morphometrical data have been reported in the literature regarding the origin of these vessels in the capybara (Ibáñez Orihuela et al., 2019). The origin of the celiac artery has been reported to occur between the twelfth thoracic vertebrae and the first lumbar vertebra in the rabbit (Abidu-Figueiredo et al., 2008) or between the pillars of the diaphragm, at the level of the first lumbar vertebrae, in carnivores (Barone, 2006b; Evans and De Lahunta, 2013), which are in line with our guinea pig findings, whereas the capybara seems to have a more caudal origin of the two vessels in comparison with other mammals.

In the capybara, the **celiac artery** trifurcated into the splenic artery, which continued as left gastroepiploic artery in the greater omentum, the left gastric artery, and the hepatic artery, analogously to what has been reported for humans, equidae and carnivores (Barone, 2006b) and what has been reported for this species by previous authors (Ibáñez Orihuela et al., 2019). In the guinea pig, on the other hand, five different modes of branching of the celiac component of the celiacomesenteric trunk (CT) were observed. In most cases, the CT first emitted the gastrosplenic artery at a distance of  $8.07 \pm 1.54$  mm from the aorta, which gave rise to the left gastric and splenic arteries, and, subsequently, at a distance of  $2.88 \pm 1.70$  mm from the latter, it detached the hepatic artery. In some cases, the gastrosplenic artery contracted anastomosis with the abdominal aorta cranially to the origin of the CT; this occurrence has also been observed by Shively and Stump (1975) in a minority of cases. Shively and Stump (1975), moreover, report that the gastrosplenic artery in the guinea pig originated at a distance of about 10 mm from the aorta and, about 2 mm after this, the hepatic artery originated; it follows, therefore, that the values found in this study are almost in line with what was reported by the aforementioned authors. The other patterns of the branching of the CT include the gastrosplenic artery originating from the abdominal aorta, with the CT emitting the hepatic artery, and the gastrosplenic and hepatic arteries originating from the confluence of a common trunk (referred to by Shively and Stump, 1975 as “celiac artery”) detached from the CT; finally, the gastrosplenic artery being absent with the CT giving rise to the splenic artery and, subsequently, to a common trunk which, in turn, gives rise to the left gastroepiploic and the left gastric arteries. This latter occurrence has not been reported in the literature, whereas the other patterns have been described (Shively and Stump; 1975; Bednářová and Malinovský, 1990). As for the division patterns of the gastrosplenic artery, in the majority of cases, it divided into the left gastric artery and the splenic artery. This first pattern was observed by Shively and Stump (1975) in 54.20% of subjects and by Perneckzy (1969) in 53.30% of cases. In the chinchilla, the presence of a gastrosplenic artery has been reported. In this species, in fact, the celiac artery divides into four branches: the left gastric, the hepatic, the splenic, and the gastrosplenic arteries (Özdemir et al., 2013).

In humans, equidae and carnivores, however, the celiac artery trifurcates into the splenic artery, the left gastric artery and the hepatic (Barone, 2006b), analogously to the capybara of the present study. In the rabbit, on the other hand, the celiac artery first emits the splenic and then the left gastric artery, which gives off the hepatic artery (Abidu-Figueiredo et al., 2008). In the literature, it has been reported that the left gastric artery originates from the celiac artery in ruminants, equidae, carnivores (Barone, 2006b) and chinchillas (Özdemir et al., 2013), analogously to the capybaras of the present study, whereas it takes origins from the splenic artery in pigs, and from the hepatic artery in rabbits (Barone, 2006b); contrary to what happens

in the previously mentioned species, in the guinea pig, the left gastric artery derives from the gastrosplenic artery.

In 38.9 % of cases, guinea pigs presented two left gastric arteries originating from the gastrosplenic, whereas all capybaras presented a single left gastric artery. Our finding in the guinea pig is confirmed by a previous study by Bednářová and Malinovský (1990), who reported the presence of double left gastric arteries in this species. Similarly to the guinea pig, also in carnivores sometimes the left gastric artery appears to be double, while in the rabbit it always divides into an anterior and posterior branches (Barone, 2006b). A peculiarity that was observed in one guinea pig was the presence of a right gastric artery originating from the gastrosplenic artery, instead of from the hepatic, which anastomosed with its left counterpart at the level of the lesser curvature of the stomach.

In the capybaras of the present study, the left gastric artery originating from the celiac, distributed to the lesser curvature of the stomach where it finally anastomosed with the right gastric artery originating from the hepatic artery, in accordance with what had previously been reported for this species (Ibáñez Orihuela et al., 2019)

Similarly to the guinea pig and capybara, also in carnivores and humans (Barone, 2006b), the right and left gastric arteries anastomose at the level of the lesser gastric curvature. However, in these species (Barone, 2006b), contrary to what happens in the guinea pig, but analogously to the capybara, a gastrosplenic artery has never been reported, and the left gastric artery originates from the celiac artery, while the right gastric artery always originates from the hepatic. In the rabbit, on the other hand, both the left gastric and the right gastric arteries originate from the hepatic artery; however, in this species, the right gastric artery does not contract direct anastomosis with the branches of the left gastric artery (Barone, 2006b).

In the guinea pig, the **hepatic artery** originated from the CT independently or from a common trunk with the gastrosplenic artery. In the majority of cases, the common hepatic artery emitted the cystic artery, followed by the proper hepatic artery, the right gastric artery, and continued as gastroduodenal artery, which terminated by bifurcating into the right gastroepiploic which anastomosed with the left counterpart coming from the splenic artery at the greater gastric curvature, and the cranial pancreaticoduodenal artery. The origin of the hepatic artery in the guinea pig has been reported to occur from the CT (Shively and Stump, 1975; Bednářová and Malinovský, 1990), analogously to the present study, from the gastrosplenic artery (Bednářová and Malinovský, 1990) or from a so-called celiac artery, which gives origin to the hepatic and gastrosplenic arteries (Shively and Stump, 1975).

These data regarding the hepatic artery of the guinea pig are partially in accordance with previous reports by Shively and Stump (1975), who, however, report that the hepatic artery, right before branching into the hepatic hilum, emit the right gastric artery and the cystic artery, whereas Bednářová and Malinovský (1990) report the presence of a hepatomesenteric trunk deriving from the celiacomesenteric trunk, that emits a common hepatic artery which, before reaching the hepatic hilum, detaches the proper hepatic artery and the right gastric artery. Similarly to our findings, also according to Bednářová and Malinovský (1990), in the guinea pig, the common hepatic artery continues as gastroduodenal artery, which ends by bifurcating into the right gastroepiploic artery and into the cranial pancreaticoduodenal artery.

In the capybara, the hepatic artery originated from the celiac artery in all instances, and then gave off the pancreatic arteries, the cranial pancreatic duodenal artery, the right gastric artery, and the gastroduodenal artery, which, in turn, emitted the right gastroepiploic that anastomosed with its left counterpart at the level of the greater curvature of the stomach. Unlike

the guinea pig, therefore, where the cranial pancreatic duodenal artery originates from the gastroduodenal artery, these vessels directly originate from the hepatic artery in the capybara. The origin of the cranial pancreatic duodenal artery in the capybara has not been reported for this species in previous studies (Ibáñez Orihuela et al., 2019) The cranial pancreaticoduodenal artery, in both species, anastomosed with the caudal pancreaticoduodenal originating from the cranial mesenteric artery, which, in the guinea pig, represents the direct continuation of the celiacomesenteric trunk. The right gastroepiploic originating from the gastroduodenal, and the left gastroepiploic, originating from the splenic, in both species anastomose at the level of the greater gastric curvature.

In the capybara, the hepatic artery entered the hepatic hilum by branching off into a right and left hepatic arteries. This same occurrence was not observed in guinea pigs. Unlike the guinea pig, but in accordance with the capybara, in the chinchilla, the hepatic artery originates from the celiac artery and first detaches a left lateral branch, then a left medial branch and, finally, a right branch destined for the liver parenchyma (Özdemir et al. 2013). In the chinchilla, the gastroduodenal artery and the right gastroepiploic artery originate from the right gastric artery (Özdemir et al. 2013); this data are in contrast with our findings in the guinea pig and capybara, where the gastroduodenal artery represented the continuation of the hepatic artery, while the right gastroepiploic artery represented the termination of the gastroduodenal artery.

The celiacomesenteric trunk of the guinea pig, after detaching the hepatic artery, continued as the **cranial mesenteric artery**, in line with what was reported by Shively and Stump (1975) for the guinea pig. The cranial mesenteric artery of the guinea pig emitted, in succession, the middle colic artery, the caudal pancreatic duodenal artery, the right colic artery, 5 to 10 jejunal arteries, and then continued as ileocolic artery.

In the capybara, on the other hand, the cranial mesenteric artery originates from the aorta, instead of from the CT, like in guinea pigs, and gives off the caudal pancreatic duodenal artery, which anastomosed with its cranial counterpart, the right colic, the middle colic, two cecal branches, ileal arteries, and a common jejunal trunk, which gives rise to multiple jejunal arteries, and continued as ileocolic artery. Our findings in the capybara partially differ from those previously reported in the literature for this species (Ibáñez Orihuela et al., 2019), especially in the sequential order of the collaterals emitted by the cranial mesenteric artery. Specifically, according to these authors, the cranial mesenteric artery emits, in order, the caudal pancreatic duodenal, the jejunal arteries, the ileocolic artery and finally the right and middle colic arteries; therefore, the ileocolic artery is not considered by the cited authors to be the continuation of the cranial mesenteric, and the right and middle colic arteries are emitted at its termination instead of towards its initial portion, as it was seen to occur in the capybaras (and guinea pigs) studied.

In the guinea pig, the middle colic artery, originated from the cranial mesenteric artery and directed towards the ascending, spiral and transverse colon, anastomosed with the left colic artery, originating from the caudal mesenteric artery, at the level of the descending colon. Shively and Stump (1975), on the other hand, report that, in the guinea pig, the middle colic artery, coming from the cranial mesenteric artery, anastomoses with the colic artery, continuation of the ileocolic artery. The middle colic artery in the rabbit and in humans, originates from the cranial mesenteric artery, after this detaches the caudal pancreaticoduodenal artery (Barone, 2006b); in the guinea pig, on the other hand, the middle colic artery originated before the caudal pancreaticoduodenal artery. These reports, however, are in line with what was observed in the capybaras of our study, where the middle colic artery originated after the emission of the caudal pancreaticoduodenal. In the guinea pigs observed, the cranial mesenteric artery originated, subsequently, the caudal pancreaticoduodenal artery, which ran in the mesoduodenum to supply the right lobe of the pancreas and the proximal duodenum, to finally anastomose with the cranial homologue, similarly to what has been described for the others

domestic mammals (Barone, 2006b) and for the guinea pig (Shively and Stump, 1975), as well as to what was seen in the capybaras under study. It has been observed that, in two guinea pigs, the caudal pancreaticoduodenal artery originated from the first jejunal artery; this exception has not been reported in the literature, and it was not observed in the capybara. The cranial mesenteric artery of the guinea pig then detached, at the level of the first jejunal arteries, the right colic artery, directed to the ascending colon. This data is in agreement with what Shively and Stump (1975) reported in the guinea pig, which, however, also report a case in which the right colic artery originated from a common trunk with the middle colic artery. In the capybara, on the other hand the right colic artery originated from the cranial mesenteric artery before the emission of the common jejunal trunk giving rise to the jejunal arteries. In two guinea pigs, the right colic artery appeared to be double. This finding is in agreement with what Barone (2007) reported for ruminants and rabbits; however, this has not been reported for the capybara, nor was observed in the subjects of our study. In carnivores, ruminants and rabbits, however, the right colic artery originates from the ileocolic artery (Barone, 2006b). Contrary to these reports, in the capybaras of our study, on the other hand, the right colic artery originated from the cranial mesenteric artery.

The cranial mesenteric artery, in the guinea pig, gave rise to a number of jejunal arteries that ranged from a minimum of 5 to a maximum of 10, with 7 being the average number of branches; the first jejunal artery originated at the same level as the right colic artery. This range of variability, in the guinea pig, is more in line with that reported by Shively and Stump (1975), between 4 and 9. It differs more from that reported for the guinea pig by Luther (1923), Favre (1967) and Pernecky (1969), ranging from a minimum of 10 to a maximum of 12 jejunal arteries. In the capybaras of our study, a mean number of 10 jejunal arteries was counted. The number of jejunal arteries in the capybara has not been previously reported in the literature (Ibáñez Orihuela et al., 2019)

The cranial mesenteric artery, after detaching the jejunal arteries, continued, in both species, as the **ileocolic artery** destined for the large intestine. The well-developed cecum of the guinea pig and capybara was irrigated by multiple caecal branches originating from the ileocolic artery. Specifically, in the guinea pig, the ileocolic artery provided several branches for the apex, body and base of the caecum, detached several ileal branches and ended by bifurcating into the branch for the base of the cecum directed to the mesenteric edge of the organ, and the colic branch of the ileocolic artery. The results of the present study are in line with those reported by Shively and Stump (1975) for the guinea pig, who reported the presence of a branch for the apex of the caecum, from one to three branches intended for the body of the cecum and two or three other branches intended for the base of the cecum. In the capybara, the ileocolic artery gave off a branch for the proximal colon, and terminated by bifurcating into an ileal artery and a voluminous caecal artery destined for the base of the cecum. In the guinea pig, the termination of the ileocolic consists of a large vessel destined for the base of the cecum, as well. The detailed description of the termination of the ileocolic artery in the capybara has not been provided in the consulted literature (Ibáñez Orihuela et al., 2019). In rabbits, a species characterized by a well-developed cecum, two main caecal arteries are present: the dorsal caecal artery, which originates at the height of the middle colic artery, and the ventral caecal artery (Barone, 2006b). The ileocolic artery, in the rabbit, ends by bifurcating into a voluminous ventral caecal artery and in the colic branch of the ileocolic (Barone, 2006b). The colic branch of the ileocolic is referred to by Shively and Stump (1975) as the colic artery, which runs along the ascending colon and anastomoses with the right and middle colic arteries. It was considered more correct in our case to refer to it as colic branch of the ileocolic artery, in line with the nomenclature used by Barone (2007), to indicate the vessel destined for the initial part of the ascending colon in all species.

The right and left adrenal glands of the guinea pig were perfused by the **adrenal arteries** of the corresponding side, which originated from the corresponding cranial renal artery at various

levels or, in a minority of cases, directly from the abdominal aorta cranial to the origin of the renal arteries. In accordance with the results of the present study, Shively and Stump (1975) describe, in the guinea pig, the presence of three or four thin adrenal branches that can originate from the renal artery, from the cranial abdominal artery or from the caudal phrenic artery of the corresponding side. In the capybara, the voluminous adrenal glands were vascularized by the caudal phrenic artery, originating from the abdominal aorta cranially to the origin of the celiac artery, or by adrenal arteries originating from the renal arteries. The vascularization of the adrenal glands of the capybara has been scarcely studied, and the presence of adrenal arteries has not been previously reported in the literature for this species (Ibáñez Orihuela et al., 2019). In domestic mammals of veterinary interest, with the exception of the horse, the cranial pole of the adrenal gland receives blood from the cranial adrenal branches, which originate from the corresponding caudal phrenic artery; the caudal pole, on the other hand, is supplied by the caudal adrenal branches coming from the corresponding renal artery. Furthermore, in carnivores and ruminants, the presence of accessory adrenal branches originating from the lumbar arteries, the celiac artery or the cranial abdominal artery has been reported (Barone, 2006b). Therefore, the adrenal arteries originating from the renal arteries in the guinea pigs of the present study likely correspond to those that Barone (2007) identifies as caudal adrenal branches; in fact, like these, they are headed dorsocaudally towards the caudal pole of the adrenal gland. Differently, in those cases in which the adrenal arteries derived from the caudal phrenic artery, originating from the aorta, cranial to the kidney, it is likely that they correspond to those which Barone (2007) defines cranial adrenal branches; this last occurrence is applicable also to the capybara adrenal arteries.

The **renal arteries** of the guinea pig, originating in correspondence of the second/third lumbar vertebrae, were found to be single, double or even triple in the guinea pigs studied. Unlike the guinea pig, they were found to be single on both sides in all the capybaras studied, which is in line with a previous study carried out in this species (Ibáñez Orihuela et al., 2019). Regarding the renal arteries of the guinea pig, Potter et al. (1958) had described the presence of single renal arteries, while Luther (1923) and Favre (1967) had observed the presence of double renal arteries, one cranial and one caudal, on both sides. According to Perneczky (1969), Shively and Stump (1975), and Mažensky and Flešarova (2017), on the other hand, the renal arteries could have a single or double origin on both sides. The presence of a third renal artery, however, has never been reported for this species in the literature. The occasional presence of an accessory renal artery on one or both sides has been reported for domestic (Barone, 2006b) and wild mammals, such as the nutria (Culau et al., 2008). The presence of double renal arteries has also been reported in rabbits by Supuka et al. (2014), with the left renal artery being more frequently double than the right. In our study on guinea pigs, on the other hand, the right renal artery was found to be double in the majority of cases.

Each renal artery, in both species, divided into a lateral and a medial branch at the level of the organ hilum. This finding is in accordance with what Shively and Stump (1975) reported for the guinea pig; the division into two branches is in line with what is traditionally described for other domestic mammals such as the dog and the cat (Barone, 2006b).

In the guinea pig, the left renal arteries were found to be, on average, larger in diameter than the corresponding right ones, and, in case of double renal arteries, the cranial branch was always larger than the caudal. Similarly, in the rabbit (Santos-Sousa et al., 2015), it was found that the left renal artery was larger than the right. The more cranial origin of the right renal artery compared to the left, seen in both species studied, is also a common finding in other species, such as the rabbit, the hamster, the nutria (Barone, 2006b; Santos-Sousa et al., 2015) and other mammals (Barone, 2006b).

In the guinea pig, the renal arteries originated in correspondence of the second/third lumbar vertebrae. This finding is in accordance with previous studies in the guinea pig (Mažensky and Flešarova, 2017) who locate it between T13 and L2, and in rabbits, where it is described to occur between L2 and L3 (Supuka et al., 2014). According to Barone (2007), the renal arteries emerge at the level of the first lumbar vertebrae in equidae and humans, at the level of the second in dogs and rabbits, and at the level of L3 in ruminants, pigs and cats. The capybara kidneys originated from the abdominal aorta about 14 mm caudally to the emission of the cranial mesenteric artery; therefore, although not assessed in the present study, it can be implied that their origin occurs around L2, in accordance with reports in dogs and rabbits (Barone, 2006b), and of the guinea pigs of the present study.

The paired **ovarian arteries** of the guinea pig originated, symmetrically, at the level of the third lumbar vertebra, from the sides of the abdominal aorta, caudal to the renal arteries in the majority of females; in one instance, the right ovarian artery originated between the right cranial and caudal renal arteries, and, in another case, both ovarian arteries originated from the caudal renal arteries. This data confirms what is reported in the literature for the guinea pig, that is, the origin of the ovarian arteries from the aorta, caudally to the renal arteries or, occasionally, cranial to the caudal renal arteries (Luther, 1923; Favre, 1967; Shively and Stump, 1975). Shively and Stump (1975) report that the ovarian arteries in the guinea pig, can originate both from the aorta and from the renal arteries. Potter et al. (1958), on the other hand, reported, as the sole origin of the ovarian arteries, the renal arteries themselves, in the guinea pig. In the capybara, which presented only single renal arteries, the ovarian arteries originated from the aorta just caudally to the renal arteries of the corresponding side, analogously to the guinea pig; the origin of the ovarian arteries from the renal arteries was not evidenced in the animals studied. According to Ibáñez Orihuela et al. (2019), the origin of the renal arteries in the capybara occurs in proximity of the caudal mesenteric artery; in the capybaras of our study, however, the origin of the renal arteries was cranial but distant from the origin of the caudal mesenteric artery. The origin of the ovarian artery in equidae, pigs, rabbits, ruminants and carnivores (Barone, 2006b), occurs at the level of the aorta, between the fourth and fifth lumbar vertebrae, near the origin of the caudal mesenteric artery or slightly more cranially. Therefore, the origin of the ovarian arteries in both capybaras and guinea pigs has been seen to be more cranial than in other domestic mammals, at a greater distance from the caudal mesenteric artery. The ovarian arteries of the guinea pigs anastomosed, at the level of the broad ligament of the uterus, with the uterine branch of the uterine artery. In the capybara, the ovarian arteries irrigated the ovary and then, through uterine branches, they coursed towards the horns, body and cervix of the uterus to finally anastomose with the branches of the caudal uterine artery originating from the internal iliac artery; these findings are in accordance with previous reports in this species (Ibáñez Orihuela et al., 2019), except for the origin of the uterine artery which, according to the aforementioned authors, occurs from the common iliac trunk before its bifurcation into external and internal iliac arteries, instead of from the internal iliac artery as seen in our study. In the guinea pigs of our study, analogously to our findings in the capybaras, the uterine artery originates from the urogenital artery, derived from the internal iliac artery. The uterine artery, in less prolific species such as equidae, ruminants and humans, contracts thin anastomoses with the uterine branches of the ovarian and vaginal arteries. In the most prolific species such as pigs, carnivores and rabbits, broad ligament anastomoses are more developed (Barone, 1994); this is also in line with what was observed in the capybaras of the present study. However, it must be remembered that, in carnivores, the uterine artery is absent and, therefore, the uterine branch of the ovarian artery contracts anastomoses with the uterine branch coming from the vaginal artery (Barone, 2006b).

The paired **testicular arteries** of the guinea pig originated from the abdominal aorta, caudally to the renal arteries, in the majority of cases, or cranially to the corresponding renal artery or to the ipsilateral caudal renal arteries. Shively and Stump (1975), in line with what was observed in this study, report that the testicular arteries, in the guinea pig, originate from the abdominal aorta caudal to the renal arteries and, occasionally, cranially to the caudal renal arteries. In the capybara, on the other hand, the testicular arteries were always seen to originate caudally and in proximity to the emission of the renal arteries and cranially to the emission of the caudal mesenteric artery; this finding is in contrast with what Ibáñez Orihuela et al. (2019) reported for this species, that is, the origin of the testicular arteries in proximity of the caudal mesenteric artery. Analogously to what has been said regarding the ovarian arteries, the origin of the testicular arteries in the guinea pig and capybara is more cranial when compared to that of other domestic mammals (Barone, 2006b).

The unpaired **caudal mesenteric artery** of the guinea pig originated from the ventral aspect of the aorta, at an average distance of 20.4 mm from the emission of the CT and ended by bifurcating into the **left colic artery**, directed to the descending colon, which ended by anastomosing with the middle colic artery, and a **cranial rectal artery**, directed to the rectum. These data are in accordance with previous reports in the guinea pig (Shively and Stump, 1975), according to which

the caudal mesenteric artery originates at an average distance of 25 mm from the CT, and subsequently divides into left colic and cranial rectal arteries.

The **caudal mesenteric artery** of the capybara originated from the aorta, approximately 42 mm caudally to the emission of the testicular or ovarian arteries, and gave off the left colic artery, which anastomosed with the middle colic artery, and the cranial rectal artery, which ended by anastomosing with the caudal rectal artery. This distribution is in accordance with previous reports in this species (Ibáñez Orihuela et al., 2019) and with our findings in the guinea pig. Also in carnivores, pigs and ruminants, the caudal mesenteric artery bifurcates into the left colic artery, which anastomoses at the level of the descending colon with the middle colic artery, and in the cranial rectal artery, which is directed towards the colon or the rectum, depending on the species (Barone, 2006b).

In contrast to what we observed in the guinea pig and capybara, however, it has been reported for the guinea pig, that the left colic and the cranial rectal arteries end by anastomosing with the colic artery, originating from the ileocolic artery, at the level of the descending colon (Shively and Stump, 1975); the colic artery corresponds to the colic branch of the ileocolic artery.

In one guinea pig, a double left colic artery was evidenced in one case. The presence of a double left colic artery has not been previously reported in the literature regarding the guinea pig, the capybara, or the other domestic mammals (Shively and Stump, 1975; Barone, 2006b; Ibáñez Orihuela et al., 2019).

The caudal mesenteric artery emerged at the level of L3-L5. In other domestic mammals, the emergence of the caudal mesenteric artery, according to Barone (2007), is located between the fourth and sixth lumbar vertebrae, depending on the species, therefore more caudally than the guinea pig.

The abdominal aorta, in the guinea pig, at an average distance of 25.9 mm from the caudal mesenteric artery, terminated by bifurcating into the right and left **common iliac arteries**, which, in turn divided into an internal and an external iliac artery. The **median sacral artery** originated at the level of the aortic bifurcation into the common iliac arteries, from its dorsal aspect. The bifurcation of the aorta into the common iliac arteries occurred at the level of L7-S1. This finding is in line with what was reported by other authors for the guinea pig (Potter et al., 1958; Favre, 1967; Shively and Stump, 1976); conversely, however, Popesko et al. (1992), report that the

guinea-pig aorta ends by bifurcating into the common iliac arteries, but the presence of external iliac arteries is not reported.

In the capybara, similarly, the terminal bifurcation of the abdominal aorta into the right and left common iliac arteries occurred about 55 mm caudally to the emission of the caudal mesenteric artery and, after approximately 30 mm, each common iliac artery bifurcated into the external and internal iliac arteries. The median sacral artery in this species arose from the dorsal surface of the aorta before its bifurcation into the common iliac arteries, therefore more cranially than in the guinea pigs of our study. These data are in accordance with what has been previously reported for the capybara (Ibáñez Orihuela et al., 2019); these authors, moreover, specified that the final bifurcation of the aorta in this species occurs at the level of L6 or L7. Unlike what was observed in the guinea pig, but similarly to what has been reported for the capybara (Ibáñez Orihuela et al., 2019), in other domestic mammals (Barone, 2006b), the bifurcation of the aorta occurs at the level of the last or penultimate lumbar vertebrae, depending on the species and, therefore, more cranially than in the guinea pig. In humans and rabbits, the internal and external iliac arteries of each side also originate from the common iliac arteries and, at the level of the bifurcation of the aorta, the median sacral artery detaches (Barone, 2006b). In carnivores, equidae and ruminants, on the other hand, the common iliac arteries are not present, but the aorta ends by dividing into five branches: it first emits the paired external iliac arteries, then the paired internal iliac arteries and, finally, an uneven and slender branch, the median sacral artery, which continues in the tail (Barone, 2006b). While in the guinea pig the median sacral artery was seen to originate at level of the bifurcation of the common iliac arteries, in the rabbit (Barone, 2006b), it originates from the aorta about one centimetre before its terminal bifurcation; this finding is more closely in line with what we observed in the capybaras of our study, where the median sacral artery originated from the aorta before its final bifurcation. In the others domestic mammals (Barone, 2006b), in which the common iliac arteries are not present, the median sacral artery originates at the point of separation of the two internal iliac arteries. In humans and equidae, on the other hand, the median sacral artery is vestigial (Barone, 2006b).

## CARDIOVASCULAR SYSTEM

The **heart** of the guinea pig and capybara was globoid in appearance, although more conical and laterally-flattened in the guinea pig in comparison with the capybara. In the guinea pig, it was seen to extend from the second rib to the fourth or fifth intercostal space, slightly more caudally than previously reported data (O'Malley, 2005). The cranio-caudal extension of the capybara heart, on the other hand, between the second intercostal space and the fifth intercostal space, is in accordance with previous reports (Magariños et al., 2018). Moreover, the guinea pig heart had a more pronounced ventrocaudal inclination over the sternum, in comparison with the capybara's. In both species, the heart was surrounded by a double-layer pericardium, as it had already been reported for both species (O'Malley, 2005; Magariños et al., 2018) with, however, the fibrous and the serous layers being very closely interconnected. The cardiac measurements previously reported in the literature for the guinea pig heart are partially in accordance with our findings. The long axis was, on average 2 cm, which are in line with the previously-reported 21 cm (Hoffmann, 1956); according to these authors, however, the maximum diameter at the heart base was 6 mm, which is in contrast with the 17 mm of our study, measured, however at the level of the maximum cranio caudal length perpendicular to the short axis. In the guinea pig, the right ventricular lumen and, in some instances, also the left, contained a well-developed septo-marginal trabecula. In the literature, however, the presence of these trabeculae in the guinea pig heart has been reported in the right ventricle only (Breazile and Brown, 1976; Hargaden and Singer, 2012). In the capybara, the ventricles were also seen to contain numerous carneous trabeculae, with the well-developed septo-marginal



trabecula being identified in the right ventricle only, which is in accordance with a previous study in this species (Magariños et al., 2018). The appearance of the internal walls of the capybara ventricles was peculiar and it resembled that of the pectinate muscles normally seen in the atria: this is probably ascribable to the presence of numerous septomarginal trabeculae interspersed among the well-developed papillary muscles, especially in the right ventricle, which had also been previously reported (Magariños et al., 2018).

As for the irrigation of the myocardium, from our study on capybara hearts, it emerged that it was vascularized solely by the **left coronary artery** and its collaterals: specifically, by the interventricular paraconal branch directed to the left ventricle, which then continued towards the caudal margin and gave off the right subsinusal branch. In all the animals studied, the right coronary artery was not evidenced. The atresia of the right coronary artery in the capybara has been seldom reported (Sejín et al., 2003). Other authors, on the other hand, state that the capybara heart is vascularized mainly by the well-developed left coronary artery and its branches, but also by the less-developed right coronary artery and its collaterals (Magariños et al., 2018). These authors, however, analogously to our findings, reported the noteworthy presence of large anastomoses among the branches of the left coronary artery (Magariños et al., 2018). The vascularization of the guinea-pig heart was not assessed in the present study; however, it has been reported that the guinea pig heart is irrigated by four main arterial vessels, which are the left circumflex branch and the paraconal interventricular branch, originating from the left artery, as well as by the right coronary artery and the right conus arteriosus branch (Vicentini et al., 1991). Therefore, it differs from what we observed in our study in the capybara, for the presence of a right coronary artery.

Histologically, the ventricular walls and the valves are lined internally by endothelium, myocardium and covered externally with the epicardium. In the myocardium, abundant connective tissue containing vascular vessels was interspersed among the cardiac muscle cells. No noteworthy differences were evidenced between the two species, or with the histological organization of the cardiac muscle seen in other species (Eurell and Frappier, 2006).

As for the **large vessels**, the large arteries, such as the aorta, and the large veins, such as the caudal vena cava, were histologically evaluated in both species. For the macroscopical study of the abdominal aorta and its collaterals in the two species, please see the section dedicated to the gastrointestinal system. Histologically, the aorta, in both species, being an elastic artery, was characterized by a prominent tunica interna (intima), with a thick subendothelial layer of collagen, elastic fibers, and smooth muscle cells. The thickest tunic, however, was the tunica media composed of layers of smooth muscle cells interspersed with abundant elastic laminae that predominate. The adventitia consisted in longitudinally-arranged bundles of collagen and elastic fibers. The histological organization of an elastic artery such as the aorta corresponds to the typical pattern seen in other domestic species (Eurell and Frappier, 2006). In the caudal vena cava, the predominant tunica, on the other hand, was the tunica externa, containing many bundles of longitudinally-oriented smooth muscle, together with elastic fibers. No noteworthy differences were evidenced between the two species regarding the histological organization of the arteries versus that of the veins, which showed the typical differences also seen in other domestic animals (Eurell and Frappier, 2006).

## URINARY SYSTEM

The guinea pig and capybara **kidneys** were, in both cases, elongated and with a more oval, bean-like shape in the guinea pig, with an elliptical shape in the capybara; these data are

in line with those previously reported for each species (Resoagli et al., 2009; Hargaden and Singer, 2012), but in contrast with Yousif (2019)'s report that the guinea pig left kidney is heart-shaped. The measurements of the length and width of the guinea pig kidneys in our study, which are, respectively, 20.1 mm, and 12.7 mm, with the left kidney slightly more voluminous than the right, are in line with what has been previously reported in the literature for this species, that is 18-21 mm for the length, and 12-14 mm for the width (Hargaden and Singer, 2012). The capybara kidneys weighed, on average, 67 grams for the right one, and 85 grams for the left; the mean length of the capybara right kidney was 11.6 cm, the mean width 4.9 cm, and the mean height 2.6 cm; the left kidney measured 12.3 cm in length, 5.3 in width, and 2.7 in height; in this species as well, analogously to the guinea pig, the left kidney was slightly more voluminous than the right. No morphometrical data regarding the capybara kidneys were found in the consulted literature. The topography of the guinea pig kidneys, located retroperitoneally at the level of L2 for the right kidney, and L3 for the left, however, was slightly more caudal than that previously reported (T12-L3) (Cooper and Schiller, 1974). The similar topography of the capybara kidney, retroperitoneal, at the level of the first two lumbar vertebrae, is the same as that previously described for this species (Resoagli et al., 2009). In any case, the right kidney was located more cranially than the left in both the guinea pig and the capybara, which is in accordance with the topography seen in most other domestic mammals and rodents (Cozzi et al., 2006; Barone, 2006b). The paired adrenal glands were located craniomedially (in the guinea pig), or medially (in the capybara) to the corresponding kidney. The guinea pig and capybara kidneys were, in both cases, found to be unipapillar with a large renal pelvis and a single longitudinal renal papilla. These findings are in line with previous reports for these species (Sejín et al., 2003; Queesenberry et al., 2004), as well as with the renal anatomy of other rodents such as rats, mice, rabbits (Cozzi et al., 2006), and domestic carnivores such as dogs and cats (König and Liebich, 2011). The guinea pig kidneys were seen to be vascularized by single, double, or even triple renal arteries on each side, with the triple pattern never been observed previously in the literature (Pernecky, 1969; Shively and Stump, 1975, Mažensky and Flešarova, 2017). In the capybara, a single right and left renal artery was evidenced in all the animals studied; in this species, the presence of double renal arteries has not been reported before (Ibáñez Orihuela et al., 2019). The occasional presence of an accessory renal artery on one or both sides has been reported for domestic mammals (Barone, 2006b), including the rabbit (Supuka et al., 2014), and wild mammals, such as the nutria (Culau et al., 2008). Macroscopically, the kidney, in cross-section, had distinct outer cortex that appeared darker and lighter inner medulla, in a ratio of approximately 1: 1. This finding is in line with previous studies in the guinea pig kidney (Yousif, 2019). Histologically, the renal structure of the kidneys, in both species, resembled that classically described in the other domestic mammals (Eurell and Frappier, 2006; König and Liebich, 2011) and laboratory rodents (Cozzi et al., 2006). The renal parenchyma was composed of well-demarcated outer cortex and inner medulla in both species. The cortex consisted of cortical lobules delimited by interlobular arteries, containing well-recognizable renal corpuscles intermingled among numerous transversally or longitudinally-cut proximal and distal convoluted tubules. In the renal corpuscle, the glomerulus was surrounded by the glomerular capsule and presented a visible macula densa of the iuxtaglomerular apparatus located at the vascular pole of the renal corpuscle. The medullary rays containing long, straight tubules were visible in the cortical labyrinth. The histological structure of the kidney in these species is confirmed by previous studies carried out in the capybara (Sejín et al., 2003) and the guinea pig (Yousif, 2019).

The gross and microscopic anatomy of the **ureters** and **urinary bladder** did not present substantial differences with the other domestic species (König and Liebich, 2011). The ureters of both species had a lumen with a stellate appearance, due to the folds of the mucosa, in accordance with previous studies in the guinea pig (Yousif, 2019), whereas, in the capybara the

literature regarding the normal histological appearance of the urinary bladder and ureters is scarce. The ureters consisted of four tunics (mucosa, lamina propria submucosa, muscularis and serosa), with the mucosa lined by transitional epithelium, as seen in other domestic mammals (Eurell and Frappier, 2006). The urinary bladder of both species presented a mucosa characterized by extensive folds, especially in the capybara, and lined with transitional epithelium, that appeared more flattened than in the ureters. The guinea pig had a pear-shaped bladder and entirely located in the pelvic cavity, as previously reported for this species (Hargaden and Singer, 2012). The guinea pig bladder mucosa seemed to lack a trigone at the level of the opening of the ureters, as usually seen in other species (König and Liebich, 2011), which is in accordance with previous reports in this species (Hargaden and Singer, 2012).

## MALE GENITAL SYSTEM

The **testes** were located in a scrotum that, in the case of the capybara, was poorly-developed and not as obvious as that of the guinea pig. The well-developed epididymis was well developed, located on the dorso-lateral surface of the testis, and composed of a distinguishable head, body and tail. In both species, the inguinal canals were widely open, as it occurs in other species such as the rabbit, the rat (Cozzi et al., 2006) and the chinchilla (Spotorno et al., 2004). A cartilaginous *os penis* was evidenced in both the male guinea pig and capybara; this structure is also present in other species such as the rat and mouse (Cozzi et al., 2006), and the dog (Barone, 2006b). The penis was S-shaped in both species, and, in the guinea pig, it presented white spurs on the glans surface.

The peculiarity of the male genital system of these species stands in the great development of the **accessory sexual glands**, in the guinea pig especially. These were only two in the capybara: the well-developed vesicular glands and the prostate, which were identified in all the animals studied. In the guinea pig, on the other hand four accessory glands were identified in all animals, as previously described in the literature (Cooper and Schiller, 1975a): the well-developed and well distinguishable paired seminal vesicles, with a similar appearance to those seen in the capybara, although more developed in the guinea pig, were seen in all animals studied. The prostate gland and coagulating glands were in close contact, with poorly demarcated limits, with the coagulating glands having a more cranio-lateral topography. A prostate gland was identified in all subjects, located at the base of the seminal vesicles. In the chinchilla, on the other hand, it has been reported that the presence of a prostate gland is variable (Spotorno et al., 2004). The well-developed bulbourethral glands were recognizable, lobulated, and located caudally to the prostate gland and dorsally to the pelvic urethra. Some differences occur with other similar rodents and lagomorphs: unlike the guinea pig, in the chinchilla (Spotorno et al., 2004) and in the rabbit (Cozzi et al., 2006), the coagulating glands are absent. The rat, on the other hand, presents an additional accessory gland, that is not present in the guinea pig: the preputial gland (Cozzi et al., 2006).

The presence, in the guinea pig (but not in the capybara), of a penile intromittent sac (sacculus urethralis) located within the penis below the urinary meatus, which everts during copulation, is typical of this species (Cooper and Schiller, 1975a) and has also been reported in another caviomorph rodent, the chinchilla (Spotorno et al., 2004). When manually everted, two cartilaginous styles protruded from the intromittent sac of the guinea pig penis. These were also observed on histology. These have been extensively reported in the literature in the guinea pig (Cooper and Schiller, 1975a; Hargaden and Singer, 2012), although their function, not correlated with inducing ovulation in the female, is still to be clarified. These were not present in the capybara, nor have been described to occur in other domestic species, to the author's

knowledge. Extensive spurs distributed throughout the dorsal and ventral surface of the glans and intromittent sac were evidenced in the guinea pigs studied. Their role, however, unlike the cat, where they serve as a mechanism to induce ovulation (König and Liebich, 2011), is unknown.

Histologically, no noteworthy differences were evidenced between the capybara and guinea pig male genital systems, with the exception of cartilaginous structures within the penile urethra of the guinea pig, ascribable to the horny styles typical of this species, that were also evidenced macroscopically. The seminiferous tubules of the testes were lined with stratified spermatogenic epithelium, characterized by Sertoli and spermatogenic cells, as typically seen in other domestic species (Eurell and Frappier, 2006) and laboratory rodents (Cozzi et al., 2006). The histological appearance of the testes of a prepubertal male capybara was characterized by the presence of immature spherical primary spermatids in the lumen of the seminiferous tubules and the absence of Leydig cells in the wide intertubular compartment. In the adult guinea pig testes, on the other hand, Leydig cells were evidenced in the interstitium between seminiferous tubules. It has been reported that the peculiarity of the histological analysis of the capybara and guinea pig testes, is the abundance of Leydig cells and lymphatic tissue in the wide intertubular compartments, as opposed to canids and equids, for instance (Fawcett et al., 1973; Paula and Walker, 2013). The intertubular compartment was particularly abundant in the capybara testes, whereas in the guinea pig, it was not as well-developed, which is in contrast with the cited literature. The epididymis and deferent ducts, on histology, were lined by a pseudostratified columnar epithelium, with a greater amount of basal cells and shorter microvilli in the deferent ducts in comparison with the epididymis. In both tissues, the ductal lumen was filled with maturing spermatozoa. This organization does not differ from the typical histological architecture of these structures described in other species (Eurell and Frappier, 2006). The seminal vesicles, in both species, were lined by a pseudostratified columnar glandular epithelium; in the capybara, however the organ had a reticular, net-like appearance due to the presence of septa that subdivided the organ into well-delimited alveoli, which were not as well-demarcated in the guinea-pig vesicular glands. In both species, however, in line with the typical histological organization of this tissue, epithelial folds projected into the secretory alveoli (Eurell and Frappier, 2006).

## **FEMALE GENITAL SYSTEM**

The substantial macroscopic difference between the guinea-pig and capybara **uterus**, is the presence of a double cervix in the capybara, as opposed to the single cervix of the guinea pig. In both cases, however, the uterus is bicornate with well-developed elongated and V-shaped uterine horns. In another hystricomorph rodent, the chinchilla, two cervices have been described, analogously to the capybara (Spotorno et al., 2004). In the rat and rabbit as well, the uterus is bicornate with a double cervix having a double opening into the vagina (Cozzi et al., 2006). In contrast to the latter species, however, the capybara was seen to have a double cervix with a single opening into the vagina. In the mouse, on the other hand, the uterus is simple bicornate with a single cervix, analogously to the guinea pig (Cozzi et al., 2006). The guinea pig uterus, if compared to that of other domestic mammals of veterinary interest, closely resembles that of the dog, characterized by two long V-shaped horns, a uterine body, a single cervix, and a vagina (König and Liebich, 2011). The interior of the vagina, in both the guinea pig and capybara, presented longitudinal folds of the mucosa. Histologically, the uterine horns and body were lined by an endometrium with pseudostratified columnar cells that formed multiple mucosal folds and presented numerous uterine glands, especially in the capybara. The

myometrium was composed of two muscular layers separated by an intermediate vascular zone, which, in the capybara, was interspersed within the inner muscular layer. The uterine cervix, on the other hand, was lined by a simple columnar epithelium, with primary and secondary folds, and containing goblet cells and numerous submucosal venous plexuses; abundant mucus was evidenced in the lumen, demonstrating the mucous secretory activity of the epithelial cells.

In both species, the oval-shaped **ovaries**, dark pink-red in color and flattened dorsoventrally, were located caudolaterally to the corresponding kidney. They were completely covered by the ovarian bursa, analogously to the bitch (König and Liebich, 2011). Histologically, no substantial differences in the histological analysis of the ovary were evidenced between the two species or with other domestic mammals (Eurell and Frappier, 2006). In cross section, the different stages of development and regression of follicles and corpora lutea were identified in the ovarian cortex, including primary, secondary and tertiary follicles, atretic tertiary follicles, corpora lutea, and regressing corpora lutea.

## **LYMPHATIC SYSTEM**

### **SPLEEN**

The **spleen**, in both species, was located in the left cranial abdomen, on the left lateral surface of the greater curvature of the stomach and connected to it through the gastrosplenic ligament. It was proportionally more developed in the guinea pig, than it was in the capybara. The roughly triangular spleen of the capybara resembled, in terms of shape, that of horses, with the wider portion located cranially, at the level of the organ hilum. In the guinea pig, on the other hand, the spleen was elongated and slightly- oval shaped, and with rounded cranial and caudal poles, resembling more closely the spleen seen in species such as pigs, dogs and cats (König and Liebich, 2011). The spleen of the guinea pig is relatively large in comparison with most rodents and rabbits (O'Malley, 2005, Cozzi et al., 2006). In the guinea pig, the splenic margins were always found to be relatively smooth and continuous, with few shallow incisures, therefore the spleen in this species can be considered unilobed. This macroscopical description is in contrast with H Qasem et al. (2015), according to whom the guinea pig spleen margins are highly fissured, giving it an appearance that resembles more closely that of the capybara spleen. Indeed, unlike the guinea pig, the capybara spleen presented fissured margins, and 3 to 7 shallow marginal sulci were identified, especially on its dorsal edge, giving it a polylobed appearance. This finding is in line with Germinaro et al. (1997), reporting that the spleen of the capybara can either present unfissured continued margins, or it can be divided up to 7 lobes total. Our findings regarding the capybara spleen are in contrast with Makita et al. (1998)'s description of the presence of only two deep and sharp sulci on the dorsal edge of the organ, subdividing it into two portions from the rest of the body. In our case, the sulci were shallow and rounded, giving the capybara spleen tapered margins, instead of the presence of actual lobes separated from the rest of the splenic body. From our macroscopic study of the spleen in the two species, and from the comparison with the literature, therefore, it appears that the macroscopic appearance of the spleen can present large interindividual variability regarding the lobature and fissuration of the margins.

The histological architecture of the spleen in both species was in accordance with that classically described for other domestic mammal species (Cozzi et al., 2006; Eurell and Frappier, 2006; König and Liebich, 2011), with most of the splenic parenchyma consisting in the red pulp, composed of venous sinuses and splenic cords forming a reticular network, and in the white pulp, composed of lymphatic nodules and periarterial lymphatic sheaths. No

noteworthy differences were evidenced between the histological appearance of the splenic tissue in the two species.

In the young adult guinea pigs, aged approximately 1 year, a residue of **thymus**, embedded in abundant adipose tissue, was evidenced in the cranial mediastinum cranially to the heart (thoracic lobe) and extending to the ventral cervical region, near the thoracic inlet (cervical lobe). The paired cervical lobes of the thymus in young guinea pigs, are usually particularly developed and extending till the caudal angle of the mandible, according to previous studies (Cooper and Schiller, 1975a; O'Malley, 2005). On the other hand, the presence of a cervical thymic lobe has been reported to be inconsistent in pigs and ruminants, and rudimental in horses and carnivores (König and Liebich, 2011). A thymus was not observed in the capybaras of our study, and the literature regarding this lymphatic organ in this species is scarce.

## ENDOCRINE SYSTEM

The **adrenal glands** of the capybara and guinea pig were, in both species, particularly well-developed and proportionally voluminous in comparison with those usually observed in other domestic mammals (Cozzi et al., 2006). They were yellowish-brown in colour and slightly triangularly-shaped in the capybara, pyramidally-shaped in the guinea pig. They were embedded in adipose tissue and located craniomedially (in the guinea pig) or medially (in the capybara) to the corresponding kidney, in the retroperitoneal space. In cross section, the more developed lighter outer cortex was well demarcated from the darker inner medulla. Histologically, the capsule, the cortical layer (zona glomerulosa, intermedia, fasciculata, reticularis) and the medullar layers were all well distinguishable. In the cortex, the outermost zone was formed of cell clusters, analogously to ruminants and humans (Eurell and Frappier, 2006), instead of arches or columnar cells, as seen in horses, pigs and carnivores (Eurell and Frappier, 2006). This finding is in contrast with Abass (2017)'s report that the zona glomerulosa of the capybara adrenal gland consists of rounded or arched clusters of columnar cells near the capsule and cuboidal cells near the deeper layer. The well-represented zona fasciculata contained cells that were arranged in a radiating columnar or reticular manner and were separated by sinusoids; these cells appear vacuolated due to extraction of lipids during processing. The cells in the zona reticularis appeared as cords of polyhedral cells separated by sinusoidal capillaries. In the medulla, large columnar epinephrine-producing cells and smaller norepinephrine-producing cells can be found (Eurell and Frappier, 2006); in our study, they were arranged into clusters and cords and appeared more basophilic, in accordance with previous histological description of this organ in the capybara (Abass, 2017).

The macroscopical and microscopic assessment of the **thyroid gland** was carried out in the guinea pig only. In this species, it consisted of well-developed right and left smooth and uniform oval-shaped lobes, caudally connected by a well-developed glandular isthmus (measuring 1 mm in width) that was present in the majority of subjects. The thyroid lobes extended from the caudal border of the cricoid cartilage of the larynx to the 5th to 8th tracheal ring, where they were connected by the glandular isthmus, which surrounded the trachea ventrally. The thyroid gland of the guinea pig was located slightly more cranially than that of dogs and cats, which extend up to the 8th or 10th tracheal ring, respectively (König and Liebich, 2011). The topography of the thyroid gland in the guinea pigs of our study, however, is in line with that previously reported for this species (Yamasaki, 1995). The presence of an isthmus has

been reported to occur in a minority of subjects by previous studies (Yamasaki, 1995); in our study, on the other hand, it was evidenced in the majority of animals. The glandular ventral isthmus connecting the two lobes of the guinea pig thyroid gland resembled that usually seen in bovines, where it is particularly developed and wide (König and Liebich, 2011). In dogs and horses, on the other hand, it is composed of connective tissue and is poorly-developed (König and Liebich, 2011). Histologically, the colloid-filled thyroid follicles were delimited by a simple cubic epithelium, resting on a basal lamina containing capillaries and parafollicular cells, with the typical aspect seen in other domestic species (Eurell and Frappier, 2006).

An internal **parathyroid gland** was not evidenced, histologically, within the thyroid parenchyma of the guinea pig, nor in its proximity. An internal parathyroid gland, incorporated within the thyroid parenchyma, has been evidenced in most other domestic mammals, such as carnivores, horses and ruminants, with the exception of the pig, where it is absent (König and Liebich, 2011). Therefore, it could be hypothesized that guinea pigs lack an internal parathyroid gland, as it occurs in pigs, as well. A greater number of thyroid samples must be collected and histologically analysed, in order to confirm this preliminary data. Previous studies have assessed the histological structure of the parathyroids of the guinea pig, however not specifying the anatomical topography of internal and external parathyroid glands. The literature regarding the thyroid and parathyroid glands of the capybara is scarce. Further studies will be necessary to investigate the anatomy of these organs in this species.

Due to the prominent concavity of the pituitary fossa of the sella turcica, typical of this species (Alves, 2019), the **hypophysis** of the capybara, located in the pituitary fossa between the optic chiasm and the mammillary body, on the ventral surface of the diencephalon, was found to be more developed and prominent than that seen in the guinea pig; this finding is in accordance with previous studies, reporting the peculiarity that the pituitary gland of the capybara is more developed than that of other rodents and domestic mammals (Alves, 2019). From the histological analysis of the pituitary gland in the capybara, the classical ultrastructural organization was observed, with the adenohypophysis consisting of glandular epithelial tissue, the pars intermedia of the adenohypophysis divided the *pars distalis* from the *pars nervosa* and was composed of colloid-filled cavities lined with follicular cells. The *pars nervosa* of the neurohypophysis contained neurosecretory axons, pituicytes and capillaries, as well as Herring's bodies, dilatations of the nervous fibers forming focal accumulations of secretory vesicles. The histological appearance did not present any notable differences with that classically described in other domestic mammals (Eurell and Frappier, 2006).

## CENTRAL NERVOUS SYSTEM

The gross anatomical morphology of the **cerebrum**, brain stem and cerebellum in the guinea pig and capybara did not differ significantly from that of other rodents (Hargaden and Singer, 2012) and mammals (Barone, 2006b; König and Liebich, 2011). Indeed, in longitudinal section, the encephalon showed all the five portions classically described in the literature for other domestic mammals (Barone, 2006b; König and Liebich, 2011): the prosencephalon divided into a telencephalon with the cerebral hemispheres, and a diencephalon, including the pineal gland, the pituitary gland, the mammillary body, the interthalamic adhesion and the optic nerves; the mesencephalon; and the rhombencephalon, comprising the metencephalon (pons and cerebellum) and the myelencephalon (medulla oblongata). The cerebral ventricles were also visible. However, some noteworthy macroscopical interspecific analogies and differences were observed in the analysed subjects. In both species, the olfactory bulbs were prominent and elongated and protruding over the oral margin of the frontal lobe, especially in the capybara

cerebrum, due to their developed sense of smell; this characteristic is also shared by other rodents, such as rats and mice, as well as by rabbits (Cozzi et al., 2006). Moreover, the temporal lobes of the encephalon were particularly developed and wide in both the guinea pig and capybara, in accordance with previous studies (Campos and Welker, 1976; Ferreira et al., 2022), and analogously to the rabbit's cerebrum, which therefore appears overall wider and taller, in comparison with other laboratory rodents (Cozzi et al., 2006); the temporal lobe contains the auditory area (König and Liebich, 2011); therefore, the great development of this lobe in these species might be associated to their extremely developed and keen sense of hearing, which they both need to have since they are prey species. The capybara forebrain structures were proportionally larger than the corresponding guinea pig areas, which had already been observed in previous studies (Campos and Welker, 1976). The most significant macroscopic difference between the encephalon of the guinea pig and that of the capybara, however, was the higher degree of gyrification of the cerebral cortex and the more conspicuous neocortical fissures in the capybara cerebrum, as opposed to the guinea pig's lissencephalic cerebrum, lacking evident cerebral convolutions. These findings are in line with previous anatomical descriptions in both species, and are correlated to the capybara's higher capacity of information processing in the neocortex, so as to establish complex social relationships, than the guinea pig and other similar rodents (Campos and Welker, 1976; Ferreira et al., 2022). In other rodents, such as rats and mice, and lagomorphs, such as the rabbit, the cerebrum is also lissencephalic, analogously to the guinea pig's (Cozzi et al., 2006). A previous study of the sensory areas of the cerebral neocortex in the two species, has shown that the representation of the buccal area (lips and perioral areas) in the main somatic sensory cortex is particularly large in both species, with the head representation constituting about 80% of the surface of the somatic sensory cortex of the mapped brain of these species (Campos and Welker, 1976).

Another difference that was noted was the higher development of the hypophysis of the capybara, in comparison with the guinea pig hypophysis. This had been reported in previous studies, and is due to the prominent concavity of the pituitary fossa of the sella turcica, typical of this species, which accounts for the greater development of the pituitary gland in capybaras, in comparison with other rodents, including the guinea pig (Alves, 2019).

The weight of the adult capybara encephalon was, on average, 54.3 grams total, of which the cerebrum weighing 49 grams and the cerebellum 5.3 grams. These quantitative data are in line with the mean 52 grams reported by Campos and Welker for the capybara brain (1976). The weight of the adult guinea pig brain was 2.9 grams, which is inferior than the 4 grams previously reported in the literature (Cooper and Schiller, 1975a), however this data might have been influenced by several factors, including the fixation process and the sex of the animal, as well as the inclusion of the cerebellum in the calculation. Both cerebral hemispheres of the guinea pig measured 2.28 cm in length by 2.3 cm in width at the level of the temporal lobe, which is roughly in line with what had been reported for this species (2.1cm x 2.25 cm) (Cooper and Schiller, 1975a); the guinea pig brain, unlike that of other rodents such as rats and mice (Cozzi et al., 2006), therefore, due to the great lateral development of the temporal lobes, appears roughly triangular and with comparable widths and lengths. The capybara brain, analogously to the guinea pig's, is less elongated than most rodents (Cozzi et al., 2006), and, in this species, it even tends to be larger than longer, with a mean length of 57 mm, and a mean width of 58 mm. Moreover, in the capybara, it was observed that the female encephalon tended to be more elongated and with a greater length than the male's, with the weight of the encephalon being only slightly larger in the male.

Furthermore, both the guinea pig and capybara were characterized by a compact **cerebellum**, composed of two lateral cerebellar hemispheres, and a well-developed median



vermis, which towered over the adjacent hemispheres. This characteristic has also been observed in other rodents, such as rats and mice (Cozzi et al., 2006); in primates, on the other hand, the vermis does not stand out over the lateral hemispheres (Cozzi et al., 2006). In both the guinea pig and capybara, the folia were transversally arranged, as it usually occurs in other domestic species (König and Liebich, 2011). In the capybara, especially, a large caudoventral floccular lobe was evidenced, in accordance with reports by Mones and Ojasti (1986); the nodulofloccular lobe is related to the integration of vestibular information for eye and head movement control, as well as for the control of axial muscles for balance (Drake et al., 2020). In longitudinal section, the cerebellum showed an extensive arborescent ramification of the white matter (*arbor vitae*), as classically seen in all mammals of veterinary interest (König and Liebich, 2011).

From a histological point of view, the cerebral cortex and cerebellum did not show any noteworthy differences with other domestic mammals (Cozzi et al., 2006; Eurell and Frappier, 2006). The cerebellum was composed of an external layer of pia mater covering the cerebellar surface and extending into the sulci that separate the folia, an outer cerebellar cortex and an inner white matter (or medulla), which extended into the center of each cerebellar folium. The cortex covering the white matter consisted of a deeper granular layer, and intermediate piriform cell layer, comprising the Purkinje cells), and the outer molecular layer, which was less cellular than the deeper layers. From a stereological study of the guinea pig cerebellum, has emerged that the total Purkinje cell count is higher in the guinea pig than in other rodents, such as the rat (De Silva et al., 2021), which could be correlated to more developed motor and cognitive functions.

The histological organization of the cerebral cortex consisted in the classically-reported six cortical layers, which were well-recognizable in the animals studied. From outer to inner, these were: the molecular layer with tangentially-oriented neuropils, the external granular layers with small interneurons, the external pyramidal layer with medium-sized pyramidal neurons, the internal granular layer with small stellate neurons, the internal pyramidal layer with medium-to-large pyramidal neurons sending their axons into the white matter, and finally, the fusiform layer, with spindle-shaped neurons sending axons into the white matter. The underlying white matter presented nerve fibers directed to and from the cortex. Therefore, the organization of the capybara cerebrum did not differ from that classically described in other mammalian species (Eurell and Frappier, 2006).

## CONCLUSIONS

From the gross and microscopic morphological and morphometrical anatomical study of the different system of the guinea pig and capybara, several analogies and differences emerged. The most noteworthy are summarized below.

### RESPIRATORY SYSTEM

The **nasal plane** of the capybara lies in a dorsal position, due to the adaptation of this species to a semi-aquatic life, unlike that of guinea pigs, which are mainly terrestrial.

The well-developed nasal septum of the capybara was complete; conversely, in the guinea pig, it was found to be fenestrated, allowing the communication between the two nasal fossae.

A well-developed system of **paranasal pneumatic sinuses** in the frontal, maxillary, and lacrimal bones of the capybara and guinea pig, was evidenced; guinea pigs, however, lacked a frontal sinus.

In the guinea pig, the **larynx** had a more squared shape, whereas, in the capybara it was more conical; the capybara presented well-developed vocal cords and laryngeal ventricles, whereas, in the guinea pig, the laryngeal ventricle was absent and the vocal cords poorly developed.

The thyroid cartilage was composed of a ventral body and two lateral rectangular laminae in both species; it presented poorly-developed rostral and caudal horns in the capybara, whereas in the guinea pig the rostral horn was well-developed.

The **trachea** of the guinea pig and capybara was composed of incomplete cartilaginous rings, bridged dorsally and on their inner side by a trachealis smooth muscle. In the guinea pig, the rings were more C-shaped, whereas in the capybara, they were more flattened in the latero-lateral direction, resulting in a U-shaped appearance. The trachea was composed, on average, by 35 tracheal rings in the guinea pigs, 40 in the capybara.

The **right lung** of the guinea pig and the capybara consisted of four lobes: cranial, middle, accessory and caudal lobes, separated by deep fissures. In the capybara, the accessory lobe was further divided, by an accessory intralobar fissure, into a medial and a lateral portions.

The **left lung** was composed of three lobes in the guinea pig: a bipartite cranial lobe, a caudal lobe and an accessory lobe (typical of this species), whereas it was composed of two lobes, cranial and caudal, in the capybara.

From the anatomo-topographic and morphometric study of the guinea-pig and capybara **primary, lobar and segmental bronchi and their satellite arteries and veins**, it emerged that the guinea pig showed an articulated bronchial tree, as opposed to the more simplified bronchial tree of the capybara. Specifically, the right and left cranial lobar bronchi bifurcated into cranial and caudal branches, which in turn, provided numerous segmental branches. In the capybara, on the other hand, the right and left cranial lobar bronchi only had dorsal and ventral segmental branches that originated from them.

In both species, the veins, unlike the arteries, did not maintain a close relationship with the corresponding bronchial branches throughout their course, with the arteries being generally located dorso-laterally (capybara) or laterally to the respective bronchus, whereas the veins tended to be located on the ventromedial (capybara) or medial (guinea pig) side of the bronchi.

In both species, from the study emerged that the bronchial tree of both the guinea pig and the capybara exhibited dichotomous branching.

## GASTROINTESTINAL SYSTEM

The guinea pig and capybara had a common dental formula (20: I 1/1, C 0/0, P 1/1, M 3/3), and all **teeth** were seen to be elodont and aradicular. Large occlusal surfaces, composed of lamellar prisms, of the molariform teeth were evidenced in both species, which is an adaptation of these species to the masticatory function typical of a herbivorous diet; moreover, the large dimension of the upper third molars in comparison with the other molariform teeth was seen in the capybara only.

The well-developed **deep masseter**, passing through the large infraorbital foramina to insert anteriorly to the complete zygomatic arch on the incisor and maxillary bones, which is related to gnawing efficiency, was observed in both species.

In the capybara, the width of the **tongue** broadened moving towards its root, whereas in the guinea pig, the apex and body had a similar width, with the root being thicker and broader and covered with lingual papillae.

In both species, the terminal portion of the **oesophagus** entered the fundus of the stomach near the lesser curvature and formed with it an angular or cardiac incisure.

The histological appearance of the oesophagus in the capybara was characterized by a highly keratinized stratified squamous epithelium composed of an evident stratum granulosum, with a well-developed striated tunica muscularis; in the guinea pig, on the other hand, the mucosa of the oesophagus was lined with a nonkeratinized stratified squamous epithelium.

In the capybara, **the stomach** had a typical inverted J-shaped appearance, with well-developed greater and lesser curvatures, that was not seen in the simpler stomach of guinea pigs with a poorly-developed lesser curvature. Both species presented a cranial expansion of the fundic part, especially in the capybara where it formed the so-called gastric diverticulum.

Externally, the stomach of the capybara presented 2 large gastric *teniae* that delimited haustras on its surface, which were not found in the guinea pig stomach. The stomach of both species was entirely glandular, unlike that of other rodents.

The **cecum** of both species was particularly voluminous and developed; it had a thin wall and occupied most of the abdominal cavity and it was composed by a body, a base and an apex. It lacked a caecal appendix in both species. On its outer surface, it presented three (in the guinea pig) or four (in the capybara) white longitudinal *teniae ceci*, which created lateral saccular haustra.

The **colon** of the capybara, with the exception of the spiral colon, presents outer haustras along its entirety; these were not macroscopically observed in the guinea pig.

In both species, the **liver** macroscopically consisted of six lobes: the left lateral, the left medial, the right medial, the right lateral, the quadrate and the caudate lobe, further divided into a caudate and a papillary processes. In the guinea pig, the lobes were poorly demarcated and tended to blend with each other, whereas, in the capybara, the lobes were well-demarcated by deep fissures, and partially overlapping. Histologically, the **liver** lobules of the capybara had poorly-defined margins, in comparison with the hexagonal liver lobules of the guinea pig.

In both species, a well-developed, thin-walled oval **gallbladder**, was seen lying on the medial aspect of the quadrate lobe, in the guinea pig, or between the left medial lobe and the quadrate lobe, in the capybara.

The guinea-pig **pancreas**, unlike the capybara's, had a diffuse appearance and was widely distributed within the mesoduodenum, and composed of a left lobe, a body, and a

right lobe. The capybara pancreas, on the other hand, had better-defined margins, a more compact appearance, and was divided into a head, a body and a tail.

From the anatomical morphological and morphometric study of the **abdominal aorta** and its collaterals in the guinea pig and capybara, emerged that, in all the guinea pigs studied, a **celiacomesenteric trunk (CT)** was present, whereas the celiac and cranial mesenteric arteries originated separately in the capybara.

In the capybara, the **celiac artery** trifurcated into the splenic artery, which continued as left gastroepiploic artery, the left gastric artery, and the hepatic artery. In the guinea pig, on the other hand, five different modes of branching of the celiac component of the CT were observed, with the most frequently occurring being the CT first emitting the gastrosplenic artery, which in turn gave rise to the left gastric and splenic arteries, and, subsequently, it detached the hepatic artery.

The **cranial mesenteric artery**, in the guinea pig, originated from the CT, after the detachment of the hepatic artery; in the capybara, on the other hand, the cranial mesenteric artery originated from the aorta, instead of from the CT. The cranial mesenteric artery continued, in both species, as the **ileocolic artery** destined for the large intestine.

The **renal arteries** of the guinea pig were found to be single, double or even triple in the guinea pig, whereas they were found to be single on both sides in the capybara.

The **median sacral artery** in the capybara arose from the dorsal surface of the aorta before its bifurcation into the common iliac arteries, more cranially than in the guinea pig.

## CARDIOVASCULAR SYSTEM

The **heart** of the guinea pig and capybara was globoid in appearance, although more conical and laterally-flattened in the guinea pig in comparison with the capybara. Moreover, the guinea pig heart had a more pronounced ventrocaudal inclination over the sternum, in comparison with the capybara's.

The myocardium, in capybaras, was vascularized solely by the **left coronary artery** and its collaterals (atresia of the right coronary artery), whereas a right coronary artery is present in guinea pig hearts.

## URINARY SYSTEM

The guinea pig and capybara **kidneys** were, in both cases, found to be unipapillar with a large renal pelvis and a single longitudinal renal papilla.

## MALE GENITAL SYSTEM

The **accessory sexual glands** were extremely developed, especially in the guinea pig. The capybara presents well-developed vesicular glands and a prostate gland. In the guinea pig, on the other hand, four well-recognizable accessory glands were identified: the even more highly developed paired seminal vesicles, the prostate gland, the coagulating glands, and the bulbourethral glands.

In the guinea pig only, a species-specific **penile intromittent sac** (sacculus urethralis) located within the penis below the urinary meatus, was identified, which, when manually everted, presented two **cartilaginous styles** protruding outwards. These were not present in the capybara.

Histologically, the capybara and guinea-pig **testes**, were characterized by an abundance of Leydig cells and lymphatic tissue in the wide intertubular compartments.

## **FEMALE GENITAL SYSTEM**

The **uterus** was characterized by a double cervix, with a single opening into the vagina, in the capybara, by a single cervix in the guinea pig. In both cases, however, the uterus was bicornate with elongated and V-shaped uterine horns.

## **LYMPHATIC SYSTEM**

The elongated and slightly oval-shaped **spleen** of the guinea pig was proportionally more developed in this species, than it was in the capybara, where it was roughly triangularly-shaped. In the guinea pig, the spleen had a unilobed appearance, with the **splenic margins** found to be relatively smooth and continuous, with few shallow incisures; in the capybara, on the other hand, the spleen presented fissured margins, with several shallow marginal sulci, giving it a polylobed appearance.

## **ENDOCRINE SYSTEM**

The **adrenal glands** of the capybara and guinea pig were, in both species, particularly well-developed and proportionally voluminous in comparison with those usually observed in other domestic mammals. They were slightly triangularly-shaped in the capybara, pyramidally-shaped in the guinea pig.

The **hypophysis** of the capybara, located in a particularly deep and concave pituitary fossa on the ventral surface of the diencephalon, was found to be more developed and prominent than that seen in the guinea pig and most other rodents.

## **CENTRAL NERVOUS SYSTEM**

In both species, the **olfactory bulbs** were prominent and elongated and protruding over the oral margin of the frontal lobe. The **temporal lobes** of the encephalon were particularly developed and wide in both the guinea pig and capybara.

The capybara cerebrum had a higher degree of **gyrification of the cerebral cortex** and more conspicuous neocortical fissures, as opposed to the guinea pig's lissencephalic cerebrum, lacking evident cerebral convolutions.

The **cerebellum** of both the guinea pig and the capybara was composed of two lateral cerebellar hemispheres, and characterized by a well-developed median vermis, towering over the adjacent hemispheres.

In conclusion, the present study aimed to implement the basic anatomical knowledge concerning two closely-related rodent species which, given their increasing diffusion, require increasing awareness as basic contribution for other clinical fields of veterinary medicine, as well as for zootechnical and research purposes. It is hoped that the results of the present study will provide the basis for a better understanding of their comparative anatomy, with important consequent therapeutic implications.

## BIBLIOGRAPHY

1. Abass, T. A. (2017). Anatomical and histological study of adrenal gland in new natal and adult guinea pig (*Cavia porcellus*). *Kufa journal for veterinary medical sciences*, 8(1):181-191.
2. Abd AL-Rhman, S. A. (2016) Morphological and Histological Study of the Stomach in Local Rodent Species (Guinea Pig) *Cavia Porcellus*. *Journal of Biology, Agruculture and Healthcare*, 6(6):74-86.
3. Abidu-Figueiredo M., Xavier-Silva B., Cardinot T.M., Babinski M.A., Chagas M.A. (2008). Celiac artery in New Zealand rabbit: anatomical study of its origin and arrangement for experimental research and surgical practice. *Pesquisa Veterinaria Brasileira*, 28:237–240.
4. Alves, L. D. S. (2019). Anatomia descritiva do encéfalo, olho e órbita da capivara (*Hydrochoerus hydrochaeris*, Linnaeus, 1766) por meio da ressonância magnética. Tesis doctoral. Universidad Estadual Paulista “Julio De Mesquita Filho”, Sao Paulo, Brasil.
5. Amiri, M. H. and Gabella, G. (1988). Structure of the guinea-pig trachea at rest and in contraction. *Anatomy and Embryology*, 178(5):389-397.
6. Anchieta J.D.E. (1997) Carta De São Vicente 1560, Vol 7, Caderno. Conselho Nacional Da Reserva Da Biosfera Da Mata Atlântica, São Paulo.
7. Ates S., Cakir A. (2010). Comparative macroanatomy of the heart valves of the New Zealand rabbit and guinea pig. *Ankara universitesi veteriner fakultesi dergisi*, 57 (3):145-150.
8. Autino, V., Casanova, M. J., and Facal, B. (2019). Irrigación sanguínea de la pelvis y el miembro pelviano del carpincho (*Hydrochoerus hydrochaeris*). Dissertation Thesis. Universidad De La República (Uruguay). Facultad de Veterinaria.
9. Barone R. (2006a). Anatomia comparata dei mammiferi domestici. Vol. 3. Splanchnologia. 4<sup>o</sup> Edizione Edagricole, Bologna (Italia).
10. Barone R. (2006b). Anatomia comparata dei mammiferi domestici. Vol. 5. Angiologia, parte 2<sup>o</sup>. Ed. Edagricole, Bologna.
11. Barthold S.W., Griffey S.M., Percy D.H. (2016). Guinea Pig. In: Barthold SW, Griffey SM, Percy DH. *Pathology of Laboratory Rodents and Rabbits*. 4<sup>th</sup> Ed. Wiley Blackwell: 213-252.
12. Bhattacharjya M., Surendrajit K., Banerjee R. (2003). Histological, biometrical and lobar pattern of liver in guinea pig. *Geobios*, 25:267-275.

13. Bode F.F., Cao J.A., Resoagli J.M., Resoagli E.H., Millán S.G, Flores Quintana C. (2008). Linfocentros abdominal, lumbar y pelviano en el carpincho (*Hydrochoerus hydrochaeris*: Linnaeus, 1766). *Revista Veterinaria*, 19:158–160.
14. Bode F.F., Resoagli J.M., Millán S.G., Resoagli E.H. (2009). Linfocentros de la cabeza y cuello del carpincho. *Revista Veterinaria*, 20:135–137.
15. Bode F.F., Fernández J.A., Cao J.A., Resoagli J.M. (2013). Descripción del esqueleto axial del carpincho (*Hydrochoerus hydrochaeris*). *Revista Veterinaria*, 24:44-46.
16. Branco E. R., Guimarães A., Miglino M. A., Didio L. J., Nurmberger Jr R., & De Souza W. M. (1997). Pesquisa anatômica da glândula pineal em capivaras (*hydrochoerus hydrochoeris*). *Brazilian Journal of Veterinary Research and Animal Science*, 34(4):191-195.
17. Breazile J.E., Brown E.M. (1976). Anatomy. In: Wagner J.E., and Manning P.J., editors. *The Biology of The Guinea Pig*. New York: Academic Press, pp. 53-62.
18. Brewer N.R., Cruise L.J. (1994). The guinea pig heart – some comparative aspects. *Contemporary Topics in Laboratory Animal Science*, 33:64-70.
19. Brewer N.R., Cruise L.J. (1997). The respiratory system of the guinea pig: emphasis on species differences. *Contemporary Topics in Laboratory Animal Science*, 36:100-108.
20. Brisson, M. J. (1762). *Regnum animale in classes ix distributum, sive synopsis methodica sistens generalem animalium distributionem in classes ix, et duarum primarum classium quadrupedum scilicet et cetaceorum, particularem divisionem in ordines, sectiones, genera et species*. Apud CI Theodorum Haak, Leiden.
21. Brown C., Mans C. (2007). Urethral catheterization of the male guinea pig (*Cavia porcellus*). *Lab animal*, 36(7):20-21.
22. Campos G.B., Welker W.I. (1976). Comparisons between brains of a large and a small hystricomorph rodent: capybara, *Hydrochoerus* and guinea pig, *Cavia*; neocortical projection regions and measurements of brain subdivisions. *Brain, Behavior and Evolution*, 13:243-66.
23. Cao J.A., Bode F.F., Resoagli J.M., Millán S.G. (2011). Linfocentros de la cavidad torácica del “carpincho” (*Hydrochoerus hydrochaeris*, linnaeus 1766). *Revista Veterinaria*, 22:139-140.
24. Cao J.A, Flores Quintana C., Bode F.F. (2017). Caracterización morfológica del hígado del carpincho (*Hydrochoerus hidrochaeris*) *Revista Veterinaria*, 28(1):47-50.

25. Caras R.A. (2002). The cavy and the dormouse: small feasts. In: Caras R.A., A perfect harmony. The intertwining lives of animals and humans throughout history. Ed. Purdue University Press:173-177.
26. Cardim F. (1980). *Tratados Da Terra e Da Gente Do Brasil*, Vol 13, Coleção Reconquista Do Brasil. Editora Itatiaia Limitada, São Paulo.
27. Carrascal Velásquez J.C., Ortiz Bedoya S.A., Petro Hernández V.G. (2016). Caracterização microscópica das regiões esofágicas de um grupo de capivaras (*Hydrochoerus hydrochaeris*) livres no Brasil. *Revista CES Medicina Veterinaria y Zootecnia*, 11(2):73-81.
28. Carrascal Velásquez J.C. (2017). Aspectos histomorfométricos, histoquímicos e ultraestruturais do intestino grosso de capivara (*Hydrochoerus* sp). Dissertation thesis. Universidad de Medicina Veterinaria, Sao Paulo, Brasil.
29. Cheeke P.R. (1987). Nutrition Of Guinea Pigs. In: Cunha T.J. (Ed.). *Rabbit Feeding And Nutrition*. Orlando, Academic Press. pp. 344-353.
30. Cherem J. J., Ferigolo J. (2012). Descrição do sincrânio de *Cavia aperea* (Rodentia, Caviidae) e comparação com as demais espécies do gênero no Brasil. *Papéis Avulsos De Zoologia*, 52:21– 50.
31. Çiçekcibaşı A.E., Uysal I.I., Seker M., Tuncer I., Büyükumucu M., Salbacak A. (2005). A Rare Variation Of The Coeliac Trunk. *Annals of Anatomy*, 187(4):387–391.
32. Cienas A.P., Santos A.C.D., Vasconcelos B.G. (2019) Morphological characteristics of the papillae and lingual epithelium of guinea pig (*cavia porcellus*). *Acta zool.* 2019; 100: 53– 60.
33. Coccolini. R (2013). *Studio Anatomico-Topografico ed Indagine Morfometrica dei Bronchi Principali, Lobari e Segmentali nel Gatto*. Dissertation Thesis. Department of Veterinary Medical Sciences, Alma Mater Studiorum - University of Bologna, Italy.
34. Cooper G., Schiller A. (1975a). Anatomy of the Guinea Pig. *Nature* 260: 204.
35. Cooper G., Schiller A. (1975b). *Anatomy of the Guinea Pig*. Cambridge, Mass.: Harvard University Press. The Digestive System, pp. 303-324.
36. Cozzi B., Ballarin C., Peruffo A., Carù F. (2006). *Anatomia degli Animali Dida Laboratorio (Roditori Eie Lagomorfi)*. Casa Editrice Ambrosiana, Milano:29-172.



37. Culau P.D.O.V., Reckziegel S.H., Lindemann T., De Araújo A.C.P., Balzaretto F. (2007). Colaterais Do Arco Aórtico Da Capivara (*Hydrochoerus hydrochaeris*). *Acta Scientiae Veterinariae*, 35(1):89-92.
38. Culau P.O.V., Azambuja R.C., Campos R. (2008). Ramos Claterais Viscerais Da Artéria Aorta Abdominal Em Myocastor Coypus (Nutria). *Acta Scientiae Veterinariae*, 36(3):241–247.
39. De Barros Moraes P.T., Pacheco M.R., De Souza W.M., Da Silva R.A., Neto P.B., De Figueiredo Barreto C.S., Ribeiro A.A.C.M. (2002). Morphological Aspects of the Capybara Stomach (*Hydrochoerus Hydrochaeris*): Gross and Microscopic Structure. *Anatomia Histologia Embryologia*, 31:362-366.
40. De Barros Moraes P.T., De Souza W.M, Da Silva R.A., Neto P.B, De Figueiredo Barreto C.S., Ribeiro A.A.C.M. (2005). The Muscular Organization of The Stomach of Capybara (*Hydrochoerus hydrochaeris*): An Architectural View. *Annals of Anatomy*, 187:51-56.
41. Debout C., Quillec M., Izard J. (1984). Natural killer activity of Kurloff cells: a direct demonstration on purified Kurloff cell suspensions. *Cellular Immunology*, 87(2):674-677.
42. De Freitas NL, De Paula MC, Peri SHV, Dos Santos Ferraz RH (2008). Morphology of Capybara small intestine – *Hydrochoerus hydrochaeris* (Linnaeus, 1766). *Brazilian Journal of Veterinary Research And Animal Science*, 45(2):122-130.
43. De Silva M., Sadeghinezhad J., Nyengaard J.R., Aghabalazadeh Asl M., Saeidi A., De Sordi N., Chiocchetti R., Grandis A. (2021). A Design-based stereological study of the guinea-pig (*Cavia porcellus*) cerebellum. *Journal of Anatomy*, 239(2):517-528.
44. De Sordi N, Bombardi C, Chiocchetti R, Clavenzani P, Trere' C, Canova M, Grandis A. (2014). A new method of producing casts for anatomical studies. *Anatomical Science International*, 89(4):255-265.
45. Diamond J. (2002). Evolution, consequences and future of plant and animal domestication. *Nature*, 418:700–707.
46. Doidge J.M., Satchell D.G. (1982). Adrenergic and nonadrenergic inhibitory nerves in mammalian airways. *Journal of the Autonomic Nervous System*, 5:83-99.
47. Donnelly T.M., Brown C.J. (2004). Guinea pig and chinchilla care and husbandry. *Veterinary Clinics of North America: Exotic Animal Practice*, 7(2):351-373.
48. Drake R.L. Wayne Vogl A. Mitchell A.W.M., eds. (2020). Gray's anatomy for students. 4th Ed. Elsevier Inc., Philadelphia.
49. Dubost, G. (1968). Les niches écologiques des forêts tropicales sud-américaines et africaines, sources de convergences remarquables entre Rongeurs et Artiodactyles. *Revue d'Ecologie, La Terre et la Vie*, 22:3-28.

50. Dubost, G. (1988). Ecology and social life of the red acouchy, *Myoprocta exilis*; comparison with the orange-rumped agouti, *Dasyprocta leporina*. *Journal of Zoology*, 214(1):107-123.
51. Dyce K.M. Sack W.O. Wensig C.J. (2015). Anatomía Veterinaria. 4º Edición. Mc Graw-Hill Interamericana.
52. Eremin O., Wilson A. B., Coombs R. R. A., Ashb J., Plumb D. (1980). Antibody-dependent cellular cytotoxicity in the guinea pig: the role of the Kurloff cell. *Cellular Immunology*, 55(2):312-327.
53. Ernström, U., Larsson, B. (1970). Determination of thymic blood flow in guinea-pigs of different ages. *Acta Pathologica et Microbiologica Scandinavica*, 78(3):366-367.
54. Eurell, J. N., Frappier, B. L. (2006). Dellmann's Textbook of Veterinary Histology. Blackwell Publishing, Ames, Iowa.
55. Evans H.E., De Lahunta A. (2013). Miller's anatomy of the dog. 4th edition. Elsevier, St. Louis.
56. Favre P. (1967). Contribution a l'etude du systeme arteriel du cobaye (abdomen, bassin, membre pelvien). Doctoral thesis. Ecole National Veterinaire D'alfort, Paris.
57. Fawcett D. W., Neaves W. B., Flores M. N. (1973). Comparative observations on intertubular lymphatics and the organization of the interstitial tissue of the mammalian testis. *Biology of Reproduction*, 9(5):500-532.
58. Ferreira J. D., Dozo M. T., de Moura Bubadué J., Kerber L. (2022). Morphology and postnatal ontogeny of the cranial endocast and paranasal sinuses of capybara (*Hydrochoerus hydrochaeris*), the largest living rodent. *Journal of Morphology*, 283(1)66-90.
59. França L.R., Russell L.D. (1998) The Testis of Domestic Animals. In: Regadera J., Martinez-Garcia F. (Eds.). Male Reproduction. A Multidisciplinary Overview. Churchill Livingstone, Madrid, pp 197–219.
60. Gabella G. (1990). Intramural neurons in the urinary bladder of the guinea-pig. *Cell and tissue research*, 261(2):231-237.
61. Germinaro A., Branco E. R., Miglino M. A., Didio L. J., de Souza, W. M. (1997). A segmentação arterial do baço da capivara (*Hydrochoerus hydrochaeris*). *Brazilian Journal of Veterinary Research and Animal Science*, 34(4):196-202.
62. Getty R. (1982). Anatomía De Los Animales Domésticos. 5º Ed, Interamericana, México, pp. 1356-1375.
63. Goldsmith O. (1870). A History of The Earth and Animated Nature. Blackie And Son, Glasgow.

64. Hargaden M, Singer L. (2012). Guinea Pigs: Anatomy, Physiology, And Behavior. In: Suckow M.A., Stevens K.A., Wilson R.P. The laboratory rabbit, guinea pig, hamster, and other rodents. Elsevier: 576-602.
65. Harkness J.E., Murray K.A., Wagner J.E. (2002). Biology And Diseases of Guinea Pigs. In: Fox J., Anderson L.C., Loew F.M. (Eds). Laboratory Animal Medicine. Boston, Academic Press, pp. 203-246.
66. Harkness J.E., Turner P.V., Vandewoude S., Wheler C.L. (2010). Biology And Husbandry. In: Harkness J.E., Turner P.V., Vandewoude S., Wheler C.L. (Eds). Harkness And Wagner's Biology and Medicine of Rabbits and Rodents. 5<sup>th</sup> Ed. Wiley-Blackwell, pp. 45-57.
67. Harkness J.E., Wagner J.E. (1995). The Biology and Medicine of Rabbits and Rodents, 4<sup>th</sup> Ed. Baltimore: William & Wilkins, pp. 30-40.
68. Heatley J. J. (2009). Cardiovascular anatomy, physiology, and disease of rodents and small exotic mammals. *Veterinary Clinics of North America: Exotic Animal Practice*, 12(1):99-113.
69. Herrera E.A. (2013). Capybara Digestive Adaptations. In: Herrera E.A. (ed). Capybara. Springer, New York, pp. 97-106.
70. Higgins G. M. (1927). The extrahepatic biliary tract in the guinea-pig. *The Anatomical Record*, 36(2):129-147.
71. Hill A. D., Folan-Curran J. (1993). Microappendages on the atrioventricular valves of the guinea pig. *Journal of Anatomy*, 182:425.
72. Hof P. R., Glezer I. I., Condé F., Flagg R. A., Rubin M. B., Nimchinsky E. A., Weisenhorn D. M. V. (1999). Cellular distribution of the calcium-binding proteins parvalbumin, calbindin, and calretinin in the neocortex of mammals: phylogenetic and developmental patterns. *Journal of chemical neuroanatomy*, 16(2):77-116. Hoffmann, G. (1956).
73. Hoffmann G. (1956). Kurzer Abriß der Anatomie und Physiologie der Laboratoriumstiere. *Veb Gustav Fischer Verlag-Jena*, 26:34.
74. Honeycutt R. L. (2013). Phylogenetics of caviomorph rodents and genetic perspectives on the evolution of sociality and mating systems in the Caviidae. In: Honeycutt R.L. (ed). Capybara. Springer, New York, NY, pp. 61-81.
75. Houaiss A., Villar M.D.S., Franco F.M.D.M. (2001). Dicionário Houaiss Da Língua Portuguesa. Objectiva Editora Ltda, pp. Lxxiii-2922.
76. H Qasem H., O Rabee F., S Al-A A. (2015). A Comparative Anatomical and Morphological Study of Spleen in Rabbit (*Oryctolagus Cuniculus*) and Guinea pig (*Cavia porcellus*). *Journal of Kerbala University*, 11(2):147-155.
77. Hudson G. (1968). Quantitative study of the eosinophilic granulocytes. *Seminars in hematology*,

5:166-186.

78. Ibáñez Orihuela P., Salaberry Andrada H., Zunino Mac Entyre C. (2019). Irrigación sanguínea de las vísceras abdominales del carpincho (*Hydrochoerus hydrochaeris*). Dissertation Thesis. Universidad De La República (Uruguay). Facultad De Veterinaria.
79. Ichii O., Yabuki A., Ojima T., Matsumoto M., Suzuki S. (2006a). Species specific differences in the ratio of short to long loop nephrons in the kidneys of laboratory rodents. *Experimental animals*, 55(5):473-476.
80. Ichii O., Yabuk, A., Ojima T., Matsumoto M., Suzuki S. (2006b). Rodent renal structure differs among species. *Journal of veterinary medical science*, 68(5):439-445.
81. Ishaq M. (1980). A morphological study of the lungs and bronchial tree of the dog: with a suggested system of nomenclature for bronchi. *Journal of anatomy*, 131(4):589-610.
82. Jara L. F., Sánchez J. M., Alvarado H., Nassar-Montoya F. (2005). Kurloff cells in peripheral blood and organs of wild capybaras. *Journal of wildlife diseases*, 41(2):431-434.
83. Jilge V.B. (1980). The gastrointestinal transit time in the guinea-pig. *Zeitschrift fur Versuchstierkunde*, 22(4):204-210.
84. Junqueira L.C., Carneiro J. (2004). *Histologia Básica*. 10ª Ed. Guanabara Koogan, Rio De Janeiro.
85. Kapelko V.I, Navikova N.A. (1993). Comparison of functional load in rat and guinea pig hearts. *News in physiological sciences*, 8:157-160.
86. Kay J.M. (1983). Pulmonary vasculature and nerves. *The American Review of Respiratory Disease*, 128:s53-s57.
87. Klemm M. F., Exintaris B., Lang R. J. (1999). Identification of the cells underlying pacemaker activity in the guinea-pig upper urinary tract. *The Journal of physiology*, 519(3):867-884.
88. König H., Liebich H. (2011). *Anatomía De Los Animales Domésticos*. 2º Ed. Tomo I: Aparato Locomotor. Ed. Panamericana., Panamericana, Buenos Aires.
89. Kramer A.W., Marks L.S. (1965). The occurrence of cardiac muscle in the pulmonary veins of rodents. *Journal of morphology*, 117:135-150.
90. Langenfeld M., Patea E. (1977). Anatomical variants of the celiac artery in the sheep, with special reference to the celiomesenteric arterial trunk. *Anatomischer Anzeiger*, 142(3):168-174.
91. Larouche M., Diep C., Sillitoe R.V., Hawkes R. (2003) Topographical Anatomy of The Cerebellum in the Guinea Pig, *Cavia Porcellus*. *Brain Research*, 965:159-69.
92. Legendre, L. F. (2003). Oral disorders of exotic rodents. *Veterinary Clinics: Exotic Animal Practice*, 6(3):601-628.

93. Legendre L. (2016). Anatomy and disorders of the oral cavity of guinea pigs. *Veterinary Clinics: Exotic Animal Practice*, 19(3):825-842.
94. Linnaeus, C. (1758). *Systema naturae, per regna tria naturae secundum classes, ordines, genera, species cum characteribus, differentiis, synonymis locis*. Tomus I. 10th ed. Laurnetii. Salvii, Holmiae.
95. Linnaeus, C. (1766). *Systema naturae, per regna tria naturae secundum classes, ordines, genera, species cum characteribus, differentiis, synonymis, locis*. 12th ed. Laurnetii Salvii, Holmiae, 1:1-533.
96. Lord E., Collins C., deFrance S., LeFebvre M. J., Pigière F., Eeckhout P., Matisoo-Smith E. (2020). Ancient DNA of guinea pigs (*Cavia* spp.) indicates a probable new center of domestication and pathways of global distribution. *Scientific reports*, 10(1):1-9.
97. Luay O.H. (2016). Some macroscopic and microscopic observation on the pituitary gland of guinea-pig *Cavia culteri*. *Basrah journal of veterinary research*, 15(4):125-131.
98. Luther E. (1923). Vergleichende anatomische untersuchugen über die aorta abdominalis und ihre verzweigungen beim meerschweinchen und kaninchen. Thèse de doctorat vétérinaire, Hannover.
99. Macdonald D.W, Herrera E.A. (2012) Capybara Scent Glands and Scent-Marking Behavior. In: Moreira J.R., Ferraz K.M., Herrera E.A., Macdonald D.W. (Eds). *Capybara: Biology, Use and Conservation of an Exceptional Neotropical Species*. Springer, New York, pp 185–193.
100. Magariños L., Benech A., Vazquez N., Pérez W. (2018). Aspectos macroanatómicos del corazón del carpincho (*Hydrochoerus hydrochaeris*). *International Journal of Morphology*, 36(1):235-242.
101. Makita T., Kakuni M., Shintaku T., Imada T., Kiso Y., Kumakura A., Endo H. (1998). Anatomical records of the splancheology of capybara. *Yamaguchi Journal of Veterinary Medicine*, 25:41-52.
102. Mann F.C., Foster J.P., Brimhall S. D. (1920). The relation of the common bile duct to the pancreatic duct in common domestic and laboratory animals. *The Journal of Laboratory and Clinical Medicine*, 5(4):203-206.
103. Manning P.J., Wagner J.E., Harkness J.E. (1984). Biology And Diseases of Guinea Pig. In: Fox J.G., Cohen B.J., Loew F.M. (Eds). *Laboratory Animal Medicine*. Academic Press, Orlando, pp. 150-181.
104. Marcgrave De Liebstad G. (1648) *Historiæ Rervm Natvarlivm Brasiliæ, Libri Octo: Quorum Tres Priores Agvnt De Plantis. Quartus De Piscibvs. Quintus De Avibvs. Sextus De*

Quadrupedibus & Serpentibus. Septimus De Insectis. Octavus De Ipsa Regione, & Illius Incolis. Franciseum Hackium, Leiden.

105. Mares M.A., Ojeda R.A. (1982). Patterns of diversity and adaptation in South American hystricognath rodents. In: Mares M.A., Genoways H.H. (Eds). *Mammalian Biology in South America*. University of Pittsburgh, Linesville. Pp 393-432.
106. Mattei A. (1966). Anatomie de l'appareille genital femelle du cobaye. Doctoral thesis. Ecole National Veterinaire D'alfort, Paris.
107. Maženský D., Flešárová S. (2017). Arrangement of renal arteries in guinea pig. *Anatomical Record*, 300:556–559.
108. Mazzi V. (1977). *Manuale di tecniche istologiche e istochimiche*. Piccin ed., Padova.
109. Møller M., Baeres F.M. (2002). The anatomy and innervation of the mammalian pineal gland. *Cell and tissue research*, 309(1):139-150.
110. Mones A. (1984). Estudios sobre la familia hydrochoeridae. Xiv: révisión sistematica (Mammalia: rodentia). *Senckenbergiana biológica*, 65(1-2):1-17.
111. Mones A., Ojasti J. (1986). *Hydrochoerus hydrochaeris*. *Mammalian species*, 264:1–7.
112. Morales E. (1995). *The Guinea Pig: Healing, Food And Ritual In The Andes*. Tucson (AZ), University Of Arizona Press.
113. Moreira J.R. (1995). The reproduction, demography and management of capybaras (*Hydrochaeris hydrochaeris*) on Marajó island – Brazil. Doctorate Thesis, University of Oxford, Oxford, UK.
114. Moreira J.R., Alvarez M.R., Tarifa T., Pacheco V., Taber A., Tirira D.G., Herrera E.A, Ferraz K.M.P.M.B., Aldana Dominguez J., Macdonald D.W. (2013). Taxonomy, Natural History and Distribution of the Capybara. In: Moreira J.R., Ferraz K.M.P.M.B, Herrera E.A., Macdonald D.W. (Eds). *Capybara*. Springer, New York, NY; pp. 3-37.
115. Moreira, J. R., Clarke, J. R., & Macdonald, D. W. (1997). The testis of capybaras (*Hydrochoerus hydrochaeris*). *Journal of Mammalogy*, 78(4):1096-1100.
116. Moreira J.R., Macdonald D.W. (1996). Capybara use and conservation in South America. In: Taylor V.J., Dunstone N. (Eds). *The exploitation of mammal populations*. Springer, Drodrecht; pp. 88-101.
117. Moreto A. O., Oliveira F. D., Bertassoli B. M., Assis Neto, A. C. (2017). Comparative morphology of the respiratory organs of capybaras (*Hydrochoerus hydrochaeris*). *Pesquisa Veterinária Brasileira*, 37:269-277.

118. Myers P., Espinosa R., Parr C.S., Jones T., Hammond G.S., Dewey T.A. (2006). Rodent Jaws. The animal diversity web.  
[Http://animaldiversity.ummz.umich.edu/site/topics/mammal\\_anatomy/rodent\\_jaws.html](http://animaldiversity.ummz.umich.edu/site/topics/mammal_anatomy/rodent_jaws.html)
119. Nenzi A., Venturoli L., Gambini F., De Sordi N., Diana A., Grandis A. (2008). Studio anatomotopografico e morfometrico dei bronchi lobari, delle loro principali diramazioni e dei vasi satelliti nel cane. Atti Del LXII Conv. Naz. S.I.S.Vet., 24-27 Settembre 2008, S. Benedetto Del Tronto (Ap). 23-24.
120. Neuhaus J., Dorschner, W., Mondry J., Stolzenburg J. U. (2001). Comparative anatomy of the male guinea-pig and human lower urinary tract: histomorphology and three-dimensional reconstruction. *Anatomia, histologia, embryologia*, 30(4):185-192.
121. Nickel R., Schummer A., Seiferle E. (1979). The viscera of the domestic mammals. Digestive System – The Alimentary Canal. 2<sup>nd</sup> Ed. Verlag Paul Parey, Berlin; pp. 101-138.
122. Nishikimi M., Kawai T., Yagi K. (1992). Guinea pigs possess a highly mutated gene for L-gulonono-gamma-lactone oxidase, the key enzyme for L-ascorbic acid biosynthesis missing in this species. *Journal of Biological Chemistry*, 267(30):21967-21972.
123. Nixon J. M. (1974). Breathing pattern in the guinea-pig. *Laboratory animals*, 8(1):71-77.
124. Nowak R.M. (1999). Walker's Mammals of The World. 6th Ed. Baltimore, Md, Johns Hopkins University Press. pp. 1667–1669.
125. O'Donnell S. R., Saar N., Wood L. J. (1978). The density of adrenergic nerves at various levels in the guinea-pig lung. *Clinical and Experimental Pharmacology and Physiology*, 5(4):325-332.
126. Ojasti, J. (1973). Estudio Biológico del Chigüire o Capibara. Fondo Nacional De Investigaciones Agropecuarias. Fonaiap, Caracas. 274 p.
127. O'Malley B. (2005). Guinea Pigs. In: O'Malley B. (ed). *Clinical Anatomy and Physiology of Exotic Species*. Philadelphia, Elsevier Saunders: 197-208.
128. Orti R.M., García P.M., Soriano J.G. (2004). Roedores – Cobayo Domestico. Atlas De Anatomia De Animales Exoticos. Masson, pp. 19-21.
129. Özdemir V., Demirkan A. Ç., Akosman M. S. (2013). Subgross and macroscopic investigation of the coeliac artery in the chinchilla (*Chinchilla lanigera*). *Folia Morphologica*, 72(3):258-262.
130. Paula T.A.R., Walker N.J. (2013). Reproductive morphology and physiology of the male capybara. In: Moreira J., Ferraz K., Herrera E., Macdonald D. (Eds). *Capybara*. Springer, New York, NY.
131. Peceño M.C. (1983). Estudio Citogenético Y Genético Evolutivo Del Chigüire Género *Hydrochaeris*. Trabajo Especial De Grado, Universidad Simón Bolívar, Caracas.

132. Percegon L.S., Aita C., Cairo I., Wouk A.F., Riella M.C. (2004). Evaluation of capybara (*hydrochaeris hydrochaeris*) as a potential donor for pancreatic islet xenotransplantation. Dissertation Thesis. University Of Paraná, Curitiba, Brazil.
133. Pereira F. M. A. M., Bete S. B. D. S., Inamassu L. R., Mamprim M. J., Schimming B. C. (2020). Anatomy of the skull in the capybara (*Hydrochoerus hydrochaeris*) using radiography and 3D computed tomography. *Anatomia, Histologia, Embryologia*, 49(3):317-324.
134. Percy D.H., Barthold S.W. (2001). Guinea Pig. In: Pathology of Laboratory Rodents and Rabbits. 2nd Ed. Blackwell, Ames Iowa, pp. 209-247.
135. Pernecky A. (1969). The branches of the abdominal aorta in the guinea pig. *Anatomischer anzeiger*, 125(4):443-453.
136. Pignon C., Mayer J. (2020). Guinea Pigs. In: Queesenberry K.E., Mans C., Orcutt C., Carpenter J.W. (Eds). Ferrets, Rabbits, And Rodents: Clinical Medicine And Surgery. 4<sup>th</sup> Ed. St. Louis, Missouri: Elsevier Saunders, pp. 270-297.
137. Popesko P., Rajtová V., Horák J. (1992). A Colour Atlas of The Anatomy of Small Laboratory Animals. Volume One: Rabbit-Guinea Pig. Wolfe Publishing Ltd., London.
138. Potter G. E., Jones W. D., Hermann C. L. (1958). The circulatory system of the guinea pig. *Bios*, 29:3-13.
139. Pradere J. D., González F., Ruiz A. Z., Correa, A. (2006). Anatomía del Útero y Ovarios del Capibara (*Hydrochoerus hydrochaeris*): Irrigación Arterial. *Revista de la Facultad de Ciencias Veterinarias, UCV*, 47(1):25-32.
140. Pritt S. (1998). The history of the guinea pig (*Cavia porcellus*) in society and veterinary medicine. *Veterinary heritage*, 21:12-16.
141. Pritt S. (2012). Guinea Pigs: Taxonomy And History. In: Suckow M.A., Stevens K.A., Wilson R.P. (Eds). The Laboratory Rabbit, Guinea Pig, Hamster, And Other Rodents. San Diego: Elsevier, pp. 563-574.
142. Privado-Filho J.R. (2000). Vascularizacao Arterial em Pancreas de Capivara, *Hydrochoerus Hydrochaeris* (Linnaeus, 1766). Dissertation Thesis. Jaboticabal: Universidade Estadual Paulista, Facultad de Ciencias Agrarias e Veterinarias.
143. Queesenberry K.E., Donnelly T.M., Hillyer E.V. (2004). Biology, Husbandry, and Clinical Techniques of Guinea Pigs and Chinchillas. In: Queesenberry K.E., Carpenter J.W. (Eds). Ferrets, Rabbits and Rodents: Clinical Medicine and Surgery. 2<sup>nd</sup> Ed. Elsevier, New York, pp. 232-244.



144. Reckziegel S. H., Lindemann T. (2017). A systematic study of the brain base arteries in capybara (*Hydrochoerus hydrochaeris*). *Journal of Morphological Sciences*, 18(2):0-0.
145. Reckziegel S. H., Schneider F. L., Edelweiss M. I. A., Lindemann T., Culau P. O. V. (2017). Anatomy of the caudal cerebral artery on the surface of capybara (*Hydrochoerus hydrochaeris*) brain. *Journal of Morphological Sciences*, 21(3):0-0.
146. Resoagli J.M., Fernández J.A., Bode F.F., Cao J., Llano E.G, Marinkovic S. (2009). Aparato Urogenital Hembra Del Carpincho. Facultad De Ciencias Veterinarias-Unne. Sitio Argentino De Producción Animal.
147. Rhodi J. (1959). Ultrastructure of the tracheal ciliated mucosa in the rat and man. *Annals of Otolaryngology, Rhinology, & Laryngology*, 68:964-974.
148. Richerson G. B., Getting P. A. (1992). Medullary respiratory neurons in the guinea pig: localization and firing patterns. *Brain research*, 591(1):79-87.
149. Rosas C., Belgica Vasquez P., del Sol M. (2010). Histological and Histochemical description of the liver of the guinea pig (*Cavia porcellus*). *International Journal of Morphology*, 28(1):151-156.
150. Rowe D. L., Honeycutt R. L. (2002). Phylogenetic relationships, ecological correlates, and molecular evolution within the Cavoidea (Mammalia, Rodentia). *Molecular Biology and Evolution*, 19(3):263-277.
151. Santos-Sousa C. A., Stocco A. V., Mencialha R., Jorge S. F., Abidu-Figueiredo M. (2015). Morphometry and vascularization of the rabbit kidneys (*Oryctolagus cuniculus*). *International Journal of Morphology*, 33(4):1293–1298.
152. Schlesinger R. B., McFadden L. A. (1981). Comparative morphometry of the upper bronchial tree in six mammalian species. *The Anatomical Record*, 199(1):99-108.
153. Sekhon H., Sun J. P., Churg A., Wright J. (1995). Pulmonary capillaries are smaller in the centre than in the periphery of the guinea-pig lung lobule: possible contributory mechanism for the centrilobular location of emphysema?. *International journal of experimental pathology*, 76(2):145–148.
154. Sejin C. J., Choque N., Fuentes E. E., Lombo P. E. (2003). Aplicación de angioteécnicas en el estudio anatómico del riñón, hígado y corazón de chigüiros (*Hydrochoerus hydrochaeris*). *Orinoquia*, 7(1-2):12-15.
155. Shively M. J., Stump J. E. (1975). The systemic arterial pattern of the guinea pig: the abdomen. *The Anatomical Record*, 182(3):355-366.
156. Shively M. J., Stump J. E. (1974). The systemic arterial pattern of the guinea pig: the head, thorax, and thoracic limb. *American Journal of Anatomy*, 139(2):269-284.
157. Sisk D.B. (1976). Physiology. In: Wagner J.E., Manning P.J. (Eds). *The Biology Of The Guinea Pig*. San Diego, Academic Press, pp. 63-92.

158. Sonmez O. F., Odaci E., Bas O., Kaplan S. (2010). Purkinje cell number decreases in the adult female rat cerebellum following exposure to 900 MHz electromagnetic field. *Brain research*, 1356:95-101.
159. Spines R. L. (1982). Anatomy of the guinea-pig cecum. *Anatomy and Embryology*, 165(1):97-111.
160. Spotorno A. E., Zuleta C. A., Valladares J. P., Deane A. L., Jiménez J. E. (2004). Chinchilla laniger. *Mammalian species*, 2004(758):1-9.
161. Stan, F. G. (2018). Comparative Study of the Liver Anatomy in the Rat, Rabbit, Guinea Pig and Chinchilla. *Bulletin of the University of Agricultural Sciences & Veterinary Medicine Cluj-Napoca. Veterinary Medicine*, 75(1).
162. Supuka P., Mazensky D., Danko J., Supukova A., Petrovova E. (2014). Anatomical description of the renal arteries and veins in the European rabbit. *Biologia*, 69(8):1059-1064.
163. Tagliavia C. (2014). Studio anatomotopografico ed indagine morfometrica dei bronchi principali, lobari e segmentali nel coniglio, nel furetto, e nella cavia. Tesi Di Laurea. Scuola Di Agraria E Medicina Veterinaria, Università Di Bologna, A.A. 2013-2014. Relatore Chiar.Mo Prof. A. Grandis.
164. Tantawy A. H., Elzoghby E. M., Attia H. F., Emam M. A. (2022). Electron microscopy and immunohistochemistry using indicators of apoptosis and proliferation on guinea pig parathyroid gland. *Advances in Animal and Veterinary Sciences*, 10(1):131-138.
165. Tenani S. C., de Melo A. P. F., Rodrigues R. F. (2010). Study of the arterial vascularization in capibara hearts (*Hydrochaeris hydrochaeris*-Carleton, MD 1984). *Brazilian Journal of Veterinary Research and Animal Science*, 47(3):204-208.
166. Timm K.I., Jahn S.E., Sedgwick C.J. (1987). The palatal ostium of the guinea pig. *Laboratory Animal Science*, 37:801-802.
167. Trindade De Veglia H. (2016). El sistema de conducción atrioventricular en corazones de carpincho (*Hydrochoerus capibara*). Laboratorio De Anatomía Del Desarrollo - Sitio Argentino De Producción Animal, Facultad De Medicina – Unne.
168. Vazquez N., Senos R., Pérez W. (2012). Anatomy of the gross intestine of the capybara (*Hydrochoerus hydrochaeris*). *American Journal of Animal and Veterinary Sciences*, 7(2):92-95.
169. Venturoli L. (2008). Studio anatomo-topografico ed indagine morfometrica dei bronchi principali, lobari e segmentali nel cane. Dissertation Thesis. Department of Veterinary Medical Sciences, Alma Mater Studiorum - University of Bologna, Italy.
170. Vicentini C. A., Orsi A. M., Dias S. M. (1991). Anatomical observations of the coronary artery vascularization in the guinea pigs (*Cavia porcellus*, L.). *Anatomischer Anzeiger*, 172(3):209-212.

171. Vucetich M.G., Deschamps C.M., Perez M.E. (2012). Paleontology, evolution and systematics of Capybara. In: Moreira J.R., Ferraz K., Herrera E.A., Macdonald D.W. (Eds). *Capybara: Biology, use and conservation of an exceptional neotropical species*. Springer, New York, pp. 39-59.
172. Wagner J.E. (1976). Introduction And Taxonomy. In: Wagner J.E., Manning P.J. (Eds). *The Biology of the Guinea Pig*. New York: Academic Press, Inc., pp. 1-4.
173. Watanabe I. S., Dos Santos Haemmerle C. A., Dias F. J., Cury D. P., Da Silva M. C. P., Sosthines M. C. K., Miglino M. A. (2013). Structural characterization of the capybara (*Hydrochaeris hydrochaeris*) tongue by light, scanning, and transmission electron microscopy. *Microscopy Research and Technique*, 76(2):141-155.
174. Webb S.D., Marshall L.G. (1982). Historical biogeography of recent south American land mammals. In: Mares M.A., Genoways H.H. (Eds). *Mammalian biology in South America*. University of Pittsburgh, Linesville, pp. 39-52.
175. Weir B. J. (1974). Notes on the origin of the domestic guinea pig. In: Rowlands I.W., Weir B.J. (Eds). *The biology of hystricomorph rodents*. Academic Press, pp 437-446.
176. Weir B. J. (1974b). Reproductive characteristics of hystricomorph rodents. *Symposia of the Zoological Society of London*, 34:265-301.
177. Widdicombe J. (1996). The tracheobronchial vasculature: a possible role in asthma. *Microcirculation*, 3:129-141.
178. Woods C.A. (1982). The history and classification of south American Histricognath rodents: reflections on the far away and long ago. In: Mares M.A., Genoways H.H. (Eds). *Mammalian biology in South America*. University of Pittsburgh, Linesville , pp. 337-392.
179. Yamasaki M. (1995). Comparative anatomical studies on the thyroid and thymic arteries. III. Guinea pig (*Cavia cobaya*). *Journal of anatomy*, 186(2):383.
180. Yousif R. R. (2019). Anatomical and histological study of kidney, ureter and urinary bladder in male guinea pig (*Cavia porcellus*). *Iraqi Journal of Veterinary Medicine*, 43(1):75-84.